

**Faculty of Science and Engineering
Department of Chemistry**

**Applications of Chemometrics to the Analysis
and Interpretation of Forensic Physical
Evidence**

Georgina Yasmin Sauzier

**This thesis is presented for the Degree of
Doctor of Philosophy
of
Curtin University**

July 2016

Declaration

To the best of my knowledge and belief, this thesis contains no material previously published by any other person except where due acknowledgement has been made.

This thesis contains no material which has been accepted for the award of any other degree or diploma in any university.

Signature:

Date: 13/07/2016

Abstract

Forensic investigations often depend upon the recovery and analysis of physical evidence to reconstruct the events surrounding a crime. Though consensus standards have been established in this regard, these typically rely on the interpretation of complex data by an examiner, leading to apprehensions regarding human error or bias. Additionally, there are limited rigorous studies concerning the appropriate handling of forensic exhibits to maximise their evidential value. Recent decades have therefore seen an increased interest in developing more objective methods for assessing evidentiary significance, as well as statistically validated sampling and handling procedures. This may be achieved by employing multivariate statistics, or chemometrics, to provide objective measures of analytical data using well-established statistical protocols. This dissertation describes a series of investigations applying chemometrics to various aspects of forensic physical evidence examination, with a specific focus on textile fibres, writing inks and explosive residues.

Microspectrophotometry (MSP) and chemometric pattern recognition were first used to conduct simulated “questioned versus known” comparisons on several blue-dyed acrylic fibre sets. Fisher’s Exact test was applied to the resultant data, providing a quantitative measure of sample similarity or dissimilarity. The majority of fibre sets formed distinct groupings on the basis of their overall dye composition, giving a true exclusion in 108 of 110 comparisons. Comparison of fibres within the same set resulted in a true inclusion in 10 out of 11 scenarios, with the one false exclusion attributed to a lack of spectral reproducibility. This methodology, whilst not infallible, could thus provide a more objective and statistical basis on which forensic examiners can support their conclusions in court.

Chemometrics with diffuse reflectance visible spectroscopy was then investigated as an *in situ* characterisation method for inks on paper. Analysis of spectra from 35 blue ballpoint inks found several to be clearly distinguishable, though others exhibited overlap. A subsequent discriminant model resulted in 88.4 % of spectra being correctly assigned to the source pen or supplier. This model could be used to generate probative information from a questioned document, or could alternatively be utilised as a rapid, non-destructive screening method for document examination.

Analysis of six ballpoint inks stored under various office conditions found that they remained chemically stable for at least 14 months in the dark. Conversely, inks exposed to light could exhibit spectral changes within just one week, resulting in altered predictions using the chemometric model. This could prove beneficial when attempting to detect alterations made to a document using the same pen as the original entry at a later date. Multivariate calibration was employed in an attempt to model these changes for ink dating purposes, but the estimations afforded by these models proved unreliable. Artificial ageing experiments found that both heat and ultraviolet light play a role in the ageing process, and that accelerated ageing using these factors gives a reasonable depiction of short-term ageing under natural conditions.

Further work in this area employed a video spectral comparator (VSC) as a means of obtaining visible spectra from handwritten ink entries, rather than the larger deposits employed previously. The VSC was found to give lower specificity between similar inks, with a classification accuracy of only 31.7 % achieved using an independent test set. Discriminant models based upon chromaticity values or fluorescence spectra were similarly unsuccessful. Fluorescence was then utilised as an initial binary classifier. Chemometric analysis was conducted on the visible spectra of fluorescent and non-fluorescent inks, giving improved separation. Further specificity could be achieved by categorising the fluorescent inks according to their observed fluorescence intensity. However, as this was done based on personal opinion, a level of human bias could be introduced to the results.

Finally, experimental design was utilised with gas chromatography-mass spectrometry (GC-MS) to determine optimum sampling, storage and extraction procedures for the recovery of smokeless powder residues from steel surfaces. The optimised protocols were successfully applied to post-blast residues deposited on steel witness plates through detonation of a pipe bomb device, with a rate of detection exceeding 95 % for both nitroglycerin and diphenylamine. These results provide a high level of confidence that explosive events involving smokeless powder formulations will be readily identified using the suggested parameters. The methodology employed here may also be readily applied to a variety of other explosive compounds, and thus assist in establishing 'best practice' procedures for explosive investigations.

Acknowledgements

I would like to acknowledge the many, many people who have made this project possible – and, on occasion, even fun.

First and foremost, I must thank Professor Simon Lewis for his guidance and encouragement (however dubious) throughout this research. He deserves no small measure of respect for having tolerated me this long. Secondly, to Emeritus Professor Bill van Bronswijk for bestowing wise counsel, reviewing my manuscripts with only as much red ink as strictly necessary, and occasionally reminding me not to take things too seriously. I am also indebted to Associate Professor John Goodpaster at Indiana University-Purdue University, Indianapolis (IUPUI), for hosting me in his laboratory and providing me use of his vast expertise on trace evidence and chemometrics. I will forgive you for making me do all of those fibre statistics if you forgive me for using all of your SPME vials (twice).

I would like to acknowledge Dr Stephen Morgan (University of South Carolina) for the provision of fibre samples, as well as Eric Reichard, Dana Bors, Wil Kranz and Marie Diez (IUPUI) for obtaining the MSP spectra. Additionally, thanks are due to both Dana and Jordan Ash (IUPUI) for their assistance with the explosives studies, and for not complaining about me hogging their GC. I would like to extend appreciation to the Indianapolis PD Bomb Squad (specifically Sergeant Leonard Langland and Officer Benjamin Cook) and the city of Martinsville, Indianapolis for facilitating the pipe bomb trial – without which this research project would have been considerably less interesting. I must also acknowledge the various students at IUPUI who assisted in the tedious preparation of witness plates or collection of post-blast samples. Thanks also to Geoff Day (Australian Federal Police) and Jasmina Clyburn (U.S. Bomb Data Centre) for providing statistics regarding reported explosive incidents, such that this work could be placed within the appropriate context.

I must thank John Coumbaros for allowing me to access the instrumentation at ChemCentre, as well as Rees Powell for providing training in Raman spectroscopy. Likewise, many thanks to Tonya Trubshoe and John McGinn (Document Examination Solutions, WA) for allowing me to regularly troop in and out of their office to use their VSC. I would like to acknowledge Peter Giles for conducting initial proof-of-concept tests regarding ink analysis, and Peter Chapman for his assistance with visible spectroscopy (as well as keeping me on my toes).

On a personal note, much gratitude is due to Jay Siegel and Maggie Wilke for being the best hosts (and tour guides) I could have asked for. My time in Indianapolis would not have been nearly as enjoyable without them. I must also thank the ‘Goodpaster Group’ at IUPUI for helping me find my feet, saving the GC (and subsequently a large portion of my project), and introducing me to such wonders as Marco’s Pizza buffet. Your collective craziness truly made me feel at home.

On that subject, I must also thank the Curtin Forensic & Analytical Chemistry Research Group for making this journey much more entertaining than I would have imagined. Our numerable shenanigans will serve to remind me that work *and* play are equally important, and that it’s sometimes easier to ask forgiveness than permission. I am also grateful to all of my friends, both in university and out, for giving me the occasional break from my PhD and only asking “*are you done yet?*” every few months or so.

Last but by no means least; I would like to thank my family and Allan for their everlasting support. They might not have understood anything I’ve been doing for the past three and a half years, but even when I had my doubts, they have always believed that I would make it.

Publications

This dissertation contains work which has been submitted for publication in the following peer reviewed journals:

G. Sauzier, P. Giles, S.W. Lewis and W. van Bronswijk. *In situ studies into the characterisation and degradation of blue ballpoint inks by diffuse reflectance visible spectroscopy*. Analytical Methods, 2015. **7**(12): p. 4892-4900. †

G. Sauzier, D. Bors, J. Ash, J.V. Goodpaster and S.W. Lewis. *Optimisation of recovery protocols for double-base smokeless powder residues using a central composite design and total vaporisation (TV) SPME/GC-MS*. Talanta, 2016. **158**: p. 368-374

G. Sauzier, E. Reichard, W. van Bronswijk, S.W. Lewis and J.V. Goodpaster. *Chemometrics as a means of improving the confidence of “questioned versus known” fiber comparisons using microspectrophotometry*. Forensic Chemistry, 2016 (accepted).

† Front cover article.

In addition, the following peer reviewed articles were published during the course of this dissertation:

G. Sauzier, M. Maric, W. van Bronswijk and S.W. Lewis. *Preliminary studies into the effect of environmental degradation on the characterisation of automotive clear coats by attenuated total reflectance infrared spectroscopy*. *Analytical Methods*, 2013. **5**(19): p. 4984-4990. †

K.J. van der Pal, **G. Sauzier**, M. Maric, W. van Bronswijk, K. Pitts and S.W. Lewis. *The effect of environmental degradation on the characterisation of automotive clear coats by infrared spectroscopy*. *Talanta*, 2016. **148**: p. 715-720.

† Front cover article.

Conference Presentations

Selected aspects of the work contained within this thesis have been presented, or have been accepted for presentation, at the following conferences:

Oral Presentations

Discrimination and classification of blue-dyed acrylic fibres using microspectrophotometry with chemometrics, 22nd ANZFSS International Symposium on the Forensic Sciences, 2014, Adelaide.

- Awarded ‘Highly Commended’ certificate for a meritorious presentation in the Chemical Criminalistics stream.

Optimisation of protocols for the recovery of smokeless gunpowder residues using solid phase microextraction with gas chromatography-mass spectrometry, Inaugural CUPSA Conference, 2015, Perth.

In situ studies into the characterisation and degradation of blue ballpoint inks by diffuse reflectance visible spectroscopy, RACI 23rd R&D Topics Conference, 2015, Melbourne.

In situ studies into the characterisation and ageing of blue ballpoint inks by diffuse reflectance visible spectroscopy, accepted for presentation at the 23rd ANZFSS International Symposium on the Forensic Sciences, 2016, Auckland.

- Keynote presentation in the Document Examination stream.

Poster Presentations

Preliminary studies into the ageing of blue ballpoint ink on paper using UV-Vis and chemometrics, Inaugural RSC Analytical Science Twitter Poster Conference [online], 2015.

Optimising the recovery of smokeless gunpowder residues using experimental design and TV-SPME/GC-MS, RACI 23rd R&D Topics Conference, 2015, Melbourne.

- Awarded Runner-Up Sciex Poster Prize

Discrimination of handwritten blue ballpoint inks using VSC spectroscopy and chemometrics, 2nd RSC Analytical Science Twitter Poster Conference [online], 2016.

Optimised recovery of smokeless gunpowder residues using experimental design with TV-SPME/GC-MS, accepted for presentation at the 23rd ANZFSS International Symposium on the Forensic Sciences, 2016, Auckland.

Table of Contents

Declaration	i
Abstract	ii
Acknowledgements	iv
Publications	vi
Conference Presentations	viii
Table of Contents	x
List of Figures	xv
List of Tables	xix
List of Abbreviations	xxii
Chapter 1: Introduction	1
1.1 Introduction	2
1.2 Issues in the interpretation of forensic analytical data	3
1.3 Chemometric techniques	5
1.3.1 Principal component analysis (PCA)	5
1.3.2 Discriminant analysis (DA)	8
1.3.3 Partial least squares regression (PLSR)	9
1.3.4 Central composite design (CCD)	9
1.4 Chemometrics in forensic science	10
1.4.1 Drugs and pharmaceuticals	11
1.4.1.1 Amphetamine-type stimulants	11
1.4.1.2 Opiates	11
1.4.1.3 Cocaine	12
1.4.1.4 Pharmaceuticals	12
1.4.2 Document analysis	13
1.4.2.1 Paper	13
1.4.2.2 Writing inks	14
1.4.3 Explosives and related materials	15
1.4.3.1 Low explosives and propellants	15
1.4.3.2 High explosives	16

1.4.3.3	Adhesive tapes	17
1.4.4	Fire debris	17
1.4.5	Paint	18
1.4.5.1	Architectural paint	19
1.4.5.2	Automotive paint	19
1.4.6	Hairs and fibres	20
1.4.7	Soils	21
1.4.8	Other transfer evidence	22
1.4.8.1	Impressions	22
1.4.8.2	Biological materials	22
1.4.8.3	Glass	23
1.4.8.4	Cosmetics	23
1.4.9	Future directions and challenges	24
1.5	Textile fibres	25
1.5.1	Classes of textile fibres	26
1.5.2	Forensic analysis of textile fibres	27
1.5.2.1	Microscopy	27
1.5.2.2	Colourant analysis	27
1.5.2.3	Infrared and Raman spectroscopy	28
1.6	Writing inks	28
1.6.1	Classes of writing ink	29
1.6.2	Forensic analysis of writing ink	30
1.6.2.1	Visual examinations	30
1.6.2.2	Infrared and Raman spectroscopy	31
1.6.2.3	Chromatographic methods	31
1.7	Explosives	31
1.7.1	Classes of explosives	32
1.7.2	Forensic analysis of explosives	33
1.7.2.1	Microscopy and microchemical testing	33
1.7.2.2	Separation methods	33
1.7.2.3	Infrared and Raman spectroscopy	34
1.8	Aims and overview	34

Chapter 2: Improving the confidence of “questioned versus known” fibre comparisons using microspectrophotometry and chemometrics	36
2.1 Introduction	37
2.2 Experimental	39
2.2.1 Samples	39
2.2.2 Microspectrophotometry	39
2.2.3 Raman spectroscopy	40
2.2.4 Data analysis	41
2.3 Results and discussion	43
2.3.1 Preliminary considerations	43
2.3.2 Fibre characterisation using Raman spectroscopy	43
2.3.3 Correlation between fibre spectra and component dyes	44
2.3.4 Distribution of the spectral dataset	47
2.3.5 Simulated “Q vs. K” comparisons	51
2.3.5.1 Fibres from same source	51
2.3.5.2 Fibres from different sources	52
2.4 Conclusions	55
Chapter 3: Chemometric characterisation and ageing studies of blue ballpoint inks on paper using diffuse reflectance visible spectroscopy	56
3.1 Introduction	57
3.2 Experimental	60
3.2.1 Sample collection and preparation	60
3.2.2 Ageing studies	60
3.2.2.1 Natural ageing	61
3.2.2.2 Artificial ageing	61
3.2.3 Photographic recording	62
3.2.4 Visible spectroscopy	63
3.2.5 Data analysis	63
3.3 Results and discussion	64
3.3.1 Preliminary considerations	64
3.3.2 Distribution of blue ballpoint inks	64
3.3.3 Discriminant analysis	67

3.3.4	Characterisation of naturally aged samples	71
3.3.5	Development of dating models for light-exposed samples.....	84
3.3.6	Characterisation of artificially aged samples	90
3.4	Conclusions	93
Chapter 4: Chemometric characterisation of blue ballpoint inks on paper using a video spectral comparator		94
4.1	Introduction	95
4.2	Experimental	96
4.2.1	Sample preparation	96
4.2.2	Data collection.....	96
4.2.2.1	Method development.....	97
4.2.2.2	Reflectance spectra and chromaticity measurements.....	97
4.2.2.3	Fluorescence characterisation.....	97
4.2.3	Data analysis	97
4.3	Results and discussion	98
4.3.1	Preliminary considerations.....	98
4.3.2	Method development	98
4.3.3	Compatibility of VSC spectra with the existing spectrophotometer model	99
4.3.4	Distribution of the spectral dataset	99
4.3.5	Discriminant analysis.....	102
4.3.6	Chromatic data	104
4.3.7	Fluorescence spectroscopy.....	107
4.3.7.1	Spectral distribution	107
4.3.7.2	Fluorescence as an initial classifier	109
4.4	Conclusions	114
Chapter 5: Optimisation of recovery protocols for smokeless powder residues with subsequent analysis by gas chromatography-mass spectrometry.....		115
5.1	Introduction	116
5.2	Experimental	118
5.2.1	Reagents and materials	118
5.2.2	Preliminary experiments	119

5.2.2.1	Preparation of standard solutions.....	119
5.2.2.2	Smokeless powder deflagration.....	119
5.2.2.3	Factor screening.....	120
5.2.3	Optimisation experiments.....	120
5.2.3.1	Preparation of standard solutions.....	120
5.2.3.2	Smokeless powder quantification.....	121
5.2.3.3	Central composite design.....	121
5.2.3.4	Sample preparation.....	121
5.2.4	Pipe bomb trial.....	122
5.2.5	Sample extraction.....	123
5.2.6	Instrumental analysis.....	124
5.3	Results and discussion.....	126
5.3.1	Preliminary considerations.....	126
5.3.2	Smokeless powder deflagration.....	128
5.3.3	Factor screening.....	130
5.3.4	Smokeless powder quantification.....	133
5.3.5	Central composite design.....	135
5.3.5.1	Optimisation.....	135
5.3.5.2	Main effects and factor interactions.....	137
5.3.6	Pipe bomb trial.....	140
5.4	Conclusion.....	143
 Chapter 6: Conclusions and Future Work.....		144
 References.....		149
 Appendices.....		182

List of Figures

Figure 1.1: Diagram illustrating the generation of the first principal component (PC) for a simplified dataset described by variables X, Y and Z (based on Unscrambler® X user manual). Dashed lines indicate the projection of each sample onto the PC. ...	6
Figure 1.2: 3-dimensional PCA scores plot of infrared spectra acquired from a large population of automotive clear coats, showing the grouping of samples according to their country of vehicle manufacture.	7
Figure 1.3: PCA loadings plot for infrared spectra acquired from a large population of automotive clear coats, showing wavenumber regions correlated with each PC.	7
Figure 1.4: Schematic comparison of a circumscribed, inscribed and face-centred central composite design for two continuous factors.	10
Figure 1.5: Classification of textile fibres according to source.	26
Figure 1.6: Microscopic image of an ink line on paper showing defects characteristic of a ballpoint writing implement; (a) excess ink deposition and (b) skipping of the ink line.	30
Figure 2.1: MSP microscope images of blue acrylic fibre exemplars utilised for Q vs. K comparisons.	40
Figure 2.2: Raman spectra acquired from blue-dyed acrylic fibre sets. (*) denotes signals identified as instrumental artifacts.	44
Figure 2.3: Normalised MSP spectra (averaged across five replicates) for acrylic fibres containing (top) Blue 3; (middle) Blue 41; and (bottom) Blue 147 as their primary dye.	46
Figure 2.4: Scree plot depicting the cumulative variance in the blue acrylic fibre dataset retained by each PC.	47
Figure 2.5: 3-dimensional PCA scores plot (employing PCs 1,2,3 and PCs 1,2,4) showing the distribution of blue acrylic fibres based upon their corresponding MSP spectra. Left and right images show the improved separation of Fibre Sets C and D upon the inclusion of PC4.	49
Figure 2.6: Factor loadings plot of PCs 1-4 for PCA of the entire blue acrylic dataset.	50
Figure 2.7: Pre-processed MSP spectra acquired from five individual fibres taken from (top) fibre set A and (bottom) fibre set H, illustrating differing relative intensities between the two major peaks at 600 nm and 650 nm.	54

Figure 3.1: Chemical structures, chemical names and common names of methyl violet homologues (chloride counter-ions not shown).....	58
Figure 3.2: Anticipated degradation pathways of methyl violet dyes in ballpoint inks deposited on paper, shown for crystal violet: (a) oxidative N-demethylation and (b) photooxidative cleavage of the central C-phenyl bond.....	59
Figure 3.3: Scree plot depicting the cumulative variance in the Cary 4000 blue ballpoint ink dataset retained by each PC.	65
Figure 3.4: 3-dimensional PCA scores plots generated using the first four PCs, highlighting the distribution of the blue ballpoint ink population based upon their corresponding Cary 4000 visible spectra. Circles indicate Pilot brand and Bic brand pens, which are separated along PC4.....	66
Figure 3.5: 3-dimensional PCA scores plot showing separation of (a) Celco Retractable and (b) PaperMate FlexGrip Elite inks, despite visually similar spectra.	67
Figure 3.6: 3-dimensional PCA projection plot showing the distribution of fresh and aged inks stored open to air in the dark following various periods of exposure. Red arrow indicates Office Basics spectrum identified as an outlier.	72
Figure 3.7: 3-dimensional PCA projection plot showing the distribution of fresh and aged blue ballpoint inks stored in plastic sleeves in the dark following various periods of exposure.	75
Figure 3.8: Photographic images of six blue ballpoint ink deposits stored open to light, (a) immediately following deposition; then following (b) 2 months, (c) 6 months and (d) 14 months of exposure.	77
Figure 3.9: 3-dimensional PCA projection plot showing the distribution of fresh and aged blue ballpoint inks exposed to light following various periods of exposure, with spectra and photographic images (recorded under identical conditions) obtained at each interval for the Celco Retractable ink.	79
Figure 3.10: Spectra of Celco Retractable, Keji Ballpoint, Office Basics, PaperMate Profile and Pilot G-2 05 ink deposits stored open to light; (a) immediately after deposition and (b) following 14 months of exposure.	80
Figure 3.11: Factor loadings of the first three PCs for PCA conducted on the population of 35 blue ballpoint inks.	81
Figure 3.12: 2-dimensional PLSR scores plots showing the distribution of six blue ballpoint inks exposed to light following various periods of exposure. Spectra collected at intervals within the first month of exposure have been colour-coded as a single group, but were treated as separate variables in the regression analysis.	85

Figure 3.13: Reference values versus estimated values by PLSR models for the age estimation of six blue ballpoint inks exposed to light over a 14 month period.....	87
Figure 3.14: 3-dimensional PCA projection plot showing the distribution of inks aged naturally for one week and those artificially aged for 24 hours by (a) thermal exposure; and (b) UV irradiation, compared to freshly deposited ink.....	92
Figure 4.1: Pre-processed reflectance spectra of a Pentel Rolly ink deposit acquired using the Cary 4000 UV-Visible spectrophotometer and VSC5000.....	99
Figure 4.2: Scree plot depicting the cumulative variance in the VSC blue ballpoint ink dataset retained by each PC.....	100
Figure 4.3: 3-dimensional PCA scores plots generated using the first four PCs, highlighting the distribution of the blue ballpoint ink population based upon their corresponding VSC visible spectra. Circles indicate Staedtler Triplus and Staedtler 430 inks, which are separated from the main population along PC4.	101
Figure 4.4: Pre-processed calibration and validation spectra (averaged across five replicates) obtained from Bic Cristal ink deposits.....	102
Figure 4.5: 3-dimensional scatter plot showing the distribution of the blue ballpoint ink population based upon their tristimulus values.	105
Figure 4.6: 2-dimensional PCA scores plots showing the blue ballpoint ink population based upon (top) raw; and (bottom) unit vector normalised tristimulus values.	106
Figure 4.7: Fluorescence spectrum recorded from an Office Choice ink deposit (inset image) using the VSC spot source at 645 – 720 nm excitation and 778 nm longpass filter.....	107
Figure 4.8: 3-dimensional PCA scores plot showing the distribution of strongly fluorescent blue ballpoint inks according to their fluorescence spectra, highlighting the large variation between replicates resulting from spectral deviations.	108
Figure 4.9: 3-dimensional PCA scores plots showing the distribution of non-fluorescent inks according to their visible spectra, highlighting improved separation of Artline Clix and Office Basics inks. Left and right views show plots generated using (left) PCs 1, 2 and 3; and (right) PCs 1, 2 and 4.	110
Figure 4.10: 3-dimensional PCA scores plots showing the distribution of fluorescent inks according to their visible spectra, (left) using PCs 1, 2 and 3; and (right) using PCs 1, 2 and 4. Improved separation of the PaperMate Ink Joy 300 and Staedtler 430 inks (circled) was achieved along PC4. Red arrow indicates PaperMate FlexGrip Elite replicate identified as an outlier based on visual inspection of the spectra as shown.	111

Figure 4.11: Photographic image of inks evaluated as exhibiting (top) strong; (middle) moderate; and (bottom) weak fluorescence when excited at 645 – 720 nm and viewed through a 778 nm longpass filter.....	112
Figure 4.12: 3-dimensional scores plots showing the distribution of (a) weakly fluorescent; (b) moderately fluorescent; and (c) strongly fluorescent inks according to their visible spectra. Plot (c) has been shown using (left) PCs 1, 2 and 3; and (right) PCs 1, 2 and 4.	113
Figure 5.1: Pipe bomb detonation trial set-up showing galvanised steel witness plates attached to each side of the welded metal frame surrounding the device.	122
Figure 5.2: GC-MS chromatogram acquired from a standard solution of nitrobenzene (NB), nitroglycerin (NG), diphenylamine (DPA) and ethyl centralite (EC) analysed using the TV-SPME-2 method. (*) denotes minor peak attributed to dinitroglycerin. Note that peaks have been auto-scaled for clarity.	128
Figure 5.3: Average percentage recoveries of nitroglycerin, diphenylamine and ethyl centralite using various sampling methods. Error bars represent the standard deviation across three replicates.	131
Figure 5.4: Average percentage recoveries of nitroglycerin, diphenylamine and ethyl centralite using various sampling methods following 3 days of sample storage. Error bars represent the standard deviation across three replicates.	133
Figure 5.5: Response surface plots for the recovery of nitroglycerin and diphenylamine (isopropanol-wetted swabs) and ethyl centralite (dry swabs) stored under refrigerated conditions, as a function of extraction and storage time. Arrows indicate optimum points on each response surface.....	139
Figure 5.6: Photographs of the PVC pipe bomb trial set-up, a) prior to; b) during; and c) following initiation of the device.	141
Figure 5.7: Heat maps showing the distribution of NG on witness plates (a) on each side; (b) above and below the PVC pipe bomb device. Colour scale is normalised to the highest nitroglycerin peak area recovery. (*) denotes the top edge of plates surrounding the device.	142

List of Tables

Table 2.1: Dye compositions of eleven blue acrylic fibre sets utilised in this study.	39
Table 2.2: General form of a contingency table generated from a Q vs. K comparison.	42
Table 2.3: Spectral features attributable to dyes contained in the blue acrylic fibres.	44
Table 2.4: Statistical values obtained from Q vs. K comparisons conducted on blue acrylic fibres originating from the same set. (*) denotes that the spectra for the ten fibres in these fibre sets were each acquired over multiple consecutive days.	52
Table 2.5: Statistical values obtained from Q vs. K comparisons conducted on fibres from different sets.	53
Table 3.1: Models and assigned numeric identifiers for all pens in the sample population. (*) denotes inks also selected for the preparation of validation samples; (†) denotes inks selected for ageing studies.	62
Table 3.2: Individual clusters of blue ballpoint pen inks observed to be visually indistinguishable using PCA based on their Cary 4000 visible spectra.	67
Table 3.3: Number of correct and incorrect classifications for samples in the calibration set using a four-PC LDA model. Labels in brackets indicate assigned groups. The overall classification accuracy was 97.7 %.	68
Table 3.4: Number of correct and incorrect classifications for samples in the validation set using a four-PC LDA model. Labels in brackets indicate assigned groups. The overall classification accuracy was 71.7 %.	69
Table 3.5: Discriminant values of Bic Economy validation samples against the Bic Orange Fine and Bic Economy classes.	70
Table 3.6: Averaged discriminant values and associated standard deviations for Office Basics and PaperMate Ink Joy 300 validation samples against the two nearest classes. Values are averaged across five replicates.	70
Table 3.7: Number of misclassified replicate spectra for Office Basics Ballpoint and PaperMate Profile ink samples stored open to air in the dark, at various intervals following ink deposition. Labels in brackets indicate assigned groups.	73
Table 3.8: Number of misclassified replicate spectra for Keji Ballpoint, Office Basics Ballpoint and PaperMate Profile inks stored in plastic sleeves in the dark, at various intervals following ink deposition. Labels in brackets indicate assigned groups.	74

Table 3.9: Number of misclassified replicate spectra for six blue ballpoint ink samples stored open to light, at various intervals following ink deposition. Labels in brackets indicate assigned groups.....	76
Table 3.10: Mean and standard deviations of LDA discriminant values for aged Celco Retractable ink against the predicted class(es), compared to true ink of that class. Values are averaged over five replicate spectra.....	83
Table 3.11: Number of selected factors and corresponding percentage of total variance for PLSR models of blue ballpoint inks exposed to light over a 14 month period.	84
Table 3.12: Mean and standard deviations of estimated ageing periods for validation blue ballpoint ink deposits exposed to light, compared to actual ageing periods. Values are averaged over five replicate spectra.	88
Table 3.13: Correlation coefficients and root mean square error of calibration (RMSEC) values obtained for PLSR models of blue ballpoint inks exposed to light over a 14 month period.	90
Table 4.1: Models and assigned numeric identifiers for pens utilised as validation samples.	96
Table 4.2: Number of correct and incorrect classifications for samples in the VSC calibration set using a four-PC LDA model. Labels in brackets indicate assigned groups. The overall classification accuracy was 96.7 %.....	103
Table 4.3: Number of correct and incorrect classifications for samples in the VSC validation set using a four-PC LDA model. Labels in brackets indicate assigned groups. The overall classification accuracy was 31.7 %.....	104
Table 5.1: Factors and levels tested for optimising the recovery of DBSP residues using a face-centred central composite design.	121
Table 5.2: Extraction parameters utilised for DBSP recovery experiments.....	123
Table 5.3: Instrumental parameters for GC-MS analysis of explosives samples. ...	125
Table 5.4: Chemical structures and selected physical properties of nitroglycerin, diphenylamine, ethyl centralite and nitrobenzene.	127
Table 5.5: Concentrations (parts-per-billion) of target explosive components recovered from deflagration trials of 0.2 – 0.6 g of Alliant Red Dot DBSP.....	129
Table 5.6: Concentrations (parts-per-billion) and standard deviation of target explosive components recovered from four replicate deflagration trials of 0.3 g of Alliant Red Dot DBSP.	130

Table 5.7: Average percentage recoveries (from three replicates) of nitroglycerin, diphenylamine and ethyl centralite using four sampling methods, following 15 minute, 30 minute or 60 minute extraction periods.	132
Table 5.8: Correlation coefficients of calibration curves generated for nitroglycerin, diphenylamine and ethyl centralite.	134
Table 5.9: Quantified mass percentages (averaged across three replicates) and precision of nitroglycerin, diphenylamine and ethyl centralite in Alliant Red Dot DBSP.	134
Table 5.10: Model fitting test results for response surface models constructed for nitroglycerin, diphenylamine and ethyl centralite based upon their GC-MS peak areas.	135
Table 5.11: CCD optimised parameters and corresponding desirability for the recovery of nitroglycerin, diphenylamine and ethyl centralite from Alliant Red Dot DBSP.	137
Table 5.12: p-values for all individual factors or two-way factor interactions in the recovery of Alliant Red Dot DBSP residues on steel.	137
Table 5.13: Relative GC-MS peak areas (normalised to maximum recovery) of target analytes from galvanised steel witness plates following detonation of a PVC pipe bomb containing Alliant Red Dot DBSP. Values are averaged across 16 samples.	141

List of Abbreviations

ANOVA	Analysis of variance
ASTM	American Society for Testing and Materials
ATF	Bureau of Alcohol, Tobacco, Firearms and Explosives
ATR	Attenuated total reflectance
CCD	Central composite design
CE	Capillary electrophoresis
CIE	Commission Internationale de l'Eclairage (International Commission on Illumination)
DA	Discriminant analysis
DBSP	Double-base smokeless powder
DP	Discriminatory power
DPA	Diphenylamine
DR	Diffuse reflectance
EC	Ethyl centralite
EDX	Energy-dispersive X-ray
FT	Fourier Transform
GC	Gas chromatography
GSR	Gunshot residue
HMX	Cyclotetramethylene tetranitrate (High Melting eXplosive)
HPLC	High performance liquid chromatography
IC	Ion chromatography
ICP	Inductively coupled plasma
IED	Improvised explosive device
IR	Infrared
IUPUI	Indiana University-Purdue University, Indianapolis
K-M	Kubelka-Munk
LDA	Linear discriminant analysis
LIBS	Laser-induced breakdown spectroscopy
MS	Mass spectrometry
MSP	Microspectrophotometry
NAS	National Academy of Sciences

NB	Nitrobenzene
NG	Nitroglycerin
NIPALS	Non-linear iterative partial least squares
NIR	Near-infrared
PC	Principal component
PCA	Principal component analysis
PETN	Pentaerythritol tetranitrate
PLS-DA	Partial least squares discriminant analysis
PLSR	Partial least squares regression
PVC	Polyvinyl chloride
Q vs. K	Questioned versus known
RDX	Cyclotrimethylene trinitramine (Research Department eXplosive)
RMSEC	Root mean square error of calibration
RSD	Relative standard deviation
SEM	Scanning electron microscopy
SIMCA	Soft independent modelling of class analogy
SPME	Solid phase microextraction
SWGMAAT	Scientific Working Group on Materials Analysis
SWGDOC	Scientific Working Group for Forensic Document Examination
SVM	Support vector machine
TATP	Triacetone triperoxide
TLC	Thin layer chromatography
TNT	Trinitrotoluene
TWGFEX	Technical Working Group for Fire and Explosions Analysis
TV	Total vaporisation
UV	Ultraviolet
UV-Vis	Ultraviolet-visible
VSC	Video spectral comparator

Chapter 1: Introduction

1.1 Introduction

The primary objective of many forensic investigations is the establishment of links between persons, places and/or objects of interest. These links are commonly drawn and supported using physical, or material, evidence. Many items of physical evidence are macroscopic items such as documents, clothing or weapons. However, this category also includes microscopic amounts of physical matter commonly referred to as 'trace evidence', which may include fingermarks, soil, glass, paint, hair, fibres, or explosive particulates.^[1-3]

Physical evidence often plays a pivotal role in reconstructing the series of events surrounding a crime, and may be used to prove or disprove a point in question based upon its discernible characteristics. As stated by Paul L. Kirk:

“Physical evidence cannot be wrong, it cannot perjure itself, it cannot be wholly absent. Only human failure to find it, study and understand it, can diminish its value.”^[4]

In addition, trace physical evidence can be instrumental in providing evidence of association. This value stems from the exchange principle developed by Edmond Locard, who posited that physical contact between two surfaces will likely result in a cross-transfer of matter between them, however minute.^[3, 5] The recovery and analysis of these traces may therefore be used to demonstrate direct or indirect contact between a perpetrator, victim and/or crime scene.

An issue arises, however, in the interpretation of physical evidence by forensic examiners. Many forensic disciplines, especially those involving pattern evidence such as marks or impressions, are primarily reliant on visual comparisons of images or chemical data. The subjective nature of these comparisons has led to concerns regarding potential human error and cognitive bias. Although this issue has been of particular relevance to pattern analysis, it also relates to the “eye-balling” of chemical data across a wide range of forensic analyses. This was highlighted in a broadly publicised report by the United States National Academy of Sciences (NAS) in 2009, which determined that more rigorous protocols were required to guide the subjective interpretations relied upon within many forensic disciplines.^[6]

Following the publication of the NAS report, as well as a similar inquiry conducted by the British House of Commons Science and Technology Committee,^[7] there have been strengthened efforts to establish statistically validated bases for assessing evidential value. One such approach is the use of chemometrics; a discipline that employs well-established statistical protocols to model chemical data. An increasing volume of scientific literature has emerged regarding the application of chemometric techniques to the discrimination and classification of forensic evidence. Chemometric tools may also be used to investigate factors affecting these analyses through the use of experimental design methods, which as of yet remain largely underutilised within a forensic context.

This dissertation outlines a program of research examining the application of chemometric techniques to the analysis and interpretation of physical evidence, as well as studying factors pertaining to its appropriate collection and storage. It is anticipated that these studies will assist in developing statistically validated operating procedures for forensic investigators.

1.2 Issues in the interpretation of forensic analytical data

Examination of physical evidence typically includes the use of various instrumental techniques, which generate a large volume of multivariate data in the form of spectra, chromatograms or similar output.^[8, 9] Interpretation of this data typically relies upon visual inspections or comparisons by a forensic examiner.^[2, 10] This may prove challenging when spectra appear visually similar, or when several samples must be compared simultaneously.^[11] The visual complexity of the data may also obscure trends or relationships between samples that may prove useful to an investigation, leading to probative information being overlooked.^[12]

Moreover, it has become increasingly recognised that examiners may be prone to cognitive or social biases that have the potential to affect their examinations.^[13-15] These may arise due to a number of factors, such as the examiner's prior expectation of results, knowledge of investigative details, or predisposition to assist the team that has retained their services.^[16, 17] This has led to a number of highly publicised cases, such as the erroneous association of Brandon Mayfield to the 2004 Madrid train bombings, or the flawed testimony provided by FBI hair examiners that resulted in an ongoing review of over 30,000 criminal cases.^[18, 19]

The 2009 NAS report highlighted several issues regarding current interpretation protocols relating to forensic evidence. In particular, the report identified the need for more rigorous and objective means of evaluating forensic evidence, as well as fundamental research regarding accuracy and reliability in forensic disciplines:

“A body of research is required to establish the limits and measures of performance and to address the impact of sources of variability and potential bias. Such research is sorely needed, but it seems to be lacking in most of the forensic disciplines that rely on subjective assessments of matching characteristics.”^[6]

The publication of the NAS report resulted in several initiatives in the United States aimed at improving forensic management and practice, such as the establishment of the National Commission on Forensic Science as a federal advisory group; formation of Organisation of Scientific Area Committees to develop documentary standards or guidelines; and attempts within Congress to introduce legislation promoting stronger oversight and fundamental research.^[20-23] Several studies also emerged examining the reliability of current procedures and improved examination protocols in disciplines such as fingerprint examination,^[24-26] bitemark analysis,^[27] toolmark comparisons;^[28, 29] shoeprint comparisons;^[30] and DNA analysis.^[21, 31]

An increased interest has also been developed in the use of statistical methods as a more objective means of assessing and describing forensic evidence, rather than comparative descriptions such as a ‘strong’ or ‘weak’ association. One area of interest is the use of Bayesian statistics to assign probability values to proposed events, such as the likelihood of a recovered fibre originating from a suspect’s garment versus some other source. This probabilistic approach, initially used primarily in DNA analysis, has also been applied to the forensic comparison of shoeprints, glass fragments and ballistics.^[32-35] However, calculation of the odds for a given event relies upon knowledge of several factors – in the case of a recovered fibre for example, data may be required regarding the number of garments produced over a given period, the number distributed within a geographical region, and the frequency of garments exhibiting properties consistent with those of the recovered sample. Such data is not always readily available, leading to debate concerning the applicability of Bayes’ theorem to a forensic context.^[36-38]

1.3 Chemometric techniques

Emerging in the 1970s, chemometrics is a discipline that uses statistical approaches to analyse and model chemical information.^[39] These techniques provide objective and quantitative measures of collected data, thus addressing concerns of human bias in forensic examinations.^[11, 40] Furthermore, the use of chemometric methods may reveal or explain trends not clearly evident from the raw information alone. As well as improving the discrimination of data, this may be vital in generating investigative leads or gathering forensic intelligence.^[41]

Chemometric techniques, of which only those used in this work are described here, can be divided into three main areas of application. Pattern recognition techniques such as principal component analysis (PCA) and linear discriminant analysis (LDA) are frequently applied to the discrimination and classification of samples, whilst calibration methods such as partial least squares regression (PLSR) are suited to the quantitative prediction of sample properties.^[42-44] Finally, experimental design techniques such as central composite designs (CCDs) may facilitate the design and optimisation of experimental procedures.^[45, 46]

1.3.1 Principal component analysis (PCA)

A common objective of pattern recognition is to identify latent trends within a dataset, also referred to as unsupervised learning or exploratory data analysis. This is often difficult when examining data obtained from analytical techniques, which may generate hundreds to thousands of variables for any given sample. PCA reduces the dimensionality of data by transforming the original set of correlated variables into orthogonal variables referred to as principal components, or PCs.^[12, 42, 47] Each successive PC is calculated to describe the maximum proportion of remaining variance, such that the majority of information is retained within the first few PCs. The number of useful PCs is therefore much fewer than the number of original variables. A graphical representation of this process is shown in Figure 1.1 for a simplified dataset containing three variables. Samples of the dataset can be represented as data points in a feature space described by the initial variables; X, Y and Z. Each PC is determined by finding the direction along which the remaining dispersion of the data points is the greatest.^[40] Projection of the samples onto the components then allows the dataset to be described using the PCs in place of the original variable set.

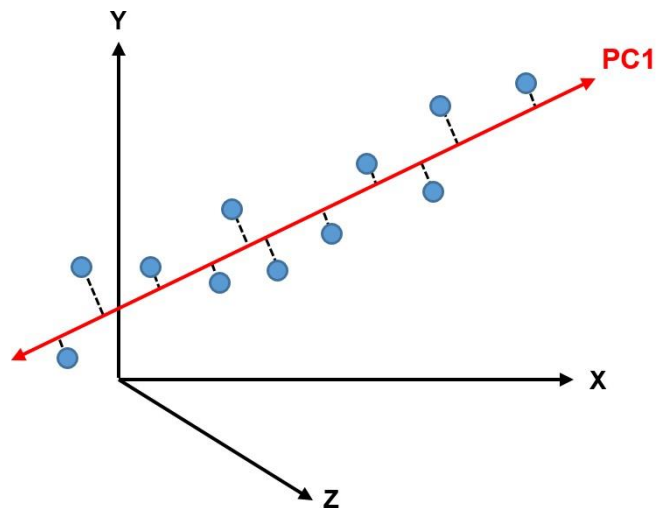


Figure 1.1: Diagram illustrating the generation of the first principal component (PC) for a simplified dataset described by variables X, Y and Z (based on Unscrambler® X user manual). Dashed lines indicate the projection of each sample onto the PC.

PCA transforms the original data matrix (X) into separate scores (T) and loadings (P) matrices, as given by the following equation:

$$\mathbf{X} = \mathbf{TP} + \mathbf{E}$$

This may be done through analysis of either the correlation or the covariance matrix.^[12, 42] The correlation method mean centres and scales the data such that each variable is equally weighted, thus accounting for different measurement units or unit variances. The covariance method, used throughout this thesis, applies mean centring without data scaling. This method is preferred where the measurement units and variance magnitudes are comparable across all variables.

As the majority of variation from the original dataset is retained by the first few PCs, multiplying the scores and loadings for these PCs allows the original dataset to be approximated. The discrepancy between the actual original data and this approximation is described by the residuals matrix (E), which largely encompasses random variation or noise within the dataset.^[48] The scores of a sample attained against any two or three PCs may be used as a new coordinate system, generating a scores plot wherein samples sharing similar characteristics are grouped together (Figure 1.2).^[49, 50] The scores plot thus allows clusters of similar samples to be identified, as well as the discrimination of samples whose scores are substantially different.

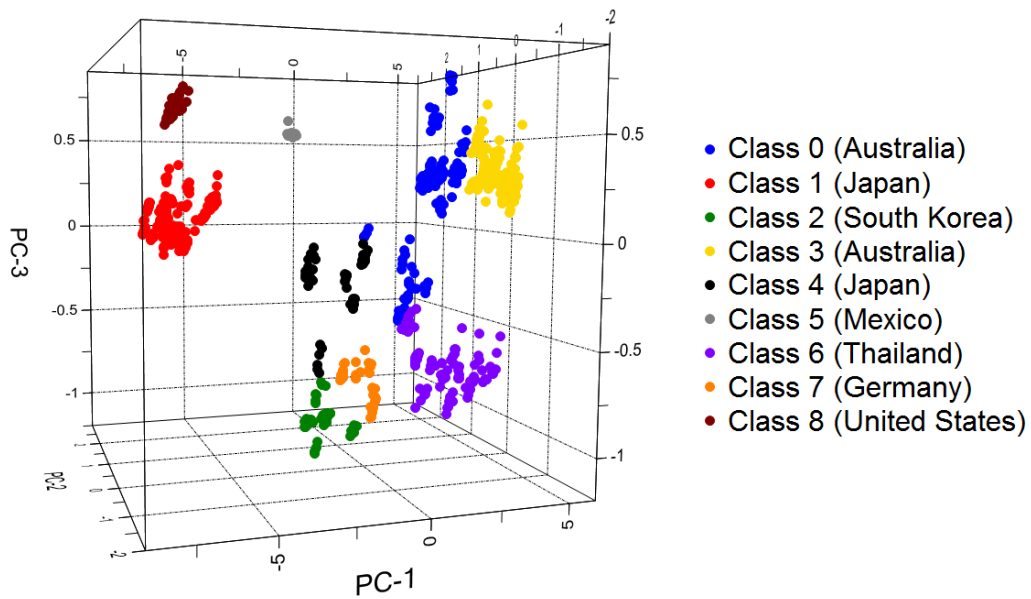


Figure 1.2: 3-dimensional PCA scores plot of infrared spectra acquired from a large population of automotive clear coats, showing the grouping of samples according to their country of vehicle manufacture.

Additionally, the PCA loadings may be examined to identify how variables of the original dataset are weighted against a particular PC (Figure 1.3). Variables with highly positive or negative loading values are significant in determining a sample's score along that component.^[47, 51] PCA hence not only allows the separation of samples, but can reveal the basis for this separation according to the underlying features of the sample.

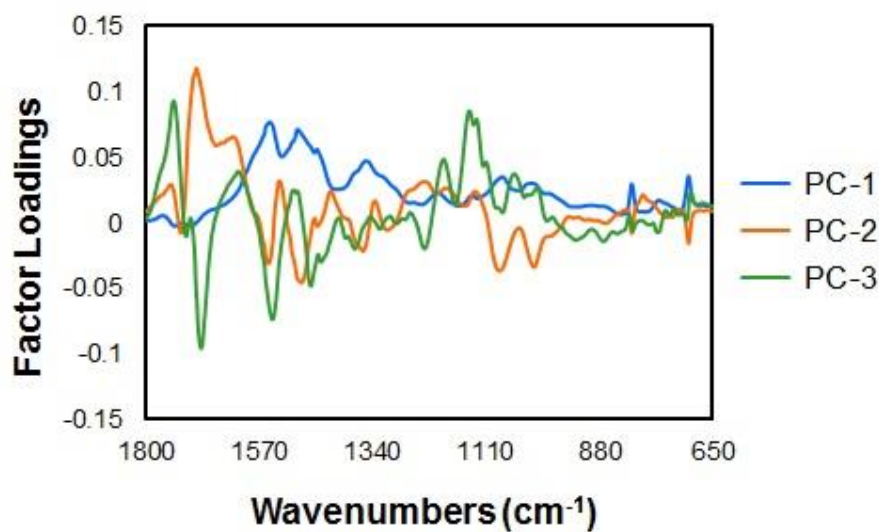


Figure 1.3: PCA loadings plot for infrared spectra acquired from a large population of automotive clear coats, showing wavenumber regions correlated with each PC.

1.3.2 Discriminant analysis (DA)

Following the identification of sample groupings within a dataset, it is often of interest to develop classification models (supervised learning) to assign future samples to a corresponding group. DA is applied to datasets with pre-specified groupings to build a discriminant function, expressed as a combination of input variables, such that the ratio of between-group to within-group variance (known as the Fisher ratio) is maximised.^[41, 52, 53] Where it is assumed that the covariance matrices of the classes are equal, such that the separating surface between the classes is linear, this method is specifically referred to as linear discriminant analysis (LDA).

As the sample size of each group must exceed the number of variables, DA is often performed after data reduction techniques such as PCA, with the first few PCs being substituted in place of the original variable set.^[11, 54] The subsequent model is then used to reclassify the samples of the training data (re-substitution), providing a percentage rate of correct classification.^[55] It should be noted that the use of the same data to both build and evaluate the model often leads to over-optimistic predictions of its performance.^[40, 54] For this reason, a more rigorous test of the model's predictive efficacy should be obtained through cross-validation procedures using separate training and testing data.

The most frequent form of cross-validation is the leave-one-out method, in which a single sample is removed from the dataset and a discriminant function constructed from the remaining data. The resultant model is used to predict a classification for the test sample, and the process then reiterated for every sample in the dataset.^[12, 56] A variant is the bootstrap, also known as leave- p -out validation, in which a number (p) of samples are randomly omitted as a test set during each repetition.^[12, 54] In both of these methods, the overall predictive ability is calculated as the average correct classification rate across all iterations. The most robust and reliable validation method is test set validation, wherein the dataset is divided into mutually exclusive training and validation sets.^[11, 57] The training set should ideally comprise approximately two thirds of the original data and is used to construct the model, with the test or validation set then being used to evaluate its performance.^[58] By utilising independent data to define and assess the model, this form of validation provides a more realistic indication of the model's predictive capability.^[40, 56, 57]

1.3.3 Partial least squares regression (PLSR)

For datasets consisting of predictor (X) and response (Y) variables, the relationship between the X and Y matrices can be modelled using regression techniques. Where both the predictors and responses are quantitative properties, these methods are referred to as calibration. The development of calibration models is valuable in allowing predictions to be made of unknown sample parameters based on their related and directly measurable properties, though as with pattern recognition, deriving relationships between a large quantity of variables often proves challenging.

PLSR addresses this problem by reducing the original variable set into a lesser number of combined variables or factors, in a similar fashion to PCA.^[57, 59] These factors are calculated such that the covariance between X and Y is maximised, i.e. greater weight is applied to predictor variables that are highly correlated with response, under the assumption that these will be more accurate for predictive purposes.^[40, 42, 50] This is in contrast to other multivariate calibration methods such as principal component regression, which apply heavier weighting to predictors that show the greatest amount of variation, regardless of whether this variation is related to a change in response.^[40]

1.3.4 Central composite design (CCD)

Although pattern recognition and regression methods are valuable tools for data interpretation, the results are often highly dependent on the initial data quality.^[40] The appropriate design of experimental procedures is thus of utmost importance. A CCD is one of several methods commonly used in response surface methodology; a collection of techniques aimed at modelling the relationships between multiple explanatory factors and a dependent response in a minimal number of experiments.^[46, 60] This data can be used to determine optimal factor settings that will provide an optimal response, as well as assessing potential factor interactions.

A CCD is derived from a two-level factorial design; wherein each factor variable has two discrete levels ('low' and 'high' settings) and experimental runs comprise all possible combinations of levels across all factors.^[11, 61] This is augmented with replicated centre points, in which all factors are set to a median value; and a set of axial (or star) points. The axial points are identical to the centre points, with the exception of a single factor that will take on values both above and below the median.^[45, 60, 62]

The purpose of the axial points is to allow the detection and modelling of any curvature in the response surface. This cannot be achieved using the simpler factorial designs.

The distance of the axial points from the centre value, termed α , will determine the specific model design as shown in Figure 1.4. Selection of the axial points to extend past the factorial space ($\alpha > 1$) will result in a circumscribed CCD, whereas a design with axial points falling within the factorial range ($\alpha < 1$) is termed inscribed.^[63-65] Although a circumscribed design covers a larger investigative range, an inscribed design may be needed if variable settings outside of the factorial levels are not readily or safely achievable.^[61]

Alternatively, the axial points may be chosen such that the low and high values are equal to the factorial points ($\alpha = 1$), giving rise to a face-centred design.^[61, 66] Unlike circumscribed or inscribed designs, a face-centred CCD is non-rotatable, i.e. it does not provide a uniform prediction error across the investigated range.^[65] On the other hand, as there are only three rather than five levels to be investigated per factor, a face-centred design requires substantially fewer experimental runs. Additionally, a face-centred design is well suited to scenarios where variable settings between or beyond the factorial points are not practicable.

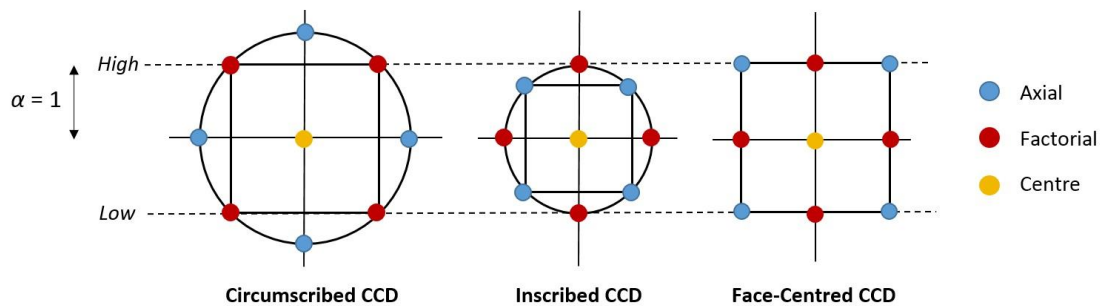


Figure 1.4: Schematic comparison of a circumscribed, inscribed and face-centred central composite design for two continuous factors.

1.4 Chemometrics in forensic science

Recent decades have seen an increased volume of research applying chemometric tools to forensic disciplines. This section provides a broad survey of chemometric applications to various forms of forensic physical evidence, including illicit drugs, documents, explosives, paints, fibres and soils.

1.4.1 Drugs and pharmaceuticals

A large proportion of research concerning the forensic application of chemometrics has focussed on drugs of abuse. Early work in this field was largely concerned with batch comparisons and impurity profiling of illicit drugs for the purpose of gathering forensic intelligence.^[67-76] This remains a key area of interest, with several studies over the last decade using chemometrics for the qualitative and quantitative analysis of illicit drugs such as amphetamine-type stimulants, opiates and cocaine.

1.4.1.1 Amphetamine-type stimulants

Andersson *et al.* employed partial least squares discriminant analysis (PLS-DA) and statistical distance metrics to identify linked samples of amphetamine analysed by gas chromatography mass spectrometry (GC-MS).^[77] The resulting discriminant models were able to successfully identify linked and non-linked samples, in addition to distinguishing those synthesised by different routes. However, no quantitative information concerning sample composition or similarity was derived. Proof-of-concept research by Goh *et al.* instead used field-portable attenuated total reflectance Fourier Transform infrared (ATR-FTIR) spectroscopy with PLSR to quantify solid mixtures containing methylamphetamine, glucose and caffeine, with predicted concentrations of these components typically within 6 % w/w of known values.^[78] Similar work by Hughes *et al.* on a larger sample set resulted in models able to quantify samples containing as little as 0.3 % w/w methamphetamine.^[79] The ability of this model to distinguish methamphetamine from structurally similar drugs is yet to be determined.

1.4.1.2 Opiates

Research by Moros *et al.* utilised diffuse reflectance near-infrared (DR-NIR) spectroscopy and PLSR to quantify heroin in seized illicit street drugs, resulting in the accurate quantitation of validation samples ranging from 6 – 34 % w/w purity.^[80] However, it should be noted that the validation set consisted of only 10 samples, and no replicate spectra were acquired to gauge the predictive reproducibility. Turner *et al.*, using FTIR spectroscopy, achieved successful and reproducible separation of heroin samples originating from three different poppy cultivars.^[81] This work was also able to identify and distinguish between five component opiates of the poppy heads, though only morphine could be reliably quantified.

In addition to spectroscopic methods, more recent studies have utilised inductively coupled plasma (ICP) as a more sensitive method of analysis based upon elemental composition. Chan *et al.* applied ICP-MS to street heroin samples seized in Malaysia, identifying two separate classes of samples.^[82] It was noted, though, that class similarities did not necessarily indicate batch linkages, as the profiled elements could have been introduced from contaminant sources in separate distribution chains. Later work by Liu *et al.* employed the same technique to distinguish opiate samples originating from the Golden Crescent and Golden Triangle; Asia's two principal areas of illicit opium production.^[83] Ten elements and seven elemental ratios were found to markedly differ between samples originating from the two regions, and a subsequent discriminant model gave a 97 % prediction accuracy of 175 validation samples.

1.4.1.3 Cocaine

Dujourdy *et al.* studied the source determination of hydrochloride cocaine samples based upon the headspace profiling of residual solvents.^[84] Cluster analysis was largely able to separate samples seized in Bolivia, Peru or Columbia, with a limited capacity to also discriminate between hydrochloride (salt) and base forms of cocaine. Separate studies by Rodrigues *et al.* and Groberio *et al.* on Brazilian seizures were able to reliably distinguish between salt and base samples based upon their IR spectra, with the latter also establishing PLSR models for the quantification of cocaine and selected common adulterants.^[85-87] Monfreda *et al.*, while not providing quantitative analysis, applied PCA to FTIR spectra to again separate base and salt forms, and visually distinguish pure samples from those adulterated with common cutting agents.^[88]

1.4.1.4 Pharmaceuticals

In addition to illicit drugs, recent studies have also investigated pharmaceutical products, particularly in regard to counterfeit medications. Researchers at the University of Lausanne have explored several approaches toward counterfeit identification and profiling. Roggo *et al.* employed Raman spectroscopy with support vector machine (SVM) models to distinguish between 25 therapeutic product families, and postulated that this methodology could potentially be applied to detect counterfeit substitutes.^[89] Been *et al.* then utilised NIR and Raman spectroscopy with pattern recognition to successfully distinguish six genuine batches of a pharmaceutical product from 27 counterfeit seizures.^[90]

Dégardin *et al.* combined the above approaches; using Raman spectroscopy with SVM models in a two-step method to detect counterfeit products and compare them against a known reference database.^[91] The resulting methodology successfully discriminated counterfeit seizures from genuine products, and identified several seizures of similar chemical profiles. An external validation set of generic brand medications was also recognised as being distinct from both the brand-name medications and existing counterfeit products.

More recent work by Custers *et al.* utilised ATR-FTIR spectroscopy to characterise brand-name, generic and counterfeit erectile dysfunction medications, with PCA enabling discrimination based on the active pharmaceutical ingredients.^[92] Although k-nearest neighbours classification and regression tree analysis were unsuccessful in classifying the majority of spectra, soft independent modelling of class analogy (SIMCA) provided 100 % discrimination of counterfeit tablets from both genuine and generic brand products.

1.4.2 Document analysis

Despite the increasing trend toward electronic communication and transactions, physical documents are still widely used in financial, legal and personal matters.^[93] An array of research has hence examined the application of chemometrics to various aspects of forensic document analysis.

1.4.2.1 Paper

Kher *et al.* utilised infrared spectroscopy techniques with pattern recognition tools to distinguish between 14 white or yellow paper substrates.^[94] PCA of spectra collected using ATR-FTIR spectroscopy was able to distinguish almost 68 % of possible pairings, while the analysis of diffuse reflectance infrared Fourier transform spectra gave 100 % discrimination using cross-validation. An approach by Sarkar *et al.* employed statistical correlation measures and *t*-testing with laser-induced breakdown spectroscopy (LIBS) to match 10 unknown paper substrates with a known database.^[95] 100 % correct identification was achieved; although as these substrates were all acquired from a single source, the applicability of the method to a wider range of substrates is not yet established.

1.4.2.2 Writing inks

In addition to paper, several studies have been conducted regarding the characterisation of writing inks. The majority of these articles have focussed on blue ballpoint pens; one of the most widespread types of writing instrument. The successful discrimination and classification of blue ballpoint inks using secondary ion or ICP mass spectrometry,^[96,97] vibrational spectroscopy,^[98-102] chromatographic methods,^[99, 103, 104] ultraviolet-visible (UV-Vis) spectroscopy,^[105, 106] and image processing^[107] have been described in the open literature.

Of particular interest, Denman *et al.* conducted surface analysis of ballpoint inks on paper using time-of-flight secondary ion MS, providing *in situ* analysis of both organic and inorganic components with no interference from the underlying substrate.^[97] This was able to discriminate 41 out of 45 pairs of inks (sourced from seven different pen models), and in one case was able to distinguish between separate batches of the same pen. Braz *et al.* employed Raman spectroscopy for the non-destructive, *in situ* analysis of over 300 pens, representing 38 pen models sourced from 12 known brands.^[101] This was successful in distinguishing between inks of different brands, models or batches, as well as identifying the main colourants present. Later work used Raman mapping with multivariate curve resolution to generate images of pen ink crossings, resulting in the correct sequence of ink application being identified in over 60 % of cases.^[102]

A smaller volume of research has also been published on the characterisation of black writing inks. da Silva *et al.* employed PLS-DA to distinguish 55 inks of six different types based on their visible spectra, and demonstrated the applicability of this method in a casework scenario to identify the pen type, brand and model used on several pages of a questioned document.^[108] Work by Adam *et al.* used UV-Vis spectroscopy and PCA to distinguish 25 black ballpoint inks,^[109] and later analysed a subset of these pens in pairwise comparisons by luminescence spectroscopy, resulting in 60 % of handwritten samples being successfully discriminated.^[110] Silva *et al.* employed NIR hyperspectral imaging to identify alternations made to documents by the obliteration or adding of text.^[111] This methodology was able to identify 82 % of added text forgeries, and 85 % of instances in which crossed lines were deposited using different inks.

1.4.3 Explosives and related materials

Explosive events have become of increasing concern over recent decades, with a large number of high-profile incidents resulting in mass civilian casualties. Chemometrics can provide a rapid means of assessing the large volumes of data generated from an explosives investigation, as well as distinguishing key signatures of various explosive materials.

1.4.3.1 Low explosives and propellants

In a series of three articles, Bueno *et al.* described the identification and discrimination of gunshot residues (GSR) using a combination of Raman and FTIR data.^[112-114] The first of these employed NIR Raman microspectroscopy to differentiate GSR particles originating from different calibre ammunition.^[112] Differentiation algorithms based on SVM and PLS-DA resulted in 9 mm and 0.38 calibre residues being successfully distinguished with only one misclassified spectrum. In the second paper, Raman and FTIR data were combined into a single dataset to improve statistical discrimination, yielding increased sensitivity and specificity compared to the original method.^[113] Finally, automated Raman microspectroscopic mapping was used as a novel approach for GSR detection on adhesive tape.^[114] Validation tests resulted in true positive rates of 85 % for organic residues and 90.4 % of inorganic residues, and a size detection limit of 3.4 μm was proposed.

Ceto *et al.* demonstrated a system for the identification of subjects involved in firearm-related incidents based on electroanalysis with chemometric data treatment. This approach was successfully able to distinguish subjects with no GSR exposure, secondary exposure, and exposure related to the loading and firing of ammunition. Steffen, using energy dispersive X-ray (EDX) and ICP-MS, was able to separate 15 primers from different ammunition brands based on their elemental and isotopic composition. Fernandez de la Ossa *et al.* took a broader approach, using NIR hyperspectral imaging with PLS-DA to successfully distinguish black powder, smokeless powders, nitrocellulose and ammonium nitrate residues in handprints.^[115] This holds potential as a non-invasive technique for explosives security screening, although limits of detection and the potential impact of skin contaminants are still under investigation.

1.4.3.2 High explosives

Several authors have examined the analysis of explosives using chemometrics in combination with laser-induced spectroscopy or emission techniques;^[116-122] electrochemical analysis;^[123-125] vibrational spectroscopy;^[126-128] ion mobility spectrometry;^[129, 130] or isotope ratio mass spectrometry.^[131]

Gottfried *et al.* demonstrated the detection of cyclotrimethylene trinitramine (RDX) and non-explosive residues on various surfaces using LIBS and PLS-DA.^[119] Models were constructed for each substrate based on nine peak intensities and 20 peak ratios, acquired from a 25 m distance. A detection rate of at least 90 % was achieved on all surfaces, though non-explosive residues on wood or travertine gave false positive rates exceeding 10 %. A combined model incorporating all substrates gave a true positive rate of 88.6 % and false positive rate of 12.7 %, with almost all false positives originating from wood, travertine or cardboard. Despite the issues encountered with these surfaces, the ability of LIBS to acquire spectra from a distance of several metres makes this a highly promising method for the remote detection of explosives.

Ceto *et al.* described the simultaneous determination of five nitro-containing explosive compounds using cyclic voltammetry.^[123] Voltammetric responses were pre-processed using discrete wavelet transform and the resulting coefficients analysed by PCA, distinguishing the pure components from five commercial mixtures. An artificial neural network was constructed to individually quantify RDX, trinitrotoluene (TNT) and pentaerythritol tetranitrate (PETN) in each mixture, yielding highly accurate estimates for both the training and validation sets. It was suggested that this methodology could be expanded to peroxide explosives such as triacetone triperoxide (TATP) that may prove challenging to analyse using traditional detection techniques.

Buxton and Harrington examined the use of ion mobility spectrometry with multivariate mixture analysis to distinguish PETN and cyclotetramethylene tetranitrate (HMX) residues from potential interferents encountered during airport baggage screening.^[129] Modification of the instrument to allow temperature programming yielded greater sensitivity and selectivity in comparison to standard thermal desorption; however, the analysis time was increased from 5 to 20 seconds. This could potentially be problematic during peak periods when the throughput demanded for luggage screening is extremely high.

1.4.3.3 Adhesive tapes

In addition to post-blast residues, valuable information may be obtained from other components of an explosive device such as tape wrappings. Goodpaster *et al.* employed PCA and discriminant analysis (DA) to characterise 67 electrical tape rolls from the reference collection of the Bureau of Alcohol, Tobacco, Firearms and Explosives (ATF), according to their surface texture and elemental composition.^[132] 36 classes were identified within the dataset, to which samples could be assigned with up to 94 % accuracy. A subsequent study employed FTIR spectroscopy and DA to classify 72 tape rolls to their nominal brand based on spectra acquired from the tape backing and adhesive, with accuracy rates of up to 99 %.^[133] This model was additionally utilised to correctly associate two fragments of blast-damaged tape from a detonated pipe bomb to their respective brands of origin.

1.4.4 Fire debris

Each year, deliberately lit fires cause significant damage to people, property and the environment. Various studies have thus explored the use of chemometrics to extract key information from fire debris analysis, as reviewed by Martín-Alberca *et al.*^[134] Of particular interest, Sinkov *et al.* applied PLS-DA and SIMCA classification to the GC-MS data acquired from 220 casework arson samples.^[135] Chromatograms were first aligned based on a spiked ladder of perdeuterated n-alkanes, with variable selection and model optimisation performed using a lab-written program. This resulted in all 55 validation samples being correctly assigned as either gasoline-containing or gasoline-free, although no determination could be made regarding the type of gasoline used or any other classes of accelerant present.

Research by Bodle and Hardy employed solid phase microextraction (SPME)-GC and SIMCA to distinguish five classes of accelerants, with a cross-validation accuracy of 97.2 %.^[136] Waddell similarly utilised several multivariate methods to distinguish ignitable liquid classes based upon their GC-MS total ion spectra. An initial approach using quadratic DA resulted in a 70.9 % validation accuracy based on samples produced in laboratory and field-test burns.^[137] A subsequent article evaluated SIMCA as an alternative classification scheme compared to inspection by an examiner. It was found that whilst the examiner achieved a 90.5 % classification accuracy compared to 79.1 % using SIMCA, the false positive rate also increased from 8.9 % to 15.0 %.^[138]

Chemometric methods have also been used to discriminate accelerants within a class according to their refining process, brand or other distinguishing features.^[139-145] Monfreda and Gregori for example were able to separate 50 unevaporated gasoline samples of five brands based on GC-MS determination of their aromatic compound content.^[143] For two brands, it was additionally possible to link the chemical characteristics of samples to the crude oil employed. Balabin *et al.* were also successful in separating classes of liquid gasoline according to their refining site, refinery stream or octane rating using NIR spectroscopy and nine multivariate classifiers.^[139]

A limitation when establishing chemometric classifiers for arson investigations is the potential impact of sample weathering or degradation. Additionally, the analysis of 'neat' samples does not take into account the various matrix interferences found in casework samples. Baernkopf *et al.* thus developed a methodology to associate post-burn ignitable liquid residues to the corresponding neat liquid, with discrimination from matrix interferences.^[146] Six ignitable liquids were burned on carpet, extracted using passive headspace extraction and analysed by GC-MS. PCA resulted in the six liquids being discriminated based upon their alkane and aromatic content, while Pearson product moment correlation coefficients were able to correctly associate all residues to their neat liquid equivalent.

Turner and Goodpaster subjected simulated samples containing gasoline to weathering and microbial degradation in soils prior to analysis by GC-MS and PCA.^[147] Volatile components were found to be susceptible to weathering, while mono-substituted aromatics or long-chain alkanes were most affected by microbial action. Highly substituted aromatics were found to be most resistant to weathering or degradation, and hence these compounds can be suggested as ideal targets for analysis.

1.4.5 Paint

Paint coatings are applied to many manufactured articles in order to protect or aesthetically improve the item's surface. Subsequently, paint chips and smears are commonly encountered as forensic transfer evidence, and their analysis may prove essential in obtaining investigative leads.

1.4.5.1 Architectural paint

Muehlethaler *et al.* analysed 34 red household paint samples using both FTIR and Raman spectroscopy combined with unsupervised chemometric analysis.^[148] PCA of the FTIR data was able to distinguish samples based on their binder type (alkyd or acrylic resin) and presence or absence of calcium carbonate, whilst Raman spectroscopy differentiated samples according to their pigment composition. The same authors later applied FTIR with supervised and unsupervised methods to analyse 74 red, green and blue spray paints.^[149] Iterative PCA was able to discriminate over 90 % of samples in each category upon inspection of the scores plot, and SIMCA models gave an approximately 95 % classification accuracy of a separate validation set.

Chemometric methods have also proved a valuable tool in the analysis of paints used in artworks.^[150-153] Of particular interest, Rosi *et al.* combined PCA with reflection micro IR spectroscopy to map cross-sectioned paint from simulated ancient easel paintings. This methodology permitted characterisation of the layer sequence according to the inorganic pigments and organic binders present in each layer. Although these studies were originally conducted from an art provenance and conservation standpoint, the established methodology could potentially be applied to the forensic investigation of art forgery.

1.4.5.2 Automotive paint

Liszewski *et al.* and Mendlein *et al.* were able to identify broad classes of automotive clear coats based on their UV microspectrophotometry (MSP) or micro Raman spectra, although these could not be correlated to the make, model or manufacturing year of the source vehicles.^[154, 155] Later studies by Maric *et al.* employed FTIR and Raman spectroscopy with pattern recognition to discriminate the clear coat or primer surfacer layers from a range of Australian and international vehicles.^[156-158] This ultimately revealed 19 classes related to the vehicles' manufacturer, model and in some instances specific year ranges or manufacturing plants. Further work established that the presence of post-manufacture coatings or long-term environmental exposure could cause erroneous identifications when relying solely on analysis of the upper clear coat, though these samples could be identified as atypical.^[159, 160] Nevertheless, it was suggested that the full paint layer sequence be collected where possible, as analysis of the lower clear coat or underlying layers could still provide reliable information.

Several studies by Lavine *et al.* investigated the use of genetic algorithms to match automotive clear coats against the IR spectral library of the Paint Data Query database.^[161-166] Successful discrimination was made between 2000 – 2006 model Chrysler and General Motor vehicles according to their assembly plant, allowing identification of the model, line or manufacturing year of the source vehicles. However, as the samples utilised in this study originated solely from North American manufacturing plants, the methodology currently has limited applicability within an international context.

1.4.6 Hairs and fibres

Two of the most frequently encountered forms of evidence in forensic investigations are hairs and fibres. The wide range of potential colours or morphologies can make these forms of evidence highly discriminating, and thus of high forensic interest.

Barrett *et al.* investigated the discrimination of red-dyed hair samples based upon their UV-Vis MSP absorbance spectra.^[167] Hierarchical cluster analysis identified three clusters of samples that were visually consistent with different shades of red. PCA identified the same groupings, and inspection of the loadings plot suggested that this separation was based on differences in the intensity of absorbance peaks related to both the hair and the dye. Discriminant analysis yielded an 89.1 % classification accuracy based on cross-validation, and 75 % using an external validation set. Additionally, it was found that successive washing of the hair samples led to a significant loss of dye colour within three weeks of application, which could lead to incorrect classifications.

Chemometric methods have also been applied in several studies to discriminate textile fibres.^[168-176] Causin *et al.* utilised pyrolysis GC-MS with PCA to differentiate colourless polyacrylonitrile-based fibres of similar morphological features.^[168] The sample set comprised 36 fibres acquired from 11 manufacturers, with fibres from certain manufacturers differing by batch, manufacturing plant, or intended end-use. Fibres from one manufacturer were able to be uniquely identified based on the presence of methyl methacrylate as a co-monomer. The remaining samples were divided into two clusters according to the presence or absence of vinyl acetate, although no further separation according to any categorical factors was achieved.

Morgan *et al.* applied PCA and LDA to analyse a database of over 5,000 MSP spectra acquired from approximately 500 dyed textile fibres.^[175] Both UV-Vis absorbance and fluorescence spectra were found to provide discriminating information, depending on the fibre set under analysis. In general, however, UV-Vis spectroscopy was determined to be the best single discriminating technique, allowing 78.9 % of fibres to be differentiated. It should be noted that in this study, all fibres of a particular colour were compared simultaneously, whereas casework scenarios more commonly utilise pairwise comparisons between a recovered fibre and one from a known source. It is thus possible that pairwise comparisons of this sample set would have led to improved discrimination between similar fibres.

1.4.7 Soils

Soil particulates may yield probative information in both criminal and environmental forensic investigations. There have hence been a number of studies applying chemometrics to discriminate or classify soils of different origins.^[177-183] Thanasoulis *et al.* were able to distinguish soils collected from five different sites due to differing relative concentrations of aromatic groups in their fulvic and humic acid fractions, with an 85.0 % classification accuracy.^[177] Dragović and Onjia described the classification of soils originating from 15 locations in Serbia and Montenegro, by applying PCA to radionuclide data collected by gamma-ray spectrometry.^[178] An overall 86.0 % correct classification was achieved, on par with results achieved by Thanasoulis *et al.*

Bonetti and Quarino were able to separate soil samples collected from 12 New Jersey state parks based on their particle size distribution, pH and organic content.^[182] Chemometric analysis was initially performed solely on the particle size data, with error rates then found to decrease with the inclusion of the remaining data. Final error rates of 33.3 % and 3.3 % were obtained for soils collected during the summer and fall seasons respectively, with the high error rate of the former attributed to the collection of samples at 15 metre intervals. This indicates a high level of heterogeneity even amongst soils within a relatively limited geographical area, which may prove challenging when establishing the provenance of a questioned soil sample.

1.4.8 Other transfer evidence

1.4.8.1 Impressions

As discussed previously, the NAS report recommended the “*raising of standards for scientific examination of all forms of physical evidence*”. This could be argued as especially important for disciplines such as impression evidence, which currently rely on direct visual comparisons between recovered (questioned) and known reference samples. Petraco *et al.* reported the use of chemometrics to evaluate the ‘uniqueness’ of shoe impressions related to accidental mark or wear patterns.^[184] Partial impressions left by five shoe pairs of the same brand and style, worn by a single person over 30-day periods were converted into feature vectors based on the number and location of any accidental marks. The vectors of 116 impressions were then subjected to PCA and discriminant analysis to assign each impression to the corresponding shoe pair, resulting in cross-validation accuracies of 77 % to 100 %.

A similar methodology was later applied to the statistical discrimination of toolmark impressions.^[29] An image processing program was used to convert the striation marks left by nine different screwdrivers into binary feature vectors, with PLS-DA and PCA-SVM then employed to match each screwdriver to its corresponding impression. The classification performances of each model were assessed through cross-, leave-one-out and bootstrap validation, yielding classification accuracies of 97 % or greater with both classifiers.

1.4.8.2 Biological materials

A number of recent studies have reported the use of chemometric methods for the detection, identification or discrimination of bodily fluids. Sikirzhytski *et al.* used confocal Raman microscopy with discriminant analysis to differentiate between blood, semen and saliva; while Sikirzhytskaya *et al.* applied NIR Raman spectroscopy to discriminate mixtures of semen and blood from their pure components.^[185, 186] Edelman demonstrated the capability of visible reflectance hyperspectral imaging with chemometric mixture analysis for the enhanced visualisation of blood stains on fabric.^[187] This method was found to be effective even for diluted blood stains on black material, provided that a minimal concentration of 25 % whole blood was present. Li *et al.* attempted to estimate the age of equine bloodstains (employed as an analogous material for human blood) based on their visible reflectance MSP spectra.^[188]

Initial results produced a correct classification rate exceeding 90 %; however, this was obtained using a single blood deposit for both training and test purposes, with only 10 replicate spectra making up each set. The correct classification rate fell to 54.7 % when using an external test set obtained from a second bloodstain.

Exploratory chemometric tools have also been utilised to investigate the composition of latent fingerprint deposits. Girod and Weyermann used GC-MS and cluster analysis to classify fingerprints from 25 donors into 'poor' or 'rich' lipid categories.^[189] Fingerprint replicates of selected donors were tested as a validation set, with 86 % being correctly classified. It was proposed that this model could be exploited for research purposes in order to select ideal donors for given compounds of interest. Frick *et al.* later employed PCA to examine the lipid composition of fingerprints collected from over 100 donors.^[190] Although variations between different donors were apparent, no correlation to specific donor traits could be discerned.

1.4.8.3 Glass

Zadora and Brozek-Mucha applied cluster analysis with scanning electron microscopy (SEM)-EDX to differentiate glass samples into use-type groups based on their elemental content.^[191] Employing a logarithmic transformation of selected element concentrations revealed three clusters consistent with the three glass types (car headlamp, car window or container) under examination, with only four objects lying outside of these clusters. A later study described the use of naïve Bayes classifiers and SVM models to separate glass samples originating from car or building windows and those from bulbs or headlamps.^[192] Classification accuracies of 90 % or greater were achieved across ten training and validation sets using both classification methods.

1.4.8.4 Cosmetics

An emerging area of interest in forensics is the examination of cosmetic products. Kulikov *et al.* employed wavelength-dispersive X-ray fluorescence spectrometry for the elemental analysis of 39 cosmetic powders.^[193] Cluster analysis and PCA were able to clearly discriminate between samples possessing traditional ingredient or mineral-based formulations, and also distinguish specific manufacturers of the latter. Salahioglu *et al.* later demonstrated the use of Raman spectroscopy to discriminate lipstick samples deposited on textile fibres, cigarette butts and paper tissues.^[194]

Thirty spectra each of ten different lipsticks were subjected to PCA and k-nearest neighbours classification, attaining accuracy rates up to 98.7 %.

1.4.9 Future directions and challenges

As evident from the literature, chemometric methods show great potential for assisting examiners in several fields of forensic science. However, there is a great deal of further work to be done before these methods can be routinely implemented in forensic laboratories. One such challenge lies in the appropriate evaluation of model performance. For studies in which the primary objective is to differentiate between classes of samples, model performance is typically assessed based on the percentage of samples correctly assigned to their expected class. However, high classification accuracies are not necessarily an indicator of good discrimination, as ‘correct’ assignments may arise purely by chance. If the sample size under consideration is relatively small, this may cause the overall classification accuracy to become greatly inflated, thus over-estimating the model’s capabilities.^[195, 196]

Similarly, the performance of regression models is frequently judged based on the correlation coefficient, r , with the assumption that a higher r implies better quality of the regression line. It is important to note that while this value indicates the strength of the linear relationship between two variables, it does not provide evidence of causality. If a sufficiently high number of variables are considered, there is a reasonable likelihood that some of these variables will be randomly correlated over a limited range. Consequently, the probability of spurious correlations increases as the number of measured variables approaches the number of samples analysed, again leading to false optimism regarding the model’s potential.^[196]

There is also a need to define what constitutes ‘good’ classification in chemometric models. This is particularly important for methods such as LDA in which samples are assigned on the basis of the ‘closest fit’, regardless of whether the sample in question is adequately described by the existing data. Previous studies have demonstrated that samples assigned to a given class through chemometric techniques may in fact be atypical, as revealed upon further inspection of the output data.^[156, 159, 160] Despite this, there is a tendency to accept the immediate results produced from chemometric analyses without critical evaluation as to their quality.

In addition, more thorough investigations are required concerning the factors that may affect chemometric models. ‘Real’ samples may be subject to ageing or weathering prior to their collection as evidence, thus affecting classifications by a model based on new samples produced under controlled conditions. Moreover, the amount of information that can be discerned using chemometrics is inherently limited by the quality of input data. This in turn may be dependent on the strategies utilised in the collection, preservation and chemical analysis of forensic exhibits. Experimental design techniques have the potential to optimise experimental procedures and thus identify ‘best protocols’ for evidence collection and handling. To date, these methods have remained largely unexplored within a forensic context.

Further work is thus required to probe the capabilities and limitations of chemometrics as applied to forensic disciplines. The research described in this dissertation takes steps in this direction with regards to the forensic analysis of three commonly encountered forms of physical evidence; textile fibres, pen inks and explosive residues.

1.5 Textile fibres

Textile fibres form the basic unit of yarns, fabrics and other textile materials. They may be defined as elongate structures with a length at least 100 times their diameter, which also exhibit physical characteristics amenable to textile manufacture such as flexibility, strength and durability.^[197-199] The use of fibres to create textile products can be traced back to at least the 6th or 7th century BC.^[200] In modern society, textiles account for a vast array of products such as clothing, carpets, linens, and upholstery. This prevalence has led textile fibres to be one of the most commonly encountered forms of forensic trace evidence during criminal investigations.

The forensic significance of fibres lies in their high tendency to shed and be transferred through physical contact.^[201, 202] Furthermore, textile fibres can exhibit a vast array of physical and chemical characteristics, many of which are selected or designed for use in particular end products.^[10, 203, 204] In addition to features inherent to the fibre itself, many textiles are further modified through the use of colourants and other additives. These may include delustrants (usually titanium dioxide) to reduce sheen and improve opacity, chemical treatments to adjust properties such as wetting and adhesion, or anti-static conductors.^[203, 205, 206] Variations in these distinguishing features can greatly enhance the significance attached to a positive fibre association.

1.5.1 Classes of textile fibres

Textile fibres are most commonly classified according to their origin as either natural or manufactured.^[198, 207] Natural fibres are derived wholly from plant, animal or mineral sources, and exist naturally in their fibrous state. As shown in Figure 1.5, plant fibres can be more specifically defined as originating from bast (stem), leaves, seeds or fruit; whereas animal fibres may be obtained from wool, hair or secretory glands.^[208] Manufactured fibres are those which are artificially created through spinning and/or extrusion processes, and may be further classified as either derived or synthetic. Derived fibres such as rayon are regenerated from natural sources such as cellulose (polymeric) or glass (non-polymeric), whilst synthetic fibres such as polyester are produced solely from synthetic chemical pre-cursors.^[10, 204]

Fibres may also be discussed in terms of their length.^[207, 208] Most natural fibres, with the exception of silk, have a finite length and are thus considered staple fibres. Those with a continuous or near-continuous length, such as silk and manufactured fibres, are instead referred to as filaments. These can be cut into discrete lengths to form manufactured staples. Alternatively, fibres may be categorised based upon their chemical composition as cellulosic (plant derived), protein (animal derived), polymeric (plant derived and synthetic) or inorganic (mineral, glass or metallic).^[209]

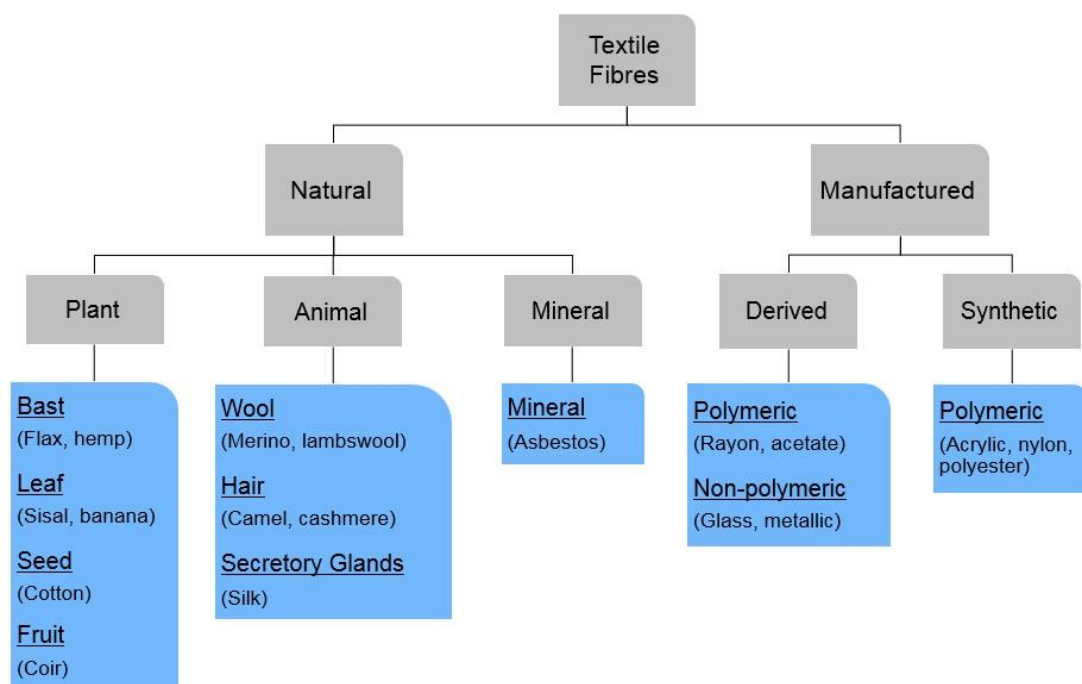


Figure 1.5: Classification of textile fibres according to source.

1.5.2 Forensic analysis of textile fibres

Forensic fibre examiners typically employ several analytical techniques in sequence to characterise various features of the sample. As per guidelines published by the American Society for Testing and Materials (ASTM) International and the Scientific Working Group for Materials Analysis (SWGMA), this begins with microscopic examination, followed by spectroscopic or chromatographic methods to provide more specific information as required.^[210-212]

1.5.2.1 Microscopy

Initial inspection of fibres begins with visual examination assisted by optical or compound microscopy, in order to observe physical characteristics such as colour, diameter, or cross-sectional shape.^[213-215] This allows many fibres to be easily and rapidly distinguished, narrowing the range of fibres required to undergo further examination. Polarised light microscopy may then be used to determine the birefringence, refractive index and dichroism of a sample.^[204, 216] This is often utilised for synthetic fibres to determine their generic polymer class, and may also provide information regarding the production or finishing of the fibre.^[209, 217] Fluorescence microscopy can also be employed to distinguish particular dyes or dye combinations based on their fluorescent behaviour,^[216, 218] while SEM may be utilised to study the fibre's surface morphology or finishing agents.^[215, 219]

1.5.2.2 Colourant analysis

As discussed above, the colour of a given fibre can be a highly discriminating characteristic. Although some colours can be distinguished visually, these assessments are subjective and may be affected by metamerism or the examiner's colour vision.^[220, 221] More objective measurements can be obtained using instrumental methods such as MSP, which provides rapid results while leaving the fibre intact.^[220, 221] Analysis may also be carried out on the dyes themselves using thin layer chromatography (TLC) or high performance liquid chromatography (HPLC).^[215, 222, 223] While chromatographic methods allow the structure of the dye to be determined, these techniques require extraction of the dye and are therefore destructive of the sample.

1.5.2.3 Infrared and Raman spectroscopy

Vibrational spectroscopy methods are highly valuable as rapid, non-destructive techniques that allow structural information to be derived from a sample without the need for extensive sample preparation. IR spectroscopy has long been recognised as a useful method for not only identifying dye components, but also identifying the polymeric composition of the fibre itself, thus allowing its generic class or sub-class to be determined.^[224-226] IR also has the added benefit of requiring minimal sample preparation, providing high signal-to-noise ratios and requiring only small sample sizes.^[220] For this reason, IR spectroscopy is frequently employed in forensic laboratories for discriminating between optically similar fibres, or as a confirmatory technique to microscopic examinations.^[220, 227]

Modern advances in Raman instrumentation have renewed interest in the potential application of Raman spectroscopy to fibre analysis. Several recent studies have highlighted the ability of Raman spectroscopy to identify or distinguish between dyes and/or pigments in coloured textile fibres.^[228-232] In addition, the complementary nature of Raman and IR spectroscopy may allow an even greater level of discrimination to be achieved between otherwise indistinguishable samples.^[233, 234] Nonetheless, issues remain in regards to the potential fluorescence masking of spectra, as well as a lack of sensitivity to minor dye components.^[216, 217, 235] As a result, Raman spectroscopy has not yet gained widespread use for fibre examination amongst practicing forensic personnel.

1.6 Writing inks

Ink can be considered as any liquid or semi-liquid material intended for the purposes of writing, printing or drawing. The history of ink dates back to ancient times, with the process of ink production known in China as early as the 3rd millennium BC.^[236] These early inks consisted of a solid carbon-glue cake ground and suspended in water, stabilised with a binding agent such as shellac or natural gums.^[237-239] This basic formulation is still employed today in the form of India inks, which are highly popular as a drawing ink due to their high colour stability and water resistance.^[237] Most modern ink formulations however are considerably more complex, having evolved to meet specific requirements such as a high colour strength and vibrancy, rapid drying time and consistencies amenable to different writing instruments.^[238, 240]

Most contemporary inks consist of several dyes or pigments carried in a solvent such as water, oil, alcohols or glycols.^[239, 241] They may also contain a variety of additives collectively referred to as the ‘vehicle’. These can include fatty acids and softeners to adjust the flow and consistency characteristics; polymeric resins to improve drying; biocides to prevent microbial growth; metallic and inorganic pigments to impart novel aesthetic effects; and pH modifiers to prevent corrosion to any metal pen components.^[238, 240, 241] This complexity, while potentially making inks a challenging material to analyse, also makes them good candidates for discrimination based on their different (and often proprietary) formulations.

1.6.1 Classes of writing ink

Writing inks can be broadly classified as either ballpoint or non-ballpoint formulations. The writing mechanisms for these inks vary, and as a result each requires specific ink properties in order to ensure the proper flow of ink onto a substrate.^[240] Ballpoint pens have a small steel ball valve at their tip that is able to freely rotate while writing, thus collecting ink from the cartridge reservoir and transferring it to the paper surface. Consequently, ballpoint inks typically employ dyes as the colourant, as pigments could result in clogging of the narrow ball tip. These dyes may constitute up to 50 % of the total ink formulation, and are generally contained in an organic solvent based on glycols or benzyl alcohol.^[242, 243] This imparts greater water resistance and also increases viscosity, providing better control over the ink flow.

Non-ballpoint inks include fountain, felt tip, roller ball and gel inks; the components of which vary according to the specific ink type and production period. Early fountain pens used iron gall inks produced from iron salts and tannic acids, which were later replaced with aqueous solutions of synthetic dyes.^[237] Although brighter and more attractive in colour, these dyes possessed poor water resistance and were prone to fading over time. Modern fountain inks thus contain pigmented dyes such as copper phthalocyanine, which exhibits superior permanence.^[244] Felt tip and roller ball inks are usually water or xylene based; the latter being water resistant; with the addition of formamide or glycols to prevent drying of the pen tip.^[245] These inks often contain metallised dyes for increased light-fastness.^[246] Gel inks are a relatively recent development, consisting of insoluble pigments suspended in a water-based gel.^[239]

These inks have a similar appearance to ballpoint inks but are insoluble in both water and strong organic solvents, making them particularly challenging to analyse.^[247]

1.6.2 Forensic analysis of writing ink

The forensic examination of inks follows a similar framework to fibres, with general guidelines published by the American Society for Testing and Materials (ASTM) International and the Scientific Working Group for Document Examination (SWGDOC) outlining a range of analytical methods amenable to ink analysis.^[248, 249]

1.6.2.1 Visual examinations

As with fibres, ink formulations often contain unique combinations of dyes and pigments, making colour a highly discriminating characteristic. Consequently, the inspection of inks begins with the determination of ink colour using microscopic examinations followed by UV-vis methods, which can provide excellent discriminatory power between visually similar samples.^[250-253] Alternative light sources such as ultraviolet or infrared illumination may then be used to reveal any luminescence characteristics of the ink. Visual examination can also identify the type of ink present based on morphological characteristics. For example, fluid inks such as fountain, roller ball or felt tip will absorb into the paper, and may bleed into the surrounding paper upon extended contact with the pen tip.^[240] Ballpoint inks by contrast are non-absorbent, merely resting on top of the paper surface, but may exhibit defects such as ‘gooping’ (excess ink deposition), skips or striations within the ink stroke (Figure 1.6).^[237]

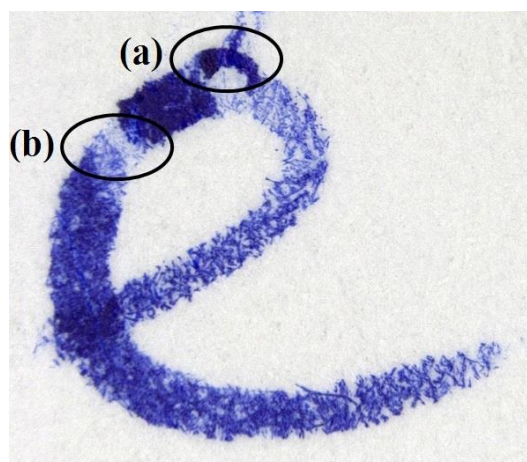


Figure 1.6: Microscopic image of an ink line on paper showing defects characteristic of a ballpoint writing implement; (a) excess ink deposition and (b) skipping of the ink line.

1.6.2.2 Infrared and Raman spectroscopy

Vibrational spectroscopy can be used to characterise not only the dyes of an ink sample, but also additives such as solvents or resins. Consequently, these methods can provide highly specific information regarding the overall ink composition. Numerous studies have illustrated the capability of Raman spectroscopy to distinguish the key organic dyes, pigments or additives present in different inks; in some instances also allowing the deposition sequence of crossed ink lines to be determined.^[101, 254-257] The primary drawbacks to this technique are its low sensitivity to components with weak Raman scattering, and fluorescence masking caused by certain ink dyes or paper substrates.^[101, 254] In these instances, IR spectroscopy is an ideal complementary method, as weak bands in the Raman spectrum often correspond to strong bands in the IR region and vice versa. IR has similarly been shown to have high discriminating power for similar ink samples based on their main components, including the determination of crossed ink lines.^[242, 250, 258, 259]

1.6.2.3 Chromatographic methods

Chromatographic techniques such as GC and TLC may be used to separate and identify individual ink components. TLC is widely used as it is relatively inexpensive, simple to perform and the results can be easily interpreted or compared to an existing database.^[260-263] GC is also commonly employed to compare organic, volatile components such as resins or solvents. Unlike TLC, the use of reference databases has limited utility in the GC analysis of inks due to the gradual loss of these volatile components following deposition of the ink on paper, thus altering its chemical profile.

On the other hand, this also makes GC an ideal method for monitoring changes in the volatiles content over time, and thus developing dating curves for the age estimation of inks. Several examples of such dating curves can be found in the literature.^[264-267]

1.7 Explosives

An explosion can be defined as a sudden conversion of potential energy into kinetic energy, resulting in violent physical disruption of the surrounding environment.^[268-270] Although these events can result from natural phenomena, they are more commonly the result of chemical explosives; compounds or mixtures consisting of a fuel and an oxidant that react to produce a large volume of gaseous products.^[271, 272]

The earliest chemical explosive was black gunpowder; a mixture of sulfur, charcoal, and potassium nitrate thought to have been developed in China during the 9th century.^[273] This remained the only known explosive until the discovery of nitrated alternatives such as nitrocellulose (guncotton) and nitroglycerin in the 19th century.^[274] Today, the ATF lists over 230 explosive materials and mixtures subject to federal monitoring and regulation in the United States.^[275]

In recent decades, explosive events have become an increasingly common occurrence both in large-scale incidents (i.e. terrorist activity) and also smaller ‘volume crimes’ such as theft or vandalism.^[276-278] Over the five-year period between January 2008 and December 2013, over 1600 bombing events were reported in Australia, and nearly 6700 in the United States.^[279, 280] As a result, the development of new and improved methods for the analysis of explosive residues remains a key area of forensic interest.

1.7.1 Classes of explosives

Explosive materials are generally classified as ‘low’ or ‘high’ explosives. In low explosives such as gunpowders, the oxidant (often atmospheric oxygen) is separate from the fuel, causing the reaction to be limited by the rate at which oxygen can be supplied to sustain the reaction.^[209, 281] These explosives will deflagrate (rapidly burn) with velocities up to 1,000 ms⁻¹, but do not generally explode unless restricted within a confined volume.^[241, 273, 282] High explosives by contrast incorporate fuel and oxidant moieties into a single molecule, allowing instant detonation with an extremely rapid blast velocity.^[204, 209] This produces a supersonic shock wave that causes shattering or shearing of objects within the blast radius.

High explosives may be further classified into primary or secondary charges based upon their sensitivity. Primary high explosives are relatively sensitive to detonation by shock, friction or other stimuli, and are typically used as primers for more stable explosives.^[271, 273, 282] Secondary explosives generally do not detonate until subjected to the pressure wave caused by a primary charge, and are thus used for military or commercial purposes requiring controlled detonation.^[272, 283, 284] These explosives are especially challenging from a forensic viewpoint, as they leave minimal traces for analysis.^[285]

1.7.2 Forensic analysis of explosives

In explosive events, much of the potential physical evidence at the scene may be destroyed or compromised by the explosive blast. The analysis of residues found at the scene may hence be vital in procuring investigative leads. The Technical Working Group for Fire and Explosions (TWGFEX) guidelines set out a number of analytical techniques for the identification of explosive residues as described below.^[286, 287]

1.7.2.1 Microscopy and microchemical testing

Initial analysis of explosives begins with a microscopic examination to determine physical particle characteristics that may be indicative of a particular explosive.^[10, 269] This is followed by microchemical testing, in which a small amount of sample is mixed with a reagent solution to produce a colour change or the formation of distinctive microcrystals.^[288, 289] Where bulk amounts of sample are present, testing may also involve the observation of burning characteristics such as odour or flame colour.^[269] It should be noted that these tests are strictly presumptive, and require confirmatory identification utilising an alternative analytical method.

1.7.2.2 Separation methods

Gas chromatography is one of the most frequently utilised methods for the separation and identification of organic explosive residues.^[290-293] Several studies have shown GC to be a highly sensitive analysis method for explosives such as TNT, TATP, RDX and HMX.^[294-296] A major drawback, however, is the limited capacity of GC for analysing thermally labile or non-volatile compounds such as emulsion explosives.^[297, 298] In these cases, liquid chromatography may instead be an ideal alternative.^[297, 299-302]

Ion chromatography (IC) was, until recently, considered as the best technique for inorganic explosives analysis due to its robustness, reliability, high sensitivity and selectivity.^[303-305] IC has proven to be readily applicable to improvised or emulsion explosives, and coupled IC systems have been shown to allow simultaneous separations of anionic and cationic species from a single sample.^[306-308] Recent years have also seen an increased interest in capillary electrophoresis (CE) as an alternative for inorganic analyses due to its simplicity and lower operating costs.^[309-311] The different ion selectivity provided by CE makes it useful as a complementary technique to ion chromatography, while retaining a comparable level of sensitivity.^[307, 312]

1.7.2.3 Infrared and Raman spectroscopy

Multiple studies have utilised various forms of IR or Raman spectroscopy for explosives analysis, as reviewed by McNesby.^[313] IR is an ideal method as it is non-destructive, applicable to both organic and inorganic analytes, and provides more comprehensive structural information than chromatographic methods.^[285, 314] A series of studies by Banas and co-workers employed FTIR spectroscopy to detect and distinguish multiple high explosives in residues collected from various sample surfaces.^[127, 315, 316] Primera-Pedrozo *et al.* were furthermore able to detect, distinguish and quantify several organic explosives utilising reflection/absorbance infrared spectroscopy.^[317, 318] IR spectroscopy is also attractive due to its ability to characterise non-explosive constituents of explosive formulations, such as stabilisers, plasticisers or contaminants.^[314] This may be useful in distinguishing different brands of commercially produced explosives, or in discriminating plastic or polymer-bonded explosives from their explosive components in pure form.

Various modes of Raman spectroscopy have been used to detect explosives traces from clothing or fingerprint residues, as well as providing stand-off detection of residues where physical contact of the sample with the instrument is either not possible or undesirable.^[319-322] Recent investigations by Bueno and co-workers have also utilised NIR Raman spectroscopy in conjunction with multivariate statistics for the differentiation or distribution mapping gunshot residue particles.^[112-114] These findings may warrant additional investigation into the capabilities of Raman spectroscopy applied to explosives investigations.

1.8 Aims and overview

Despite a large volume of research concerning the application of chemometric tools to forensic examinations, the full capabilities of these techniques are largely underutilised. The primary aim of this dissertation is to employ chemometric techniques to not only develop more reliable and objective comparison protocols, but also identify scientifically rigorous procedures for the collection and handling of forensic evidence. This thesis focuses specifically on the analysis of textile fibres, writing inks and explosive residues; however, the methodologies developed throughout this research are universal and may be applied to other forms of forensic physical evidence.

This dissertation comprises three main streams of investigation. The first of these, described in Chapter 2, examines the use of MSP with chemometrics to improve the confidence of "questioned versus known" fibre comparisons. Previous studies to date have focussed on the discrimination of several classes of fibres simultaneously, rather than the pairwise comparisons more typical of forensic casework scenarios. This work also employed Fischer's Exact Test as a quantitative statistical means of determining the similarity or dissimilarity of questioned versus known pairs.

Chapter 3 utilises conventional diffuse reflectance visible spectroscopy with PCA and LDA to characterise a large population of blue ballpoint inks. This chapter additionally describes investigations into the ageing of inks under office conditions over a 14 month period, and how the resulting compositional changes may affect the generated classification model. Further work in Chapter 4 focuses on the re-characterisation of the ink set using a video spectral comparator (VSC); an instrument routinely used by forensic document examiners, thus allowing the methodology to be more readily applied within an operational context.

Chapter 5 examines the use of chemometric experimental design, in the form of a central composite design, to develop statistically optimised sampling and storage protocols for the recovery of smokeless gunpowder residues. To date, such studies have been limited to the optimisation of instrumental parameters for explosives analysis. The use of experimental design to evaluate evidence collection or handling procedures remains yet to be explored explored.

Chapter 2: Improving the confidence of “questioned versus known” fibre comparisons using microspectrophotometry and chemometrics

Portions of this research have been submitted for publication in the journal *Forensic Chemistry*:

G. Sauzier, E. Reichard, W. van Bronswijk, S.W. Lewis and J.V. Goodpaster. *Chemometrics as a means of improving the confidence of “questioned versus known” fiber comparisons using microspectrophotometry*. *Forensic Chemistry*, 2016 (accepted).

2.1 Introduction

Textiles are encountered in a wide range of everyday products, and so are one of the most common forms of trace evidence encountered during forensic investigations. Fibres may provide invaluable associative evidence due to their high tendency to shed and be transferred through physical contact.^[202, 209, 323] In addition, certain classes of fibres may prove highly distinctive based on their morphology, composition or colour. The latter is a particularly discriminating feature due to the millions of shades that may be applied to textiles. More than 7,000 textile dyes and pigments are currently produced worldwide, and manufacturers will typically use combinations of these to impart specific colours to their products.^[209, 324] Furthermore, textile dyeing processes are generally carried out in batches, which may exhibit minor variations in dye form, shade or strength.^[207]

Colour and colourant analysis thus form a major aspect of forensic fibre examination. Although many colours can be distinguished visually, these examinations are subjective and may be affected by metamerism or the examiner's colour vision.^[220, 221] More objective measurements can be obtained using instrumental methods such as microspectrophotometry (MSP), which is favoured as a rapid and non-destructive method for characterising the colour of dyed fibres.^[217, 325] Various studies have shown the capability of MSP to distinguish visually similar coloured fibres based on different chromophores in the molecular structure of their dyes.^[326-330] In recent years, the use of Raman spectroscopy has also become a subject of increasing interest, with several studies highlighting its ability to rapidly identify dyes and/or pigments at concentrations as low as 0.005 % w/w.^[228, 230, 232, 331-333] Raman spectroscopy can be utilised as a confirmatory method to MSP, and may provide additional information regarding minor dye components not readily evident from MSP spectra.^[229, 231]

The majority of casework fibre examinations involve the comparison of questioned samples recovered from a crime scene and a reference material taken from a known source. Such "questioned versus known" (Q vs. K) comparisons are conducted by analysing the two samples in parallel to determine their physical and chemical characteristics.^[10, 334] It is generally assumed that if the questioned and known samples share a common origin, they will exhibit 'indistinguishable' properties.^[215]

In reality, this depends on the capability of the analytical method to detect and resolve features of interest. MSP spectra for example rarely provide a perfect ‘match’, even where these spectra originate from the same fibre. ‘Indistinguishable’ thus encompasses an acceptable range of variation between spectra of the questioned and known samples. Guidelines published by the Scientific Working Group for Materials Analysis (SWGMA) dictate that a spectral *inclusion* can be made if the questioned spectrum lies within the range of the known spectra in terms of the curve shape and absorbance values.^[335] In this case, the samples are considered to potentially originate from the same source. Conversely, if the questioned spectrum falls outside of the range produced by the known spectra, they can be *excluded* as sharing a common source.^[335]

Traditionally, the decision of whether the questioned spectra fall within range of the known has relied upon an examiner’s judgement, leading to concerns regarding human error or bias.^[6] Substantial research in recent decades has hence examined the use of chemometrics as a more objective means of comparison.^[168, 171-173, 176] Liu for example employed Raman spectroscopy with pattern recognition to distinguish cotton cellulose fibres based upon their colour, crystalline fraction and strength.^[336] Morgan *et al.* described several inter-laboratory studies employing chemometrics with UV-visible spectroscopy and fluorescence MSP to discriminate between a large population of fibres based on their dye composition and loadings.^[175] However, these studies have largely focussed on the simultaneous discrimination of several fibres, rather than the Q vs. K comparisons more typical of casework. Furthermore, there is presently a lack of quantitative measures for assessing sample similarity. The establishment of statistical cut-off criteria for an ‘inclusion’ or ‘exclusion’ result would provide an additional basis on which forensic scientists could support their findings in court.

This study investigated the potential use of MSP spectroscopy followed by chemometrics to assess the similarity or dissimilarity of several blue-dyed acrylic fibre sets. These were selected as an example of a common fibre type and dye combination. Chemometric data analysis was conducted on spectra acquired from various fibre pairs to simulate Q vs. K comparisons. Quantitative determination of the similarity was then made by comparing the resultant data using hypothesis testing. Raman spectroscopy was also investigated as an alternative means of analysing the fibre set, to determine whether this method could provide additional discrimination to MSP.

2.2 Experimental

2.2.1 Samples

Fibre samples were provided by the University of South Carolina. The sample population comprised eleven bilobal blue acrylic fibre sets with varying combinations of cationic (basic) dyes, as shown in Table 2.1. Representative images of each fibre set are provided in Figure 2.1. Fibres from each set had varying diameters as indicated.

Table 2.1: Dye compositions of eleven blue acrylic fibre sets utilised in this study.

Fibre Set	Dye composition	Diameter (μm)
Fibre A	Blue 3, Red 18, Yellow 28	17.5
Fibre B	Blue 41, Red 46, Yellow 28, Yellow 29	15
Fibre C	Blue 41, Red 46, Yellow 28	15
Fibre D	Blue 41, Red 29, Yellow 21	21.25
Fibre E	Blue 147, Red 29, Yellow 28	23.75
Fibre F	Blue 3, Blue 147	23.75
Fibre G	Blue 147, Red 46, Yellow 28	18.75
Fibre H	Blue 3, Red 18, Yellow 28	22.5
Fibre I	Blue 41, Red 29, Yellow 28	22.5
Fibre J	Blue 41, Red 18, Yellow 28	25
Fibre K	Blue 3, Red 46, Yellow 28	25

2.2.2 Microspectrophotometry

Individual fibres from each set were removed and mounted on glass microscope slides using Permount mounting media (Fisher Scientific, NJ) for analysis. Spectra were acquired from 400 – 800 nm using a CRAIC QDI 2000 microspectrophotometer calibrated using NIST traceable standards, operated in transmission mode with 150x magnification.^a An autosect optimisation, dark scan and reference scan were obtained prior to each sample analysis. Ten fibres were analysed with from each set, with five spectra taken along the length of each fibre to account for intra-fibre variation. Fifty averaged scans at a resolution of 5 nm were obtained for each spectrum.

^a All MSP spectra were acquired by Eric Reichard, Dana Bors, Wil Kranz and Marie Diez at Indiana University-Purdue University, Indianapolis (IUPUI).

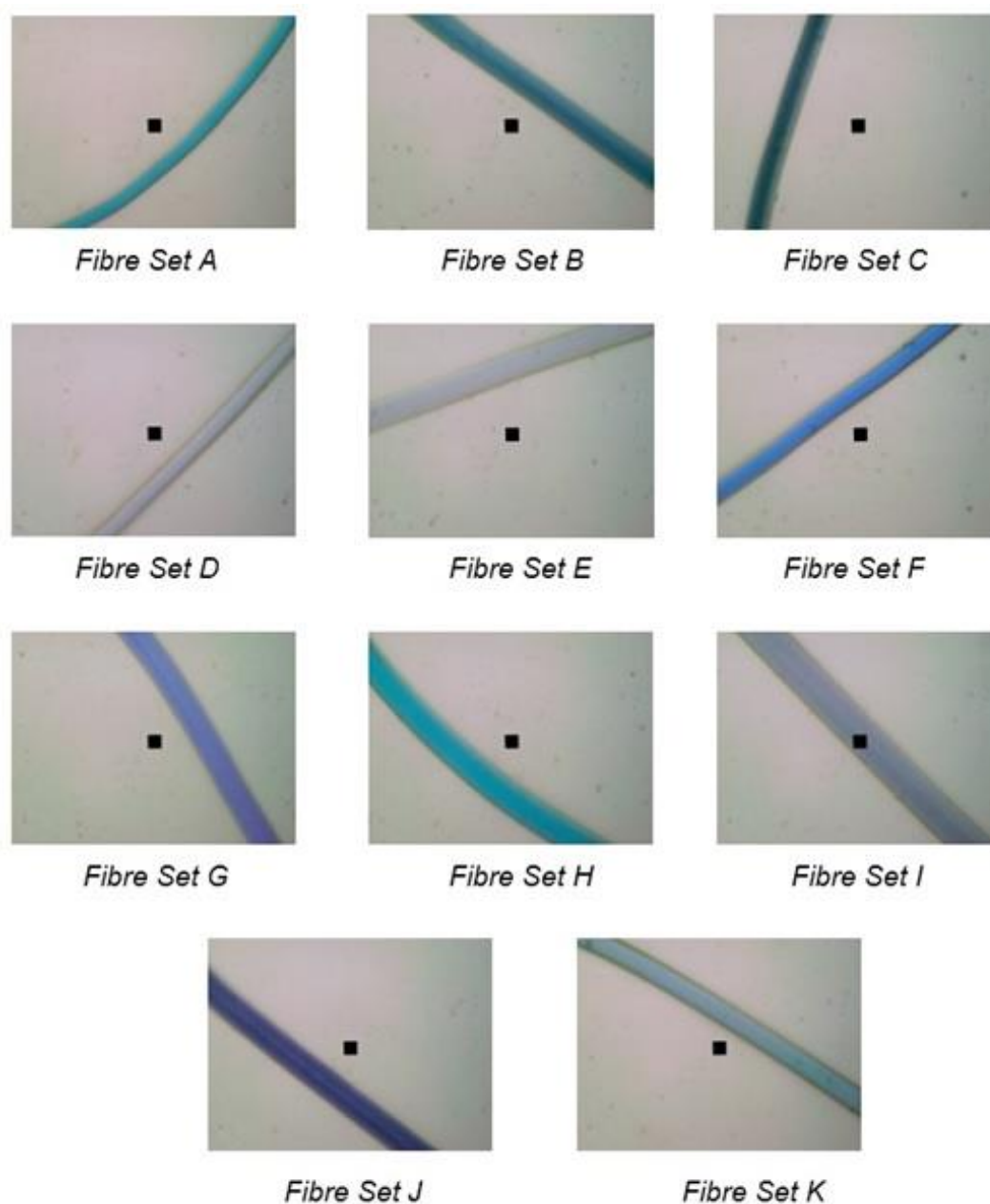


Figure 2.1: MSP microscope images of blue acrylic fibre exemplars utilised for Q vs. K comparisons.

2.2.3 Raman spectroscopy

Individual fibres from each set were randomly selected and attached to mirrored microscope slides using adhesive tape. Raman spectra were obtained using a Renishaw inVia confocal Raman microscope under 100x magnification, equipped with a near-infrared 785 nm diode laser. Data acquisition and instrument control was performed using Renishaw WiRE 3.4 software. Spectra were collected in Synchroscan mode between $100 - 3200 \text{ cm}^{-1}$, using 0.1 % laser power and a 10 second exposure.

2.2.4 Data analysis

Data pre-processing and chemometric analysis was conducted using XLSTAT (AddInSoft, Paris, France) and Unscrambler® X 10.3 (Camo Software AS, Oslo, Norway). All spectra were baseline offset to correct for light scattering and normalised to unit vector length to account for variations associated with the fibre diameter or dye concentrations. Spectra were then mean-centred and subjected to principal component analysis (PCA) using Unscrambler® X 10.3, using the non-linear iterative partial least squares (NIPALS) algorithm. 3-dimensional scores plots were generated using the scores from the first three principal components (PCs) in order to visualise the sample distribution and identify any outliers prior to further analysis.

The Q vs. K approach was undertaken by conducting PCA on different pairs of fibre sets in XLSTAT.^b In each case, the “known” sample was defined as a group of 45 spectra originating from the first nine fibres of the set, while the “questioned” sample was defined as the five spectra acquired from the last fibre analysed in the same set (to assess true inclusions and false exclusions) or different set (to assess true exclusions and false inclusions). As the fibres of each set were selected randomly, the consistent use of the last fibre in each set as the questioned sample still provided a randomised selection. Discriminant analysis (DA) was performed in XLSTAT on each pair based on their PCA scores and using the Mahalanobis distance measure. The covariance matrices were assumed to be non-equal based on Box’s *M* test for equality of covariance. The number of PCs used to construct each model was selected according to the corresponding scree plots. Prior membership probabilities were calculated from the training set to avoid classification biases due to the size difference of the questioned and known classes. This approach was repeated for all possible pairs of questioned and known samples, yielding a total of 121 comparisons amongst all eleven fibre sets.

Due to the large size difference between the questioned and known classes, the overall classification accuracy of the discriminant model could not be taken as a reliable measure of differentiation. As only five of the 50 spectra involved in each comparison originated from the questioned sample, an overall classification accuracy of 90 % would be obtained even if all five questioned spectra were assigned to the known class.

^b Generation of XLSTAT values performed by Dr. John Goodpaster (IUPUI).

The differentiation between each pair was therefore evaluated according to the percentage of questioned spectra assigned to the known class, assessing the extent to which the questioned sample fell within the boundaries of the known source. In addition, the mean membership probability of the questioned sample belonging to the known class was recorded. Fisher’s exact test was then utilised to obtain a quantitative measure of sample similarity. Contingency tables were constructed from the results of the discriminant analysis as shown in Table 2.2.

Table 2.2: General form of a contingency table generated from a *Q* vs. *K* comparison.

	Classified as “Known”	Classified as “Questioned”	Total
Known	<i>a</i>	<i>b</i>	<i>a + b</i>
Questioned	<i>c</i>	<i>d</i>	<i>c + d</i>
Total	<i>a + c</i>	<i>b + d</i>	

Fisher’s exact test statistics were calculated in XLSTAT from each contingency table according to the following formula, where *N* is the sum of *a*, *b*, *c*, and *d*.

$$p = \frac{(a+b)!(c+d)!(a+c)!(b+d)!}{a!b!c!d!N!}$$

Fisher’s exact test calculates the exact probability associated with observing a given combination of data in a contingency table.^[337, 338] This probability is summed with all other combinations of *a*, *b*, *c*, and *d* that could be obtained whilst retaining the same marginal totals, generating an overall *p*-value.^[338] The null hypothesis (*p* > 0.05 at the 95 % confidence level) is that the rows and columns of the table are independent, i.e. there is no association between the classification of spectra as belonging to the questioned or known fibres and the actual source of the spectra.^[339] This would indicate that the questioned and known fibres possess overlapping characteristics, and thus could potentially originate from a common source. Conversely, the alternative hypothesis (*p* < 0.05) is that there is an association between the actual and predicted fibre sources. This in turn implies that the questioned and known fibres are distinguishable, and that they are likely to originate from different sources.

2.3 Results and discussion

2.3.1 Preliminary considerations

Single textile fibres often exhibit varying levels of dye uptake, particularly where a multicomponent dye has been used.^[207, 220] This potential heterogeneity both among and within individual fibres requires appropriate sampling to obtain representative data for the bulk material. For synthetic textiles such as acrylics, SWGMAT guidelines recommend the examination of at least five individual fibres, with a minimum of five replicate spectra acquired for each.^[211, 335] In this study, nine to ten fibres were hence utilised in each known set to ensure representative sampling. As it is not always possible in casework scenarios to recover multiple fibres from the questioned source, single fibres were utilised as the questioned sample to simulate a challenging scenario wherein a single fibre is recovered and submitted for analysis alongside a much larger known source, such as a garment or blanket. However, the large difference in size of the questioned and known classes has the potential to affect the results obtained in this study, and this must be considered when evaluating the results.

MSP spectra from fibre sets A and H were each collected over two consecutive days, with the instrument re-calibrated on each date. In a casework scenario, the known and questioned fibres would ideally be analysed sequentially on the same day, thus minimising the risk of false exclusions due to day-to-day variations in the instrument performance. However, this is not always feasible where a large number of samples have been submitted for analysis. The re-calibration of the instrument, in addition to inherent instrumental variability, may therefore result in spectral deviations that could influence the results determined through statistical analysis.

2.3.2 Fibre characterisation using Raman spectroscopy

Attempts to characterise the fibre population using Raman spectroscopy proved unsuccessful, due to strong sample fluorescence obscuring the entire spectral region (Figure 2.2). Sharp signals were observed in several spectra, though these were not reproducible across replicate spectra and so were identified as instrumental artifacts. The likelihood of fluorescence interference when conducting Raman analysis of dyed textiles has been heavily documented in the existing literature.^[228, 230, 232, 331-333] This issue can potentially be overcome by utilising an alternative laser source, such that the wavelength of the laser falls outside of the sample's fluorescence excitation range.

In this instance, as the Raman instrument available for this study was equipped with only a single laser, no further investigation could be conducted. The following results in this chapter are thus presented solely in reference to data obtained using MSP.

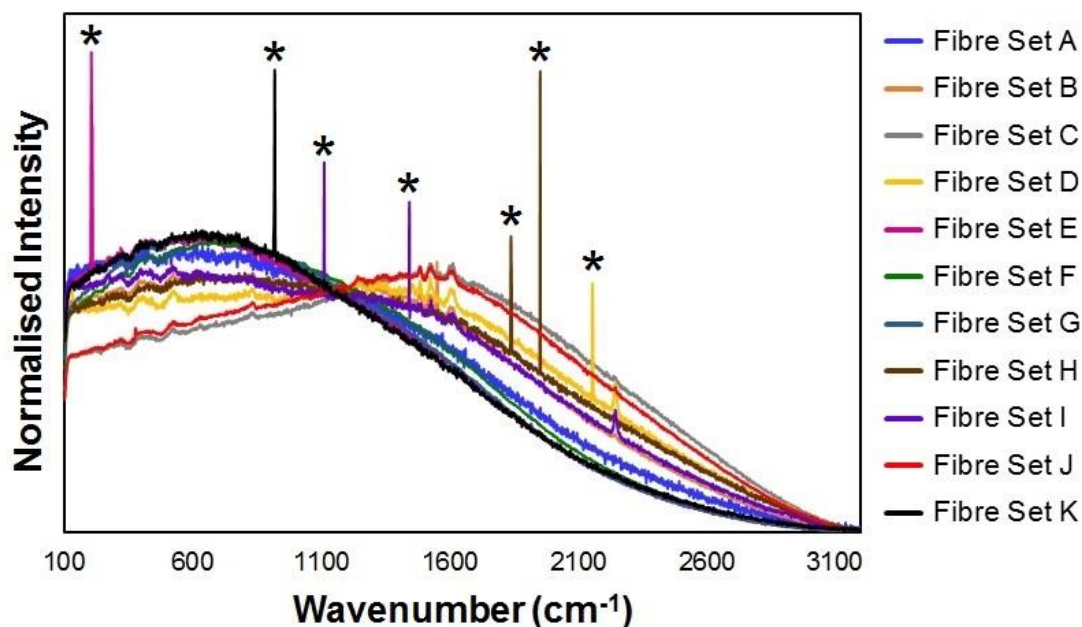


Figure 2.2: Raman spectra acquired from blue-dyed acrylic fibre sets. () denotes signals identified as instrumental artifacts.*

2.3.3 Correlation between fibre spectra and component dyes

Chemical structures of the component dyes used in this research are provided in Appendix 2.1. Though reference standards for each dye were unavailable, visual inspection of the spectra allowed broad correlations to be drawn between these dyes and specific spectral features (Table 2.3).

Table 2.3: Spectral features attributable to dyes contained in the blue acrylic fibres.

Dye	Absorbance peak/s
Blue 3	Sharp peak at 655 nm, shoulder at 600 nm
Blue 41	Peak at 625 nm, shoulder at 585 nm
Blue 147	Broad peak at 600 nm
Red 46	Peak at 545 nm
Yellow 21	Peak at 450 nm, possible peak at 425 nm
Yellow 28	Peak at 450 nm
Yellow 29	Peak at 450 nm

For the purposes of this inspection, the fibre sets were divided into three groups according to their primary blue dye: Blue 3 (sets A, F, H and K), Blue 41 (B, C, D, I and J) or Blue 147 (sets E and G). Example spectra from each of these fibre sets are shown in Figure 2.3. It was noted that spectra from sets A and H appeared visually identical, as expected given their identical dye combination.

Fibres containing Blue 3 exhibited a strong peak at 655 nm with a shoulder at 600 nm, consistent with known values for this dye.^[340-342] Sets A, H and K also showed minor peaks or shoulders at 450 nm consistent with Yellow 28.^{34, 35} No such peak was noted in the spectrum of set F, as these fibres did not contain any yellow dyes. Set K spectra exhibited a weak shoulder at 545 nm, possibly due to the presence of Red 46. Red 18, present in fibres from sets A and H, gave no distinguishable peak in the corresponding spectra. Given the broad, overlapping nature of MSP spectra, it is possible that any absorbance band from this dye was masked by the blue or yellow dyes, which would likely have been present at much greater concentrations.

Samples containing Blue 41 showed a corresponding peak at 625 nm, with a shoulder at 585 nm. It is likely that the latter resulted in the masking of any red dyes, as none of the spectra yielded observable peaks in the red (500 – 550 nm) region. Fibres containing Yellow 28 gave the expected absorbance band at 450 nm, with the exception of sets I and J, which instead exhibited broad shoulders at ca. 490 nm. It is possible that this band shift is due to the overlap or interaction between multiple dyes contained in these samples. Fibre set B (containing Yellows 28 and 29) gave a single peak in the yellow region indistinguishable from that arising solely from Yellow 28, indicating that these dyes give rise to overlapping bands centred around 450 nm. Set D gave a weak shoulder at ca. 425, consistent with Yellow 21.^[343, 344]

Both fibre sets containing Blue 147 produced a single broad band at ca. 600 nm. Any Blue 147 contained in set F could have been hence likely masked by the 600 nm shoulder of Blue 3, also explaining why this shoulder exhibited a broader peak width and greater intensity relative to the 655 nm peak compared to fibres containing only Blue 3. The Blue 147 peak may also be responsible for masking any bands in the red region caused by Red 29 (set E) or Red 46 (set G). Set G fibres gave no distinguishable peak in the yellow region despite containing Yellow 28, indicating that the concentration of yellow dye in these fibres was too low to be detected under the conditions in this study.

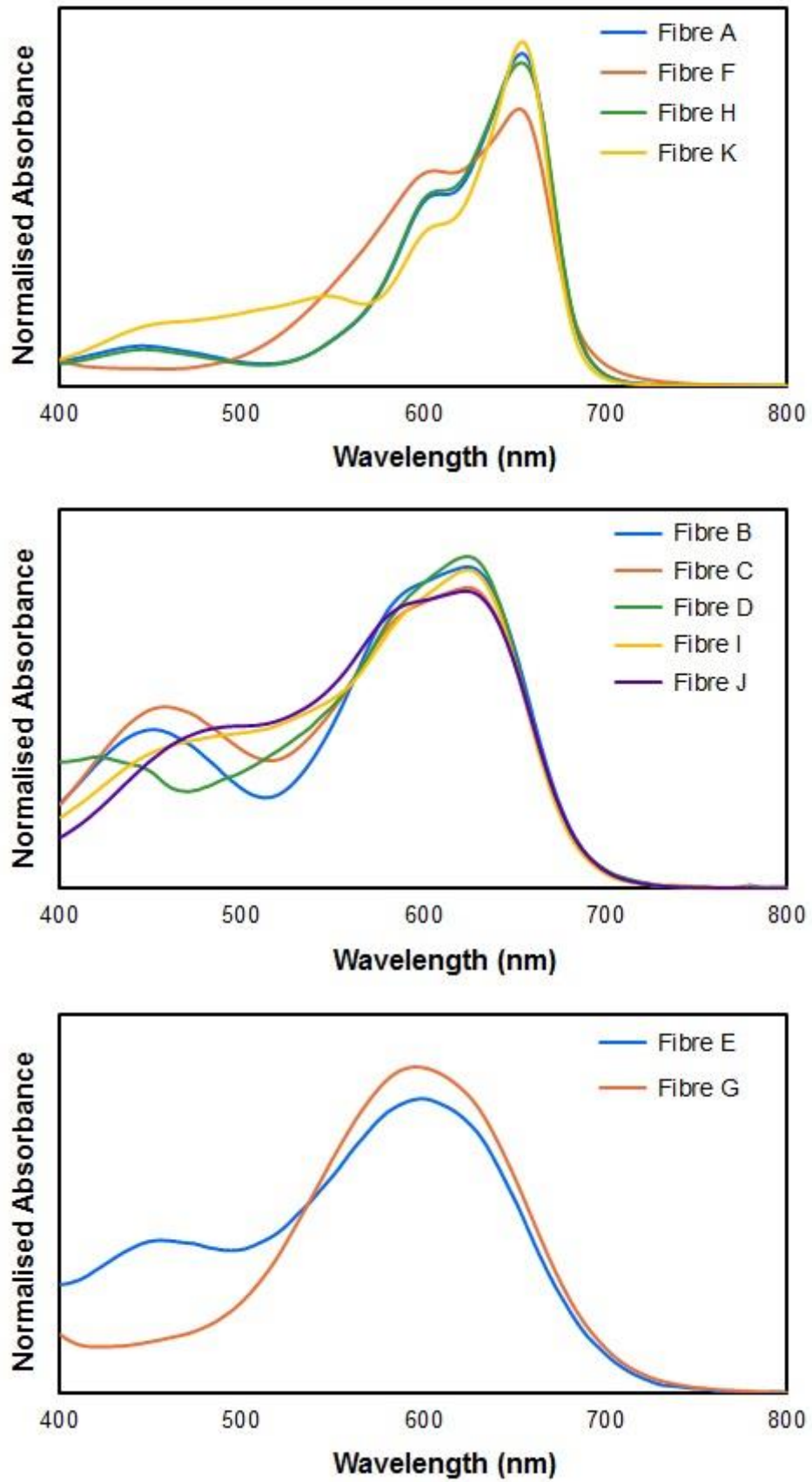


Figure 2.3: Normalised MSP spectra (averaged across five replicates) for acrylic fibres containing (top) Blue 3; (middle) Blue 41; and (bottom) Blue 147 as their primary dye.

2.3.4 Distribution of the spectral dataset

PCA was employed to reduce the dimensionality of the data by transforming the original variable set into a lesser number of orthogonal principal components (PCs).^[47, 49, 53] This was done to visualise the overall distribution of the sample population, and identify any latent patterns within the dataset that would not be readily discernible from the raw spectra.^[49]

PCA revealed that 96.6 % of total variance in the dataset could be described by the first three PCs, as illustrated in the scree plot below (Figure 2.4). The scree plot is important in determining the optimum number of PCs to be retained within the model.^[42] Retaining an insufficient number of PCs may cause information pertaining to dataset variation being lost, whilst extraneous PCs may result in the modelling of random variance or noise.^[42, 48] By assessing the variance accounted for by each individual PC, and determining the point at which the curve begins to plateau, the optimum number of PCs required to model the data can be identified.^[49, 59] In this case, the scree plot advocated the use of up to four PCs (accounting for 98.5 % of the total variation) to re-visualise the dataset.

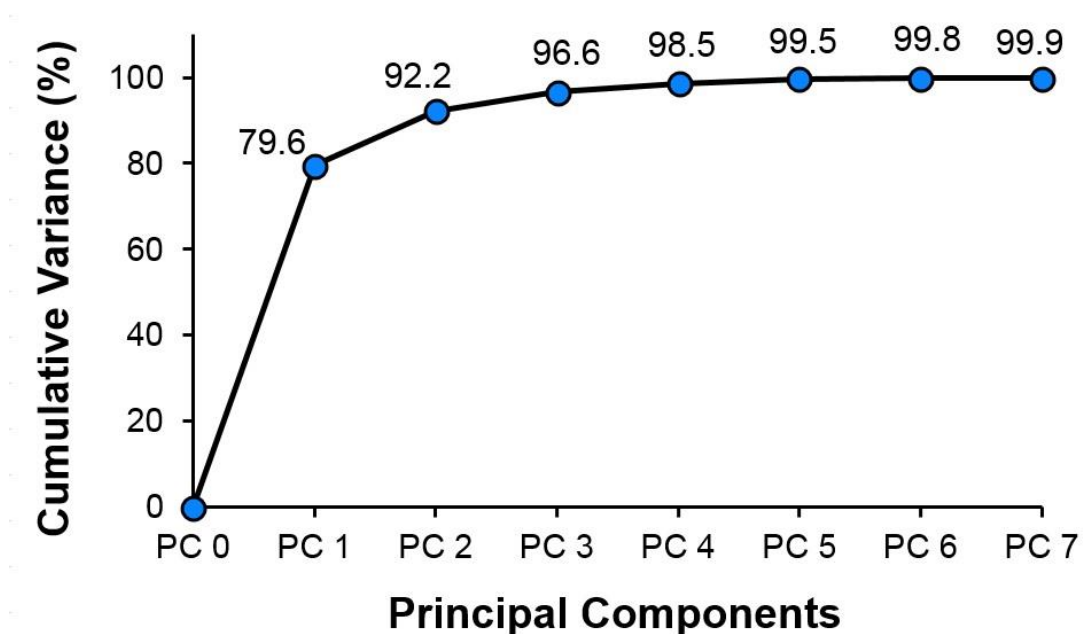
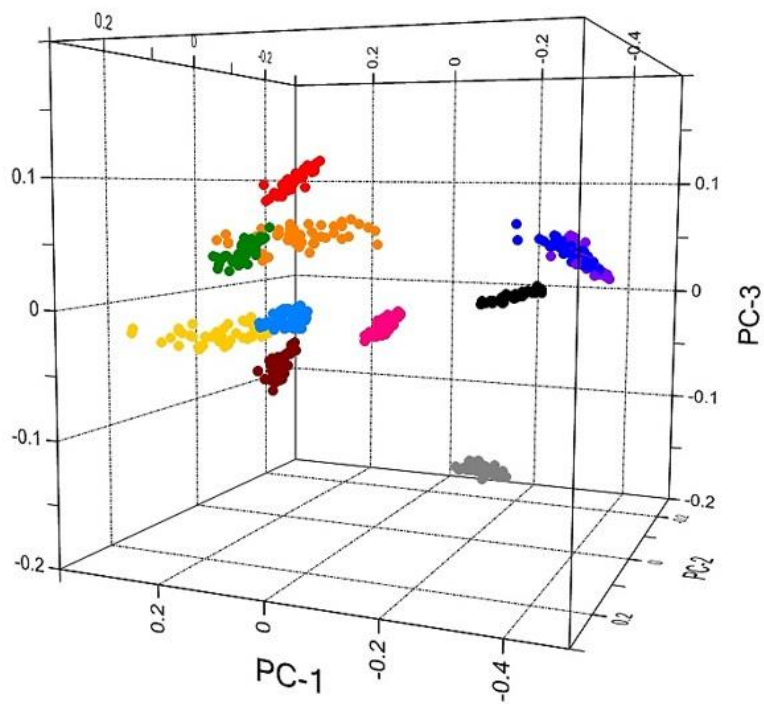


Figure 2.4: Scree plot depicting the cumulative variance in the blue acrylic fibre dataset retained by each PC.

Scores plots generated using combinations of the first four PCs resulted in most fibre sets forming visually distinct clusters, with no obvious outliers (Figure 2.5). PC4, despite accounting for only 1.9 % of variance within the dataset, was found to improve the discrimination between fibre sets C and D. These exemplars were observed to overlap when using only the first three PCs. Fibre sets A and H exhibited significant overlap, which was attributed to these fibres possessing the same dye combination (Table 2.1). It should also be noted, though, that these fibres have different diameters, and would hence be distinguishable upon a general microscopic examination.

Spectra from sets D and E exhibited a high level of spread (i.e. intra-class variance) compared to the remaining samples when employing the first three PCs. Visual inspection of the corresponding spectra (Appendices 2.2 and 2.3) revealed variation in the relative absorbance between bands in the 400 – 500 nm (yellow dye) region and those in the 600 nm (blue dye) region. This is potentially due to differing dye uptake amongst individual fibres, as discussed above. This also reinforces the importance of collecting an adequate number of fibres and replicate spectra where feasible, in order to allow representative measurements to be obtained.



- Fibre Set A
- Fibre Set B
- Fibre Set C
- Fibre Set D
- Fibre Set E
- Fibre Set F
- Fibre Set G
- Fibre Set H
- Fibre Set I
- Fibre Set J
- Fibre Set K

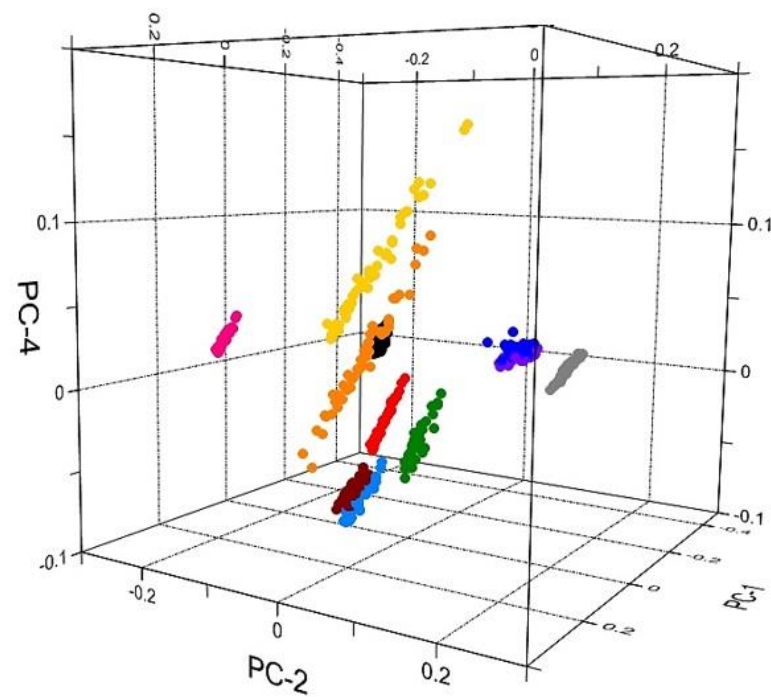


Figure 2.5: 3-dimensional PCA scores plot (employing PCs 1,2,3 and PCs 1,2,4) showing the distribution of blue acrylic fibres based upon their corresponding MSP spectra. Left and right images show the improved separation of Fibre Sets C and D upon the inclusion of PC4.

The factor loadings for the first four PCs (Figure 2.6) can be used to identify which wavelength regions are the largest contributors to variation between the fibre sets, and hence between each Q vs. K pair. PC1 has a strong positive correlation at ca. 655 nm, consistent with the absorbance band for Blue 3 dye. Samples separated along this PC may therefore be assumed to differ in their relative proportions of this dye. For example, fibres from set F (containing Blue 3) attain positive scores against PC1, while fibres from set E (instead containing Blue 147) exhibit negative scores. Similarly, PC2 has a positive correlation at 450 nm, consistent with Yellow 28 dye. Fibre pairs separated along this component are thus assumed to be dissimilar in terms of the type or concentration of yellow dye present.

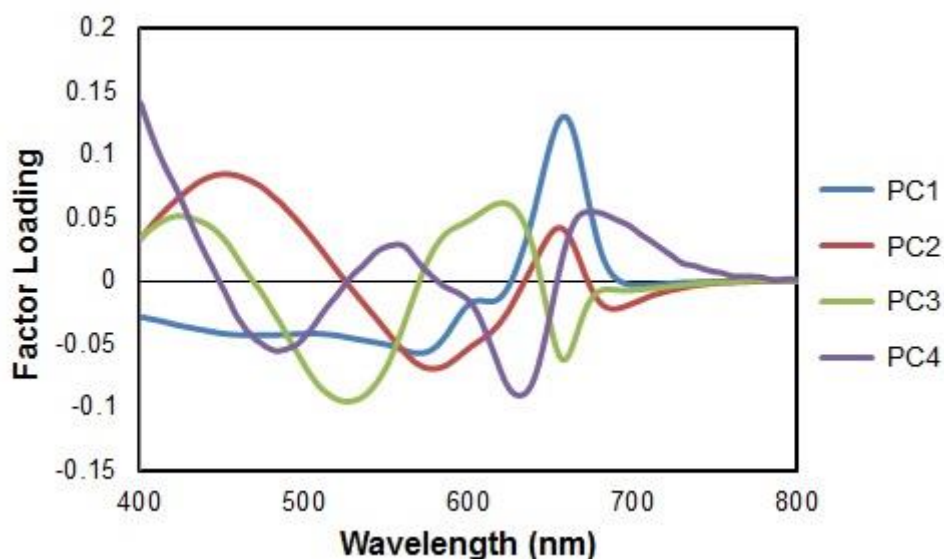


Figure 2.6: Factor loadings plot of PCs 1-4 for PCA of the entire blue acrylic dataset.

PC3 exhibits a strong negative correlation at approximately 530 nm, consistent with a local minimum in the set B spectra (Figure 2.3). Set B fibres hence obtain the most positive scores along this PC, resulting in their separation from sets C, D, I or J. Likewise, PC4 has a negative correlation at ca. 470 nm. At this wavelength, set D spectra exhibit a local minimum whilst set C spectra are near a maximum, resulting in the separation of these samples along PC4 as observed in the scores plot. PCA is thus not only valuable in qualitatively assessing the similarity of a questioned and known pair, but may reveal the chemical basis for their similarity or dissimilarity. Such relationships may be difficult to identify from visual examination of spectra, highlighting the potential utility of chemometrics in forensic applications.

2.3.5 Simulated “Q vs. K” comparisons

2.3.5.1 Fibres from same source

Simulated Q vs. K comparisons were undertaken by subjecting pairs of fibre sets to PCA and DA. Successful discrimination (100 % correct classification) was interpreted as an exclusion result wherein the fibres could be considered to originate from different sources. Poor discrimination, i.e. where three or more of the questioned spectra were assigned to the known class, was treated as an inclusion – that is, the fibres could possibly originate from a common source. The first set of comparisons were carried out between fibres of the same set, employing the last fibre as the questioned sample and the remaining nine fibres as the known sample. These spectra were expected to be non-differentiable, thus yielding an inclusion result.

This was the case for ten of the eleven fibre sets, as shown in Table 2.4. The majority of the questioned spectra from these fibre sets were assigned to the known class, implying the questioned fibre to fall within the boundaries of the known source. Furthermore, the mean membership probability of these spectra belonging to the known class exceeded 50 %. The results of Fisher’s exact test largely agreed with these initial metrics, with large p -values obtained for nine of the fibre sets. Fibre set I generated a p -value just below 0.05, resulting in an inconclusive comparison. For fibre set K, only two of the five questioned spectra were classified to the known class, and the mean membership probability for these two samples was less than 50 %. Fisher’s exact test also resulted in a rejection of the null hypothesis, giving a false exclusion. This is potentially a result of fibre heterogeneity associated with dye concentration, as previously discussed.

Overall, these results indicate that while ten of eleven “same source” comparisons gave the expected result, there is a potential for false exclusions. This may be exacerbated by the large difference in size of the questioned and known classes, despite the fact that the initial probabilities of the discriminant model took this into account.

Table 2.4: Statistical values obtained from *Q* vs. *K* comparisons conducted on blue acrylic fibres originating from the same set. (*) denotes that the spectra for the ten fibres in these fibre sets were each acquired over multiple consecutive days.

	Q = K classification (%)	Mean Membership Probability (Q = K) (%)	Fisher's Exact Test (p-value)
Fibre Set A*	100	76	1.0
Fibre Set B	100	89	1.0
Fibre Set C	100	87	1.0
Fibre Set D	100	80	0.18
Fibre Set E	100	88	1.0
Fibre Set F	100	78	1.0
Fibre Set G	100	74	1.0
Fibre Set H*	80	78	1.0
Fibre Set I	60	53	0.04
Fibre Set J	80	66	1.0
Fibre Set K	40	42	5.1 x 10 ⁻⁴

2.3.5.2 Fibres from different sources

When comparing fibres taken from different sets, the majority of samples (with exception of sets A vs. H and C vs. D) were unambiguously differentiated, yielding true exclusions in 108 of 110 comparisons. In these instances, 100 % correct classification was achieved and the membership probability of the questioned spectra belonging to the known class was determined to be 0 %. Successful discrimination of these fibre sets was expected based on their clear visual separation in the PCA scores plot. As these samples could be readily differentiated according to their PC scores, Fisher's exact test was deemed unnecessary and the results are not included here.

When fibre sets C and D were compared, there was a small probability for some of the questioned samples to be assigned to the known class (Table 2.5). This is consistent with the minor overlap noted between these sample sets in the PCA scores plot when employing the first three PCs. Nonetheless, as the probability associated with misclassification of the questioned spectra was minimal (below 5 % in each case), the samples were still considered to be separable. Fisher's exact test also indicated that the *Q* vs. *K* membership frequencies for these samples were interdependent, yielding an overall exclusion result.

Table 2.5: Statistical values obtained from *Q* vs. *K* comparisons conducted on fibres from different sets.

Questioned	Known	Q = K classification (%)	Mean Membership Probability (Q = K) (%)	Fisher's Exact Test (<i>p</i> -value)
Fibre Set C	Fibre Set D	0	3	4.7×10^{-7}
Fibre Set D	Fibre Set C	0	2	2.8×10^{-6}
Fibre Set A	Fibre Set H	60	47	8.2×10^{-3}
Fibre Set H	Fibre Set A	100	81	1.0

When comparing fibre sets A and H, the results were less conclusive. When the questioned fibre originated from set A, the majority (60 %) of questioned spectra were assigned to the known class, despite the mean membership probability being less than 50 %. Furthermore, Fisher's exact test indicated that the two samples were distinguishable. However, when a fibre from set H made up the questioned sample, all questioned spectra were assigned to the known class with a high mean membership probability, with Fisher's exact test indicating the two samples to be indistinguishable. Taken together, this indicates that fibre sets A and H were not able to be reliably differentiated.

The inability to discriminate between these sets was expected given their high degree of overlap in the PCA scores plot (Figure 2.5). These fibre sets also contained the same dye combination, although the relative concentrations (loadings) of each dye component were not determined. Interestingly, visual examination of the spectra from sets A and H revealed varying ratios of absorbance at the 655 nm peak and 650 nm shoulder (Figure 2.7). Both of these bands have been attributed to the same dye (Blue 3), and so heterogeneous dye uptake would not appear to be a contributing factor to this variation. It is possible that the deviations observed are a result of inherent instrumental variation, and this warrants future investigation.

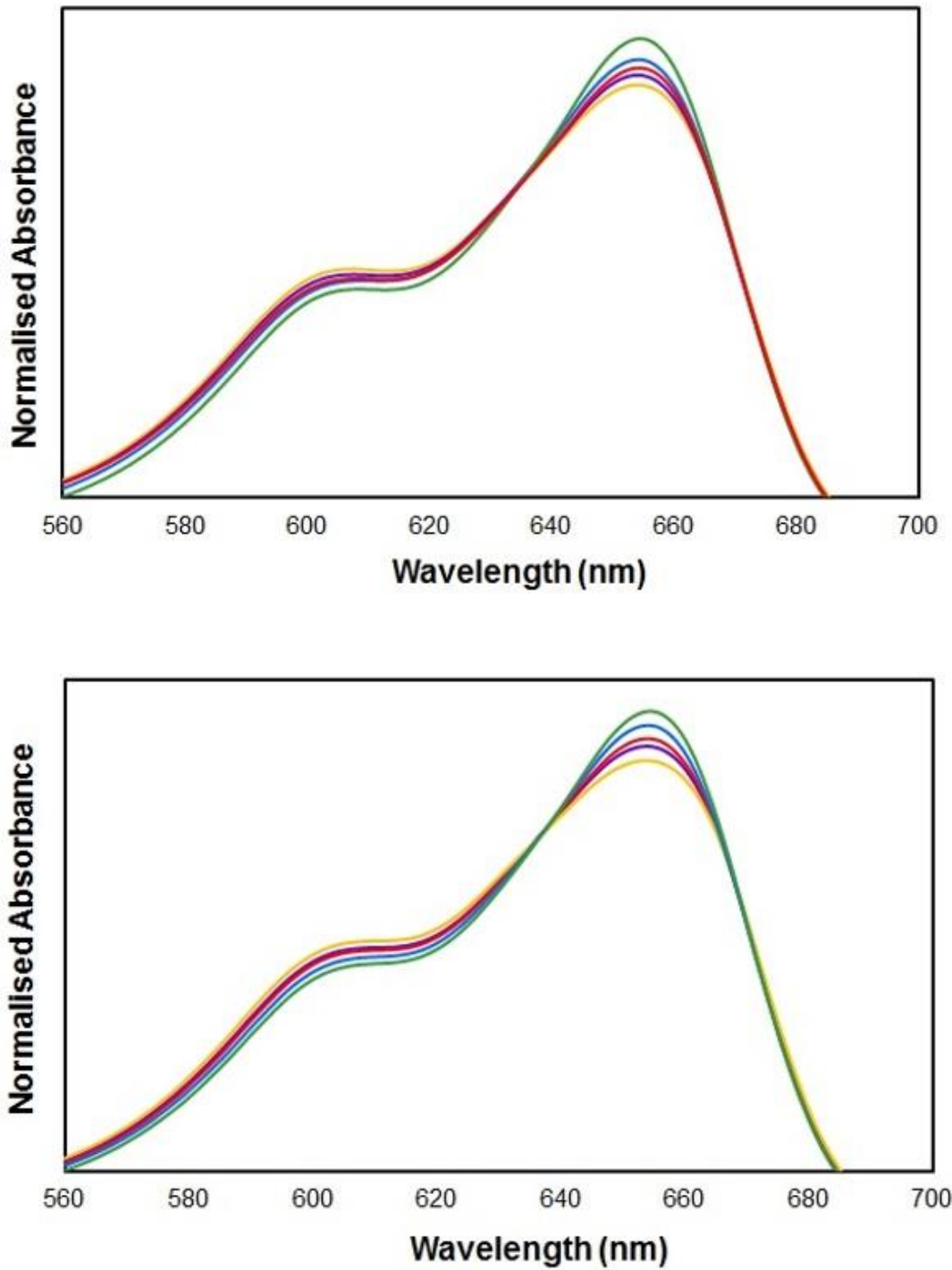


Figure 2.7: Pre-processed MSP spectra acquired from five individual fibres taken from (top) fibre set A and (bottom) fibre set H, illustrating differing relative intensities between the two major peaks at 600 nm and 650 nm.

2.4 Conclusions

The use of statistical methods with MSP shows great potential for rapidly distinguishing visually similar fibres on the basis of their dye combinations. The comparison of simulated questioned and known fibres from the same source resulted in a correct inclusion result for nine of the eleven fibre sets, although fibre set I gave potentially ambiguous results. The comparison of questioned and known fibres from different sources allowed for the differentiation of all fibre sets with the exception of fibre set A and H, which shared the same dye combination, yielding true exclusion results in 108 of 110 comparisons.

The single false exclusion, observed in fibre set K, may be attributed to a lack of reproducibility in obtaining the MSP spectra. This may result from the varying absorption of dyes in a multi-component mixture by individual fibres, or the analysis of questioned and known samples on different analysis dates. Given the impact of these factors on the results obtained through statistical analyses, it can be concluded that these methods are not infallible. Nevertheless, the use of well-documented statistical protocols for these comparisons provides a more scientifically rigorous basis on which examiners can support their findings in a court of law.

Raman spectroscopy proved unsuccessful in characterising the fibre set due to significant fluorescence interference when using a 785 nm laser source. This could potentially be overcome through the use of alternative laser sources. Infrared spectroscopy could also be investigated, as this may afford more reproducible data in comparison to MSP, in addition to providing complementary information regarding the structure of the dyes or their substrate.

This chapter has described the use of chemometric pattern recognition to characterise the variation present within a sample set. In the following chapter, these techniques will also be employed to investigate factors that may affect this characterisation, such as the ageing of samples under various conditions.

Chapter 3: Chemometric characterisation and ageing studies of blue ballpoint inks on paper using diffuse reflectance visible spectroscopy

Portions of this chapter have been published in the journal *Analytical Methods*:

G. Sauzier, P. Giles, S.W. Lewis and W. van Bronswijk, *In situ studies into the characterisation and degradation of blue ballpoint inks by diffuse reflectance visible spectroscopy*. *Analytical Methods*, 2015. **7**(12): p. 4892-900.

3.1 Introduction

The analysis and comparison of pen inks forms a key aspect of forensic investigations concerning document fraud or forgery. Modern writing inks are complex mixtures consisting of several pigments or dyes carried in a solvent such as water, oils or glycols.^[239, 241] In the case of ballpoint inks, dyes may constitute up to 50 % of the total ink formulation, and are generally contained in glycol- or benzyl alcohol-based solvents.^[237, 239, 242] Many ink formulations are patented and contain unique dye combinations, making colour a highly discerning characteristic. Several studies have hence investigated the discrimination of ballpoint inks using microspectrophotometry (MSP) or ultraviolet-visible (UV-Vis) spectroscopy.^[250-252] Recent inquiries have combined these techniques with chemometric analysis, yielding more objective assessments compared to visual examinations of data and allowing the comparison of several samples at a time.^[105, 106, 253, 345]

A limitation in the majority of these studies is the analysis of inks as solvent extracts rather than *in situ* on a paper substrate, making the methodology destructive. Another drawback is the small sample sizes employed; typically fewer than 15 inks of a given colour and type. This can result in models that exhibit poor predictive capability or reliability when applied to future samples. Furthermore, these models were generated from freshly deposited inks, with a lack of validation regarding their utility to aged samples. Following deposition, the chemical composition of an ink may rapidly change due to the evaporation of volatiles, resin polymerisation, diffusion through the substrate or photofading of dyes.^[346-349] Dye degradation poses a particular challenge for document examiners relying on MSP or UV-Vis methods, as ink from the same pen may produce very different spectral profiles depending on when it was deposited.

The most common dyes in modern blue or black ballpoint inks are synthetic triarylmethane dyes; particularly those of the methyl violet family (Figure 3.1).^[350] This dye class consists of three homologous structures derived from pararosaniline in which four, five or six of the amino hydrogen atoms have been replaced with methyl substituents. The degree of methylation determines the dye shade, with greater methylation tending toward blue-violets and lower methylation toward red-violets.^[351] The terms “methyl violet” and “crystal violet” are generally used in a forensic research context to specifically denote the penta- or hexamethyl structures respectively.

However, commercial dyes marketed as crystal or methyl violet are typically manufactured and sold as a mixture of all three homologues in varying proportions.^[352]

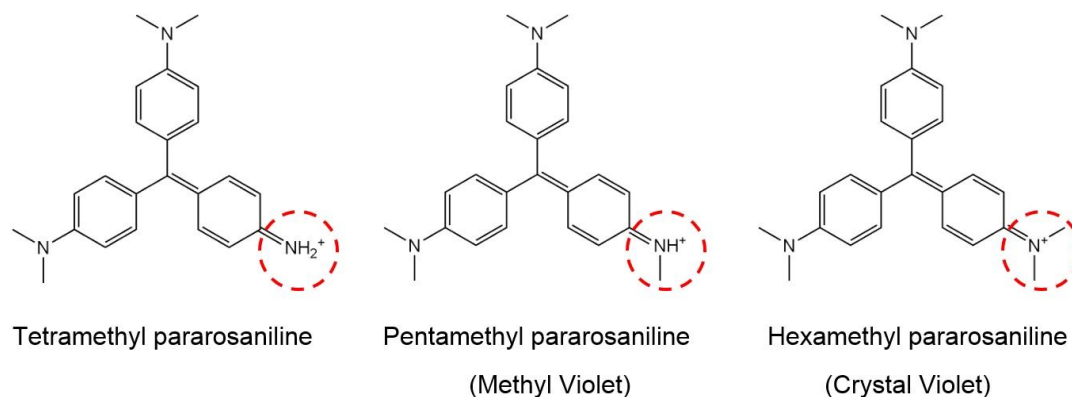


Figure 3.1: Chemical structures, chemical names and common names of methyl violet homologues (chloride counter-ions not shown).

A limitation concerning the use of these dyes in writing inks is their low photoresistance. Numerous studies have shown that methyl violets are highly prone to colour loss as a result of light exposure.^[346, 353, 354] The main degradation pathways for these dyes that can be expected to occur on paper are oxidative *N*-demethylation or photooxidative cleavage of the central C-phenyl bond, as depicted in Figure 3.2.^[354-357] These processes are known to be accelerated by the presence of titanium dioxide; a filler commonly used in paper production to impart high opacity and brightness.^[358] Li *et al.* also proposed that in an aqueous environment, hydroxide radicals formed by singlet oxygen and water could result in aromatic ring-opening reactions, though the exact mechanism or anticipated degradation products for this pathway were not specified.^[356]

A number of researchers have investigated the compositional changes that may occur in writing inks as a result of both natural and artificial ageing.^[346-349, 359, 360] Several such studies have attempted to utilise these changes in order to develop a reliable means of age estimation, as reviewed by Ezcurra *et al.*^[243] However, there is a paucity of research considering the effect of ageing on ink characterisation using chemometric techniques.

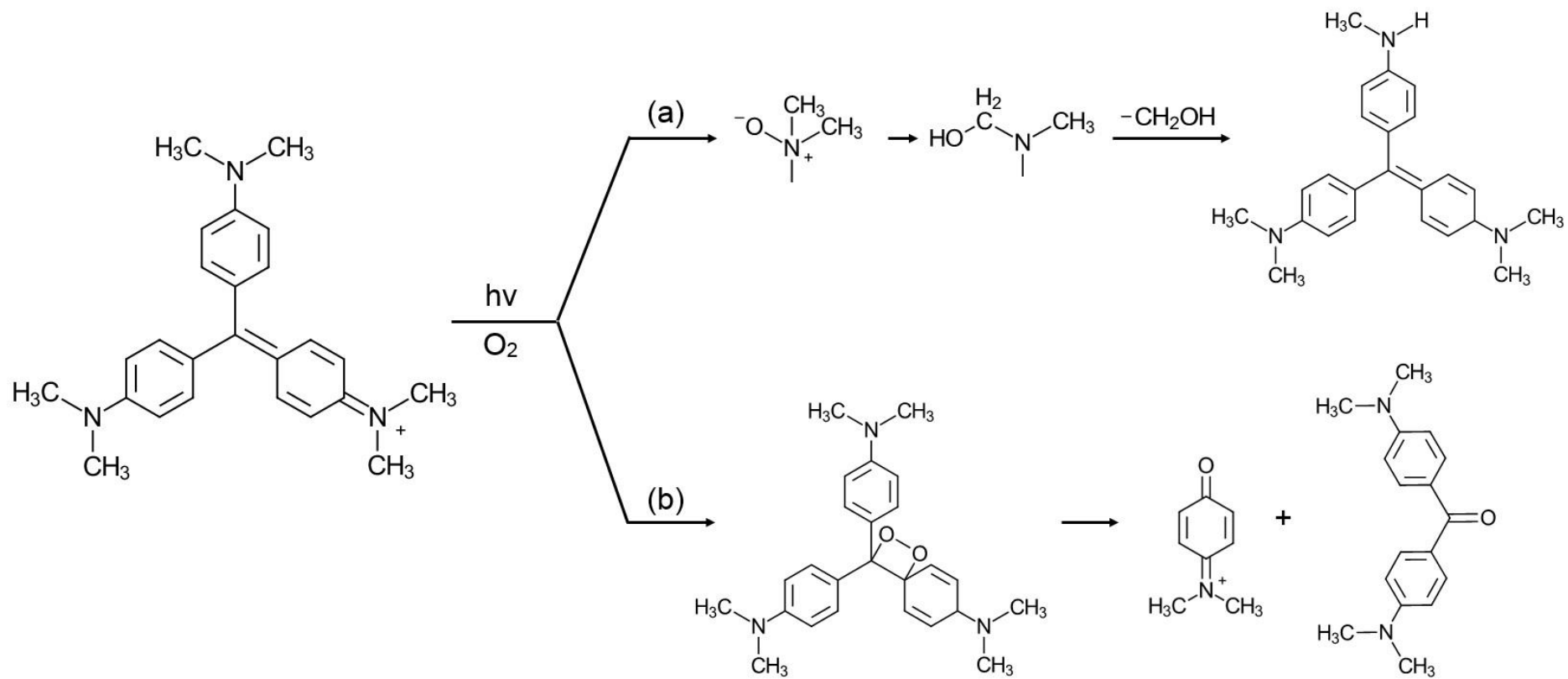


Figure 3.2: Anticipated degradation pathways of methyl violet dyes in ballpoint inks deposited on paper, shown for crystal violet: (a) oxidative N-demethylation and (b) photooxidative cleavage of the central C-phenyl bond.

One such study by Senior *et al.* found that blue ballpoint inks analysed 2, 6, 12 or 18 months after deposition on paper gave significantly different PCA scores compared to fresh ink samples, and postulated that these changes could be correlated with time to estimate when a questioned document was written.^[253] However, this study employed a limited sample set of only 10 pens, with the ink again analysed as solvent extracts rather than on paper.

In this chapter, the use of diffuse reflectance visible spectroscopy followed by chemometric data analysis was investigated as an *in situ* analysis method for ballpoint inks on paper. Visible spectra acquired from 35 blue ballpoint inks were subjected to principal component analysis (PCA) and linear discriminant analysis (LDA), establishing a statistical model for ink identification or discrimination purposes. This chapter also examines the effects of both artificial and extended natural ageing on the chemical composition of selected inks, the resultant impact on the classification model, and the potential to utilise these changes for ink dating purposes.

3.2 Experimental

3.2.1 Sample collection and preparation

35 blue ballpoint pens were obtained from office stationery supplies and various Western Australian retailers (Table 3.1). Ink from each pen was deposited onto commercial white copy paper (Fuji Xerox Professional Carbon Neutral, 80 g/m²) by filling 10 mm x 10 mm squares using parallel lines, with five replicate samples prepared using each pen to account for any inhomogeneity within the ink cartridge. An additional five replicates were prepared from 12 pens selected as an external validation set (Table 3.1). Where pens had been purchased as a packet, a different pen from the same packet was randomly selected as the validation exemplar. All pens were stored within a paper bag in a closed office cupboard when not in use.

3.2.2 Ageing studies

Inks from six newly purchased pens were selected to undergo both natural and artificial ageing (Table 3.1). These inks were deposited as 25 mm x 25 mm squares to allow replicate measures to be made from different locations on each sample.

3.2.2.1 Natural ageing

Ink deposits from the selected pens were prepared for storage in three locations representative of typical office environments, as listed below. The samples were then left to age naturally, with analysis at specific intervals following ink deposition (1 day; 1 and 2 weeks; and 1, 2, 4, 6, 8, 10, 13 and 14 months).

- i.) On an office shelf, exposed to light (on a diurnal cycle) and air
- ii.) In an office drawer, away from light but exposed to air
- iii.) In an office drawer, away from light and stored in archival plastic sleeves (Ditto A4 reinforced sheet protectors)

Additional deposits were prepared as 10 x 10 mm squares for photographic monitoring, in order to track any visually discernible changes in the ink colour over time. These samples were stored in the same three locations as the analysis samples, with photographic images taken at the same intervals (1 day; 1 and 2 weeks; and 1, 2, 4, 6, 8, 10, 13 and 14 months) following ink deposition. Further deposits were also prepared as 25 mm x 25 mm squares to act as an external validation set for ink dating purposes. These samples were stored on an office shelf exposed to light and air, with analysis carried out after 5 days and 3, 6, 14 and 21 weeks following deposition.

All natural ageing experiments were carried out in a building with controlled air-conditioning. As a climate control chamber was not available during these studies, no further attempts were made to control factors such as ambient humidity. Data collected using a Digitech QP-6013 data logger found that throughout the ageing period, the average relative humidity was 45.5 % with a standard deviation of 8.4 %. A summary of environmental data collected over the ageing period is provided in Appendix 3.1.

3.2.2.2 Artificial ageing

Thermal ageing was conducted by placing samples into a ZhiCheng ZXRD-A5055 oven at 100 °C. Aluminium foil was placed over the glass oven window to prevent the samples from being exposed to light. These samples were analysed after 20 minutes, 2 hours and 24 hours of exposure. UV accelerated ageing was conducted via irradiation with a compact fluorescent UV light (20 W, Nelson Industries, Australia) mounted overhead on a camera stand. Samples were placed approximately 17 cm below the light source and analysed following 24 and 48 hours of UV exposure.

Table 3.1: Models and assigned numeric identifiers for all pens in the sample population. (*) denotes inks also selected for the preparation of validation samples; (†) denotes inks selected for ageing studies.

Pen ID	Pen Model	Pen ID	Pen Model
1*	Bic Cristal	19†	Pilot G-2 05
2	Papermate Ink Joy 100	20	Pilot Super Grip
3	Artline Ikonic	21*	Uniball Power Tank
4	Deer Ultrafine	22*	Pilot BPS-GP
5	Artline 7210	23†	PaperMate Profile
6	PaperMate Kilometrico	24*	Bic Pro Plus
7	Bic ReAction	25*	PaperMate FlexGrip Elite
8†	Celco Retractable	26*†	Pentel Rolly
9	Bic Orange Fine	27	PaperMate Kilometrico Elite
10†	Keji Ballpoint	28*	Staedtler Triplus 426
11*†	Office Basics Ballpoint	29	Staedtler Stick Click Retractable
12	Artline Smoove	30	Pilot BP-145
13*	J.Burrows Ballpoint	31	PaperMate FlexGrip Ultra
14	Bic Round Stic	32*	PaperMate Ink Joy 300
15	Artline Flow 4-Colour Retractable	33*	Office Choice Retractable
16	Artline Clix 4-Colour	34	COS Capped Ballpoint
17	Bic Cristal Easy Glide	35	Staedtler 430
18*	Bic Economy		

3.2.3 Photographic recording

Ink samples were photographed using a Nikon D300 camera on manual exposure mode, using a 60 mm lens. The camera was mounted overhead on a camera stand at a distance of 55 cm, with illumination provided by dual incandescent light globes on each side. All samples were photographed using a 1/60 second shutter speed, f8 aperture, ISO 200 and incandescent white balance. Images were digitally captured on a desktop computer using the Nikon Camera Control Pro program (v. 2.0.0), and an auto-contrast applied using Adobe Photoshop CC (v. 2014.2.1).

3.2.4 Visible spectroscopy

Spectra were obtained using a Cary 4000 UV-Visible spectrophotometer equipped with a DRA-900 internal diffuse reflectance accessory. Baseline scans were taken using an empty sample holder and mounted halon reference plate prior to sample measurement. The instrument was operated with a reduced slit height in double beam mode, and data acquisition performed using the Cary WinUV Bio Version software (v. 4.20). Spectra were recorded over the range of 400 – 700 nm, with a scan interval of 1 nm and scan speed of 600 nm min⁻¹.

3.2.5 Data analysis

All data pre-processing and analysis was performed using the Unscrambler® X 10.3 software (Camo Software AS, Oslo, Norway). Two different pre-processing approaches were examined. In both instances, spectra were first baseline offset to 0 % reflectance to account for any scattering effects, then unit vector normalised to remove variability caused by the sample surface texture. The first approach then subjected the spectra to chemometric analysis with no further pre-treatment, while the second approach applied a Kubelka–Munk (K-M) conversion according to the equation:

$$F(R) = \frac{(1 - R)^2}{2R}$$

The offset and normalised spectra were adjusted to a maximum reflectance of 1 prior to conversion, as the K–M function poorly handles values approaching zero, such as those obtained through normalisation.^[361]

Spectra were mean-centred and subjected to PCA using the non-linear iterative partial least squares (NIPALS) algorithm. 3-dimensional scores plots were generated using the scores from up to the first four principal components (PCs) to visualise the distribution of the samples and identify any outliers. An LDA model was then constructed from the calibration set (35 pens) using the Mahalanobis distance and scores from the first four PCs, treating each pen as a distinct class. The resultant model was used to predict spectra from the validation set (12 pens), with the actual and predicted classifications compared to evaluate the efficacy of the model. The validated model was also employed to predict spectra acquired from samples undergoing ageing, in order to detect any changes in the inks over time.

Separate dating models were constructed for each of the light-exposed inks using the pre-processed spectra collected over the 14 months of exposure. This data was mean-centred and analysed using partial least squares regression (PLSR) with the NIPALS algorithm. The resulting regression models were used to predict the age of the validation ink deposits (exposed for up to 21 weeks), with the actual and predicted ages compared to evaluate the efficacy of the model.

3.3 Results and discussion

3.3.1 Preliminary considerations

The outcomes obtained through chemometric analysis can be largely dependent upon the initial pre-processing of the data.^[48] Two different approaches were thus examined in this study. The first approach used only a baseline correction and normalisation, while the second approach also applied a Kubelka–Munk (K–M) conversion. This function is frequently applied to diffuse reflectance spectra to derive quantitative information, which may be useful for discrimination purposes.^[361, 362] In this instance, it was found that the K–M function did not improve discrimination between the samples. Using an external validation set, 73 % of spectra could be correctly assigned to the individual source pen and a further 8.3 % to the pen supplier, compared to 71.7 % and 16.7 % respectively with only a baseline correction and normalisation. This is possibly due to the amplification of spectral deviations, which may occur when reflectance spectra are converted to K–M units.^[362] For this reason, the K–M function was omitted in all further data analysis, and the following discussion is presented in reference to results obtained without the conversion applied.

3.3.2 Distribution of blue ballpoint inks

PCA performed on the dataset revealed that 95.8 % of total variance was described by the first three PCs. From the scree plot (Figure 3.3), it was determined that up to four PCs (accounting for 98.0 % of variance) could be suitably employed to re-visualise the dataset. Spectra from the 35 ballpoint pen inks were thus plotted against combinations of the first four PCs, resulting in the scores plots shown in Figure 3.4. Replicates from each individual pen were clustered together, indicating good reproducibility in the sampling and analysis method. PC4, although accounting for only 2.2 % of total variance, was found to assist in discriminating between the Pilot and Bic brand pens.

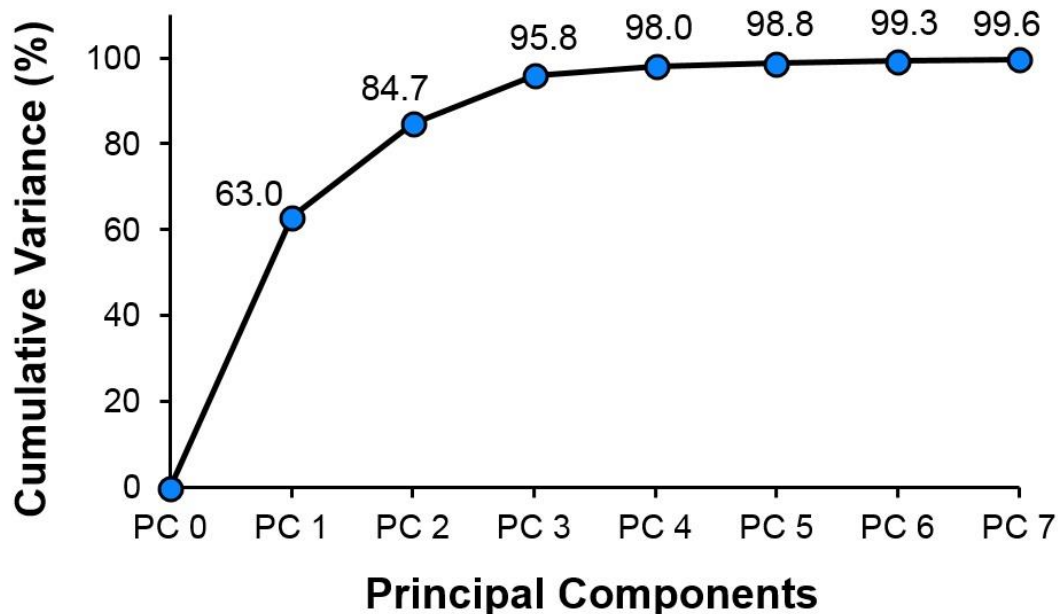


Figure 3.3: Scree plot depicting the cumulative variance in the Cary 4000 blue ballpoint ink dataset retained by each PC.

Several inks formed visually distinct groupings, allowing rapid discrimination based solely upon their visible spectra. In some cases, these spectra visually appeared very similar (Figure 3.5) and may have been difficult to distinguish based on visual comparison alone. A number of overlapping clusters were also observed in which one or more inks could not be clearly distinguished, as described in Table 3.2. PCA repeated on these individual clusters failed to improve the separation between these sets of samples (Appendix 3.2).

As Groups 1 – 3 all consisted of pens belonging to the same brand or supplier, the overlap between these samples is likely due to suppliers employing the same ink formulation across a range of different pens. Conversely, groups 4 and 5 contained a mixture of pens from different suppliers. This likeness may simply be due to these suppliers coincidentally using similar ink formulations. However, it should also be noted that although certain suppliers such as Bic manufacture their own inks,^[363] many suppliers source their inks externally. A distinction must therefore be made between the ‘supplier’ (brand) and ‘manufacturer’ of any given ink. Consequently, it is possible that budget suppliers such as COS or Office Choice may have purchased inks from the same manufacturers as larger suppliers such as Artline and PaperMate, resulting in the same ink being used across different brands.

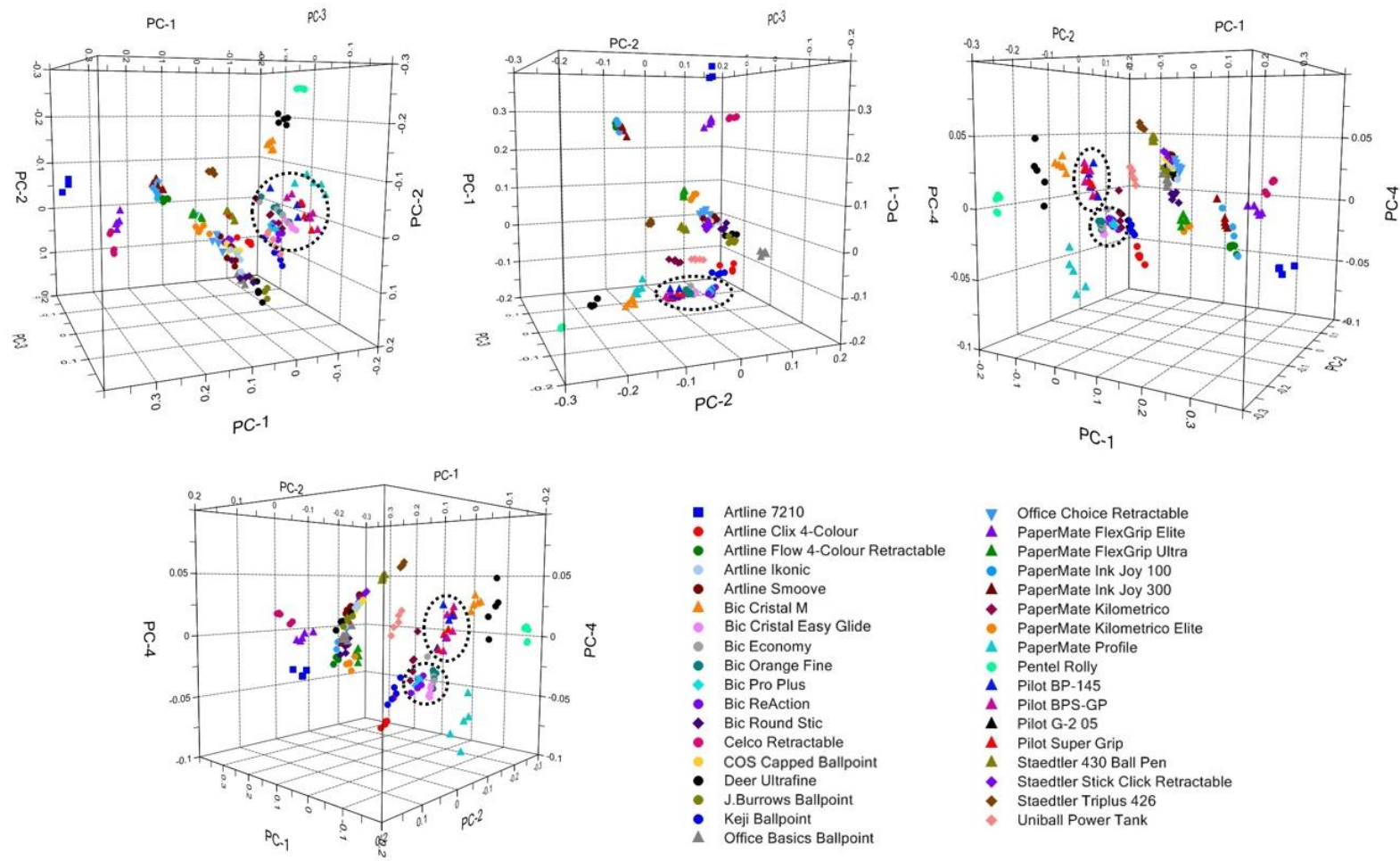


Figure 3.4: 3-dimensional PCA scores plots generated using the first four PCs, highlighting the distribution of the blue ballpoint ink population based upon their corresponding Cary 4000 visible spectra. Circles indicate Pilot brand and Bic brand pens, which are separated along PC4.

Table 3.2: Individual clusters of blue ballpoint pen inks observed to be visually indistinguishable using PCA based on their Cary 4000 visible spectra.

Cluster	Pens
Group 1	Bic Pro Plus, Bic ReAction
Group 2	Bic Cristal Easy Glide, Bic Economy, Bic Orange Fine
Group 3	Pilot BP-145, Pilot BPS-GP, Pilot Super Grip
Group 4	Artline Ikonic, Artline Smoove, COS Capped Ballpoint, Office Choice Retractable, Staedtler Stick Click Retractable
Group 5	Artline Flow 4-Colour Retractable, PaperMate Ink Joy 100, PaperMate Ink Joy 300

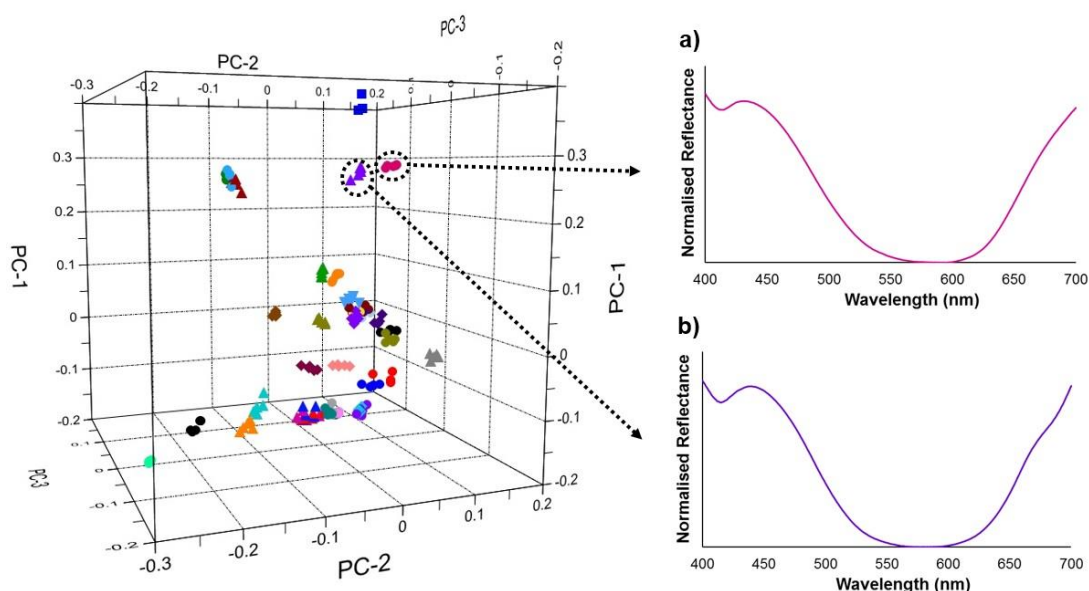


Figure 3.5: 3-dimensional PCA scores plot showing separation of (a) Celco Retractable and (b) PaperMate FlexGrip Elite inks, despite visually similar spectra.

3.3.3 Discriminant analysis

A discriminant model was constructed from the calibration set using the first four PCs, treating each ink as a discrete class. The efficacy of the model was then evaluated using a separate validation set comprising 12 inks. Six of these were deliberately chosen as exhibiting overlap or close clustering with other inks in the PCA plot, in order to observe how the model would handle these more challenging samples. The resultant model yielded correct classification accuracies of 97.7 % for the calibration set (Table 3.3), and 71.7 % for the validation set (Table 3.4).

Table 3.3: Number of correct and incorrect classifications for samples in the calibration set using a four-PC LDA model. Labels in brackets indicate assigned groups. The overall classification accuracy was 97.7 %.

Pen Model	Correct	Incorrect	% Correct
Bic Cristal	5	0	100
Papermate Ink Joy 100	5	0	100
Artline Ikonic	5	0	100
Deer Ultrafine	5	0	100
Artline 7210	5	0	100
PaperMate Kilometrico	5	0	100
Bic ReAction	5	0	100
Celco Retractable	5	0	100
Bic Orange Fine	4	1 (Bic Economy)	80
Keji Ballpoint	5	0	100
Office Basics Ballpoint	5	0	100
Artline Smoove	5	0	100
J.Burrows Ballpoint	5	0	100
Bic Round Stic	5	0	100
Artline Flow 4-Colour Retractable	5	0	100
Artline Clix 4-Colour	5	0	100
Bic Cristal Easy Glide	5	0	100
Bic Economy	4	1 (Bic Orange Fine)	80
Pilot G-2 05	5	0	100
Pilot Super Grip	5	0	100
Uniball Power Tank	5	0	100
Pilot BPS-GP	4	1 (Pilot BP-145)	80
PaperMate Profile	5	0	100
Bic Pro Plus	4	1 (Bic ReAction)	80
PaperMate FlexGrip Elite	5	0	100
Pentel Rolly	5	0	100
PaperMate Kilometrico Elite	5	0	100
Staedtler Triplus 426	5	0	100
Staedtler Stick Click Retractable	5	0	100
Pilot BP-145	5	0	100
PaperMate FlexGrip Ultra	5	0	100
PaperMate Ink Joy 300	5	0	100
Office Choice Retractable	5	0	100
COS Capped Ballpoint	5	0	100
Staedtler 430	5	0	100
	171	4	97.7

Table 3.4: Number of correct and incorrect classifications for samples in the validation set using a four-PC LDA model. Labels in brackets indicate assigned groups. The overall classification accuracy was 71.7 %.

Pen Model	Correct	Incorrect	% Correct
Bic Cristal M	5	0	100
Office Basics Ballpoint	5	0	100
J.Burrows Ballpoint	5	0	100
Bic Economy	0	5 (Bic Orange Fine)	0
Uniball Power Tank	4	1 (Bic Cristal)	80
Pilot BPS-GP	4	1 (Pilot BP-145)	80
Bic Pro Plus	2	3 (Bic ReAction)	40
PaperMate Flexgrip Elite	3	2 (J.Burrows Ballpoint)	60
Pentel Rolly	5	0	100
Staedtler Triplus 426	4	1 (Staedtler Stick Click)	80
PaperMate Ink Joy 300	5	0	100
Office Choice Retractable	1	4 (Staedtler Stick Click)	20
Total	43	17	71.7

As expected, most incorrect classifications were obtained against inks that exhibited overlap in the PCA. For example, ink from the Bic Economy pen was predicted as originating from a Bic Orange Fine. These results were confirmed upon inspection of the discriminant values; distance measures between projected samples and the centroid of a given class. In LDA, assignment of an unknown sample is made to the group yielding the smallest magnitude discriminant value, indicative of the ‘closest fit’. In this instance, it can be seen that the spectra of the Bic Economy lie closer to the centroid of the Bic Orange Fine class, thus resulting in an incorrect classification (Table 3.5). However, similar magnitude values could be obtained against both classes, and the standard deviation ranges of each class overlap, implying a high ratio of *intra*-sample to *inter*-sample variability. This suggests that the Bic Orange Fine and Bic Economy classes are not in fact well separated, and that classifications cannot be made to these groupings with confidence. It is therefore important to examine the discriminant values or other output data before accepting classifications provided by LDA, in order to assess the confidence of the result.

Table 3.5: Discriminant values of Bic Economy validation samples against the Bic Orange Fine and Bic Economy classes.

	Discriminant Values	
	Bic Orange Fine	Bic Economy
Bic Economy Validation-1	-24.2	-304.4
Bic Economy Validation-2	-11.9	-62.6
Bic Economy Validation-3	-71.5	-269.0
Bic Economy Validation-4	-24.2	-120.8
Bic Economy Validation-5	-10.4	-38.5
Average	-28.4	-159.1
Standard Deviation	24.9	120.9

It was noted that the Office Basics and PaperMate Ink Joy 300 inks were correctly predicted, despite their similar clustering with other inks in the PCA distribution. Examination of the discriminant values confirmed that these inks fell within a relatively close distance to other inks in the population (Table 3.6), although the separation in both cases was more distinct than that observed between the Bic Orange Fine and Economy. Nonetheless, classifications made to these groups should again be treated with caution.

Table 3.6: Averaged discriminant values and associated standard deviations for Office Basics and PaperMate Ink Joy 300 validation samples against the two nearest classes. Values are averaged across five replicates.

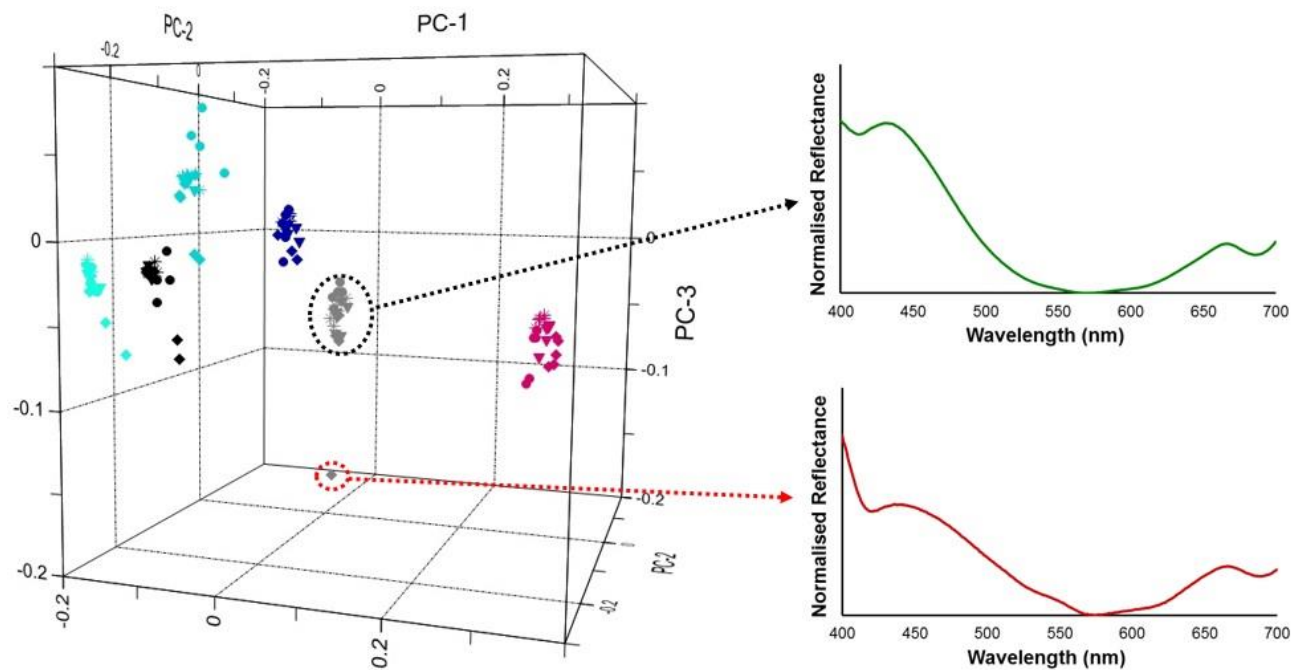
Validation Sample	Class	Average	Standard Deviation
Office Basics	Office Basics	-126.3	139.2
	Staedtler Stick Click	-2980.7	615.3
PaperMate Ink Joy 300	PaperMate Ink Joy 300	-49.0	19.2
	PaperMate Ink Joy 100	-511.4	222.4

16.7 % of spectra, while not correctly assigned to a specific pen, were assigned to the correct pen supplier. This can be seen in Table 3.4 above, in which replicates of the Bic Economy, Bic Pro Plus, Pilot BPS-GP and Staedtler Triplus inks were assigned to other pens from the same brand. With exception of the latter, this is consistent with the overlap observed between certain Bic or Pilot pens (Table 3.2), which was attributed to these suppliers possibly using the same ink in multiple pen models. Hence, even in scenarios where an unknown ink cannot be uniquely attributed to a given pen, the model may still be capable of determining the pen supplier. Alternatively, the model could also be utilised for exclusionary purposes. As seen above, examination of either the PCA scores or discriminant values clearly identifies ink formulations that are dissimilar. On this basis, it is possible to reduce the number of potential source pens that an unknown ink could belong to, narrowing the scope for further examinations.

3.3.4 Characterisation of naturally aged samples

Inks from six newly purchased pens were left to undergo natural ageing under three office conditions, with spectroscopic analysis at intervals ranging from 1 day to 14 months after deposition. This segment of study employed inks that were clearly discriminated in the PCA model, to ensure that any changes in classification could be attributed to ageing rather than coincidental overlap. Over the 14 month period, four of the six ink samples stored in the dark and open to air still gave 100 % correct predictions using the LDA model. Individual replicates of the PaperMate Profile and Office Basics inks were misclassified as early as one week after deposition; though as the remaining spectra were correctly classified, the overall classification of the ink remained unchanged (Table 3.7).

These results were confirmed through projection of the aged ink deposits onto the original PCA model, which revealed the samples to largely remain clustered with their equivalent fresh ink deposits (Figure 3.6). Both the Celco Retractable and Keji Ballpoint inks exhibit very tight clustering, indicating no discernible compositional changes within these deposits over the ageing period. The Office Basics inks are similarly grouped very closely together with exception of a single spectrum acquired at 14 months, which was the only misclassified replicate for this ink. Visual inspection revealed this spectrum to significantly differ from the remaining spectra (Figure 3.6), and so this replicate was omitted as an outlier.



- | | | |
|---------------------------------|---------------------------------------|----------------------------|
| ● Celco Retractable | ● Office Basics Ballpoint | ● Pentel Rolly |
| * Celco Retractable - 2 Months | * Office Basics Ballpoint - 2 Months | * Pentel Rolly - 2 Months |
| ▼ Celco Retractable - 6 Months | ▼ Office Basics Ballpoint - 6 Months | ▼ Pentel Rolly - 6 Months |
| ◆ Celco Retractable - 14 Months | ◆ Office Basics Ballpoint - 14 Months | ◆ Pentel Rolly - 14 Months |
| ● Keji Ballpoint | ● PaperMate Profile | ● Pilot G-2 05 |
| * Keji Ballpoint - 2 Months | * PaperMate Profile - 2 Months | * Pilot G-2 05 - 2 Months |
| ▼ Keji Ballpoint - 6 Months | ▼ PaperMate Profile - 6 Months | ▼ Pilot G-2 05 - 6 Months |
| ◆ Keji Ballpoint - 14 Months | ◆ PaperMate Profile - 14 Months | ◆ Pilot G-2 05 - 14 Months |

Figure 3.6: 3-dimensional PCA projection plot showing the distribution of fresh and aged inks stored open to air in the dark following various periods of exposure. Red arrow indicates Office Basics spectrum identified as an outlier.

The remaining three inks gave a greater overall spread, although similar levels of variance can be seen amongst replicates acquired at different intervals and those collected on the same date. Consequently, it cannot be stated with certainty whether these variations are indicative of a compositional change, or merely due to instrumental variation and inhomogeneity within the ink deposit.

Spectra from three of the inks stored in plastic sleeves out of light were also misclassified at varying points during the exposure period. As with the samples stored in the dark and open to air, this was again largely limited to single replicates (Table 3.8). The overall classification of the inks across the ageing period thus remained unchanged, with exception of the Office Basics ink at 13 months, which yielded three misclassified spectra. This caused the ink to be wrongly assigned to a J.Burrows ballpoint pen. Following an additional month, the ink was again correctly assigned with only one misclassified replicate. The previous result is hence likely to have been caused by instrumental variation, rather than an actual compositional change in the ink

Table 3.7: Number of misclassified replicate spectra for Office Basics Ballpoint and PaperMate Profile ink samples stored open to air in the dark, at various intervals following ink deposition. Labels in brackets indicate assigned groups.

Ageing Period	Pen 11 (Office Basics)	Pen 23 (PaperMate Profile)
1 Day	-	-
1 Week	-	1 (Pen 10)
2 Weeks	-	-
1 Month	-	-
2 Months	-	1 (Pen 10)
4 Months	-	1 (Pen 10)
6 Months	-	1 (Pen 10)
8 Months	-	-
10 Months	-	-
13 Months	-	-
14 Months	1 (Pen 33)	1 (Pen 1)

Table 3.8: Number of misclassified replicate spectra for Keji Ballpoint, Office Basics Ballpoint and PaperMate Profile inks stored in plastic sleeves in the dark, at various intervals following ink deposition. Labels in brackets indicate assigned groups.

Ageing Period	Pen 10 (Keji Ballpoint)	Pen 11 (Office Basics)	Pen 23 (PaperMate Profile)
1 Day	-	1 (Pen 13)	-
1 Week	-	-	-
2 Weeks	-	-	-
1 Month	-	-	-
2 Months	-	-	-
4 Months	-	1 (Pen 13)	-
6 Months	1 (Pen 18)	1 (Pen 13)	-
8 Months	-	1 (Pen 13)	-
10 Months	-	1 (Pen 13)	1 (Pen 10)
13 Months	-	3 (Pen 13)	1 (Pen 1)
14 Months	1 (Pen 18)	1 (Pen 13)	1 (Pen 10)

PCA projection again found that the aged inks largely remained clustered with their corresponding fresh deposits (Figure 3.7). Of note, spectra from the Pilot G-2 05 ink showed less intra-class variation when stored in plastic archive sleeves than when left open to air (Figure 3.6), suggesting that this ink remains more chemically stable when exposure to air is minimised. This in turn may indicate that the ink formulation is vulnerable to ageing mechanisms based on oxidation or the evaporation of volatiles. On the other hand, spectra from the Keji Ballpoint ink were more closely clustered when the sample was left open to air.

Previous research by Grim *et al.* proposed that during the demethylation of dyes such as methyl violets (as depicted in Figure 3.2), solvent molecules provide the protons to replace the lost methyl substituents.^[364] It is therefore possible that the trapping of solvent within the plastic sleeve results in the acceleration of this process, or alternatively that plasticisers contained in the sleeves undergo a chemical interaction with the ink. The discrepancy in results obtained from different inks indicates that the mechanisms of ageing can potentially vary according to the precise ink composition.

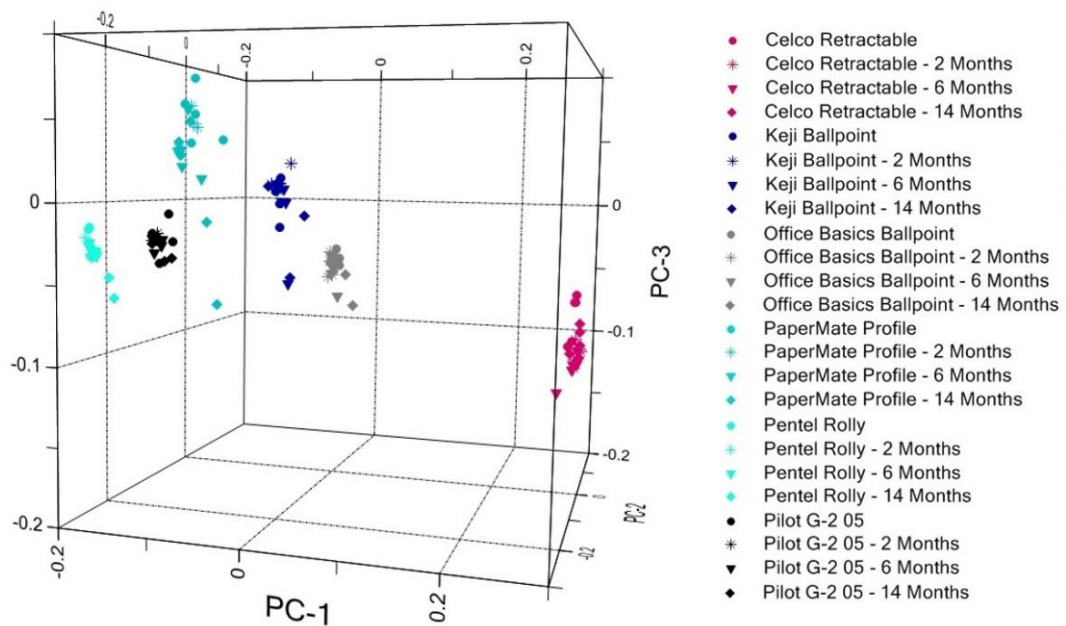


Figure 3.7: 3-dimensional PCA projection plot showing the distribution of fresh and aged blue ballpoint inks stored in plastic sleeves in the dark following various periods of exposure.

When inks were exposed to ambient light in addition to open air, two inks (Celco Retractable and PaperMate Profile) were misclassified within just one week. Upon two months of ageing, incorrect predictions were obtained for all inks except the Pentel Rolly (Table 3.9). It was noted that each of the inks aged at different rates, with the first misclassification occurring at different points within the two-month period. This is consistent with findings in previous studies, which found that the rate of ageing is at least partially dependent on the initial ink composition, such as the volatility of solvents or the stability of the various dyes and pigments.^[364-366]

Photographic images of the ink deposits show a visual colour darkening of the Celco and PaperMate ink deposits following two months of exposure (Figure 3.8), consistent with their misclassification by the model. Conversely, no clearly evident changes were discerned in the visual appearance of the Pentel, Keji, Office Basics or Pilot inks, despite erroneous classifications of the latter three. This highlights the necessity of objective colour measurement techniques when conducting forensic comparisons, as instrumental analysis may detect changes not immediately apparent through visual inspection. With exception of the Pentel Rolly all inks were noted to become visually darker upon further ageing for six months, with fading of the Celco and Office Basics inks then observed between 6 months and 14 months.

Table 3.9: Number of misclassified replicate spectra for six blue ballpoint ink samples stored open to light, at various intervals following ink deposition. Labels in brackets indicate assigned groups.

Ageing Period	Pen 8 (Celco Retractable)	Pen 10 (Keji Ballpoint)	Pen 11 (Office Basics)	Pen 19 (Pilot G-2 05)	Pen 23 (PaperMate Profile)	Pen 26 (Pentel Rolly)
1 Day	-	-	-	-	-	-
1 Week	5 (Pen 13)	-	-	-	5 (Pen 10)	-
2 Weeks	5 (Pen 13)	3 (Pen 24) 2 (Pen 18)	1 (Pen 13)	-	3 (Pen 10) 1 (Pen 20) 1 (Pen 22)	-
1 Month	5 (Pen 13)	2 (Pen 24) 3 (Pen 18)	4 (Pen 13)	-	3 (Pen 1) 1 (Pen 20) 1 (Pen 22)	-
2 Months	5 (Pen 13)	5 (Pen 11)	5 (Pen 13)	5 (Pen 22)	1 (Pen 1) 3 (Pen 20) 1 (Pen 22)	-
4 Months	5 (Pen 13)	5 (Pen 13)	5 (Pen 13)	5 (Pen 30)	4 (Pen 22) 1 (Pen 30)	-
6 Months	5 (Pen 13)	2 (Pen 13)	5 (Pen 13)	5 (Pen 27)	5 (Pen 22)	-
8 Months	5 (Pen 13)	1 (Pen 33)	5 (Pen 13)	3 (Pen 27) 2 (Pen 13)	4 (Pen 22) 1 (Pen 30)	-
10 Months	4 (Pen 13) 1 (Pen 34)	1 (Pen 33)	5 (Pen 13)	3 (Pen 29) 1 (Pen 13) 1 (Pen 33)	2 (Pen 22) 2 (Pen 16) 1 (Pen 30)	-
13 Months	3 (Pen 19) 2 (Pen 34)	5 (Pen 33)	4 (Pen 33) 1 (Pen 30)	3 (Pen 13) 2 (Pen 29)	4 (Pen 16) 1 (Pen 19)	-
14 Months	3 (Pen 19) 2 (Pen 34)	3 (Pen 33) 1 (Pen 16) 1 (Pen 24)	2 (Pen 33) 2 (Pen 30) 1 (Pen 19)	5 (Pen 13)	4 (Pen 16) 1 (Pen 19)	-

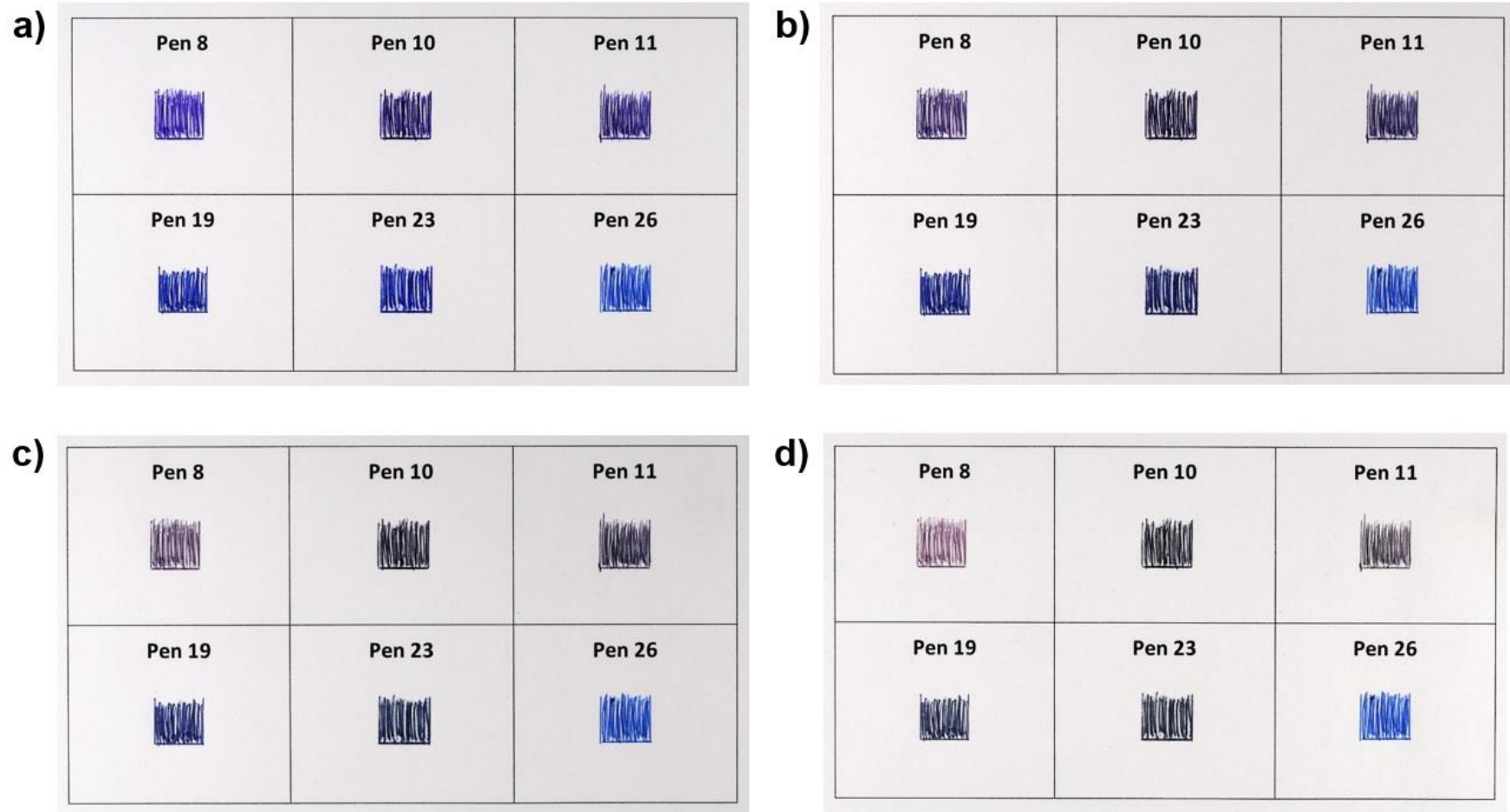
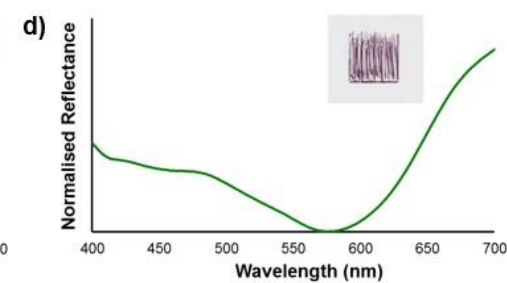
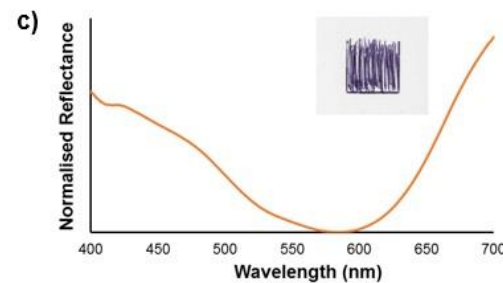
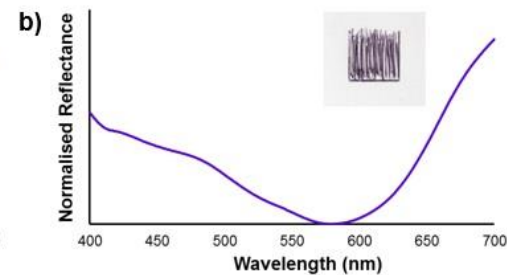
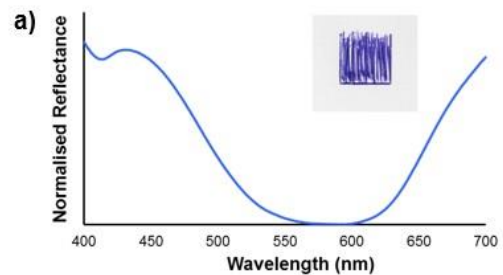
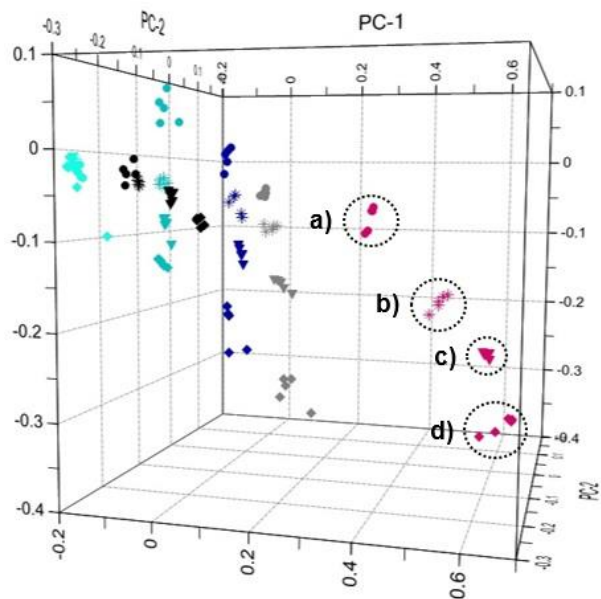


Figure 3.8: Photographic images of six blue ballpoint ink deposits stored open to light, (a) immediately following deposition; then following (b) 2 months, (c) 6 months and (d) 14 months of exposure.

Over the 14 month period, the classifications of the light-exposed inks changed several times. These classifications, as well as the changes in the visual appearance of the deposits, indicate that the ageing process of these inks is still ongoing. This is apparent in the PCA projection plot (Figure 3.9), where the aged deposits continually drift further from the baseline samples with time. The PCA projection also illustrates the different rates of ageing observed in the inks. The Celco Retractable and PaperMate Profile inks shifted the furthest from the baseline samples within the first two months, hence being the first to become misclassified. These ink formulations can thus be considered as fast-ageing. In contrast, slow-ageing samples such as the Pilot G-2 05 and Pentel Rolly remained clustered with their fresh ink equivalents until at least six months of exposure.

Spectra acquired from the Celco Retractable ink over the 14 month period exhibited a decreasing relative reflectance in the blue region (c.a. 430 nm) and increasing reflectance in the red region (700 nm), resulting in the visible colour change described above. Examination of the spectra for the remaining samples revealed that this change was observable in all inks except for the Pentel Rolly (Figure 3.10). Peaks in the blue region of the Keji, Office Basics and PaperMate Profile spectra were also found to broaden towards the red region, whilst portions of the Celco and Pilot inks underwent a shift towards the blue region.

Inspection of the PCA factor loadings (Figure 3.11) allows the spectral changes of the inks to be related to the shift in these spectra on the scores plot. As seen in Figure 3.9, the majority of inks obtained more negative scores along PC3 as the ageing period increased. This PC exhibits a positive correlation in the blue region at ca. 450 nm; hence as the reflectance decreases in this region, the scores attained along the PC become more negative. Similarly, PC1 exhibits a strong positive correlation at 700 nm, and a negative correlation between 400 – 500 nm. As the relative reflectance decreases in the blue region and increases in the red region, the scores attained along PC1 therefore become more positive, as seen for the Pilot and Celco inks.



- Celco Retractable
- * Celco Retractable - 2 Months
- ▼ Celco Retractable - 6 Months
- ◆ Celco Retractable - 14 Months
- Keji Ballpoint
- * Keji Ballpoint - 2 Months
- ▼ Keji Ballpoint - 6 Months
- ◆ Keji Ballpoint - 14 Months

- Office Basics
- * Office Basics - 2 Months
- ▼ Office Basics - 6 Months
- ◆ Office Basics - 14 Months
- PaperMate Profile
- * PaperMate Profile - 2 Months
- ▼ PaperMate Profile - 6 Months
- ◆ PaperMate Profile - 14 Months

- Pentel Rolly
- * Pentel Rolly - 2 Months
- ▼ Pentel Rolly - 6 Months
- ◆ Pentel Rolly - 14 Months
- Pilot G-2 05
- * Pilot G-2 05 - 2 Months
- ▼ Pilot G-2 05 - 6 Months
- ◆ Pilot G-2 05 - 14 Months

Figure 3.9: 3-dimensional PCA projection plot showing the distribution of fresh and aged blue ballpoint inks exposed to light following various periods of exposure, with spectra and photographic images (recorded under identical conditions) obtained at each interval for the Celco Retractable ink.

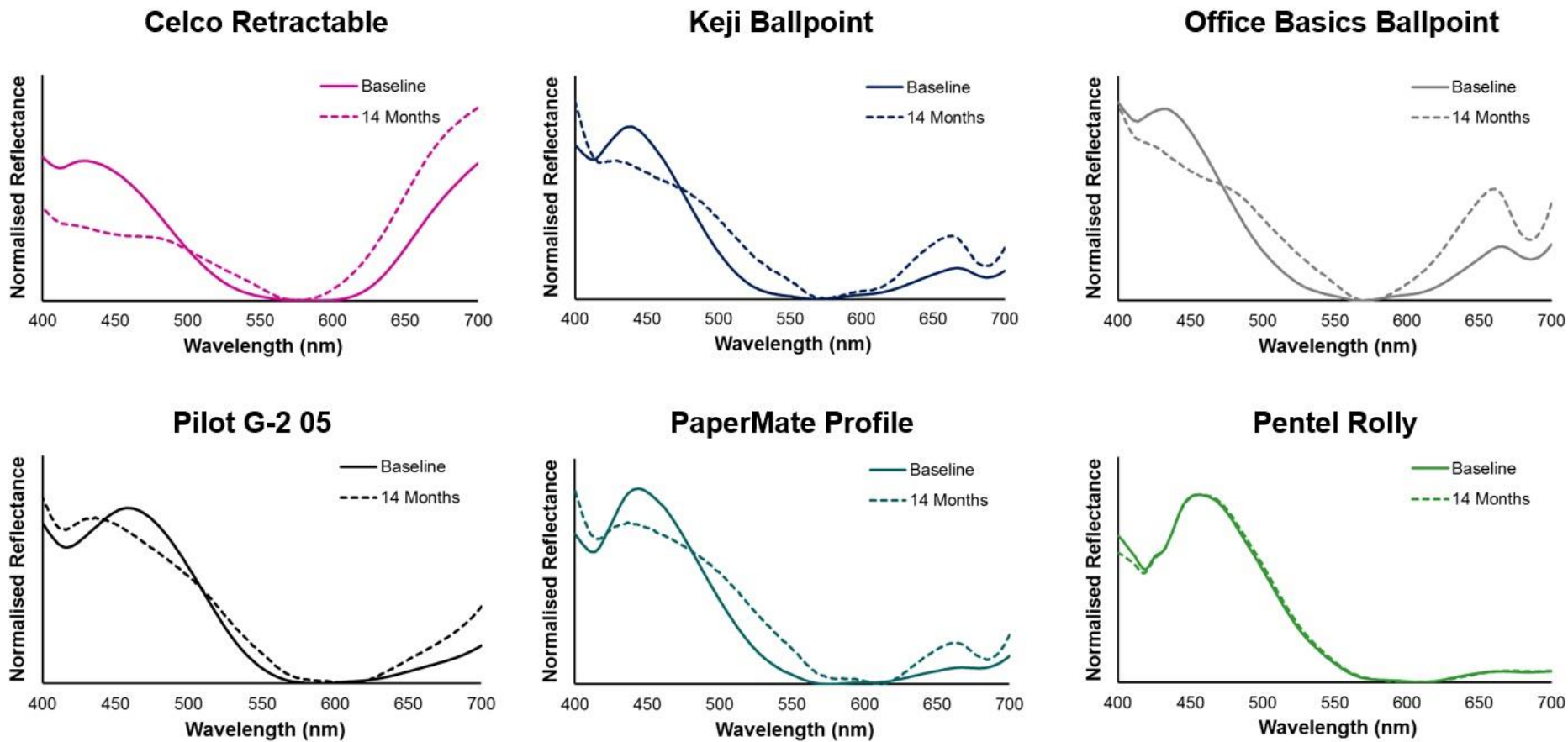


Figure 3.10: Spectra of Celco Retractable, Keji Ballpoint, Office Basics, PaperMate Profile and Pilot G-2 05 ink deposits stored open to light; (a) immediately after deposition and (b) following 14 months of exposure.

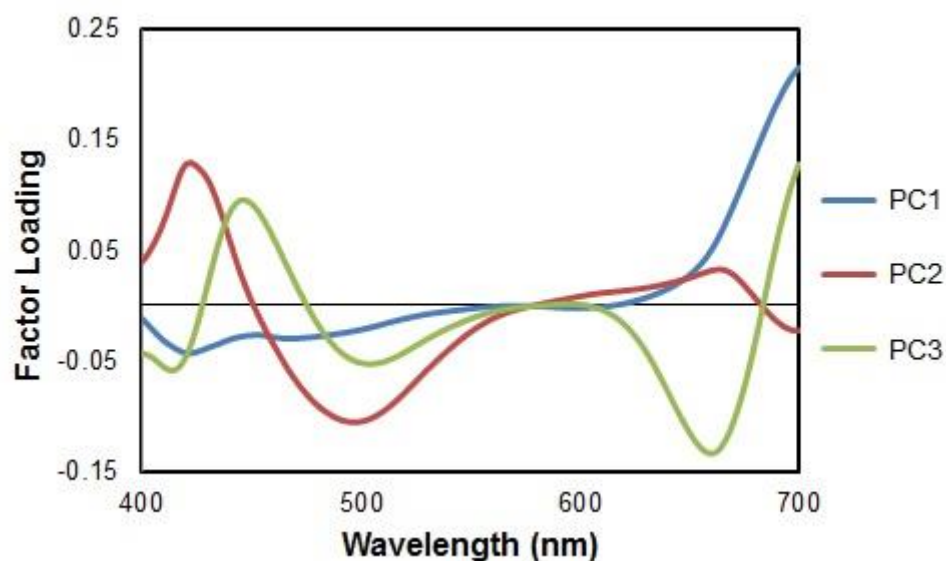


Figure 3.11: Factor loadings of the first three PCs for PCA conducted on the population of 35 blue ballpoint inks.

Due to the proprietary nature of the ink formulations and the lack of structural information discernible from visible spectra, it cannot be said with certainty which ink components are responsible for the observed ageing effects. However, as these changes were limited to samples exposed to light, it is a reasonable assumption that they can be attributed to the photofading of triarylmethane dyes such as methyl or crystal violet.

As discussed at the beginning of this chapter, triarylmethane dyes can undergo oxidative demethylation or cleavage reactions catalysed by titanium dioxide present in paper products.^[354, 358] The shade of these dyes is also influenced by their degree of methylation, with decreasing methyl substitution resulting in the dye colour shifting from blue-violet to red-violet. The red shifts observed in the spectra of the Keji, Office Basics and PaperMate inks is therefore a potential indicator of dye degradation occurring via *N*-demethylation. Conversely, the blue shifts displayed by the Celco and Pilot inks suggests that degradation processes may be occurring through alternative mechanisms such as photooxidative cleavage.

Spectral changes due to ageing pose an obvious challenge in applying chemometric models to ‘real’ samples, which may be several weeks to years old. The rapid alteration of visible spectra following deposition may result in ink entries created using the same pen being falsely excluded due to their different deposition dates or storage history.

Incorrect information could also be generated when attempting to predict or identify an aged ink on the basis of its visible spectrum. Fortunately, such samples can be identified as atypical through their discriminant values. Table 3.10 shows the discriminant values obtained by the aged Celco Retractable ink for the J.Burrows pen, to which the ink was incorrectly classified. The discriminant values against this group are several orders of magnitude larger than those from actual J.Burrows ink, demonstrating that the aged ink is not well classified.

It should also be noted that in certain investigative instances, the rapid ageing of deposited inks may in fact be beneficial. In cases of suspected fraud or forgery, it is often of interest to determine whether an ink entry could have been modified at a later date from its original creation. Examples of this may include the contemporaneous signing of legal documents or the suspected alteration of banking cheques. These analyses may be complicated if changes have been made using the same pen as the original entry. However, the results here suggest that entries completed using the same pen, as little as one week apart, may be differentiable if the document has been exposed to light during the intervening period.

Table 3.10: Mean and standard deviations of LDA discriminant values for aged Celco Retractable ink against the predicted class(es), compared to true ink of that class. Values are averaged over five replicate spectra.

Pen	J.Burrows Ballpoint		COS Capped Ballpoint		Pilot G-2 05	
	Mean	Std. Deviation	Mean	Std. Deviation	Mean	Std. Deviation
Celco Retractable – 1 Week	-7869.4	991.9	-	-	-	-
Celco Retractable – 2 Weeks	-9056.7	1469.8	-	-	-	-
Celco Retractable – 1 Month	-12078.0	1612.3	-	-	-	-
Celco Retractable – 2 Months	-11784.8	2263.4	-	-	-	-
Celco Retractable – 4 Months	-10037.4	1412.3	-	-	-	-
Celco Retractable – 6 Months	-9145.0	335.3	-	-	-	-
Celco Retractable – 8 Months	-7703.2	284.7	-	-	-	-
Celco Retractable – 10 Months	-8641.8	527.1	-	-	-20642.8	10332.8
Celco Retractable – 13 Months	-	-	-11436.1	301.4	-10145.4	3840.6
Celco Retractable – 14 Months	-	-	-11797.9	394.1	-9837.1	3603.4
J. Burrows Ballpoint	-3.2	3.7×10^{-6}	-	-	-	-
COS Capped Ballpoint	-	-	-3.2	2.9×10^{-6}	-	-
Pilot G-2 05	-	-	-	-	-3.2	3.8×10^{-6}

3.3.5 Development of dating models for light-exposed samples

The results obtained from both PCA and LDA indicate that the ageing of ink deposits under ambient light is a dynamic process, with changes continuing to occur over at least a 14 month period. These changes could potentially be used to develop chemometric models for the age estimation of unknown ink entries. With this in mind, calibration curves were generated for the inks using PLSR; a multivariate regression technique that maximizes the covariance between the predictor and response variables. PLSR models were constructed for each of the light-exposed inks using the spectra acquired over the 14 month ageing period. For each model, a scree plot was used to select the optimal number of factors to retain for regression, as summarised below.

Table 3.11: Number of selected factors and corresponding percentage of total variance for PLSR models of blue ballpoint inks exposed to light over a 14 month period.

Ink	Factors	% Total Variance
Celco Retractable	3	99.2
Keji Ballpoint	3	99.0
Office Basics Ballpoint	1	98.6
Pilot G-2 05	1	96.2
PaperMate Profile	3	98.8
Pentel Rolly	6	98.6

Scores plots were generated for each model using the first two factors, as depicted in Figure 3.12. It can be seen that the spectra of each ink generally attain more positive scores along Factor 1 with time, with exception of the Pentel Rolly ink. The latter was expected to give significant overlap between spectra of different exposure intervals, as this ink remained correctly classified even after 14 months. This result is also consistent with the previous PCA projection of these inks (Figure 3.9), in which all except the Pentel Rolly ink exhibited a clear shift along the PCs over the exposure period. Ink from the Keji and PaperMate Profile pens also show a degree of overlap between spectra collected at each analysis date, indicating that the ageing of these inks is gradual in comparison to the Celco, Office Basics or Pilot inks, in which the separation between the ageing intervals is more distinct. This contrasts with the previous characterisation of the PaperMate Profile ink by PCA as fast-ageing, and further examination of the discrepancy between the two methods would be of interest.

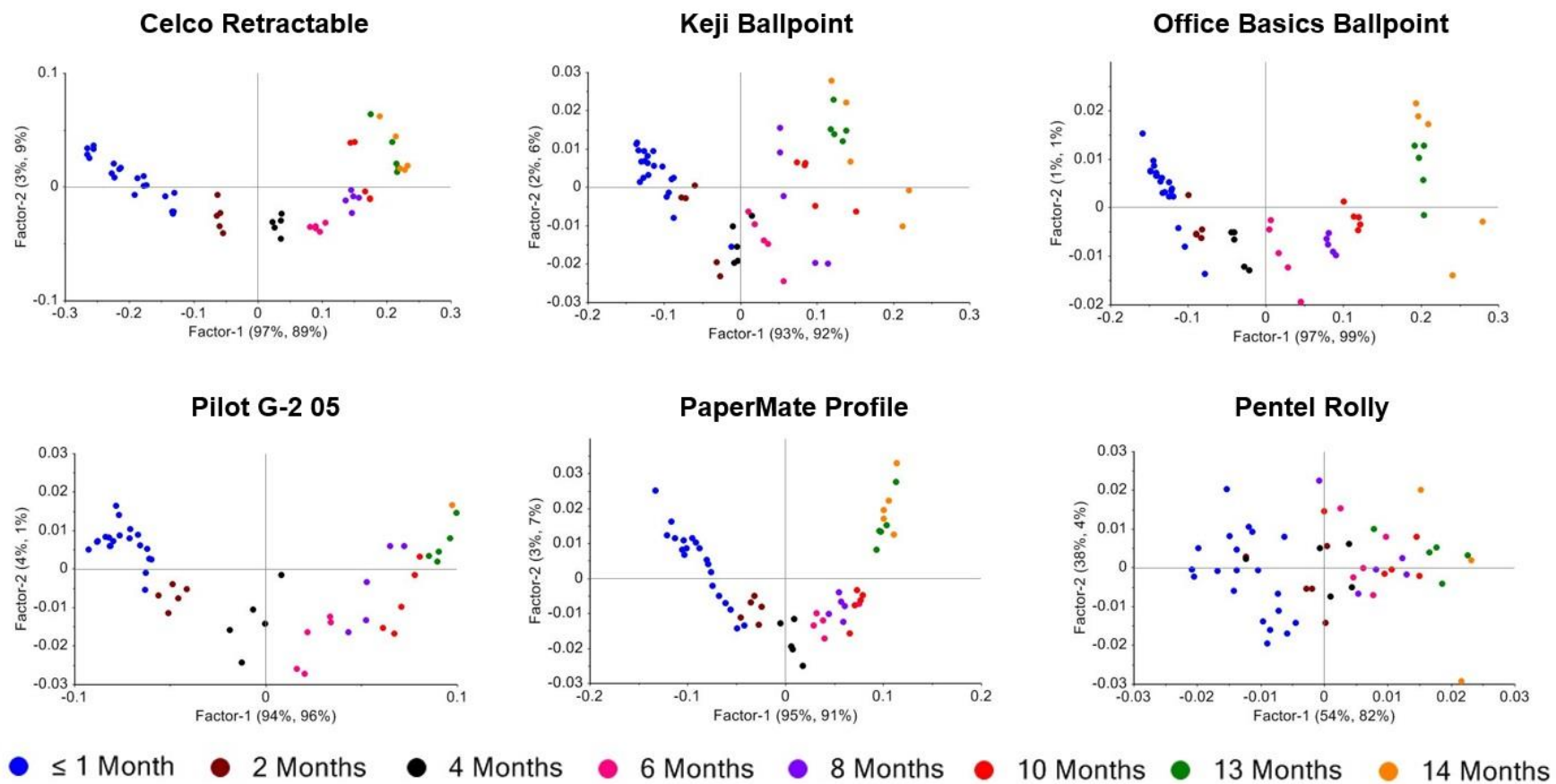


Figure 3.12: 2-dimensional PLSR scores plots showing the distribution of six blue ballpoint inks exposed to light following various periods of exposure. Spectra collected at intervals within the first month of exposure have been colour-coded as a single group, but were treated as separate variables in the regression analysis.

Dispersion graphs of the actual and predicted ageing intervals are shown in Figure 3.13. Excellent agreement was observed between the reference and estimated values both in the calibration and cross-validation, with correlation coefficients greater than 0.96 obtained for all models including the Pentel Rolly ink. Based on this high correlation, it would appear that PLSR is a highly suitable means of modelling the dataset, and that the resultant models could be expected to demonstrate good predictive capability in estimating the age of an unknown ink deposit.

The constructed regression models were evaluated using a separate validation set of ink deposits aged for up to 21 weeks. As these deposits were prepared approximately seven months after the initial ageing samples, baseline spectra from each deposit were first predicted using the discriminant model, in order to determine whether any significant compositional changes in the inks had occurred during the intervening period. All spectra were correctly assigned, indicating the inks to have remained chemically stable within the pen cartridges throughout the storage period.

These results are consistent with earlier research by Andrasko and Kunicki, who found no evidence of dye degradation in ink entries produced from the same pen up to 6 years apart.^[367] Grim *et al.* similarly found that dyes within the ink cartridges of pens stored for up to 20 years remained predominantly unchanged, although a small number of inks exhibited ageing at an even greater rate than when deposited on a paper substrate.^[360] In these studies, however, no specification was made regarding the storage conditions of the pens in between analyses. For this research, all pens were kept in a closed office cupboard when not in use. It is possible that ink ageing within the cartridge may occur in pens left exposed to light; particularly for those with a transparent housing; and this may be the subject of future investigation.

The regression results obtained for the validation samples at each analysis date are summarised in Table 3.12. Despite the high correlation coefficients obtained for each regression line, the majority of the regression models proved to be highly inaccurate, yielding age estimations substantially different from the actual age of the deposit. In fact, negative exposure times were often predicted even for ink deposits over one month old. In contrast, estimations for the Office Basics ink were reasonably accurate, with the predicted and actual ages consistently falling within two weeks of each other.

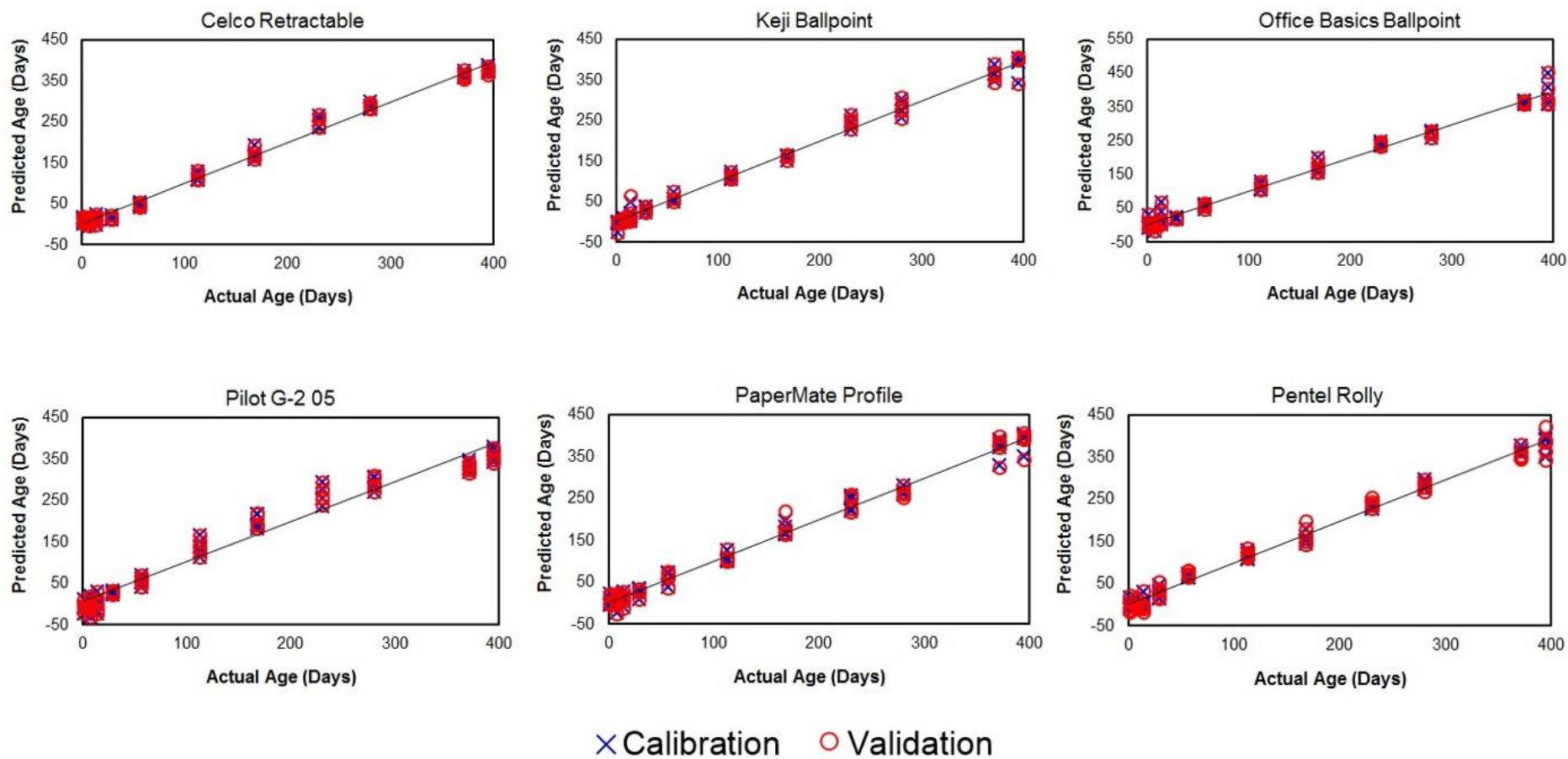


Figure 3.13: Reference values versus estimated values by PLSR models for the age estimation of six blue ballpoint inks exposed to light over a 14 month period.

Table 3.12: Mean and standard deviations of estimated ageing periods for validation blue ballpoint ink deposits exposed to light, compared to actual ageing periods. Values are averaged over five replicate spectra.

Actual Ageing Period	Estimated Ageing Period (Days)											
	Celco Retractable		Keji Ballpoint		Office Basics		Pilot G-2 05		PaperMate Profile		Pentel Rolly	
	Mean	Std. Dev.	Mean	Std. Dev.	Mean	Std. Dev.	Mean	Std. Dev.	Mean	Std. Dev.	Mean	Std. Dev.
0 Days	6.0	3.9	-29.9	7.7	0.9	6.9	-29.9	6.5	14.2	12.6	-75.1	18.1
6 Days	-10.0	3.1	-45.0	5.7	2.9	6.2	-18.3	15.3	-20.9	14.5	-31.7	20.0
21 Days	-11.9	4.6	-18.8	13.2	29.8	25.2	-9.0	6.1	-7.2	21.4	-10.7	20.0
42 Days	4.1	9.9	-10.6	8.9	44.5	5.9	32.8	20.7	27.1	29.7	29.2	13.2
98 Days	73.8	8.9	43.3	23.3	106.8	7.1	80.2	5.0	91.6	25.7	135.2	27.6
147 Days	143.0	15.4	82.4	28.6	159.7	7.2	133.3	13.6	130.4	25.8	153.5	15.0

It should be noted, however, that the age estimates for all inks were highly variable between replicate spectra collected at a given analysis date. This is evident from the standard deviations, which in several instances are greater than the actual age estimate of the ink. Further work is thus required to determine whether the results obtained from the Office Basics ink can be consistently reproduced.

Upon closer inspection of the scores plots for each ink, it can be seen that although a shift in factor scores can be observed over time, the distance between spectra of different ages is similar or greater than that amongst spectra of the same ageing period. The similar magnitudes of *intra*-group and *inter*-group variance results in poor discriminative capability between inks of different ages, and hence inaccurate age estimations using the regression models. An additional figure of merit is the root mean square error of calibration (RMSEC) values obtained for each model. The RMSEC is a measure of the dispersion of calibration samples about the regression line, measured in the same units as the response variable.^[368, 369] Table 3.13 shows that despite the high correlations achieved, the RMSEC for each model is greater than many of the predicted values, indicating a disproportionately high level of scatter around the regression line. As mentioned in Chapter 1, random correlations are likely to occur in datasets containing large numbers of variables.^[196] The high correlations observed for the models may therefore have resulted from chance correlations rather than a causal relationship. This example highlights the potential pitfalls of over-relying on correlation values, without considering additional metrics such as the RMSEC to assess the regression quality.

It can be concluded that although clear spectral changes are observable in the ink deposits as a function of ageing, these changes are insufficiently modelled using PLSR as employed in this work. It is possible that employing alternative pre-processing or regression techniques on the collected data may yield improved results. It must also be considered that successful application of these models would require knowledge of both the pen type of the ink and the storage history of the document it is deposited on, which may not be possible when conducting forensic examinations of questioned documents. Future work should hence examine not only alternate approaches to developing chemometric ink dating models, but the extent to which these models could be readily applied within an operational context.

Table 3.13: Correlation coefficients and root mean square error of calibration (RMSEC) values obtained for PLSR models of blue ballpoint inks exposed to light over a 14 month period.

Ink	Correlation (R ²)	RMSEC
Celco Retractable	0.992	12.6
Keji Ballpoint	0.990	13.9
Office Basics Ballpoint	0.986	16.8
Pilot G-2 05	0.962	27.5
PaperMate Profile	0.988	15.6
Pentel Rolly	0.993	11.2

3.3.6 Characterisation of artificially aged samples

Artificial ageing experiments were carried out to examine the individual effects of heat and UV exposure on ink degradation, and to determine whether the induced changes provided a realistic comparison with naturally aged inks exposed to light and air. Samples of the six inks utilised in the natural ageing study were heated in an oven at 100 °C as recommended by Cantu, who proposed that four minutes at this temperature would provide an equivalent ageing to three months under natural conditions.^[370] After 20 minutes to 2 hours of heat exposure, ink from the PaperMate Profile pen was misclassified as originating from a Keji ballpoint. Following 24 hours, three spectra from the Celco Retractable ink were additionally attributed to a J.Burrows ballpoint pen. These results are consistent with changes observed in the first week of natural ageing under ambient light.

As mentioned previously, Grim *et al.* suggested that the solvent acts as a source of protons for the replacement of methyl substituents in the oxidative *N*-demethylation of methyl violet dyes.^[364] Thus, while a thermal approach may be suitable for representing changes in the ink's solvent content, the removal of solvent may hinder degradation of the dye molecules, thus resulting in little change to the visible spectrum of the ink. This supports conclusions from the natural ageing study that dye photofading has the key influence on the observed ageing of the inks. Nonetheless, the changes noted in thermally treated samples despite the absence of light indicates that solvent loss is also a relevant factor.

UV accelerated ageing was conducted by irradiating ink samples under a compact UV lamp. Inks from the PaperMate Profile and Celco Retractable pens were misclassified as Keji and J.Burrows inks respectively, following 24 hours of exposure. These results are again consistent with early changes noted in samples aged naturally for one week under open conditions. Interestingly, no further misclassifications were observed between 24 and 48 hours of irradiation. Siegel *et al.* postulated that the loss of methyl groups due to UV exposure yields stable products that resist further degradation.^[353] Alternatively, given the continuing changes in naturally exposed inks, it is perhaps more likely that the photodegradation of dyes is partially due to visible light rather than solely UV. Previous studies have achieved decolourisation of crystal violet and other triarylmethane dyes using visible irradiation in the presence of zinc oxide or titanium oxide.^[356, 371]

Figure 3.14 provides a comparison of the inks artificially aged for 24 hours and those aged naturally for one week, compared to freshly deposited ink. It can be seen that inks aged by UV irradiation show a greater shift away from their fresh counterparts compared to those that were thermally aged, though in both instances the direction of these shifts is consistent with naturally aged samples. Spectral changes in the artificially aged samples are also consistent with those obtained through natural ageing (Appendix 3.3). Hence, either approach can be considered to give a realistic depiction of natural ageing processes.

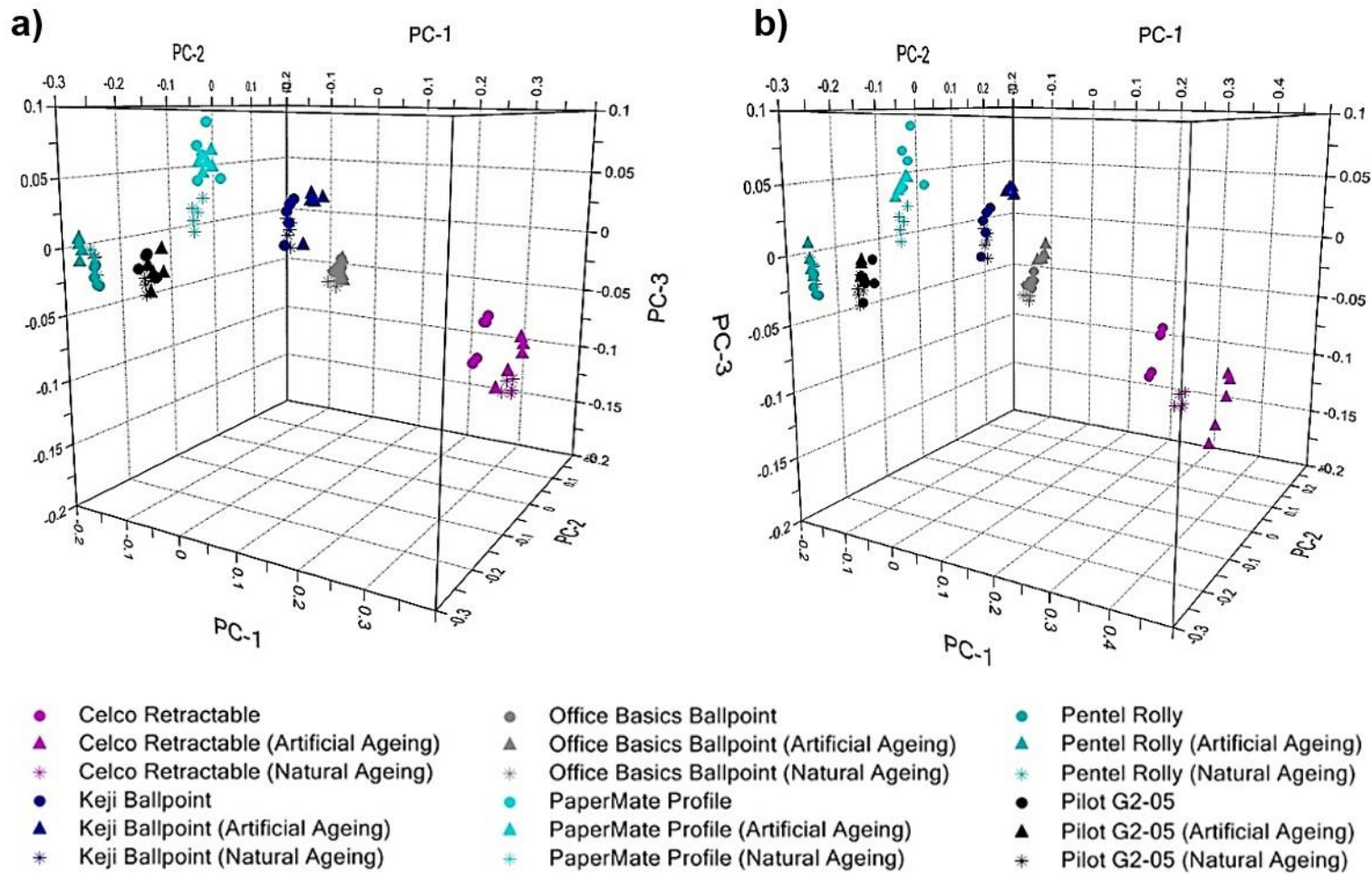


Figure 3.14: 3-dimensional PCA projection plot showing the distribution of inks aged naturally for one week and those artificially aged for 24 hours by (a) thermal exposure; and (b) UV irradiation, compared to freshly deposited ink.

3.4 Conclusions

The overall results of this study indicate that diffuse reflectance visible spectroscopy with chemometrics provides a simple, rapid and non-destructive method for distinguishing blue ballpoint inks on paper. The developed model may be employed as a screening method to compare multiple pen inks at a time, and exclude those which are dissimilar. Additionally, prediction using LDA may allow the identification of the source pen or supplier for an unknown ink where a known reference is unavailable, or where comparison with another sample is not of primary interest.

Analysis of six pen inks stored under different conditions found that inks stored in the dark could still be reliably predicted up to 14 months following deposition. Conversely, inks stored in the light could exhibit significant changes to their spectral profile within just one week, with these changes continuing over the 14 month period. This could prove beneficial when attempting to identify alterations made to a document using the same pen at a later date. PLSR was used to model these changes for ink dating purposes, but the estimations afforded by these models proved unreliable. Additionally, the application of such models would require knowledge of both the pen type and document storage conditions, which is often not possible when conducting questioned document examinations. Artificial ageing experiments determined that both thermal and UV exposure are significant in the ageing process of inks on paper, and that accelerated ageing through these mechanisms provides comparable results to short-term natural ageing under light.

It should be noted that the instrumentation used in this chapter may not be readily available within existing document examination laboratories, due to their high cost and the need for specialised accessories. The size of the ink deposits required for this methodology are also not representative of 'real' samples, such as handwriting, that are encountered in an operational context. The following chapter presents an investigation into the characterisation of more typical ink deposits using instrumentation routinely employed by practicing document examiners.

Chapter 4: Chemometric characterisation of blue ballpoint inks on paper using a video spectral comparator

4.1 Introduction

As described in Chapter 3, visible spectroscopy with chemometrics provides a rapid and non-destructive method for characterising inks on paper, as well as studying changes in their chemical composition as they age. The generated statistical model, while potentially useful as a means of forensic ink comparison, is limited in its applicability due to the relatively large (10 mm x 10 mm) ink deposits required for analysis, which are not representative of ‘real samples’ such as handwriting. Analysis of these samples requires instrumental methods with a much smaller aperture, such as micro-Raman or infrared microscopy. However, these techniques require specialised accessories that may not be available within a document examination laboratory.

An alternative method for collecting spectral data from document evidence is the use of a video spectral comparator (VSC). Developed by Foster + Freeman, this instrument is routinely utilised by forensic document examiners conducting specialised lighting examinations.^[372, 373] Samples are placed under an enclosed canopy and can be illuminated using various light sources and optical filters, allowing visualisation across the visible to near-infrared (NIR) range.^[374, 375] This may be used to discriminate between similar inks based on their differing luminescence characteristics.^[376, 377] Selected VSC models are also equipped with a video imaging system and automated spectrometer, enabling the collection of spectral and chromatic data.^[378, 379]

Within an Australian context, use of the VSC by forensic document examiners is primarily limited to the visual comparison of samples side-by-side under various viewing conditions.^[380] As a result, there are limited studies probing the discrimination of inks using their VSC spectra. Weyermann *et al.* compared VSC spectroscopy with microspectrophotometry (MSP) and laser desorption ionisation-MS in distinguishing 25 black gel inks, with the VSC yielding the lowest discriminatory power (DP) at 49 %.^[381] Reed *et al.* obtained a similarly low DP (38 %) for 14 black gel inks, though blue and red inks gave DP values of 82 % and 90 % respectively.^[374] It must be noted that these studies used different means of calculating the DP, and so the cited values are not directly comparable. Work by da Silva *et al.* employed partial least squares discriminant analysis to VSC spectra acquired from blue and black inks.^[105, 108] This methodology allowed the pen type and brand to be identified with a high degree of accuracy, but also necessitated individual models to be constructed for each class.

This study investigated the use of VSC reflectance spectra followed by pattern recognition chemometrics for the rapid characterisation of handwritten ink entries on paper. Chromaticity measurements and fluorescence characteristics were evaluated as a means of providing additional discrimination between similar ink formulations, potentially yielding more specific results.

4.2 Experimental

4.2.1 Sample preparation

This study employed the same population of 35 blue ballpoint pens described in Chapter 3. Ink from each pen was deposited onto commercial white copy paper (Fuji Xerox Professional Carbon Neutral, 80 g/m²) by writing each pen’s model identifier. An additional ink trace was prepared from 12 pens selected as an external validation set (Table 4.1). All pens were stored in a paper bag in a closed office cupboard when not in use.

Table 4.1: Models and assigned numeric identifiers for pens utilised as validation samples.

Pen ID	Pen Model	Pen ID	Pen Model
1	Bic Cristal	24	Bic Pro Plus
8	Celco Retractable	25	PaperMate FlexGrip Elite
11	Office Basics Ballpoint	26	Pentel Rolly
13	J.Burrows Ballpoint	28	Staedtler Triplus 426
18	Bic Economy	32	PaperMate Ink Joy 300
19	Pilot G-2 05	33	Office Choice Retractable

4.2.2 Data collection

Spectra and chromaticity values were obtained using a VSC5000 (Foster + Freeman, UK), with instrument control and data acquisition performed using the VSC5000 software (v.5.7). Spectra were acquired in reflectance mode using the manufacturer provided white tile as the ‘standard white’ reference. The instrument was operated under 100 % flood illumination, 50 % brightness/contrast and automatic exposure settings. Spectra were recorded over the range 400 – 1000 nm, with a scan interval of 3 nm. Validation samples were analysed one week following the calibration deposits.

4.2.2.1 Method development

Spectra were acquired using magnification levels of approximately 10 – 50x, and regions of interest ranging from 4 x 4 pixels to 16 x 16 pixels. The placement of black material around the ink trace was also investigated as a means to reduce background light scattering from the paper substrate. The exposure settings (iris, camera gain and integration time) were not investigated, as these parameters are automatically set to fixed values during spectral acquisition.

4.2.2.2 Reflectance spectra and chromaticity measurements

Using the parameters determined through method validation, five replicate spectra were obtained at different locations along each ink trace. Chromaticity coordinates were automatically generated from the VSC5000 software by analysing each spectrum using the CIE (Commission Internationale de l'Eclairage, or International Commission on Illumination) colour measurement system.

4.2.2.3 Fluorescence characterisation

Fluorescence illumination was achieved using the VSC spot lamp source. Samples were excited at 645 – 720 nm and viewed through a 778 nm longpass barrier filter. Spectra of luminescent inks were obtained in fluorescence spot mode using the same settings employed for the reflectance spectra. Three replicate spectra were obtained at different locations along each ink trace.

4.2.3 Data analysis

Data pre-processing and chemometric analysis was carried out using the Unscrambler® X 10.3 (Camo Software AS, Oslo, Norway). Spectra were interpolated to a step size of 1 nm and truncated to selected wavelength ranges. A baseline offset to 0 % reflectance and unit vector normalisation were applied to account for variation due to light scattering or the sample surface texture. All spectra were mean-centred and subjected to principal component analysis (PCA) using the non-linear iterative partial least squares (NIPALS) algorithm. 3-dimensional scores plots were generated using combinations of the first four principal components (PCs) in order to visualise the sample distribution and identify outliers. A linear discriminant analysis (LDA) model was then constructed from the calibration set using the Mahalanobis distance and scores derived from the first four PCs, treating each ink as an independent class.

This model was used to predict source pens for the validation spectra, with the actual and predicted classes compared to evaluate the model's performance.

Calibration samples were also plotted according to their tristimulus values (refer to section 4.3.6) to determine whether chromaticity measurements could improve upon the separation afforded by the reflectance spectra. Samples were first plotted using their raw tristimulus values as a 3-dimensional coordinate system. The tristimulus values were then subjected to PCA both with and without unit vector normalisation, and samples plotted using the scores obtained against the first two PCs.

4.3 Results and discussion

4.3.1 Preliminary considerations

PCA was conducted using both the visible (400 – 700 nm) and visible-NIR (400 – 925 nm) wavelength ranges, to establish whether infrared reflectance could increase separation between the inks. The wavelength region above 925 nm was omitted, as it yielded minimal variance between the spectra. The visible-NIR range was found to give no improved separation of the ink population (Appendix 4.1). The following discussion is thus presented solely in reference to results obtained using the visible range.

4.3.2 Method development

Initial research examined how factors such as the magnification or integration area would affect the quality of spectra obtained using the VSC (Appendix 4.2). A minimum 15.06x magnification was required to ensure that the ink trace comprised the full region of interest when integrating across a 16 x 16 pixel area. This feature area was found to produce the highest instrumental response in the blue region of the spectrum, as well as a more distinct reflectance maximum. Magnification below 15.06x resulted in band broadening in the blue region due to the influence of the paper substrate, whilst magnification exceeding 15.06x provided no improvement to the quality of the spectra. Similarly, the use of black masking to reduce the interference of background scattering did not appear to have any effect on spectral quality. Based on these results, all subsequent spectra were acquired using 15.06x magnification and a 16 x 16 pixel region of interest, with no attempt to reduce background scattering from the paper substrate.

4.3.3 Compatibility of VSC spectra with the existing spectrophotometer model

Classification of the validation inks was performed using the VSC spectra with the statistical model generated in Chapter 3 using a Cary 4000 UV-Vis spectrophotometer, in order to assess the compatibility of the two instruments. All 12 inks were incorrectly classified (Appendix 4.3), and significant deviations were noted between spectra collected using each instrument (Figure 4.1). These discrepancies may be due to varying wavelength sensitivities between the instruments, or the use of different ‘standard white’ reference materials. Spectra collected using the VSC also exhibited a lower signal-to-noise ratio compared to those obtained using the Cary 4000. This result was not unexpected given that the VSC is a highly specialised instrument not intended for research-level spectrophotometry, but it may affect the capability of the VSC to provide sufficiently reproducible data for discrimination purposes.

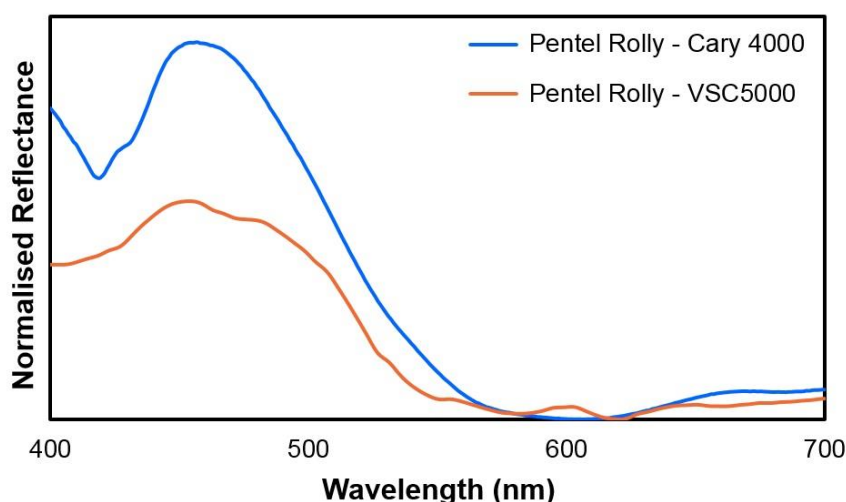


Figure 4.1: Pre-processed reflectance spectra of a Pentel Rolly ink deposit acquired using the Cary 4000 UV-Visible spectrophotometer and VSC5000.

4.3.4 Distribution of the spectral dataset

PCA performed on the calibration inks on the basis of their VSC spectra showed that 95.6 % of total variance was described by the first three PCs, and 97.3 % in the first four PCs (Figure 4.2). Scores plots were produced using combinations of the first four PCs, as shown in Figure 4.3. It was found that PC4 (accounting for 1.7 % of total variance) assisted in separating the Artline Smoove and Staedtler 430 spectra from the bulk of the ink population, and so the first four PCs were retained for subsequent discriminant analysis.

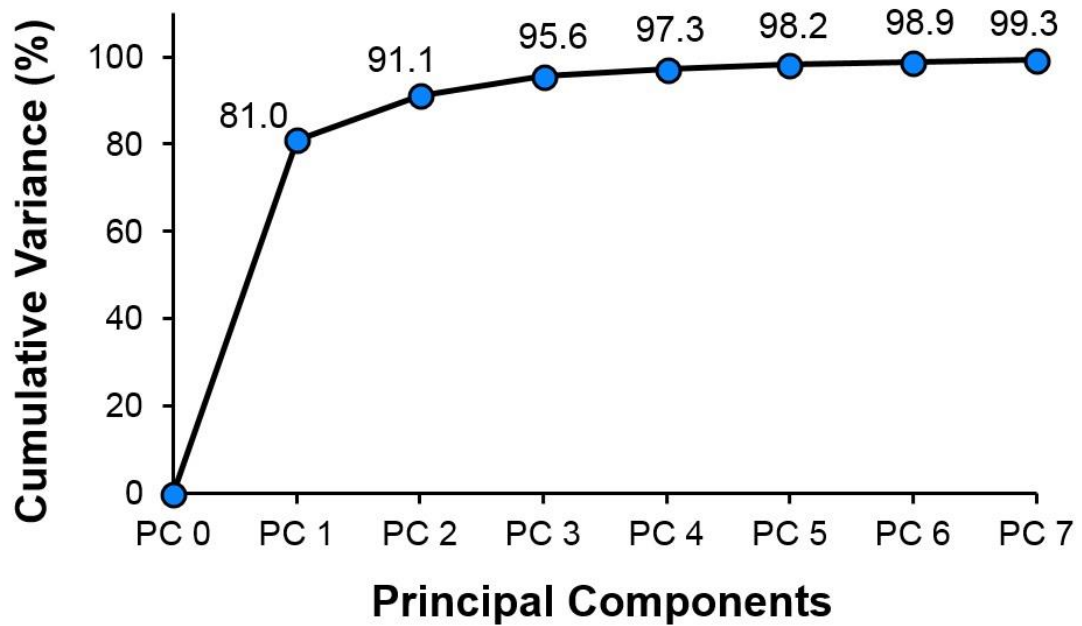


Figure 4.2: Scree plot depicting the cumulative variance in the VSC blue ballpoint ink dataset retained by each PC.

As with the PCA model constructed in Chapter 3, replicates from each pen were generally clustered together, indicating reasonable measurement reproducibility. The overall clustering patterns observed were also consistent with those in the initial model. Certain inks, such as the Bic Cristal and Pentel Rolly, were again clearly distinguishable from all other samples in the dataset. However, a larger number of formulations formed a broad, overlapping cluster in the centre of the scores plot that could not be resolved through further PCA. This indicates that the VSC5000 provides lower specificity between ink formulations in comparison to the Cary 4000.

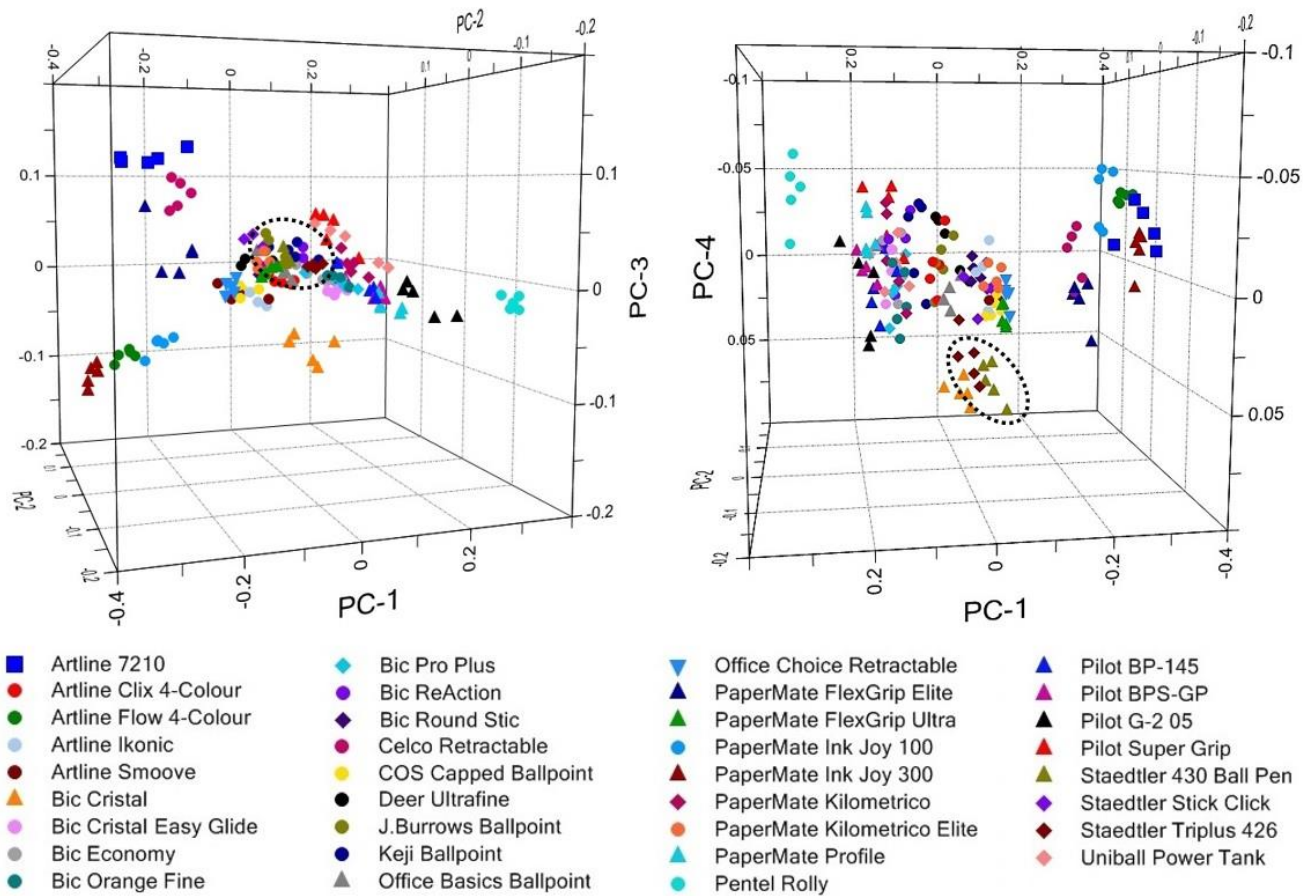


Figure 4.3: 3-dimensional PCA scores plots generated using the first four PCs, highlighting the distribution of the blue ballpoint ink population based upon their corresponding VSC visible spectra. Circles indicate Staedtler Triplus and Staedtler 430 inks, which are separated from the main population along PC4.

4.3.5 Discriminant analysis

A discriminant model was constructed from the calibration set using the scores derived from the first four PCs, treating each ink as its own class. The efficacy of the model was then evaluated using a separate validation set of 12 inks, six of which were deliberately selected as overlapping with other inks in the sample population. The resultant model yielded a classification accuracy of 96.7 % for the calibration set (Table 4.2), on par with the original model. However, the validation accuracy was significantly lower at only 31.7 % (Table 4.3). Visual inspection revealed deviations between the calibration and validation samples in the blue region (ca. 400 – 470 nm) of the spectra (Figure 4.4). This, in conjunction with the overlap observed between many of the inks in the PCA, is likely the cause of the misclassified samples.

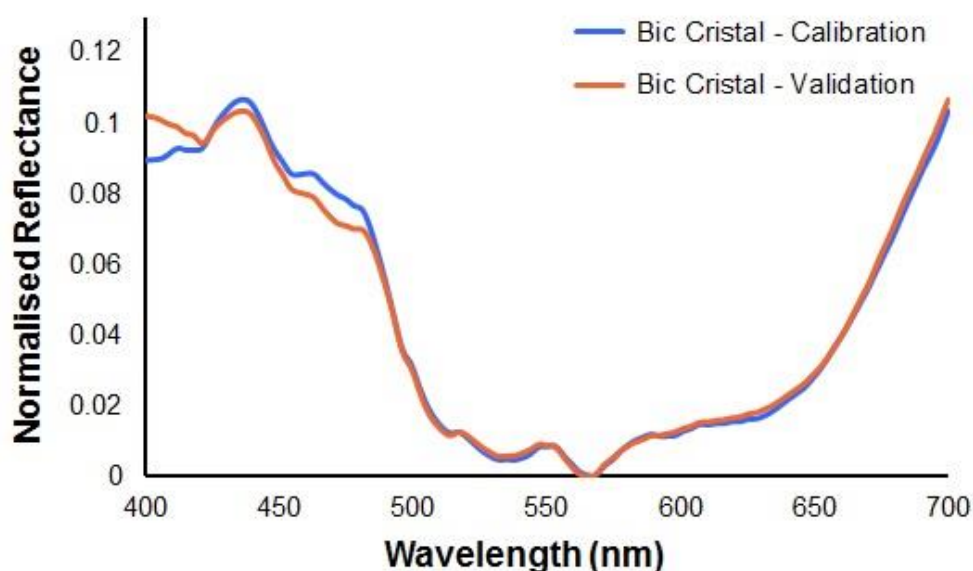


Figure 4.4: Pre-processed calibration and validation spectra (averaged across five replicates) obtained from Bic Cristal ink deposits.

As the calibration and validation spectra were acquired on separate days, systematic instrumental variation between analysis dates was considered as a prospective factor affecting the results. However, PCA showed no distinct separation between the calibration and validation spectra taken from any given ink deposit (Appendix 4.4). The discrepancies in the spectra were thus attributed to random instrumental variation or noise, as noted in section 4.3.3. Further work is needed to investigate the spectral reproducibility of the VSC, and whether corrections can be applied to compensate for the observed variations.

Table 4.2: Number of correct and incorrect classifications for samples in the VSC calibration set using a four-PC LDA model. Labels in brackets indicate assigned groups. The overall classification accuracy was 96.7 %.

Pen Model	Correct	Incorrect	% Correct
Bic Cristal	5	0	100
Papermate Ink Joy 100	5	0	100
Artline Ikonik	4	1 (COS Capped)	80
Deer Ultrafine	5	0	100
Artline 7210	5	0	100
PaperMate Kilometrico	5	0	100
Bic ReAction	5	0	100
Celco Retractable	5	0	100
Bic Orange Fine	5	0	100
Keji Ballpoint	5	0	100
Office Basics Ballpoint	5	0	100
Artline Smoove	5	0	100
J.Burrows Ballpoint	5	0	100
Bic Round Stic	5	0	100
Artline Flow 4-Colour Retractable	5	0	100
Artline Clix 4-Colour	5	0	100
Bic Cristal Easy Glide	5	0	100
Bic Economy	3	2 (Pro Plus)	60
Pilot G-2 05	5	0	100
Pilot Super Grip	5	0	100
Uniball Power Tank	5	0	100
Pilot BPS-GP	5	0	100
PaperMate Profile	5	0	100
Bic Pro Plus	2	2 (Bic Orange Fine) 1 (Bic Economy)	40
PaperMate FlexGrip Elite	5	0	100
Pentel Rolly	5	0	100
PaperMate Kilometrico Elite	5	0	100
Staedtler Triplus 426	5	0	100
Staedtler Stick Click Retractable	5	0	100
Pilot BP-145	5	0	100
PaperMate FlexGrip Ultra	5	0	100
PaperMate Ink Joy 300	5	0	100
Office Choice Retractable	5	0	100
COS Capped Ballpoint	5	0	100
Staedtler 430	5	0	100
	169	6	96.7

Table 4.3: Number of correct and incorrect classifications for samples in the VSC validation set using a four-PC LDA model. Labels in brackets indicate assigned groups. The overall classification accuracy was 31.7 %.

Pen Model	Correct	Incorrect	% Correct
Bic Cristal	1	3 (Artline Ikonic) 1 (Bic Economy)	20
Celco Retractable	1	4 (Staedtler Stick Click)	20
Office Basics Ballpoint	1	2 (J.Burrows Ballpoint) 1 (Staedtler Stick Click) 1 (Artline Clix 4-Colour)	20
J.Burrows Ballpoint	2	1 (Bic ReAction) 1 (Artline Clix 4-Colour) 1 (Office Basics Ballpoint)	40
Bic Economy	1	4 (Bic Cristal Easy Glide)	20
Pilot G-2 05	5	0	100
Bic Pro Plus	0	5 (Bic Cristal Easy Glide)	0
PaperMate FlexGrip Elite	5	0	100
Pentel Rolly	2	3 (Pilot G-2 05)	40
Staedtler Triplus 426	0	2 (Staedtler Stick Click) 2 (COS Capped Ballpoint) 1 (Office Basics Ballpoint)	0
PaperMate Ink Joy 300	0	4 (Artline Flow 4-Colour) 1 (PaperMate FlexGrip Elite)	0
Office Choice Retractable	1	4 (COS Capped Ballpoint)	20
Total	19	41	31.7

4.3.6 Chromatic data

Chromaticity values were examined as a potential means to increase the discrimination between similar inks. The VSC generates a range of chromaticity values corresponding to several CIE colour spaces; mathematical models that describe perceived colours in human colour vision as numerical values. As these colour spaces are derived from one another, chemometric analysis of the entire chromatic dataset was not expected to yield meaningful information. Instead, data analysis was restricted to the tristimulus values, which represent basic trichromatic colour measurements based upon human colour vision as X, Y and Z coordinates.

Samples were first plotted using the raw tristimulus values as 3-dimensional coordinates. This produced a single overlapping cluster with no distinct separation of any of the ink formulations (Figure 4.5). PCA was then conducted on both the raw and normalised values, with samples plotted using their scores from the first two PCs, accounting for > 99 % of total variance (Figure 4.6). This again did not result in any clear discrimination. It can be seen that replicates of each ink exhibited a very large range of variation, indicating a poor level of reproducibility. As the chromatic data is derived from analysis of the spectra, it is possible that minor deviations or noise in the spectral data is affecting the generated tristimulus values, thus yielding poor results.

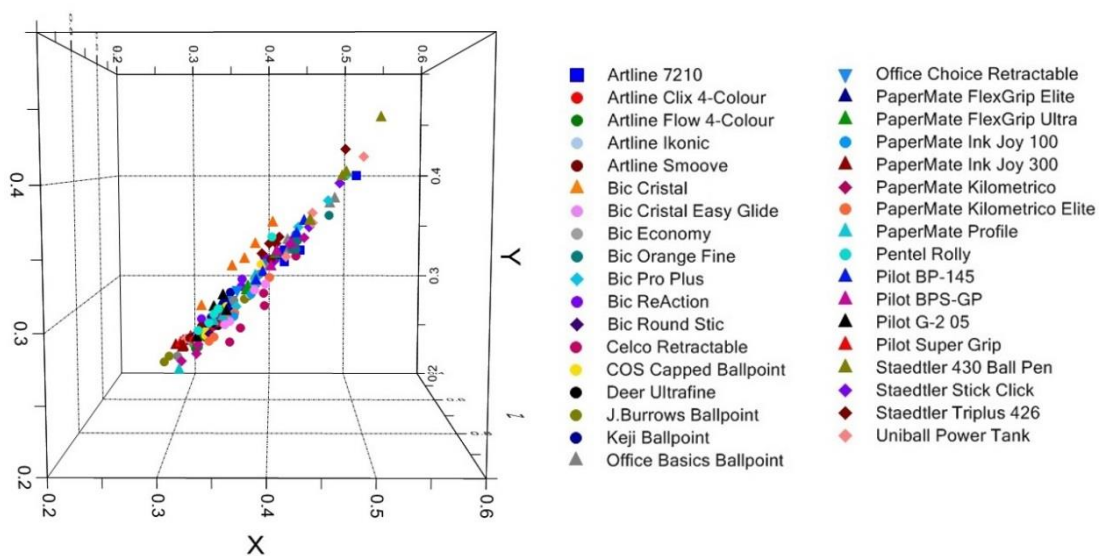


Figure 4.5: 3-dimensional scatter plot showing the distribution of the blue ballpoint ink population based upon their tristimulus values.

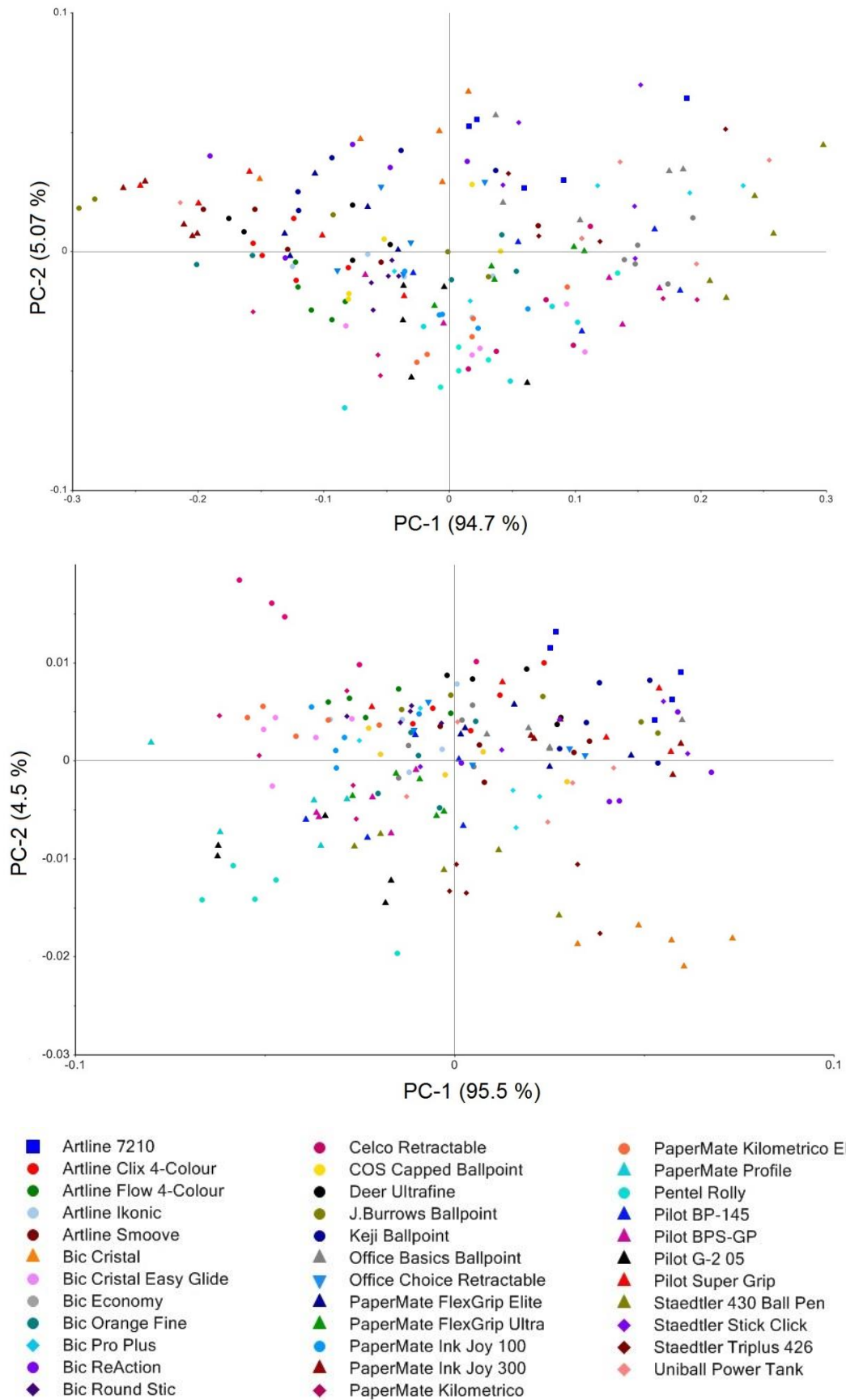


Figure 4.6: 2-dimensional PCA scores plots showing the blue ballpoint ink population based upon (top) raw; and (bottom) unit vector normalised tristimulus values.

4.3.7 Fluorescence spectroscopy

4.3.7.1 Spectral distribution

As mentioned in section 4.1, the VSC is equipped with several light sources and optical filters for specialised lighting examinations. In addition to incandescent lamps, the main unit houses vapour discharge tubes (allowing UV excitation at 254 nm, 312 nm or 365 nm) and an infrared laser diode (970 – 990 nm). Ink deposits were viewed under each of these sources to determine whether fluorescence characteristics could assist in distinguishing inks with similar visible spectra. Whilst no fluorescence was observed under ultraviolet or infrared irradiation, several inks were found to fluoresce in the NIR region (ca. 720 – 910 nm) when illuminated under red light (Figure 4.7). This is consistent with work by Sun *et al.*, who found that 18 selected blue ballpoint inks were most distinguishable when illuminated at 605 – 720 nm and observed in the NIR region.^[377]

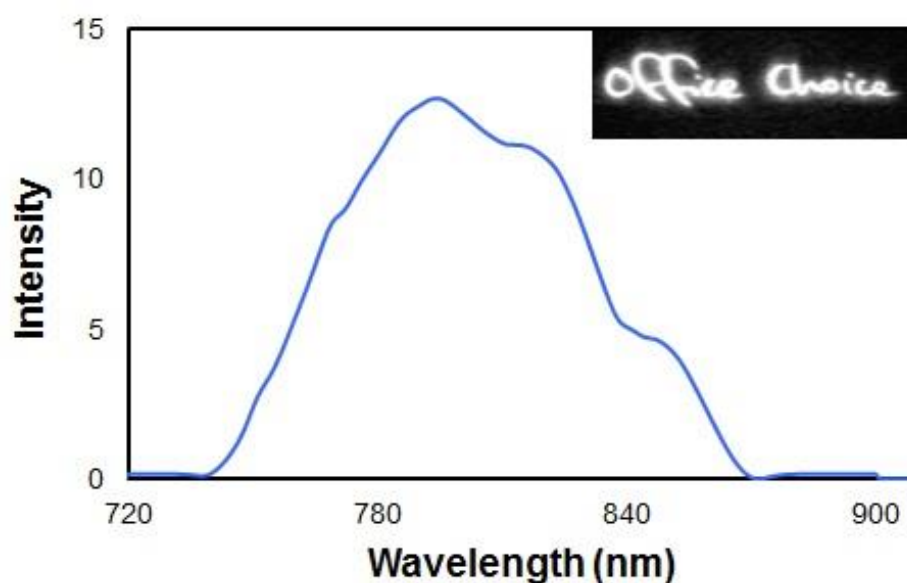


Figure 4.7: Fluorescence spectrum recorded from an Office Choice ink deposit (inset image) using the VSC spot source at 645 – 720 nm excitation and 778 nm longpass filter.

Due to limited instrumental response, fluorescence spectra could only be acquired from eight inks exhibiting strong fluorescence. PCA found no distinct separation between these inks, as shown in Figure 4.8. This was found to largely be due to the high level of variation between replicate spectra. Consequently, the use of VSC fluorescence spectra was concluded to be unsuitable for the discrimination of inks used in this study.

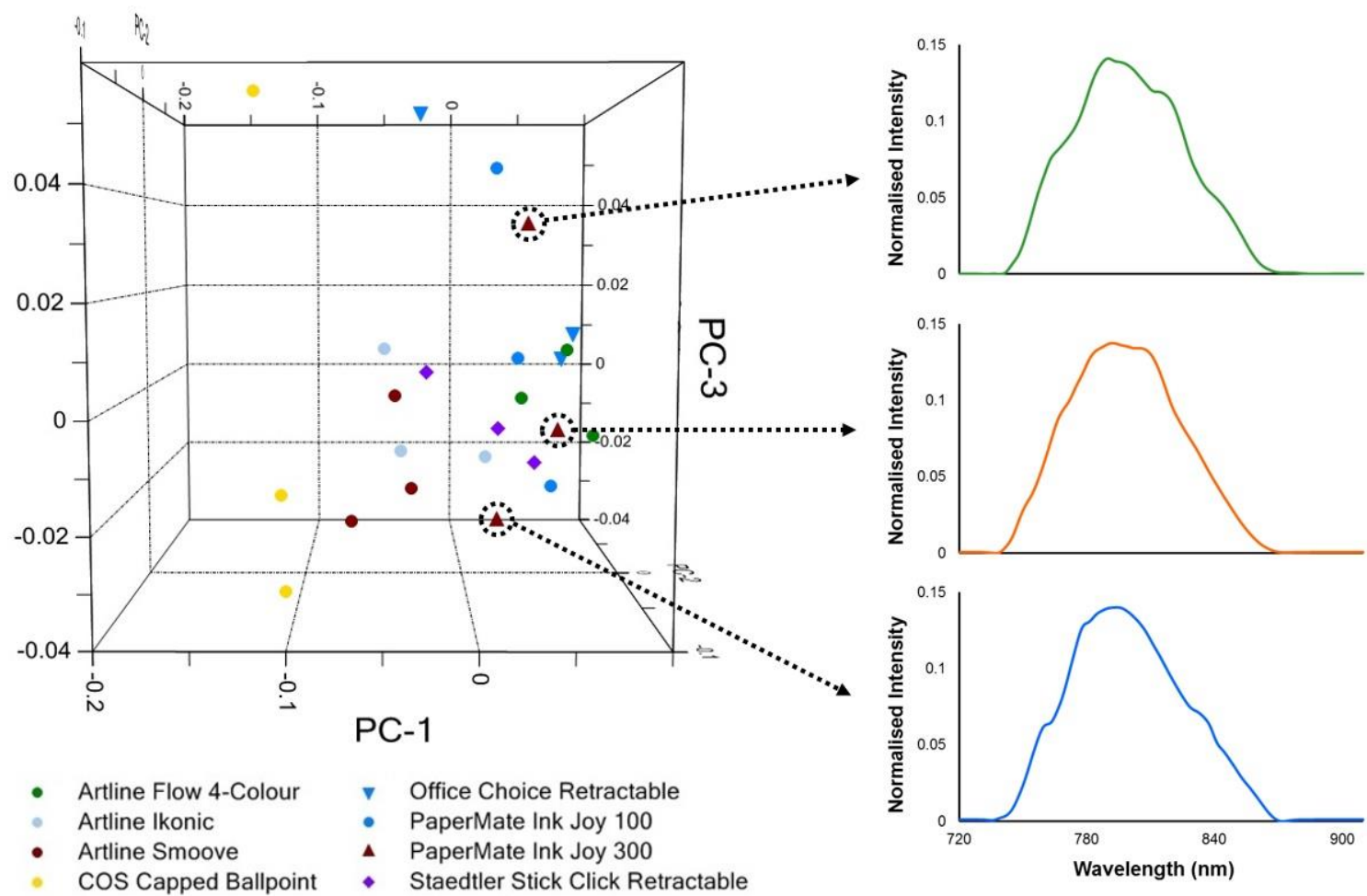


Figure 4.8: 3-dimensional PCA scores plot showing the distribution of strongly fluorescent blue ballpoint inks according to their fluorescence spectra, highlighting the large variation between replicates resulting from spectral deviations.

4.3.7.2 Fluorescence as an initial classifier

Due to the poor results obtained using fluorescence spectra, an alternative approach was taken by using the observable fluorescence properties of each ink as an initial classifier. Each ink was categorised as fluorescent or non-fluorescent, and separate PCA conducted on the visible spectra for each group. 3-dimensional scores plots were generated using the scores obtained for the first 4 PCs, accounting for > 97 % of total variance in both instances (Appendix 4.5).

Of the 35 ballpoint inks examined, ten gave no observable fluorescence under the selected instrumental settings. PCA of these inks showed that the Pentel Rolly and Bic Cristal inks were again clearly distinguishable using the first three PCs, while PC4 improved the separation of the Office Basics and Artline Clix inks (Figure 4.9). In contrast, the Bic and Keji inks remained indistinguishable, even following further PCA. The Bic inks were expected to be clustered together given that these samples could not be reliably separated by the UV-Vis model generated in Chapter 3. This was previously attributed to the manufacturer using the same or very similar ink formulation across a range of its pen models. The fact that ink from these pens also exhibit similar fluorescence phenomena supports this theory.

PCA of the fluorescent inks revealed improved separation of the PaperMate FlexGrip Elite using the first three PCs, with the exception of one replicate that overlapped with the Celco Retractable spectra (Figure 4.10). Visual inspection revealed this spectrum to significantly differ from the remaining spectra, and so this replicate was omitted as an outlier. The use of PC4 also resulted in the PaperMate Ink Joy and Staedtler 430 inks becoming more readily distinguishable.

Additional discrimination could be achieved by further dividing the fluorescent inks according to their observed strength of fluorescence. These inks were categorised as exhibiting weak, moderate or strong fluorescence (Figure 4.11) followed by subsequent PCA. It is important to note that the fluorescence intensity was judged based upon personal opinion, and this has the potential to once again introduce human subjectivity into the results.

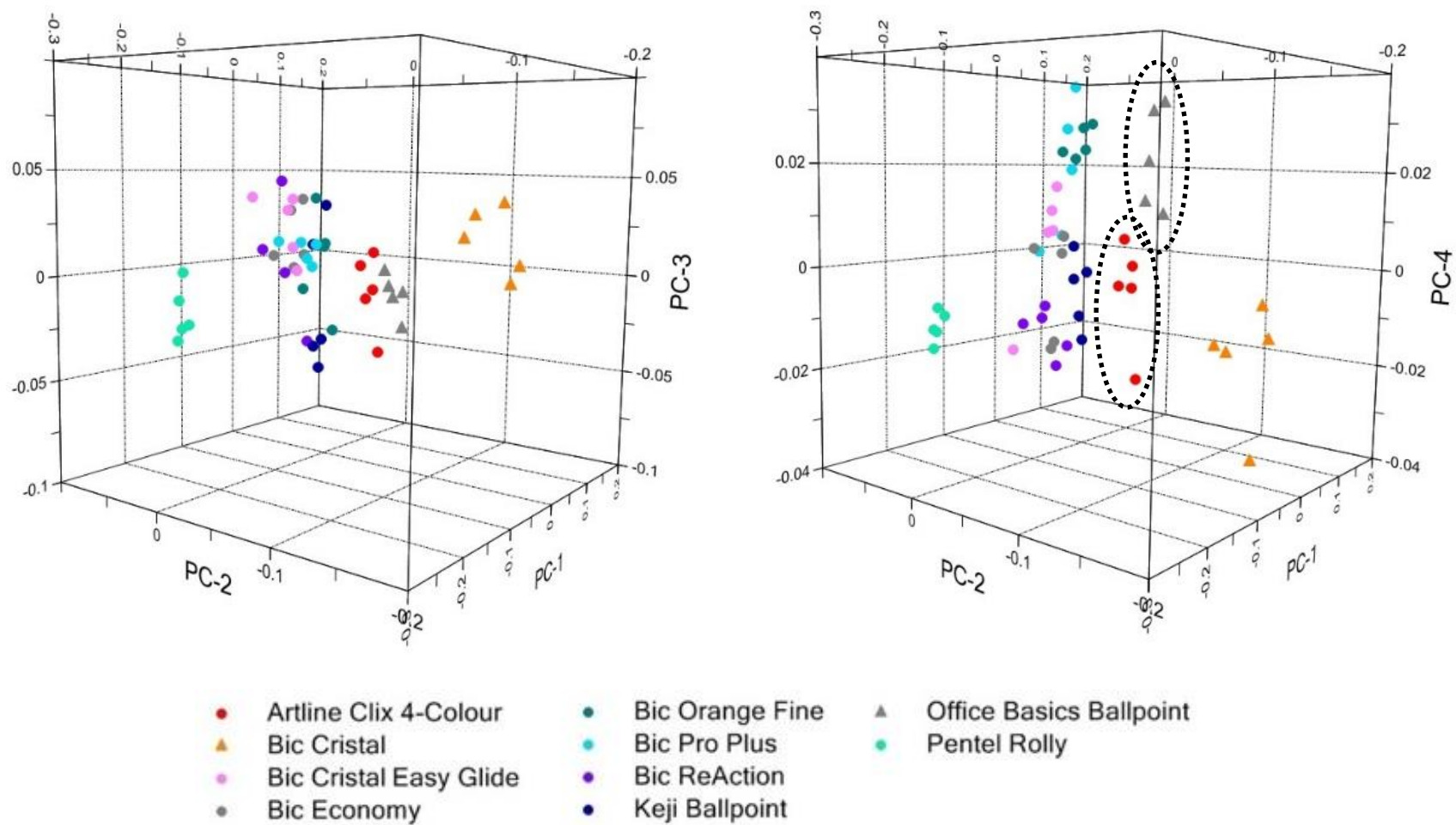


Figure 4.9: 3-dimensional PCA scores plots showing the distribution of non-fluorescent inks according to their visible spectra, highlighting improved separation of Artline Clix and Office Basics inks. Left and right views show plots generated using (left) PCs 1, 2 and 3; and (right) PCs 1, 2 and 4.

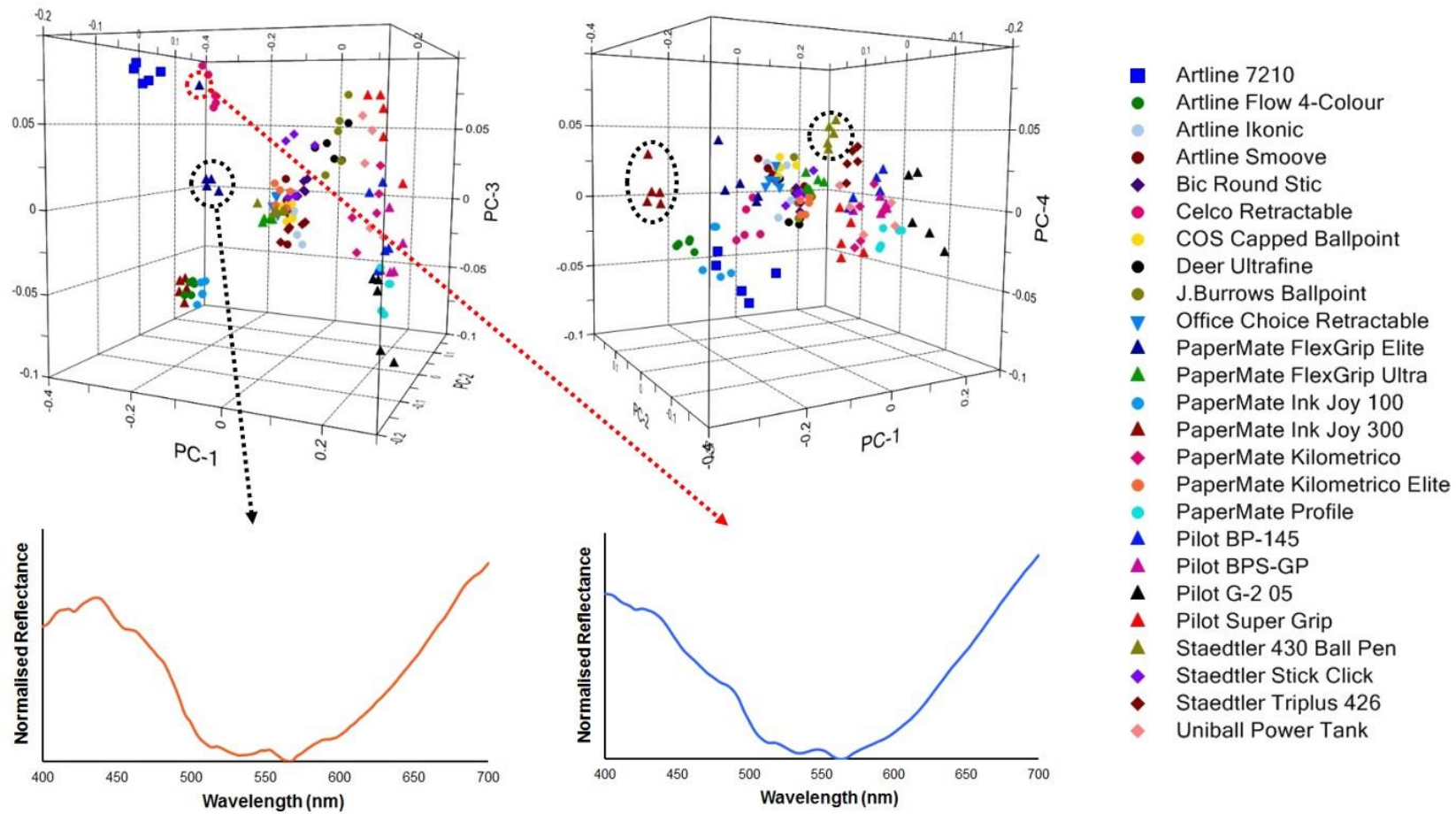


Figure 4.10: 3-dimensional PCA scores plots showing the distribution of fluorescent inks according to their visible spectra, (left) using PCs 1, 2 and 3; and (right) using PCs 1, 2 and 4. Improved separation of the PaperMate Ink Joy 300 and Staedtler 430 inks (circled) was achieved along PC4. Red arrow indicates PaperMate FlexGrip Elite replicate identified as an outlier based on visual inspection of the spectra as shown.

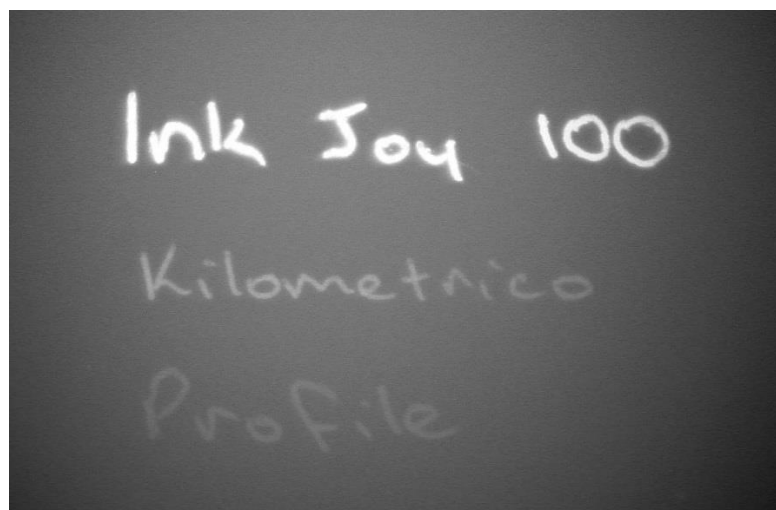


Figure 4.11: *Photographic image of inks evaluated as exhibiting (top) strong; (middle) moderate; and (bottom) weak fluorescence when excited at 645 – 720 nm and viewed through a 778 nm longpass filter.*

Weakly fluorescing inks were divided into two groups, with the PaperMate FlexGrip Ultra and Kilometrico Elite separated from the PaperMate Profile and Pilot inks along PC1 (Figure 4.12). The loadings plot (Appendix 4.6) revealed this PC to be positively correlated with the blue region (ca. 400 – 500 nm), and negatively correlated with the red region (ca. 600 – 700 nm). The FlexGrip Ultra and Kilometrico Elite inks exhibited a higher ratio of red- to blue-reflectance, thus resulting in more negative PC1 scores. Only four inks were judged to have moderate fluorescence, two of which (the Artline 7210 and PaperMate FlexGrip Elite) formed independent clusters. These inks were separated from the PaperMate Kilometrico and Pilot G-2 05 along PC1, which was again found to be due to the differing ratios of reflectance in the red region compared to the blue region (Appendix 4.7).

PCA of the strongly fluorescent inks produced three general clusters using PCs 1-3. The PaperMate Ink Joy and Office Choice inks were grouped together as expected based on earlier results, while the Celco Retractable ink was uniquely characterised. The remaining inks formed a largely overlapping cluster. Some separation of the Staedtler Triplus and Uniball Power Tank inks was noted, but due to the similar magnitudes of within-group and between-group variance, this was insufficient for reliable discrimination. The use of PC4 resulted in the PaperMate Ink Joy 300 being separated from the Ink Joy 100 and Office Retractable inks, as well as slightly improved separation of the Staedtler 430 and Triplus 426 inks.

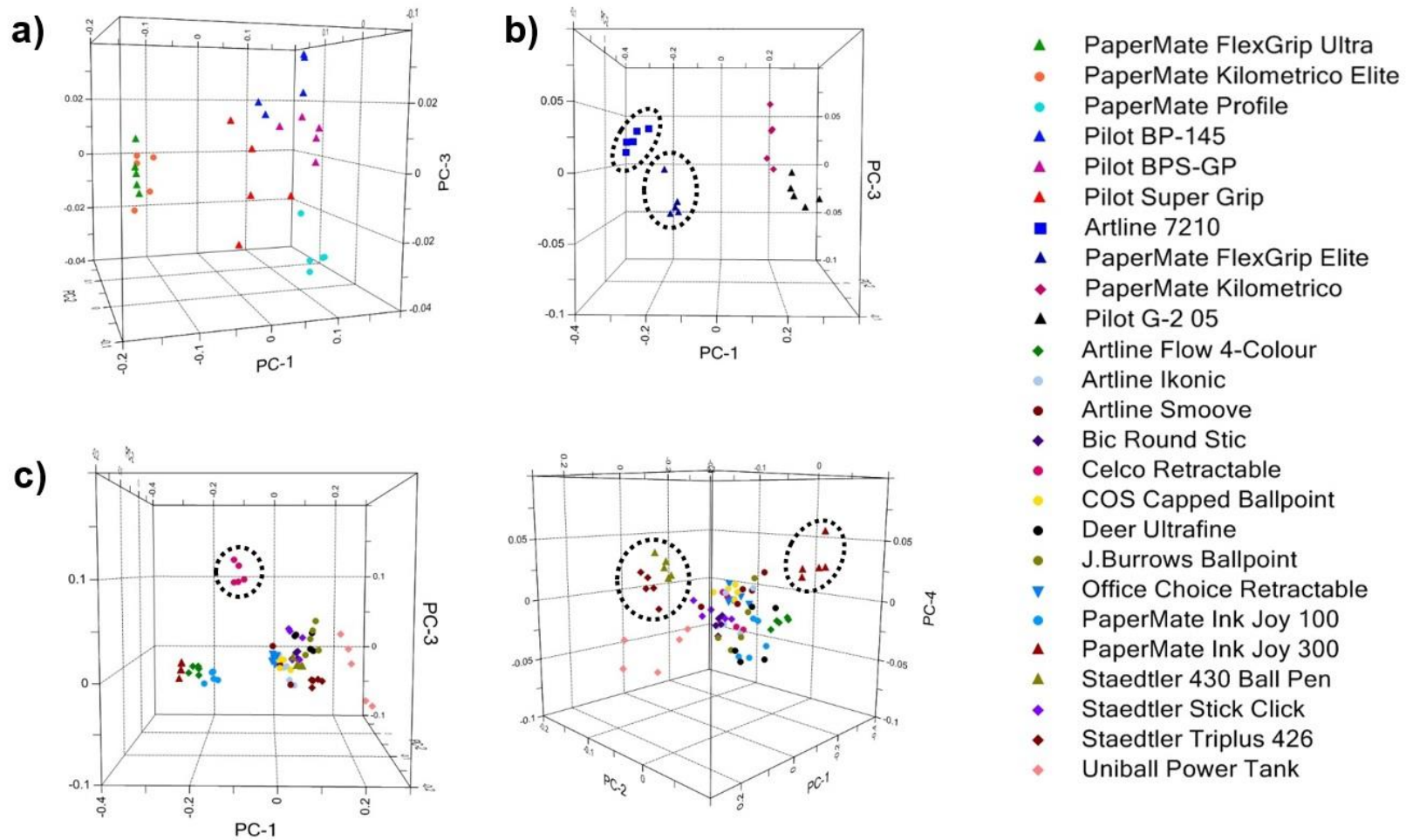


Figure 4.12: 3-dimensional scores plots showing the distribution of (a) weakly fluorescent; (b) moderately fluorescent; and (c) strongly fluorescent inks according to their visible spectra. Plot (c) has been shown using (left) PCs 1, 2 and 3; and (right) PCs 1, 2 and 4.

4.4 Conclusions

The results of this study demonstrate that the use of VSC spectroscopy with chemometrics could potentially be utilised as an objective discriminatory method for handwritten ink entries on paper, although further work is required regarding instrumental limitations. It was found that the VSC5000 gave lower specificity between similar inks in comparison to the Cary 4000 spectrophotometer used in Chapter 3. This was likely due to the lower signal-to-noise ratio provided by the VSC, resulting in lower spectral reproducibility. Consequently, a discriminant model constructed from the VSC visible reflectance spectra of the inks yielded poor classification results, with a validation accuracy of only 31.7 %.

Discriminant models based upon tristimulus values or fluorescence spectra were similarly unsuccessful, due to the large magnitude of within-group to between-group variance. An alternative approach, in which the observed fluorescence intensity of each ink was used as an initial classifier, was used to narrow the range of similar samples to undergo chemometric analysis. PCA carried out on the fluorescent and non-fluorescent inks gave improved separation of a number of inks which could not be distinguished when all inks were compared concurrently. Further specificity was achieved by categorising the fluorescent inks according to their fluorescence intensity. However, as this was done based on personal opinion, a level of human bias could be introduced to the results.

It should be noted that in this study, several inks were analysed simultaneously. In a casework scenario, ink examinations are more likely to involve the pairwise comparison of ink entries in order to establish the integrity of a document. The methods described in this chapter may hence be more appropriate and effective for “questioned versus known” comparisons as described in Chapter 2, rather than ink identification using a database model.

The work described in this dissertation thus far has been restricted to the use of pattern recognition and regression methods to aid the interpretation of physical evidence following its analysis. In Chapter 5, experimental design will instead be employed to optimise pre-analysis factors such as evidence sampling and handling. These factors may affect the quality of data generated using analytical techniques, and thus the information that may be subsequently extracted using chemometrics.

Chapter 5: Optimisation of recovery protocols for smokeless powder residues with subsequent analysis by gas chromatography-mass spectrometry

Portions of this chapter have been published in the journal *Talanta*:

G. Sauzier, D. Bors, J. Ash, J.V. Goodpaster and S.W. Lewis. *Optimisation of recovery protocols for double-base smokeless powder residues using a central composite design and total vaporisation (TV) SPME/GC-MS*. *Talanta*, 2016. **158**: p. 368-374.

5.1 Introduction

Improvised explosive devices (IEDs) are becoming an increasing topic of public concern, with high-profile incidents such as the Bali (October 2002), Boston Marathon (April 2013), and Baghdad (July 2016) bombings garnering international attention. Although the majority of media coverage has focussed on large-scale incidents attributed to terrorism, there has also been a rise in explosive incidents using smaller devices such as pipe bombs. This is particularly the case in the United States, where pipe bombs are considered to make up the vast majority of IED encounters.^[382, 383] These devices can be easily and cheaply constructed from everyday materials, and can produce a large destructive effect using low explosive powders such as black powder, black powder substitutes, pyrotechnic compositions or smokeless powder.

Smokeless powders are a class of nitrocellulose-based propellants designed to produce minimal solid residue upon deflagration. These propellants can be categorised as single-, double- or triple-base according to their composition. Single-base powder utilises nitrocellulose as the sole energetic component, while double-base smokeless powder (DBSP) also contains nitroglycerin for increased detonation velocity.^[241, 273, 384] Triple-base powders additionally employ nitroguanidine to lower the flame temperature and reduce barrel erosion, though these formulations are restricted to large calibre munitions and are hence rarely encountered in IEDs.^[274, 385] All three varieties of smokeless powder may also contain additives; for example diphenylamine or ethyl centralite; that act as stabilisers, plasticisers, or flash suppressants.^[282, 384]

Though not commonly encountered in Australia due to legal restrictions, smokeless powders are readily available in the United States, where 10 million pounds (4500 tonnes) are produced commercially per annum.^[386] They are relatively powerful propellants; decomposing at rates of up to 1,000 metres per second; and can be purchased loose at sporting goods stores in quantities of up to 25 pounds (11.3 kilograms).^[385, 386] As a result, they are highly favoured as the explosive charge for IEDs. In fact, smokeless powder devices comprised over 20 % of the approximately 4,300 explosive powder-related incidents reported to the U.S. Bomb Data Centre between 2008 and 2014.^[280] By comparison, less than 50 powder-related incidents were reported to the Australian Federal Police over the same period, and only four of these were confirmed to involve smokeless powder formulations.^[387]

The investigation of explosive events relies upon the detection and identification of residues from the scene. To this end, research to date has largely focussed on developing improved instrumental methods to yield more sensitive and selective analyses of explosive materials. However, the success of these methods is largely dependent on the sampling method, storage conditions and extraction parameters employed prior to instrumental analysis.^[10, 269, 388] Adequate research to establish appropriate sampling and handling procedures is thus of equally critical importance.

A common sampling method for explosives, particularly on large non-porous surfaces, is the use of swabbing techniques. A number of studies have evaluated the efficacy of various swabbing materials, solvents or extraction procedures in recovering organic and inorganic explosives on multiple substrates.^[389-396] The findings of these studies have been diverse, with the most effective swabbing media or solvents differing according to the substrate or target analytes selected.^[391-393] Investigations have also been conducted regarding the stability of explosive residues stored under various conditions. These studies have established that volatile explosives such as triacetone triperoxide (TATP) may rapidly evaporate at room temperature, whilst trinitrotoluene (TNT) and other nitroaromatic explosives are prone to photo-transformation.^[397, 398]

Despite several studies concerning the sampling, storage or extraction parameters of explosive traces, there is a lack of rigorous research examining particular combinations of these factors. Song-im *et al.* for example investigated a range of swab types and solvents for explosives recovery on different substrates; however, the same extraction procedure was used for all samples, and no investigation was made of different storage conditions.^[392] Similarly, DeTata *et al.* studied the efficacy of several extraction procedures in removing explosive residues from different swab types, but employed a single swab type and solvent to examine residue stability under different storage temperatures.^[389] This univariate approach fails to take into account interactions between the factors, and the effect that these interactions may have on explosives recovery. An additional limitation is the use of standard analyte solutions as simulated residues, which may not provide an accurate representation of 'real' samples generated through an explosive event. Furthermore, studies to date have relied solely upon visual assessment of the acquired data. Interaction effects may not be readily evident from the raw data, and can thus be overlooked when relying on visual inspections.

A more statistically rigorous approach is the use of multivariate chemometric techniques to identify and model interactions within the dataset. In particular, experimental design methods such as a central composite design (CCD) can be used to map the relationship between several explanatory factors and a dependent response. In addition to identifying the factor levels that will yield a target response, CCDs can be used to determine the significance and effect of factor interactions in a minimal number of experiments.^[46] Unlike simpler design methods such as factorial designs, a CCD is also capable of modelling curvilinear variable effects.^[45, 61] CCDs have recently been applied to optimise extraction and instrumental analysis parameters for explosive residues,^[399-401] however, the broader capability of experimental design to investigate initial factors such as sampling and storage methods remains unexplored.

This chapter describes the use of a CCD to optimise recovery procedures for DBSP residues analysed using total vaporisation solid-phase microextraction gas chromatography-mass spectrometry (TV-SPME/GC-MS). TV-SPME is a technique wherein a sample extract is heated to complete evaporation, and a SPME fibre used to pre-concentrate analytes from the vapour.^[402] The analytes therefore partition directly between the vapour phase and the SPME fibre, providing increased sensitivity compared to either liquid injection or headspace or immersion SPME.

TV-SPME has recently been applied to successfully detect smokeless powder residues recovered from steel pipe bomb fragments.^[403] However, it is also of investigative interest to detect residues left on witness materials, i.e. surfaces proximate to an explosive device. The optimised parameters were therefore applied to the recovery of post-blast explosive residues deposited on steel plates surrounding a pipe bomb device following detonation. All experimental work in this chapter was conducted at Indiana University-Purdue University, Indianapolis (IUPUI).

5.2 Experimental

5.2.1 Reagents and materials

Acetone and dichloromethane (Fisher Scientific, USA) were of analytical grade and used as received. Nitrobenzene and ethyl centralite (Sigma Aldrich, USA), nitroglycerin (Restek, USA) and diphenylamine (Acros Organics, USA) were all of analytical reagent grade or above.

Alliant Red Dot double-base smokeless powder was obtained from Gander Mountain (Indianapolis, IN, USA), Puritan sterile cotton-tip applicators from Fisher Scientific USA, polyvinylchloride (PVC) piping from Home Depot (Indianapolis, IN, USA) and low carbon galvanised steel sheets from Grainger Industrial Supply (Indianapolis, IN, USA). SPME fibres were acquired from Sigma Aldrich USA, and SPME vials and caps from Gerstel USA.

5.2.2 Preliminary experiments

Initial experiments were conducted to establish a suitable means of sample preparation, as well as identifying factors of interest to be examined using the central composite design. Analysis of these samples was carried out using the TV-SPME method previously optimised by Bors for the analysis of smokeless powder residues.^[403] This method is referred to below as TV-SPME-1.

5.2.2.1 Preparation of standard solutions

Individual standards of nitroglycerin, diphenylamine and ethyl centralite were prepared in dichloromethane at a concentration of 1000 mg L⁻¹. These were used to prepare mixed stock solutions at concentrations of 10 mg L⁻¹ and 50 mg L⁻¹. Mixed calibration standards in the range of 0.001 – 0.050 mg L⁻¹ were prepared by dilution of the stock solutions. All solutions were kept refrigerated at approximately 8 °C before and after analysis, in order to minimise degradation.

5.2.2.2 Smokeless powder deflagration

The initial intended method for this study was to generate explosive residues through the deflagration of smokeless powder. To assess the feasibility of this approach, a series of deflagration trials were carried out using aluminium as a recovery surface. A single layer of aluminium foil was wrapped around a tin can lid, and Alliant double-base smokeless powder placed within a 1 inch x 1 inch section marked on the foil surface. The tin can lid was mounted over a Bunsen burner at a distance of approximately 4 inches, and the powder heated until deflagration occurred. Masses of 0.2 g, 0.3 g, 0.4 g, 0.5 g and 0.6 g were tested to determine the effect of powder quantity on the amount of recoverable residues. Quadruplicate trials using 0.3 g of powder were also performed to assess the reproducibility of residue deposition.

5.2.2.3 Factor screening

Screening experiments were conducted to assess whether selected sampling, extraction or storage parameters of samples would affect recovery of the target analytes. These trials were intended not as an in-depth investigation, but to determine factors warranting further investigation through the optimisation design. Simulated residues were prepared by spiking aluminium foil with 20 μL aliquots of 50 mg L^{-1} mixed stock solution, and allowing the deposits to completely dry prior to sampling.

Four sampling methods were chosen for comparison; solvent extraction, dry swabbing, acetone-wetted swabbing and isopropanol-wetted swabbing. Samples for solvent extraction were prepared by removing the spiked section of aluminium foil using a razor blade, and transferring directly to a 12 mL glass screw-top vial. Swabbing was carried out using cotton-tip applicators. Where applicable, the cotton-tips were briefly dipped in the selected swabbing solvent and the excess allowed to evaporate for 20 seconds. The cotton-tips were rubbed back and forth across the recovery surface for 10 seconds to allow thorough sampling of the surface area whilst minimising evaporation of the solvent, and the tips transferred to 12 mL glass screw-top vials. Triplicate samples prepared using each sampling method were subjected to 15 minute, 30 minute and 60 minute extractions. Triplicate samples were also sealed using wax film and refrigerated at 8 °C for three days, followed by a 15 minute extraction.

5.2.3 Optimisation experiments

5.2.3.1 Preparation of standard solutions

In these experiments, acetone was used as the solvent rather than dichloromethane due to its lower toxicity, applicability to the extraction of PVC (which is dichloromethane soluble) and effectiveness in dissolving a wide range of explosives.^[404] Individual standards of nitroglycerin, diphenylamine and ethyl centralite were each made at a concentration of 1000 mg L^{-1} , and used to prepare a 50 mg L^{-1} mixed stock. An internal standard solution of nitrobenzene was made up at a concentration of 100 mg L^{-1} . Mixed calibration standards in the range of 0.125 – 20 mg L^{-1} were prepared by dilution of the stock. A standard solution of Alliant Red Dot DBSP was prepared at a concentration of 2.04 g L^{-1} . All solutions were refrigerated at 8 °C when not in use.

5.2.3.2 Smokeless powder quantification

In order to more realistically represent the chemical composition of post-blast residue, optimisation samples were prepared from a standard solution of smokeless powder rather than solely the target components. Quantification of this solution was carried out to determine an appropriate spiking volume. Twenty-fold and fifty-fold dilutions of the smokeless powder solution were prepared in acetone, and run in triplicate alongside the mixed calibration standards (analysed without replicates). Due to instrumental issues at the time of this experiment, samples were analysed using liquid injection GC-MS rather than TV-SPME/GC-MS, as detailed in section 5.2.6 below.

5.2.3.3 Central composite design

The central composite design was generated using Design-Expert® 9 (Stat-Ease Inc., Minneapolis, USA) to investigate sampling, storage and extraction conditions as shown in Table 5.1. A face-centred CCD ($\alpha = 1$) with five replicates of each centre point was selected. This design was chosen as only three rather than five levels are required for each factor, and because it allowed the number of storage days at each level to be restricted to integer values. This resulted in a total of 78 experiments. Analysis of the data was conducted using Design-Expert® 9, optimising the peak area recovery of nitroglycerin, diphenylamine and ethyl centralite to a maximum. Two-way analysis of variance (ANOVA) was conducted to assess the significance of any main effects or two-way factor interactions on the recovery of each target compound.

Table 5.1: Factors and levels tested for optimising the recovery of DBSP residues using a face-centred central composite design.

Factor	Levels
Swab Type	None (dry), acetone and isopropanol
Storage Location	Fume cupboard (~ 25 °C) and refrigerator (~ 8 °C)
Storage Duration	0, 3 and 6 days
Extraction Time	15, 37 and 60 minutes

5.2.3.4 Sample preparation

Low carbon galvanised steel sheets (48 inch x 48 inch x 0.019 inch) were used as the recovery surface for all samples. Each sheet was cut into 12 inch x 12 inch plates, and further divided into 3 inch x 3 inch squares by scoring grid-lines into one side of each.

The surface was cleaned using deionised water followed by ethanol and acetone, then dried at room temperature before use. Samples for each experiment were prepared by spiking 50 μL of smokeless powder solution onto squares of the galvanised steel grid, allowing the deposit to completely dry prior to sampling. Swabbing was carried out as previously described, and the tips transferred to 12 mL glass screw-top vials. Each vial was sealed using wax film, and placed in either a fume cupboard or a refrigerator for the required storage duration prior to extraction and analysis. Due to the large number of samples to be analysed, a modified instrumental analysis procedure was employed to provide a shorter run time (detailed in section 5.2.6 below). This method will subsequently be referred to as TV-SPME-2.

5.2.4 Pipe bomb trial

Assembly and detonation of the pipe bomb device was completed by the Indiana State Police Bomb Squad. A single device was constructed using PVC pipe (8 inch x 1 inch diameter) and endcaps (1 inch diameter), with an approximately 50 g charge of Alliant Red Dot DBSP. The device was suspended by wire within a welded metal frame (approximately 22 inch x 24 inch x 34 inch), with the end-caps pointing in the north and south directions. Six galvanised steel plates (12 inch x 12 inch) were attached to each side of the frame, including above and below the device, by threading metal wire through holes drilled into the corners of each plate (Figure 5.1). All plates were positioned approximately 8 – 12 inches from the device. Specific distance measurements are provided in Appendix 5.1.



Figure 5.1: Pipe bomb detonation trial set-up showing galvanised steel witness plates attached to each side of the welded metal frame surrounding the device.

A time fuse inserted through a hole in the south endcap was used to initiate the device. Following detonation, the steel plates were cut along the scored lines. The resulting segments (3 inch x 3 inch) were each given a unique alphanumeric identifier, and stored in separate polyethylene clip-seal bags prior to analysis. Sampling, storage and extraction were conducted using the optimal parameters determined by the central composite design. GC-MS analysis was performed using the TV-SPME-2 method utilised for the optimisation samples, with a modification to the ion dwell times as specified in section 5.2.6.

5.2.5 Sample extraction

Extraction was carried out as shown in Table 5.2. 3 mL, 5 mL or 10 mL of the selected extraction solvent was pipetted into each sample vial. The vials were then closed, sealed using wax film and placed onto a shaker table for the desired extraction period. 60 μL or 70 μL aliquots of the extract were transferred directly to 20 mL SPME vials for analysis. These volumes were calculated based on the properties of the solvent as the maximum volume allowing for complete vaporisation, according to the equation:

$$V_S = \left(\frac{10^{\left(A - \left(\frac{B}{T+C} \right) \right)} V_C}{RT} \right) \left(\frac{M}{\rho} \right)$$

where V_S is the aliquot volume (mL); A, B and C are the Antoine constants describing a solvent's vapour pressure at a given temperature T (K); V_C is the volume of the container (L); R is the ideal gas constant ($\text{J mol}^{-1} \text{K}^{-1}$); M is the molar mass of the solvent (g mol^{-1}); and ρ is the density of the solvent at room temperature (g mL^{-1}).

Table 5.2: Extraction parameters utilised for DBSP recovery experiments.

Sample Set	Extraction Solvent	Extraction Volume (mL)	SPME Volume (μL)
Deflagration	Dichloromethane	3	60
Factor screening	Dichloromethane	10	60
Optimisation	Acetone	5	70
Pipe bomb	Acetone	5	70

5.2.6 Instrumental analysis

All sample analyses were performed using a Thermo Scientific Ultra II gas chromatograph equipped with a DSQ II mass spectrometer and TriPlus autosampler. Instrumental control, data acquisition and peak area integration was carried out using Thermo Xcalibur software (v.2.0.7), with integration performed as per the standard software parameters. As a consequence of instrumental limitations, three GC-MS programmes were utilised in this study. In each programme, analytes were separated on a Zebron ZB-5MS column (10 m x 0.18 mm x 0.18 μ m) via splitless injection.

Helium was used as the carrier gas at a flow rate of 1.5 mL min⁻¹. Analytes were ionised using a pulsed positive ion negative ion chemical ionisation source with methane as the reagent gas. Selected ion monitoring was used to detect nitrobenzene (m/z 123 in negative mode), nitroglycerin (m/z 46 and m/z 62 in negative mode), diphenylamine (m/z 170 in positive mode) and ethyl centralite (m/z 269 in positive mode). Typical MS conditions were: solvent delay, 2 minutes; ionisation energy, 70 eV; and electron multiplier voltage, 1505 V. Further instrumental conditions are listed in Table 5.3.

Table 5.3: Instrumental parameters for GC-MS analysis of explosives samples.

Parameter	Conditions		
	TV-SPME-1	Liquid Injection	TV-SPME-2
Injection Parameters			
Sample incubation	60 °C for 5 min	N.A.	60 °C for 1 min
SPME fibre	Polyethylene glycol (PEG)	N.A.	Polydimethylsiloxane (PDMS)
SPME extraction time	20 min	N.A.	1 min
Injection volume	N.A.	1 µL	N.A.
Splitless time	0.5 minutes	0.8 minutes	0.5 minutes
Split flow	40 mL min ⁻¹	30 mL min ⁻¹	40 mL min ⁻¹
Oven Parameters			
Inlet program	200 °C $\xrightarrow{10^\circ \text{ s}^{-1}}$ 250 °C (0.21 min) (0.21 min)	200 °C $\xrightarrow{10^\circ \text{ s}^{-1}}$ 250 °C (0.21 min) (0.21 min)	200 °C $\xrightarrow{10^\circ \text{ s}^{-1}}$ 250 °C (0.21 min) (0.21 min)
Oven program	40 °C $\xrightarrow{45^\circ \text{ min}^{-1}}$ 220 °C $\xrightarrow{\text{INF}}$ 300 °C (1 min) (1 min)	40 °C $\xrightarrow{40^\circ \text{ min}^{-1}}$ 30 °C (1 min) (1 min)	40 °C $\xrightarrow{40^\circ \text{ min}^{-1}}$ 30 °C (1 min) (1 min)
Fibre conditioning	240 °C for 5 min	N.A.	240 °C for 3 min
MS Parameters			
Ion source temperature	250 °C	200 °C	200 °C
Methane flow	1.3 mL min ⁻¹	2 mL min ⁻¹	2 mL min ⁻¹
Ion dwell times	m/z 46: 5 ms m/z 62: 5 ms m/z 170: 5 ms m/z 269: 5 ms	m/z 62: 75 ms m/z 123: 75 ms m/z 170: 50 ms m/z 269: 50 ms	m/z 46: 25 ms m/z 62: 25 ms m/z 123: 25 ms§ m/z 170: 50 ms m/z 269: 125 ms

*N.A.: Not applicable; § For pipe bomb samples, m/z 123 (nitrobenzene) was removed and the dwell time of m/z 62 (nitroglycerin) increased to 50 ms.

5.3 Results and discussion

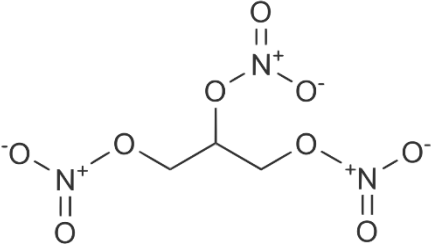
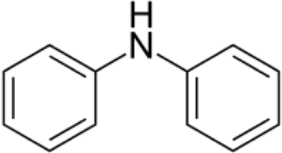
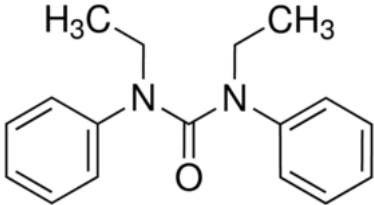
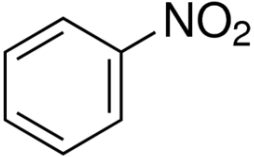
5.3.1 Preliminary considerations

As nitrocellulose is unsuitable for analysis via GC-MS, this study instead targeted nitroglycerin, diphenylamine and ethyl centralite as the components of interest. The structures and physical properties of these compounds, as well as those of nitrobenzene (used as an internal standard) are shown in Table 5.4. Diphenylamine is a stabiliser that neutralises nitrous and nitric oxides formed during nitrocellulose decomposition, which would otherwise result in autocatalytic degradation of the powder.^[405, 406] Ethyl centralite is a stabiliser and a plasticiser, making the nitrocellulose pliable and reducing its hygroscopicity.^[385, 386] Although results are presented in this chapter for all three components, the primary goal was to determine suitable recovery protocols for nitroglycerin. Under most forensic protocols, this component must be detected in order to report the presence of residues from double-base smokeless powder.^c Additives such as diphenylamine and ethyl centralite may assist in identifying the brand of powder employed, but are not themselves indicative of an explosive material.

A sample chromatogram acquired from a mixed calibration standard of nitrobenzene and the three target components is shown in Figure 5.2. It should be noted that ethyl centralite yielded a substantially lower peak area than the remaining components, which could potentially hinder its detection at low concentrations. Nitroglycerin, diphenylamine and ethyl centralite all exhibit a degree of chemical degradation, as evident by the presence of multiple chromatographic peaks. The minor peak eluting shortly before nitroglycerin was attributed to dinitroglycerin, a degradation product formed through the hydrolysis of a nitro functional group on trinitroglycerin.^[406] Previous experiments by Bors found that this peak could be reduced by employing a lower GC inlet temperature.^[403] In this instance, as the presence of dinitroglycerin was not found to interfere with the quantification of nitroglycerin, the existing GC inlet program was retained. Similarly, the minor peaks observed in the diphenylamine and ethyl centralite mass ranges were well separated from those of interest, and so no further investigation regarding their origin was conducted.

^c For example, this is standard procedure within the United States Bureau of Alcohol, Tobacco, Firearms and Explosives (ATF), as communicated by Dr. John Goodpaster (a former explosives analyst at the ATF).

Table 5.4: Chemical structures and selected physical properties of nitroglycerin, diphenylamine, ethyl centralite and nitrobenzene.

Compound	Molecular Weight	Boiling Point
<p data-bbox="453 412 630 450">Nitroglycerin</p> 	<p data-bbox="847 562 1050 600">227.1 g mol⁻¹</p>	<p data-bbox="1209 562 1299 600">50 °C</p>
<p data-bbox="440 790 644 828">Diphenylamine</p> 	<p data-bbox="847 909 1050 947">169.2 g mol⁻¹</p>	<p data-bbox="1198 909 1303 947">302 °C</p>
<p data-bbox="437 1106 647 1144">Ethyl Centralite</p> 	<p data-bbox="847 1240 1050 1279">268.4 g mol⁻¹</p>	<p data-bbox="1166 1240 1337 1279">325-330 °C</p>
<p data-bbox="453 1449 630 1487">Nitrobenzene</p> 	<p data-bbox="847 1565 1050 1603">123.1 g mol⁻¹</p>	<p data-bbox="1198 1565 1303 1603">211 °C</p>

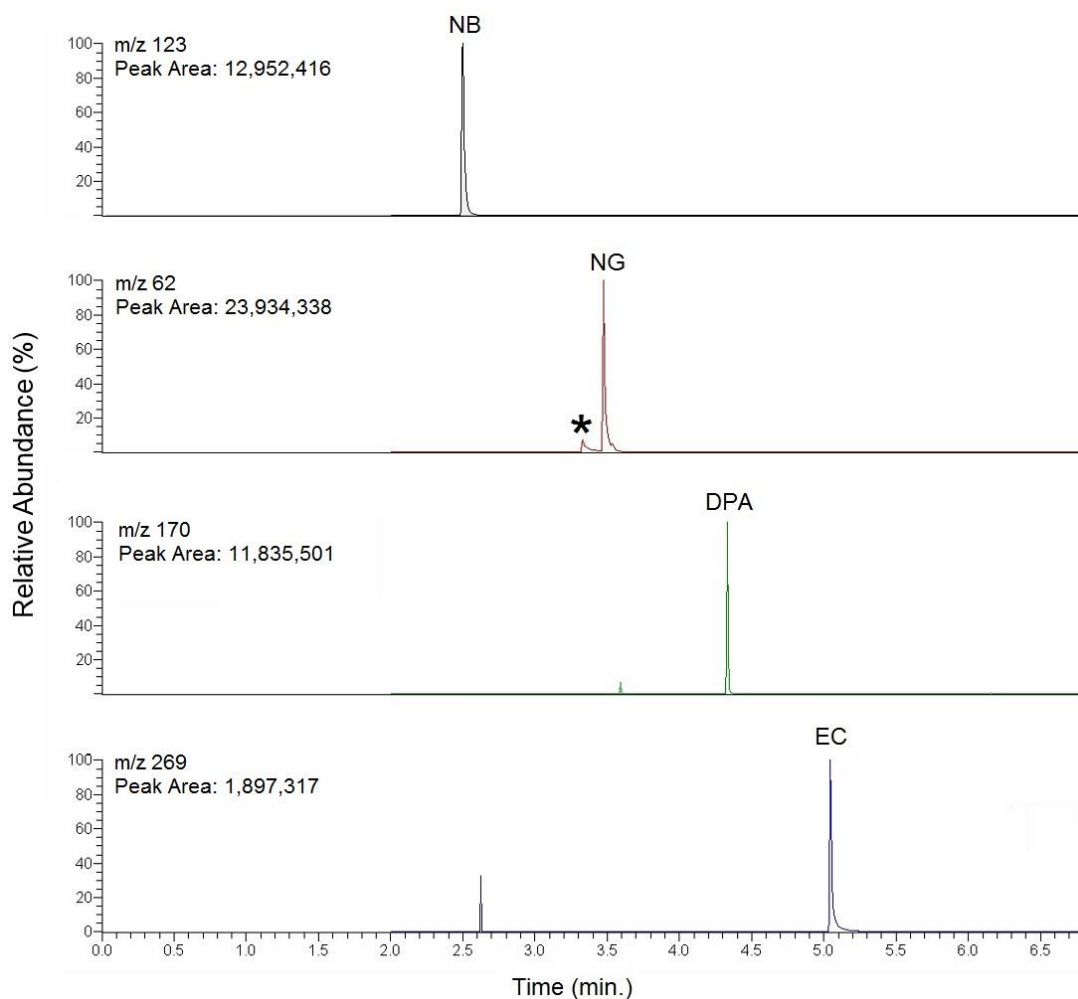


Figure 5.2: GC-MS chromatogram acquired from a standard solution of nitrobenzene (NB), nitroglycerin (NG), diphenylamine (DPA) and ethyl centralite (EC) analysed using the TV-SPME-2 method. (*) denotes minor peak attributed to dinitroglycerin. Note that peaks have been auto-scaled for clarity.

5.3.2 Smokeless powder deflagration

As mentioned above, the majority of studies to date concerning recovery protocols for explosive traces have utilised standard solutions of the target analytes as imitation residues.^[389, 390, 392-396, 398] These simulated samples may not provide an accurate representation of actual residues produced by an explosive event. Post-blast residues are significantly more complex due to the changes that occur in the explosive as it reacts, degradation processes following reaction, and potential contamination from the local environment.^[407, 408] Initial experiments were hence conducted to assess the practicality of generating ‘real’ residues for sampling through the deflagration of smokeless powder.

Various masses of smokeless powder were deflagrated under identical conditions and quantification carried out on the resulting residues, as shown in Table 5.5. Only one trial; employing 0.3 g of smokeless powder; resulted in the successful detection of all three target components. Substantially lower recoveries of all analytes were observed in the 0.2 g trial, which may be due to insufficient material being present prior to deflagration. The overall recovery of residues also appeared to decrease with larger mass quantities of the powder. A possible explanation for this phenomenon is that greater powder quantities produce a larger flame, which is more efficient in consuming the explosive material. This is consistent with assertions in the scientific literature that larger explosions in fact leave less explosive residue at the scene than smaller detonations.^[285]

Table 5.5: Concentrations (parts-per-billion) of target explosive components recovered from deflagration trials of 0.2 – 0.6 g of Alliant Red Dot DBSP.

Compound	0.2 g	0.3 g	0.4 g	0.5 g	0.6 g
NG	0.00	16.46	0.00	0.00	1.28
DPA	1.07	5.92	0.83	0.88	0.85
EC	3.43	9.41	0.00	0.00	0.00

Four replicate trials using 0.3 g of smokeless powder found that the most consistent results were obtained for nitroglycerin (Table 5.6). However, the relative standard deviation (RSD) was found to be greater than the recommended acceptable limit of 15 %, indicating a lack of precision.^[409] A greater level of variation was observed for the remaining components, with two trials failing to detect ethyl centralite altogether. This is consistent with prior studies that have found difficulty in controlling deflagration or detonation processes to obtain a reproducible deposition of residues.^[410] Due to the low quantities of target analytes recovered from the deflagration trials, as well as the lack of reproducibility between replicate trials, it was decided to conduct all subsequent studies using standard solutions of the target analytes spiked onto the recovery surface.

Table 5.6: Concentrations (parts-per-billion) and standard deviation of target explosive components recovered from four replicate deflagration trials of 0.3 g of Alliant Red Dot DBSP.

Compound	Trial 1	Trial 2	Trial 3	Trial 4	Average	Precision (% RSD)
NG	3.39	2.18	2.33	1.91	2.45	26.5
DPA	3.87	9.18	2.47	1.90	4.36	76.2
EC	15.29	0.00	0.00	24.76	10.0	121.7

5.3.3 Factor screening

In order to select factors to be investigated using the central composite design, screening trials were carried out to determine whether particular sampling methods, extraction periods or storage parameters would affect recovery of the target analytes. Triplicate samples were prepared using each of four selected sampling methods; solvent extraction, dry cotton swabbing, isopropanol-wetted cotton swabbing and acetone-wetted cotton swabbing. Cotton swabs are frequently utilised for the sampling of explosive residues due to their low cost and availability,^[392, 393] and the use of these swabs with both acetone and isopropanol has been reported in the literature.^[411-413]

The average percentage recoveries using each method are depicted in Figure 5.3. The ethyl centralite results were highly unreliable, with extremely large standard deviations and an impractically high recovery using the isopropanol-wetted swabs. The large variation in the ethyl centralite results is likely due to the low peak areas obtained, resulting in minor deviations producing a much larger percentage effect. Additionally, some error may be attributed to the instrumental analysis parameters utilised, which were optimised for the detection of nitroglycerin rather than ethyl centralite.^[403] As ethyl centralite has a very low vapour pressure, the vaporisation of this analyte may have been inconsistent, contributing to the large variation between replicates. The inaccurate recovery (exceeding 300 %) obtained using the isopropanol-wetted swabs was attributed to uncertainty associated with the calibration. The low peak areas generated by ethyl centralite resulted in a poor signal-to-noise ratio, making it difficult to accurately integrate these peak areas. Consequently, the ethyl centralite recovery could not be determined with confidence.

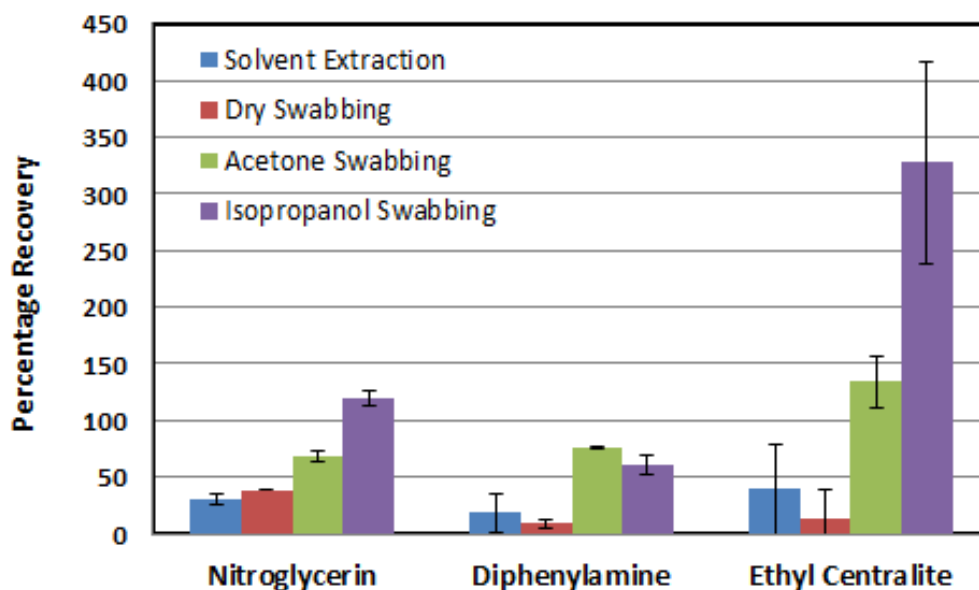


Figure 5.3: Average percentage recoveries of nitroglycerin, diphenylamine and ethyl centralite using various sampling methods. Error bars represent the standard deviation across three replicates.

Nonetheless, the results indicate that wetted cotton swabbing was the most effective overall recovery method, followed by solvent extraction and dry swabbing. This indicates that the presence of a solvent is highly desirable for recovering residues adhering to the surface. Interestingly, the use of isopropanol-wetted swabs gave a higher recovery of nitroglycerin whilst acetone gave a higher recovery of diphenylamine. This is potentially due to the relative solubilities of the two components in each solvent. It was hence decided to investigate the use of dry, acetone-wetted or isopropanol-wetted swabbing using the central composite design, to determine whether the difference in recoveries obtained from each method could be considered significant.

The comparison of sampling methods was repeated using 30 minute and 60 minute extraction times, as it was anticipated that a longer extraction interval may improve recovery. As shown in Table 5.7, increasing the extraction time improved overall recoveries using the solvent extraction and dry swabbing methods. On the other hand, recoveries from the solvent-wetted swabs decreased over the extended extraction time. The differing results obtained from the wetted and dry swabs indicates an interaction between the swabbing method and extraction duration, warranting further investigation through the central composite design.

Table 5.7: Average percentage recoveries (from three replicates) of nitroglycerin, diphenylamine and ethyl centralite using four sampling methods, following 15 minute, 30 minute or 60 minute extraction periods.

Compound	Solvent Extraction	Dry Swab	Acetone Swab	Isopropanol Swab
15 Minutes				
NG	31.0	39.0	67.9	119.1
DPA	18.4	9.2	75.6	61.0
EC	39.7	14.1	134.0	327.3
30 Minutes				
NG	47.7	40.4	52.1	83.7
DPA	52.5	21.1	70.1	51.9
EC	70.5	49.4	148.7	240.6
60 Minutes				
NG	51.9	40.8	46.7	54.3
DPA	62.1	24.9	45.3	48.4
EC	69.4	61.4	159.2	102.6

Whilst the above samples were extracted and analysed within an hour of residue collection, this is often not achievable in casework scenarios due to the time required to transport samples from the scene to the laboratory, as well as the large number of samples submitted for analysis. In these instances, samples must be appropriately stored until they are able to be processed. Triplicate samples were prepared using each sampling method and kept in a refrigerator for three days prior to extraction and analysis, to determine whether a loss of residues would occur while in storage. Refrigerated conditions were selected in order to minimise the evaporation of volatile residues such as nitroglycerin. Despite this, evaporation of solvent from the swab material still occurred, as evident from condensation observed in the storage vials.

Average recoveries from each sampling method are depicted in Figure 5.4. Comparison with Figure 5.3 shows that recoveries of the solvent extraction and dry-swabbing samples increased after storage, but decreased for the wet-swabbing samples. A potential explanation is that the solvent-dissolved residues penetrate further into the swab than those collected through dry swabbing, and become strongly adhered to the swab material as the solvent evaporates. This would result in the residues becoming more difficult to remove upon extraction, decreasing recovery.

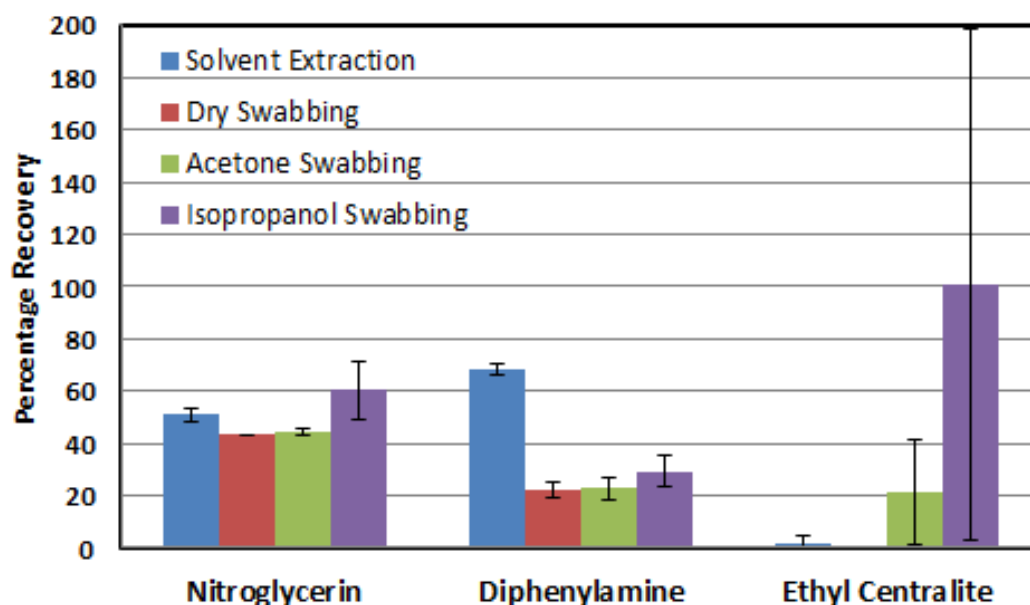


Figure 5.4: Average percentage recoveries of nitroglycerin, diphenylamine and ethyl centralite using various sampling methods following 3 days of sample storage. Error bars represent the standard deviation across three replicates.

In this instance, a longer extraction period may improve the recovery from swabs that are stored prior to analysis. It was hence decided to investigate storage time as part of the experimental design to evaluate the importance of storage duration in analyte recovery, and also to determine whether an interaction could be identified between the storage and extraction intervals. As there was insufficient time during these initial experiments to determine the effect of sample storage at room temperature, it was additionally decided to investigate storage at room temperature versus refrigerated conditions.

5.3.4 Smokeless powder quantification

As described above, standard solutions of the target analytes were used as simulated residues for initial screening experiments, in order to ensure consistent residue deposition across all samples. However, these solutions omit potential interferences caused by other components of the explosive material such as opacifiers, burn modifiers or dyes. For the optimisation study, it was hence decided to prepare samples from a standard solution of smokeless powder rather than solely the target components. This was anticipated to more accurately represent the chemical composition of post-blast smokeless powder residues.

Quantification of the solution was performed to determine an adequate spiking volume for sample preparation. The manufacturer-reported mass percentages of each component were 4 – 40 % nitroglycerin, 0 – 1 % diphenylamine and 0 – 1 % ethyl centralite.^[414] Twenty-fold and fifty-fold dilutions of the powder solution were run in triplicate alongside mixed calibration standards, using nitrobenzene as an internal standard. Excellent linearity was obtained for all three components, with correlation coefficients (calculated using the relative peak area) exceeding 0.99 for all target components (Table 5.8).

Table 5.8: Correlation coefficients of calibration curves generated for nitroglycerin, diphenylamine and ethyl centralite.

Component	Calibration Range	Correlation Coefficient
Nitroglycerin	0.125-20 mg L ⁻¹	0.994
Diphenylamine	0.125-10 mg L ⁻¹	0.997
Ethyl Centralite	0.125-10 mg L ⁻¹	0.999

Quantification results are presented in Table 5.9. Nitroglycerin was quantified using peak areas integrated from the fifty-fold dilution, whilst diphenylamine and ethyl centralite were quantified from the twenty-fold dilution. Good precision was obtained for nitroglycerin and diphenylamine, with RSD values better than the recommended 15 % limit. The precision for ethyl centralite was substantially lower, as expected given the large variation in results obtained during initial experiments. Nonetheless, as the mass percentages of each component were within the ranges reported by the manufacturer, these values were considered to be acceptable. On the basis of these results, 50 µL was selected as a spiking volume to ensure readily detectable analyte concentrations (in the approximate range of 0.1 – 5 mg L⁻¹) upon extraction to 5 mL.

Table 5.9: Quantified mass percentages (averaged across three replicates) and precision of nitroglycerin, diphenylamine and ethyl centralite in Alliant Red Dot DBSP.

Component	Mass Percentage	Precision (% RSD)
Nitroglycerin	26.2 %	13.59
Diphenylamine	0.72 %	6.33
Ethyl Centralite	0.55 %	27.65

5.3.5 Central composite design

5.3.5.1 Optimisation

A face-centred CCD was used to develop response surface models for each target analyte as a function of the selected sampling, storage and extraction parameters, in order to identify the optimum parameters leading to maximum recovery. Model fitting tests were used to assess the quality of the model for each component (Table 5.10). The coefficient of determination, R^2 , measures the percentage of response variation that can be explained by the model.^[415] A drawback to relying on this metric is that it is dependent on the number of factor variables or parameters relative to the sample size.^[61] The adjusted R^2 value, corrected for the number of variables modelled, is thus usually taken as a more accurate indicator of explanatory power.^[61, 416] The predicted R^2 measures the model's predictive capability toward new observations, and may reveal overfitting to the experimental data.^[416]

As seen in Table 5.10, the adjusted R^2 was below 65 % for all components, signifying that a large proportion of variation in explosive recovery remains unexplained by the regression models. This variation is likely attributed to factors not included in the experimental design, such as the time interval between residue deposition and sampling. Additionally, low determination coefficients are frequently obtained when the response (i.e. recovery) variation between individual factor levels is small relative to the variation across the full factor range.^[61] It is therefore possible that the low determination coefficients in this design are at least partially due to only small variations in recovery existing between particular factor levels.

Table 5.10: Model fitting test results for response surface models constructed for nitroglycerin, diphenylamine and ethyl centralite based upon their GC-MS peak areas.

Model parameter	Nitroglycerin	Diphenylamine	Ethyl Centralite
Model significance	< 0.001	< 0.001	0.004
R^2	55.3 %	71.0 %	40.1 %
Adjusted R^2	43.6 %	63.3 %	24.4 %
Predicted R^2	35.5 %	54.8 %	5.0 %
Lack-of-fit	0.999	0.928	0.865

The predicted R^2 values for each component were below 55 %, indicating low predictive precision. The values for ethyl centralite were particularly low, with a large disparity noted between the adjusted and predicted R^2 . This suggests that the ethyl centralite model is overfitted to the experimental data, likely due to unnecessary parameters introducing random variation. The predicted R^2 could be improved by reducing the number of parameters in the design; however, this could adversely affect the modelling of the remaining components. As the recovery of ethyl centralite was not of primary interest to this study, the full set of parameters was therefore retained.

ANOVA found that the regression models for all three components were significant in modelling response variation ($p < 0.005$) with no substantial lack of fit ($p > 0.85$), indicating significant trends modelled within the dataset despite the low R^2 values. These models may hence still provide valuable information regarding the effect of the investigated factors on explosives recovery. This example illustrates the importance of evaluating experimental design results based upon the full data available, rather than relying solely on a single metric such as R^2 .

The optimum parameters and corresponding desirability for each component are shown in Table 5.11. The desirability is a measure of how suited the parameters are to producing an optimum response, with values ranging from 0 (least desirable) to 1 (most desirable). Nitroglycerin and diphenylamine gave the same optimum parameters, with excellent desirability in both instances. The parameters for ethyl centralite, on the other hand, differ from the previous components and show a much lower desirability. This is likely due to the lower detection rate of ethyl centralite (82 %) in comparison to the other components (100 % detection). The overall optimum parameters, while the same as those determined for nitroglycerin and diphenylamine, thus exhibit a decreased desirability due to the poor response expected from ethyl centralite. Regardless, as the desirability towards nitroglycerin was very high, these parameters were retained for the pipe bomb detonation samples.

Table 5.11: CCD optimised parameters and corresponding desirability for the recovery of nitroglycerin, diphenylamine and ethyl centralite from Alliant Red Dot DBSP.

	Nitroglycerin	Diphenylamine	Ethyl Centralite	Overall
Swab Type	Isopropanol	Isopropanol	Dry	Isopropanol
Storage Location	Fridge	Fridge	Fridge	Fridge
Storage Duration	0 Days	0 Days	6 Days	0 Days
Extraction Time	20 Minutes	15 Minutes	60 Minutes	15 Minutes
Desirability	1.000	0.996	0.672	0.777

5.3.5.2 Main effects and factor interactions

Two-way ANOVA was used to evaluate the effect of each factor on the subsequent explosives recovery, and results are shown in Table 5.12. The choice of swabbing solvent was not identified as a critical factor for any of the three target components, possibly due to the similarity in recoveries obtained using acetone and isopropanol. Similarly, extraction time alone was not found to be significant.

Table 5.12: *p*-values for all individual factors or two-way factor interactions in the recovery of Alliant Red Dot DBSP residues on steel.

Parameter(s)	NG	DPA	EC
Sampling solvent	0.999	0.500	0.541
Storage location	0.049	< 0.001	< 0.001
Storage duration	0.292	< 0.001	0.003
Extraction time	0.627	0.391	0.327
Storage duration curvature	< 0.001	< 0.001	0.028
Extraction time curvature	0.925	0.472	0.695
Storage duration * Extraction time	0.058	0.012	0.176
Storage duration * Sampling solvent	0.964	0.478	0.408
Storage duration * Storage location	0.612	0.716	0.387
Extraction time * Sampling solvent	0.876	0.646	0.271
Extraction time * Storage location	0.838	0.865	0.788
Sampling solvent * Storage location	0.203	0.563	0.842

Diphenylamine and ethyl centralite recoveries were found to be significantly lower in samples stored at room temperature than those under refrigerated conditions ($p < 0.001$). Conversely, storage temperature had low significance on the recovery of nitroglycerin ($p = 0.049$). It was expected that losses would occur at higher temperature due to residue evaporation, and that this would be most pronounced in the recovery of nitroglycerin due to its higher volatility than diphenylamine or ethyl centralite. The results obtained here instead suggest that the decreased recoveries are more likely due to solvent evaporation from the swab material, resulting in increased binding of the residues as reported by DeTata *et al.*^[389] The greater recovery of nitroglycerin indicates that this component exhibits a lesser degree of binding to the swab material, allowing it to be more readily extracted when the swab is re-wetted.

Both diphenylamine and ethyl centralite were found to be significantly affected by the storage duration, with longer storage periods proving detrimental to the former ($p < 0.001$) whilst appearing to improve recoveries of the latter ($p = 0.003$). This is evident from the response surface plots (Figure 5.5), which illustrate how recoveries of each component vary as a function of the storage duration and extraction time. It was anticipated that a minimum delay between sampling and analysis would provide the highest recovery, and so the result obtained for ethyl centralite was unexpected. At present, there is insufficient evidence to speculate as to the cause for this result, and this warrants future investigation.

Interestingly, the response surface plots of both diphenylamine and nitroglycerin exhibit a response curvature associated with the storage duration of samples, in which those stored for 3 days exhibit much lower recoveries than those stored for 0 or 6 days. This curvature was found to be significant for both compounds ($p < 0.005$). Although the initial decrease in recovery could be anticipated due to residue loss or decomposition while in storage, the increased recovery between three and six days of storage was not anticipated. Due to the analysis of samples across multiple days, this curvature may be a result of block effects as previously discussed. Further work is hence required to determine whether the results obtained here can be reproduced, or are the result of extraneous variations in the data.

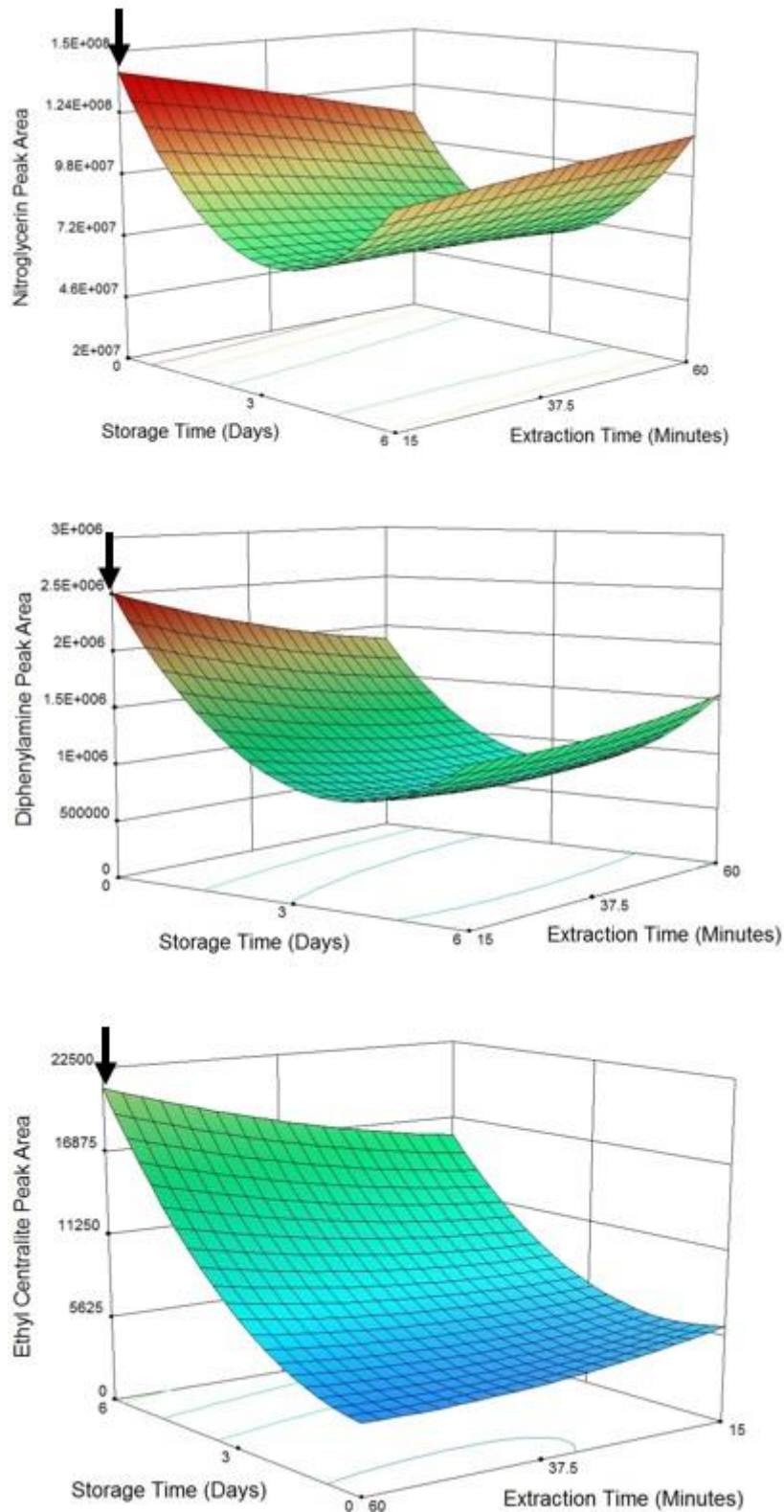


Figure 5.5: Response surface plots for the recovery of nitroglycerin and diphenylamine (isopropanol-wetted swabs) and ethyl centralite (dry swabs) stored under refrigerated conditions, as a function of extraction and storage time. Arrows indicate optimum points on each response surface.

Interactions between the different factors were generally found to be insignificant, with exception of the storage and extraction times. The combination of these factors was found to be influential on the recoveries of diphenylamine ($p = 0.012$) and ethyl centralite ($p = 0.028$), with longer extractions required for samples stored over 3 or 6 days than those analysed on the same day as preparation. These findings again support the hypothesis that increased residue binding onto the swab material occurs whilst in storage, thus requiring a longer extraction period to remove the residues for analysis. This interaction demonstrates the value of a CCD, as univariate optimisation of the extraction time following three or six days of storage could produce a false optimum extraction time of 60 minutes. By employing a CCD to model the entire response surface, it can be seen that the true optimum is in fact obtained when both the storage and extraction time are minimised.

5.3.6 Pipe bomb trial

In order to validate the suitability of the optimised protocols within an operational context, a PVC pipe bomb detonation was conducted to produce real post-blast residues for recovery. Previous work by Bors employed TV-SPME/GC-MS for the recovery of DBSP residues from steel pipe bomb device fragments.^[403] Although the device itself is a key source of post-blast residues, traces may also be recovered from “witness” materials surrounding the explosive charge.^[408] This trial therefore aimed to recover residues on surfaces proximate to the device, rather than the device itself.

Galvanised steel was chosen as the witness surface as it is a common non-porous material that could be expected to survive an explosive blast and accumulate post-blast residues suited to sampling using the techniques described above. Following detonation of the device (Figure 5.6), each plate was divided into 16 areas for processing using the CCD-optimised parameters. This resulted in excellent rates of detection for nitroglycerin (99.0 %) and diphenylamine (95.8 %), and moderate detection of ethyl centralite (64.6 %) across the 96 samples analysed.



Figure 5.6: Photographs of the PVC pipe bomb trial set-up, a) prior to; b) during; and c) following initiation of the device.

The average relative peak area recoveries from each witness plate are provided in Table 5.13, and the relative quantities of nitroglycerin from individual samples illustrated in Figure 5.7. The highest overall recoveries were obtained from plates facing the sides of the device (east and west), rather than the end-caps. This is consistent with previous observations that the initial containment failure of PVC pipe bomb devices initiates in the pipe body, with the explosive plume primarily expanding from the sides of the device.^[417] The heat map also reveals that the explosive residues are more heavily concentrated on samples toward the south end of the device. This is likely due to residues being expelled through the hole drilled in the south end-cap for the time fuse, or the breach of the container originating closer to the south end-cap.

Table 5.13: Relative GC-MS peak areas (normalised to maximum recovery) of target analytes from galvanised steel witness plates following detonation of a PVC pipe bomb containing Alliant Red Dot DBSP. Values are averaged across 16 samples.

Plate Position	Nitroglycerin	Diphenylamine	Ethyl Centralite
East	1.00	1.00	1.00
West	0.95	0.68	0.51
North	0.00	0.01	0.00
South	0.34	0.21	0.14
Top	0.54	0.33	0.78
Bottom	0.47	0.38	0.87

It should be noted that in pipe bombs constructed from steel, the first breach of the container has been observed to occur at the end-caps of the device rather than the pipe body.^[417, 418] This would prospectively result in a differing distribution of post-blast residue on surrounding surfaces, and this should be investigated in future studies.

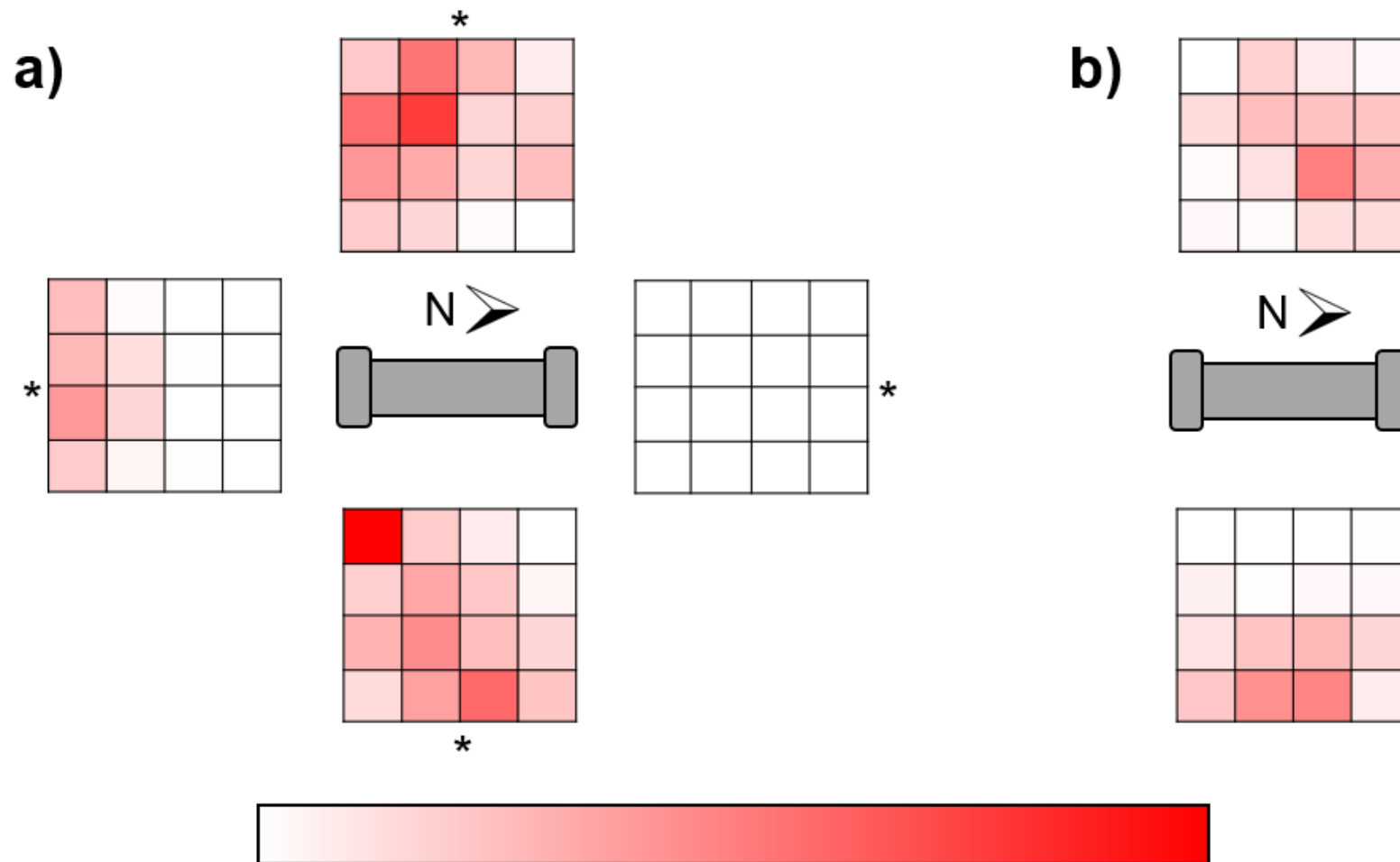


Figure 5.7: Heat maps showing the distribution of NG on witness plates (a) on each side; (b) above and below the PVC pipe bomb device. Colour scale is normalised to the highest nitroglycerin peak area recovery. (*) denotes the top edge of plates surrounding the device.

5.4 Conclusion

The use of a CCD in combination with TV-SPME/GC-MS analysis was able to develop statistically validated protocols for the sampling, storage and extraction of DBSP residues resulting from an explosive event. The resulting parameters were successfully applied to post-blast residues produced from a pipe bomb detonation, with a rate of detection exceeding 95 % for both nitroglycerin and diphenylamine. The elucidated parameters therefore provide a high level of confidence that IED events involving DBSP formulations will be readily identified. The distribution of post-blast residues about the device was also found to be consistent with previous observations regarding the fracturing pattern of PVC pipe bomb devices.

Storage temperature was identified as the most significant individual factor affecting the explosive recovery, with greater recoveries obtained when samples were stored under refrigerated conditions. Minimum storage durations were generally found to be ideal, and a substantial curvature in recovery also observed across the 0 – 6 day period tested. The latter is potentially the result of block effects in the experimental design. Nonetheless, the presence of both curvature and significant factor interactions highlight the necessity of multivariate optimisation methods in order to detect and adequately model higher-order interactions within complex datasets.

As discussed at the beginning of this chapter, while smokeless powders are common in the United States, they are rarely encountered in countries such as Australia due to legal restrictions. In these jurisdictions, explosive incidents are more likely to involve mining munitions such as TNT, or homemade peroxide explosives such as TATP and ammonium nitrate-based explosives. Future work is therefore required determine optimum protocols for a wider range of explosives encountered in different geographical contexts. Ultimately, such studies will assist in establishing more rigorously validated standards for explosive investigations.

Chapter 6: Conclusions and Future Work

The aim of this dissertation was to develop more objective analysis and interpretation protocols for physical evidence through the use of chemometric techniques. The studies detailed in this thesis have shown the utility of chemometrics not only for the improved discrimination of samples, but also for the exploration of factors affecting sample characterisation, and subsequent optimisation of evidentiary procedures. Specific conclusions are provided below for each chapter, along with proposals for future work.

Chapter 2 demonstrated the use of microspectrophotometry (MSP) with chemometrics and hypothesis testing to measure sample similarity or dissimilarity, specifically in regards to “questioned versus known” comparisons of blue-dyed acrylic fibres. It was noted that spectral deviations as a result of sample heterogeneity or instrumental variation have the potential to lead to false exclusions. Nonetheless, this methodology offers a quantitative means of describing the strength of a fibre association, addressing the need to express comparative evidence in probabilistic rather than subjective terms. Due to the limited sample range, further work is required to determine whether similar results can be obtained with other fibre or dye types. Natural fibres such as cotton or wool are of particular interest due to their prevalence and greater level of natural variation, which will provide a more challenging test of the methodology described.

Raman spectroscopy was examined as a means of obtaining complementary information regarding both the fibre dyes and substrate, but proved unsuccessful due to significant fluorescence interference. This could potentially be overcome by using alternative laser sources. Alternatively, future work could instead investigate the characterisation of the fibres using infrared microspectroscopy, which has been shown to provide discrimination between undyed acrylic fibres based on their co-monomer content.^[419] Another factor worthy of investigation is the effect of damage or degradation (e.g. by repeated wear or laundering) on the characterisation of textiles, as this may affect their probative value in questioned versus known comparisons.

In Chapter 3, diffuse reflectance visible spectroscopy with chemometric analysis was used to characterise and classify a population of 35 blue ballpoint inks. The developed statistical model could potentially allow identification of the pen type from which a questioned ink entry was made, or exclude dissimilar ink formulations from further examination. Certain inks proved to be difficult to separate on the basis of colour alone.

Further studies could therefore make use of micro-Raman or infrared microscopy to instead target vehicle components such as solvents or resins, which may assist in discrimination.

Monitoring of six inks stored under various conditions over 14 months found that they remained chemically stable in the dark. Conversely, changes in both the spectral profile and visible colour of the deposit could occur in as little as one week when left exposed to light. Although posing a challenge to ink identification, this may in fact prove beneficial in detecting document alterations. The observed changes are consistent with the degradation of triarylmethane dyes such as methyl violet through *N*-demethylation, though this cannot be stated with certainty as the composition of the studied inks is unknown. In future, chromatographic methods could be applied to identify ink constituents that may be of specific interest. Ink dating curves constructed using partial least squares regression (PLSR) proved unsuccessful due to a high level of dispersion about the regression line. It should also be noted that the use of these models would require knowledge of the ink composition and document storage history, which may not be feasible in casework scenarios involving questioned documents.

Artificial ageing via ultraviolet (UV) or thermal exposure over 24 hours was able to reproduce the effects of short-term light exposure, though no subsequent changes were noted. It has been postulated in the literature that that the loss of methyl groups due to UV irradiation yields stable products resistant to further degradation, whilst the removal of solvent through heating may hinder the dye degradation pathway.^[353, 364] Further work in this area would benefit from the use of a climate control chamber to more thoroughly investigate the effects of varying both light and temperature. This would also facilitate investigations regarding the impact of humidity, which was not controlled in this study but is likely to be influential on the ink ageing process.

The study of ink analysis was extended in Chapter 4 through the use of a video spectral comparator (VSC) to obtain spectral and chromatic data from handwritten ink traces. This instrument is routinely utilised by forensic document examiners conducting specialised lighting examinations, allowing the results of this study to be more readily applied within an operational context. The distribution of the ink population based upon the VSC spectra was broadly consistent with results in Chapter 3, although less specificity was obtained due to the lower spectral reproducibility of the VSC.

Future studies should incorporate testing on other VSC5000s to determine whether this limitation is inherent to all other instruments of this model, or only with the instrument utilised in this study. It would also be of interest to determine whether improved results can be obtained using the more recent VSC6000 or VSC8000 models.

The use of fluorescence as an initial classifier prior to chemometric analysis yielded improved separation of a small number of inks. Additional discrimination could be achieved by categorising the fluorescent inks according to their relative fluorescence intensity, though this was done based on personal opinion and could introduce subjectivity into the results. In future, the use of quantitative fluorescence microscopy may be able to establish objective cut-off values for 'strong' or 'weak' fluorescence.

The ink studies in both Chapters 3 and 4 employed a very specific range of pen inks on a single substrate, all sourced from Western Australia. Additional studies involving a range of ink types (such as gel, roller-ball and felt-tip varieties) on different substrates should be conducted to determine whether similar results can be achieved. There is also a need to expand the sample set to incorporate international suppliers. This will allow the potential application of this model to a broader geographical context, as well as providing a more rigorous assessment of batch variations. Furthermore, ink formulations are constantly being redesigned to improve characteristics such as colour or viscosity, and this will necessitate the consistent addition of new data through continued sample collection.

Chapter 5 illustrated the use of a central composite design to optimise the sampling, storage and extraction parameters for double-base smokeless powder residues analysed by total vapourisation solid-phase microextraction gas chromatography-mass spectrometry (TV-SPME/GC-MS). Storage temperature was found to be the most significant factor influencing recovery, with considerable losses observed when samples were stored at room temperature rather than under refrigerated conditions. Longer storage periods were found to be detrimental to recovery, requiring a greater extraction period to remove the residues from the swab material. Interestingly, a substantial curvature associated with the storage duration was noted for nitroglycerin and diphenylamine, the cause of which could not be stated with absolute certainty. This result highlights the necessity of multivariate optimisation methods in order to detect and adequately model higher-order interactions within complex datasets.

The optimum parameters identified through the central composite design were successfully applied to post-blast residues produced from a pipe bomb detonation, with a rate of detection exceeding 95 % for both nitroglycerin and diphenylamine. The use of these parameters therefore provides a high level of confidence that explosive events involving double-base smokeless powders will be readily identified. The distribution of residues on witness materials surrounding the device was found to be consistent with previous observations regarding the fracturing pattern of polyvinyl chloride (PVC) pipe bomb devices. It is expected that steel devices would produce a differing residue distribution on surrounding surfaces, and this should be investigated in future studies.

It should be noted that although gunpowders are widely used in the United States, they are rarely encountered in countries such as Australia due to legal restrictions. In these jurisdictions, explosive incidents are more likely to involve mining munitions such as trinitrotoluene (TNT) or homemade peroxide explosives, e.g. triacetone triperoxide (TATP). Additional work is therefore required to determine optimum protocols for a wider range of explosives encountered in different geographical contexts. The methodology presented in Chapter 5 may also be applied to alternative forms of physical evidence. As with explosives analysis, the use of experimental design within a broader forensic context has been largely limited to the optimisation of instrumental analysis, rather than pre-analysis procedure such as sample collection or storage. The use of multivariate optimisation techniques will allow the development of scientifically rigorous evidential procedures across multiple forensic disciplines.

Finally, whilst the work in this dissertation has demonstrated the applicability of chemometrics to forensic examinations, it must also be considered how the results of these examinations may be presented in court. Current approaches to the presentation of evidence vary between jurisdictions. For example, fibre analysts in the United States commonly employ a frequentist approach as per Scientific Working Group on Materials Analysis (SWGMAT) guidelines, whilst European (and to an extent, Australian) examiners utilise the Bayesian approach recommended by the European Network of Forensic Science Institutes.^[212, 420, 421] Future research is needed to examine how chemometric methodologies can be integrated within each of these frameworks, in order to gain acceptance in the legal system.

References

1. Coyle, T., *Trace and Contact Evidence*, in *Crime Scene to Court: The Essentials of Forensic Science*, P. White, Editor. 2010, RSC Publishing: Cambridge. p. 106-126.
2. Roux, C. and J. Robertson, *Trace Evidence Overview*, in *Encyclopedia of Forensic Sciences*, J.A. Siegel and P.J. Saukko, Editors. 2013, Academic Press: Waltham. p. 279-285.
3. Saferstein, R., *Forensic Science: From the Crime Scene to the Crime Lab*. 2009, Upper Saddle River, NJ: Pearson Education.
4. Kirk, P.L., *Crime Investigation: Physical Evidence and the Police Laboratory*. 1953, New York: Interscience.
5. Locard, E., *The analysis of dust traces: Part 1*. The American Journal of Police Science, 1930. **1**(3): p. 276-298.
6. National Academy of Sciences, *Strengthening Forensic Science in the United States: A Path Forward*. 2009, Committee on Identifying the Needs of the Forensic Sciences Community, National Research Council: Washington DC.
7. Science and Technology Committee, *The Forensic Science Service*. 2011: London.
8. Jackson, A.R.W. and J.M. Jackson, *Introduction to Forensic Science*, in *Forensic Science*. 2011, Pearson Education: Harlow, England. p. 1-14.
9. Smith, R., *Chemometrics*, in *Forensic Chemistry: Fundamentals and Applications*, J.A. Siegel, Editor. 2016, John Wiley & Sons: Chichester, UK. p. 469-503.
10. Saferstein, R., *Criminalistics: An Introduction to Forensic Science*. International ed. 2011, Upper Saddle River, NJ: Pearson Prentice Hall.
11. Brereton, R.G., *Chemometrics: Data Analysis for the Laboratory and Chemical Plant*. 2003, London: John Wiley & Sons.
12. Morgan, S.L. and E.G. Bartick, *Discrimination of Forensic Analytical Chemical Data using Multivariate Statistics*, in *Forensic Analysis on the Cutting Edge: New Methods for Trace Evidence Analysis*, R.D. Blackledge, Editor. 2007, John Wiley & Sons: New Jersey. p. 333-374.
13. Christensen, A.M., et al., *Error and its meaning in forensic science*. Journal of Forensic Sciences, 2014. **59**(1): p. 123-126.
14. Dror, I.E., D. Charlton, and A.E. Péron, *Contextual information renders experts vulnerable to making erroneous identifications*. Forensic Science International, 2006. **156**(1): p. 74-78.
15. Kassin, S.M., I.E. Dror, and J. Kukucka, *The forensic confirmation bias: Problems, perspectives, and proposed solutions*. Journal of Applied Research in Memory and Cognition, 2013. **2**(1): p. 42-52.

16. Boehm-Davis, D.A., *Human factors and cognitive bias in forensic science*, in *First Public Meeting of the National Commission on Forensic Science 2014*: Washington, DC.
17. Murrie, D.C., et al., *Are forensic experts biased by the side that retained them?* *Psychological Science*, 2013. **24**(10): p. 1889-97.
18. Hsu, S.S., *FBI admits flaws in hair analysis over decades*, in *The Washington Post*. 2015: Washington, D.C.
19. OIG, *A Review of the FBI's Handling of the Brandon Mayfield Case*. 2006, Office of the Inspector General, Oversight & Review Division, National Institute of Justice.
20. White House Office of Science and Technology Policy. *Strengthening Forensic Science: A Progress Report*. 2014; Available from: http://www.whitehouse.gov/sites/default/files/microsites/ostp/forensic_science_progress_2-14-14.pdf.
21. Butler, J.M., *U.S. initiatives to strengthen forensic science & international standards in forensic DNA*. *Forensic Science International: Genetics*, 2015. **18**: p. 4-20.
22. *Forensic Science and Standards Act of 2012*.
23. *Criminal Justice and Forensic Science Reform Act of 2011*.
24. Abraham, J., et al., *Modern statistical models for forensic fingerprint examinations: A critical review*. *Forensic Science International*, 2013. **232**(1-3): p. 131-150.
25. Neumann, C., et al., *Quantifying the weight of fingerprint evidence through the spatial relationship, directions and types of minutiae observed on fingerprints*. *Forensic Science International*, 2015. **248**: p. 154-171.
26. Ulery, B.T., et al., *Accuracy and reliability of forensic latent fingerprint decisions*. *Proceedings of the National Academy of Sciences*, 2011. **108**(19): p. 7733-7738.
27. Pretty, I.A. and D. Sweet, *A paradigm shift in the analysis of bite marks*. *Forensic Science International*, 2010. **201**(1-3): p. 38-44.
28. Baiker, M., et al., *Quantitative comparison of striated toolmarks*. *Forensic Science International*, 2014. **242**: p. 186-199.
29. Petraco, N.D.K., et al., *Addressing the National Academy of Sciences' challenge: A method for statistical pattern comparison of striated tool marks*. *Journal of Forensic Sciences*, 2012. **57**(4): p. 900-911.
30. Hancock, S., R. Morgan-Smith, and J. Buckleton, *The interpretation of shoeprint comparison class correspondences*. *Science & Justice*, 2012. **52**(4): p. 243-248.

31. Kloosterman, A., M. Sjerps, and A. Quak, *Error rates in forensic DNA analysis: Definition, numbers, impact and communication*. Forensic Science International: Genetics, 2014. **12**: p. 77-85.
32. Biedermann, A. and F. Taroni, *Bayesian networks for evaluating forensic DNA profiling evidence: A review and guide to literature*. Forensic Science International: Genetics, 2012. **6**(2): p. 147-157.
33. Sjøstad, K.-E., D. Lucy, and T. Andersen, *Lead isotope ratios for bullets, forensic evaluation in a Bayesian paradigm*. Talanta, 2016. **146**: p. 62-70.
34. Skerrett, J., C. Neumann, and I. Mateos-Garcia, *A Bayesian approach for interpreting shoemark evidence in forensic casework: Accounting for wear features*. Forensic Science International, 2011. **210**(1-3): p. 26-30.
35. Zadora, G., *Evaluation of evidence value of glass fragments by likelihood ratio and Bayesian Network approaches*. Analytica Chimica Acta, 2009. **642**(1-2): p. 279-290.
36. *R vs T*. 2010, EWCA Crim 2439.
37. Jayaprakash, P.T., *On the limitations of probability in conceptualizing pattern matches in forensic science. Response to "On the value of probability for evaluating results of comparative pattern analysis" by Alex Biedermann and Franco Taroni [Forensic Sci. Int. 232 (2013) e44-e45]*. Forensic Science International, 2014. **239**: p. e10-e11.
38. Taylor, D., et al., *An illustration of the effect of various sources of uncertainty on DNA likelihood ratio calculations*. Forensic Science International: Genetics, 2014. **11**: p. 56-63.
39. Wold, S., *Chemometrics; what do we mean with it, and what do we want from it?* Chemometrics and Intelligent Laboratory Systems, 1995. **30**(1): p. 109-115.
40. Miller, J.N. and J.C. Miller, *Statistics and Chemometrics for Analytical Chemistry*. 6th ed. 2010, Harlow, England: Pearson Education.
41. Zadora, G., *Chemometrics and Statistical Considerations in Forensic Science*, in *Encyclopedia of Analytical Chemistry*, R.A. Meyers, Editor. 2006, John Wiley & Sons: New Jersey.
42. Otto, M., *Chemometrics: Statistics and computer application in analytical chemistry*. 2nd ed. 2007, Weinheim, Germany: Wiley-VCH.
43. Brereton, R.G., *Applied Chemometrics for Scientists*. 2007, Chichester, England: John Wiley & Sons. 145-191.
44. Brereton, R.G., *Pattern recognition in chemometrics*. Chemometrics and Intelligent Laboratory Systems, 2015. **149B**: p. 90-96.

45. Anderson, M.J. and P.J. Whitcomb, *Response Surface Methods for Optimization*, in *DOE Simplified: Practical Tools for Effective Experimentation*. 2000, Productivity Press: New York. p. 135-145.
46. Bezerra, M.A., et al., *Response surface methodology (RSM) as a tool for optimization in analytical chemistry*. *Talanta*, 2008. **76**(5): p. 965-977.
47. Gemperline, P.J., *Principal Component Analysis*, in *Practical Guide to Chemometrics*. 2006, CRC Press: Boca Raton, Florida. p. 69-104.
48. Brereton, R.G., *Pattern Recognition*, in *Applied Chemometrics for Scientists*. 2007, John Wiley & Sons: Chichester, England. p. 145-191.
49. Varmuza, K. and P. Filzmoser, *Principal Component Analysis*, in *Introduction to Multivariate Statistical Analysis in Chemometrics*. 2009, Taylor & Francis: Boca Raton, Florida.
50. Lavine Barry, K. and J. Workman, *Chemometrics: Past, Present, and Future*, in *Chemometrics and Chemoinformatics*. 2005, American Chemical Society. p. 1-13.
51. Jolliffe, I.T., *Principal Component Analysis*. 2nd ed. 2002, Secaucus, NJ, USA: Springer.
52. Bensmail, H. and G. Celeux, *Regularized gaussian discriminant analysis through eigenvalue decomposition*. *Journal of the American Statistical Association*, 1996. **91**(436): p. 1743-1748.
53. Kinton, V., *Multivariate Techniques*, in *Practical Analysis of Flavor and Fragrance Materials*. 2011, John Wiley & Sons. p. 91-110.
54. Mendlein, A., C. Szkudlarek, and J.V. Goodpaster, *Chemometrics*, in *Encyclopedia of Forensic Sciences*, J.A. Siegel and P.J. Saukko, Editors. 2013, Academic Press: Waltham. p. 646-651.
55. Fujikoshi, Y., V.V. Ulyanov, and R. Shimizu, *Multivariate Statistics: High-Dimensional and Large-Sample Approximations*. 2010, New Jersey: John Wiley & Sons.
56. Somorjai, R.L., *Multivariate Statistical Methods*, in *Encyclopedia of Spectroscopy and Spectrometry*, J. Lindon, Editor. 2010, Academic Press: Oxford. p. 1704-1709.
57. Brereton, R.G., *Chemometrics and Multivariate Analysis*, in *Encyclopedia of Applied Spectroscopy*, D.L. Andrews, Editor. 2003, Wiley-VCH: Weinheim, Germany. p. 1103-1148.
58. Bhatnagar, V., *Data Mining and Analysis in the Engineering Field*. 2014, Pennsylvania: IGI Global.
59. Adams, M.J., *Chemometrics in Analytical Spectroscopy*. 2nd ed. 2004, Cambridge: Royal Society of Chemistry.

60. Khuri, A.I. and S. Mukhopadhyay, *Response surface methodology*. Wiley Interdisciplinary Reviews: Computational Statistics, 2010. **2**(2): p. 128-149.
61. Anderson, M.J. and P.J. Whitcomb, *RSM Simplified: Optimising Processes Using Response Surface Methods for Design of Experiments*. 2005, Boca Raton, Florida: CRC Press.
62. Mead, R., S.G. Gilmour, and A. Mead, *Statistical Principles for the Design of Experiments*. 2012, Cambridge: Cambridge University Press.
63. Ridge, E. and D. Kudenko, *Tuning an Algorithm Using Design of Experiments*, in *Experimental Methods for the Analysis of Optimization Algorithms*, T. Bartz-Beielstein, et al., Editors. 2010, Springer: Heidelberg, Germany. p. 265-286.
64. Li, W., *Efficiency of Manufacturing Processes: Energy and Ecological Perspectives*. 2015, Heidelberg, Germany: Springer.
65. Hibbert, D.B., *Modeling and Optimizing Analytical Methods*, in *Quality Assurance in the Analytical Chemistry Laboratory*. 2007, Oxford University Press: Oxford. p. 66-104.
66. Cavazzuti, M., *Design of Experiments*, in *Optimization Methods: From Theory to Design*. 2013, Springer: Heidelberg, Germany. p. 13-42.
67. Casale, J.F. and J.W. Watterson, *A computerized neural network method for pattern recognition of cocaine signatures*. Journal of Forensic Sciences, 1993. **38**(2): p. 292-301.
68. Janhunen, K. and M.D. Cole, *Development of a predictive model for batch membership of street samples of heroin*. Forensic Science International, 1999. **102**(1): p. 1-11.
69. Ryder, A.G., G.M. O'Connor, and T.J. Glynn, *Quantitative analysis of cocaine in solid mixtures using Raman spectroscopy and chemometric methods*. Journal of Raman Spectroscopy, 2000. **31**(3): p. 221-227.
70. Dams, R., et al., *Heroin impurity profiling: Trends throughout a decade of experimenting*. Forensic Science International, 2001. **123**(2-3): p. 81-8.
71. Ryder, A.G., *Classification of narcotics in solid mixtures using principal component analysis and Raman spectroscopy*. Journal of Forensic Sciences, 2002. **47**(2): p. 275-284.
72. Waddell, R.J.H., N. NicDaeid, and D. Littlejohn, *Classification of ecstasy tablets using trace metal analysis with the application of chemometric procedures and artificial neural network algorithms*. Analyst, 2004. **129**(3): p. 235-240.
73. Esseiva, P., et al., *Chemical profiling and classification of illicit heroin by principal component analysis, calculation of inter sample correlation and artificial neural networks*. Talanta, 2005. **67**(2): p. 360-7.

74. Krishna Reddy, M.M., et al., *Source identification of Indian opium based on chromatographic fingerprinting of amino acids*. Journal of Chromatography A, 2005. **1088**(1–2): p. 158-168.
75. Mohana, M., et al., *Principal opium alkaloids as possible biochemical markers for the source identification of Indian opium*. Journal of Separation Science, 2005. **28**(13): p. 1558-1565.
76. Nic Daéid, N. and R.J.H. Waddell, *The analytical and chemometric procedures used to profile illicit drug seizures*. Talanta, 2005. **67**(2): p. 280-285.
77. Andersson, K., et al., *Development of a harmonised method for the profiling of amphetamines VI: Evaluation of methods for comparison of amphetamine*. Forensic Science International, 2007. **169**(1): p. 86-99.
78. Goh, C.Y., W. van Bronswijk, and C. Priddis, *Rapid nondestructive on-site screening of methylamphetamine seizures by attenuated total reflection Fourier transform infrared spectroscopy*. Applied Spectroscopy, 2008. **62**(6): p. 640-648.
79. Hughes, J., et al., *Rapid quantification of methamphetamine: using attenuated total reflectance Fourier transform infrared spectroscopy (ATR-FTIR) and chemometrics* Public Library of Science One, 2013. **8**(7): p. e69609.
80. Moros, J., et al., *Nondestructive direct determination of heroin in seized illicit street drugs by diffuse reflectance near-infrared spectroscopy*. Analytical Chemistry, 2008. **80**(19): p. 7257-7265.
81. Turner, N.W., et al., *Rapid qualitative and quantitative analysis of opiates in extract of poppy head via FTIR and chemometrics: towards in-field sensors*. Biosensors and Bioelectronics, 2009. **24**(11): p. 3322-8.
82. Chan, K.-W., G.-H. Tan, and R.C.S. Wong, *Investigation of trace inorganic elements in street doses of heroin*. Science & Justice, 2013. **53**(1): p. 73-80.
83. Liu, C., et al., *Profiling and classification of illicit heroin by ICP-MS analysis of inorganic elements*. Forensic Science International, 2014. **239**: p. 37-43.
84. Dujourdy, L. and F. Besacier, *Headspace profiling of cocaine samples for intelligence purposes*. Forensic Science International, 2008. **179**(2–3): p. 111-122.
85. Grobério, T.S., et al., *Discrimination and quantification of cocaine and adulterants in seized drug samples by infrared spectroscopy and PLSR*. Forensic Science International, 2015. **257**: p. 297-306.
86. Grobério, T.S., et al., *Quantification of cocaine hydrochloride in seized drug samples by infrared spectroscopy and PLSR*. Journal of the Brazilian Chemical Society, 2014. **25**(9): p. 1696-1703.

87. Rodrigues, N.V.S., et al., *Analysis of seized cocaine samples by using chemometric methods and FTIR spectroscopy*. Journal of the Brazilian Chemical Society, 2013. **24**(3): p. 507-517.
88. Monfreda, M., et al., *Fast profiling of cocaine seizures by FTIR spectroscopy and GC-MS analysis of minor alkaloids and residual solvents*. Science & Justice, 2015. **55**(6): p. 456-466.
89. Roggo, Y., K. Degardin, and P. Margot, *Identification of pharmaceutical tablets by Raman spectroscopy and chemometrics*. Talanta, 2010. **81**(3): p. 988-995.
90. Been, F., et al., *Profiling of counterfeit medicines by vibrational spectroscopy*. Forensic Science International, 2011. **211**(1): p. 83-100.
91. Dégardin, K., et al., *Detection and chemical profiling of medicine counterfeits by Raman spectroscopy and chemometrics*. Analytica Chimica Acta, 2011. **705**(1-2): p. 334-341.
92. Custers, D., et al., *ATR-FTIR spectroscopy and chemometrics: An interesting tool to discriminate and characterize counterfeit medicines*. Journal of Pharmaceutical and Biomedical Analysis, 2015. **112**: p. 181-189.
93. Trubshoe, T. and J. McGinn, *Forgery/Counterfeits*, in *Encyclopedia of Forensic Sciences*, M.M. Houck, J.A. Siegel, and P.J. Saukko, Editors. 2013, Academic Press: Waltham. p. 360-366.
94. Kher, A., et al., *Classification of document papers by infrared spectroscopy and multivariate statistical techniques*. Applied Spectroscopy, 2001. **55**(9): p. 1192-1198.
95. Sarkar, A., S.K. Aggarwal, and D. Alamelu, *Laser induced breakdown spectroscopy for rapid identification of different types of paper for forensic application*. Analytical Methods, 2010. **2**(1): p. 32-36.
96. Alamilla, F., et al., *Forensic discrimination of blue ballpoint pens on documents by laser ablation inductively coupled plasma mass spectrometry and multivariate analysis*. Forensic Science International, 2013. **228**(1-3): p. 1-7.
97. Denman, J.A., et al., *Organic and inorganic discrimination of ballpoint pen inks by ToF-SIMS and multivariate statistics*. Applied Surface Science, 2010. **256**(7): p. 2155-2163.
98. de Souza Lins Borba, F., R. Saldanha Honorato, and A. de Juan, *Use of Raman spectroscopy and chemometrics to distinguish blue ballpoint pen inks*. Forensic Science International, 2015. **249**: p. 73-82.
99. Kher, A., et al., *Forensic classification of ballpoint pen inks using high performance liquid chromatography and infrared spectroscopy with principal components analysis and linear discriminant analysis*. Vibrational Spectroscopy, 2006. **40**(2): p. 270-277.

100. Silva, C.S., et al., *Classification of blue pen ink using infrared spectroscopy and linear discriminant analysis*. *Microchemical Journal*, 2013. **109**: p. 122-127.
101. Braz, A., M. López-López, and C. García-Ruiz, *Studying the variability in the Raman signature of writing pen inks*. *Forensic Science International*, 2014. **245**: p. 38-44.
102. Braz, A., M. López-López, and C. García-Ruiz, *Raman imaging for determining the sequence of blue pen ink crossings*. *Forensic Science International*, 2015. **249**: p. 92-100.
103. Neumann, C. and P. Margot, *New perspectives in the use of ink evidence in forensic science: Part II. Development and testing of mathematical algorithms for the automatic comparison of ink samples analysed by HPTLC*. *Forensic Science International*, 2009. **185**(1-3): p. 38-50.
104. Kher, A.A., E.V. Green, and M.I. Mulholland, *Evaluation of principal components analysis with high-performance liquid chromatography and photodiode array detection for the forensic differentiation of ballpoint pen inks*. *Journal of Forensic Sciences*, 2001. **46**(4): p. 878-83.
105. da Silva, V.A.G., et al., *Non-destructive identification of different types and brands of blue pen inks in cursive handwriting by visible spectroscopy and PLS-DA for forensic analysis*. *Microchemical Journal*, 2014. **116**: p. 235-243.
106. Thanasoulas, N.C., N.A. Parisi, and N.P. Evmiridis, *Multivariate chemometrics for the forensic discrimination of blue ball-point pen inks based on their Vis spectra*. *Forensic Science International*, 2003. **138**(1-3): p. 75-84.
107. Berger, C.E.H., *Objective ink color comparison through image processing and machine learning*. *Science & Justice*, 2013. **53**(1): p. 55-59.
108. da Silva, V.A.G., et al., *Discrimination of black pen inks on writing documents using visible reflectance spectroscopy and PLS-DA*. *Journal of the Brazilian Chemical Society*, 2014. **25**(9): p. 1552-1564.
109. Adam, C.D., S.L. Sherratt, and V.L. Zholobenko, *Classification and individualisation of black ballpoint pen inks using principal component analysis of UV-vis absorption spectra*. *Forensic Science International*, 2008. **174**(1): p. 16-25.
110. Adam, C.D., *In situ luminescence spectroscopy with multivariate analysis for the discrimination of black ballpoint pen ink-lines on paper*. *Forensic Science International*, 2008. **182**(1-3): p. 27-34.
111. Silva, C.S., et al., *Near infrared hyperspectral imaging for forensic analysis of document forgery*. *Analyst*, 2014. **139**(20): p. 5176-5184.

112. Bueno, J., V. Sikirzhyski, and I.K. Lednev, *Raman spectroscopic analysis of gunshot residue offering great potential for caliber differentiation*. Analytical Chemistry, 2012. **84**(10): p. 4334-4339.
113. Bueno, J. and I.K. Lednev, *Advanced statistical analysis and discrimination of gunshot residue implementing combined Raman and FT-IR data*. Analytical Methods, 2013. **5**(22): p. 6292-6296.
114. Bueno, J. and I. Lednev, *Raman microspectroscopic chemical mapping and chemometric classification for the identification of gunshot residue on adhesive tape*. Analytical and Bioanalytical Chemistry, 2014. **406**(19): p. 4595-4599.
115. Fernández de la Ossa, M.Á., J.M. Amigo, and C. García-Ruiz, *Detection of residues from explosive manipulation by near infrared hyperspectral imaging: A promising forensic tool*. Forensic Science International, 2014. **242**: p. 228-235.
116. De Lucia, F.C. and J.L. Gottfried, *Classification of explosive residues on organic substrates using laser induced breakdown spectroscopy*. Applied Optics, 2012. **51**(7): p. B83-B92.
117. De Lucia, F.C., et al., *Multivariate analysis of standoff laser-induced breakdown spectroscopy spectra for classification of explosive-containing residues*. Applied Optics, 2008. **47**(31): p. G112-G121.
118. Figueroa-Navedo, A.M., et al., *Chemometrics-enhanced laser-induced thermal emission detection of PETN and other explosives on various substrates*. Journal of Chemometrics, 2015. **29**(6): p. 329-337.
119. Gottfried, J.L., F.C. De Lucia Jr, and A.W. Miziolek, *Discrimination of explosive residues on organic and inorganic substrates using laser-induced breakdown spectroscopy*. Journal of Analytical Atomic Spectrometry, 2009. **24**(3): p. 288-296.
120. Lazic, V., et al., *Analysis of explosive and other organic residues by laser induced breakdown spectroscopy*. Spectrochimica Acta Part B: Atomic Spectroscopy, 2009. **64**(10): p. 1028-1039.
121. Moros, J., et al., *New chemometrics in laser-induced breakdown spectroscopy for recognizing explosive residues*. Journal of Analytical Atomic Spectrometry, 2012. **27**(12): p. 2111-2122.
122. Pinkham, D.W., J.R. Bonick, and M.D. Woodka, *Feature optimization in chemometric algorithms for explosives detection*. Proceedings of SPIE, 2012. **8357**: p. K1-K8.
123. Cetó, X., et al., *Simultaneous identification and quantification of nitro-containing explosives by advanced chemometric data treatment of cyclic voltammetry at screen-printed electrodes*. Talanta, 2013. **107**: p. 270-276.

124. Jimenez-Perez, R., et al., *Design of a virtual sensor data array for the analysis of RDX, HMX and DMNB using metal-doped screen printed electrodes and chemometric analysis*. International Journal of Electrochemical Science, 2013. **8**(3): p. 3279-3289.
125. Polsky, R., et al., *Multivariate analysis for the electrochemical discrimination and quantification of nitroaromatic explosives*. Electroanalysis, 2009. **21**(3-5): p. 550-556.
126. Almeida, M.R., et al., *Detection of explosives on the surface of banknotes by Raman hyperspectral imaging and independent component analysis*. Analytica Chimica Acta, 2015. **860**: p. 15-22.
127. Banas, K., et al., *Multivariate analysis techniques in the forensics investigation of the postblast residues by means of Fourier Transform-infrared Spectroscopy*. Analytical Chemistry, 2010. **82**(7): p. 3038-3044.
128. Hwang, J., et al., *Fast and sensitive recognition of various explosive compounds using Raman spectroscopy and principal component analysis*. Journal of Molecular Structure, 2013. **1039**: p. 130-136.
129. Buxton, T.L. and P.D. Harrington, *Rapid multivariate curve resolution applied to identification of explosives by ion mobility spectrometry*. Analytica Chimica Acta, 2001. **434**(2): p. 269-282.
130. Fraga, C.G., D.R. Kerr, and D.A. Atkinson, *Improved quantitative analysis of ion mobility spectrometry by chemometric multivariate calibration*. Analyst, 2009. **134**(11): p. 2329-2337.
131. Pierrini, G., et al., *Evaluation of preliminary isotopic analysis (¹³C and ¹⁵N) of explosives: A likelihood ratio approach to assess the links between semtex samples*. Forensic Science International, 2007. **167**(1): p. 43-48.
132. Goodpaster, J.V., et al., *Identification and comparison of electrical tapes using instrumental and statistical techniques: I. Microscopic surface texture and elemental composition*. Journal of Forensic Sciences, 2007. **52**(3): p. 610-629.
133. Goodpaster, J.V., et al., *Identification and comparison of electrical tapes using instrumental and statistical techniques: II. Organic composition of the tape backing and adhesive*. Journal of Forensic Sciences, 2009. **54**(2): p. 328-338.
134. Martín-Alberca, C., F.E. Ortega-Ojeda, and C. García-Ruiz, *Analytical tools for the analysis of fire debris. A review: 2008–2015*. Analytica Chimica Acta.
135. Sinkov, N.A., P.M. Sandercock, and J.J. Harynuk, *Chemometric classification of casework arson samples based on gasoline content*. Forensic Science International, 2014. **235**: p. 24-31.

136. Bodle, E.S. and J.K. Hardy, *Multivariate pattern recognition of petroleum-based accelerants by solid-phase microextraction gas chromatography with flame ionization detection*. *Analytica Chimica Acta*, 2007. **589**(2): p. 247-254.
137. Waddell, E.E., et al., *Progress toward the determination of correct classification rates in fire debris analysis*. *Journal of Forensic sciences*, 2013. **58**(4): p. 887-96.
138. Waddell, E.E., M.R. Williams, and M.E. Sigman, *Progress toward the determination of correct classification rates in fire debris analysis II: utilizing soft independent modeling of class analogy (SIMCA)*. *Journal of Forensic Sciences*, 2014. **59**(4): p. 927-35.
139. Balabin, R.M., R.Z. Safieva, and E.I. Lomakina, *Gasoline classification using near infrared (NIR) spectroscopy data: comparison of multivariate techniques*. *Analytica Chimica Acta*, 2010. **671**(1-2): p. 27-35.
140. Doble, P., et al., *Classification of premium and regular gasoline by gas chromatography/mass spectrometry, principal component analysis and artificial neural networks*. *Forensic Science International*, 2003. **132**: p. 26-39.
141. Hupp, A.M., et al., *Chemometric analysis of diesel fuel for forensic and environmental applications*. *Analytica Chimica Acta*, 2008. **606**(2): p. 159-71.
142. Marshall, L., et al., *Association and discrimination of diesel fuels using chemometric procedures*. *Analytical and Bioanalytical Chemistry*, 2009. **394**(8): p. 2049-2059.
143. Monfreda, M. and A. Gregori, *Differentiation of unevaporated gasoline samples according to their brands, by SPME-GC-MS and multivariate statistical analysis*. *Journal of Forensic Sciences*, 2011. **56**(2): p. 372-80.
144. Petraco, N.D., et al., *Statistical discrimination of liquid gasoline samples from casework*. *Journal of forensic Sciences*, 2008. **53**(5): p. 1092-101.
145. Tan, B., J.K. Hardy, and R.E. Snavely, *Accelerant classification by gas chromatography/mass spectrometry and multivariate pattern recognition*. *Analytica Chimica Acta*, 2000. **422**(1): p. 37-46.
146. Baernkopf, J.M., V.L. McGuffin, and R.W. Smith, *Association of ignitable liquid residues to neat ignitable liquids in the presence of matrix interferences using chemometric procedures*. *Journal of Forensic Sciences*, 2011. **56**(1): p. 70-81.
147. Turner, D.A. and J.V. Goodpaster, *Comparing the effects of weathering and microbial degradation on gasoline using principal components analysis*. *Journal of Forensic Sciences*, 2012. **57**(1): p. 64-9.

148. Muehlethaler, C., G. Massonnet, and P. Esseiva, *The application of chemometrics on Infrared and Raman spectra as a tool for the forensic analysis of paints*. Forensic Science International, 2011. **209**(1–3): p. 173-182.
149. Muehlethaler, C., G. Massonnet, and P. Esseiva, *Discrimination and classification of FTIR spectra of red, blue and green spray paints using a multivariate statistical approach*. Forensic Science International, 2014. **244**: p. 170-178.
150. Defeyt, C., et al., *Micro-Raman spectroscopy and chemometrical analysis for the distinction of copper phthalocyanine polymorphs in paint layers*. Spectrochimica Acta Part A: Molecular and Biomolecular Spectroscopy, 2013. **115**: p. 636-640.
151. Gatta, T., et al., *Characterization of black pigment used in 30 BC fresco wall paint using instrumental methods and chemometry*. Chemistry Central Journal, 2012. **6**(Suppl. 2): p. S2.
152. Miguel, C., et al., *Combining infrared spectroscopy with chemometric analysis for the characterization of proteinaceous binders in medieval paints*. Chemometrics and Intelligent Laboratory Systems, 2012. **119**: p. 32-38.
153. Rosi, F., et al., *Multivariate chemical mapping of pigments and binders in easel painting cross-sections by micro IR reflection spectroscopy*. Analytical and Bioanalytical Chemistry, 2011. **399**(9): p. 3133-3145.
154. Liszewski, E.A., et al., *Characterization of automotive paint clear coats by ultraviolet absorption microspectrophotometry with subsequent chemometric analysis*. Applied Spectroscopy, 2010. **64**(10): p. 1122-5.
155. Mendlein, A.N., J.A. Siegel, and J.V. Goodpaster, *Instrumental and chemometric analysis of automotive clear coat paints by micro laser Raman*, in *42nd Central Regional Meeting of the American Chemical Society*. 2011, American Chemical Society: Indianapolis (United States).
156. Maric, M., et al., *Rapid characterisation and classification of automotive clear coats by attenuated total reflectance infrared spectroscopy*. Analytical Methods, 2012. **4**(9): p. 2687-2693.
157. Maric, M., et al., *Synchrotron FTIR characterisation of automotive primer surfacer paint coatings for forensic purposes*. Talanta, 2014. **118**: p. 156-161.
158. Maric, M., et al., *Characterisation and classification of automotive clear coats with Raman spectroscopy and chemometrics for forensic purposes*. Journal of Raman Spectroscopy, 2016.
159. Sauzier, G., et al., *Preliminary studies into the effect of environmental degradation on the characterisation of automotive clear coats by attenuated total reflectance infrared spectroscopy*. Analytical Methods, 2013. **5**(19): p. 4984-4990.

160. van der Pal, K.J., et al., *The effect of environmental degradation on the characterisation of automotive clear coats by infrared spectroscopy*. *Talanta*, 2016. **148**: p. 715-720.
161. Lavine, B.K., et al., *Development of search prefilters for infrared library searching of clear coat paint smears*. *Talanta*, 2014. **119**: p. 331-340.
162. Lavine, B.K., et al., *Search prefilters for mid-infrared absorbance spectra of clear coat automotive paint smears using stacked and linear classifiers*. *Journal of Chemometrics*, 2014. **28**(5): p. 385-394.
163. Lavine, B.K., et al., *Search prefilters for library matching of infrared spectra in the PDQ database using the autocorrelation transformation*. *Microchemical Journal*, 2014. **113**: p. 30-35.
164. Lavine, B.K., et al., *Search prefilters to assist in library searching of infrared spectra of automotive clear coats*. *Talanta*, 2015. **132**: p. 182-190.
165. Lavine, B.K., A. Fasasi, and M. Sandercock, *Improving PDQ database search strategies to enhance investigative lead information for automotive paints*. *Microchemical Journal*, 2014. **117**: p. 133-137.
166. Lavine, B.K., et al., *Wavelets and genetic algorithms applied to search prefilters for spectral library matching in forensics*. *Talanta*, 2011. **87**: p. 46-52.
167. Barrett, J.A., J.A. Siegel, and J.V. Goodpaster, *Forensic discrimination of dyed hair color: II. Multivariate statistical analysis*. *Journal of Forensic Sciences*, 2011. **56**(1): p. 95-101.
168. Causin, V., et al., *Forensic analysis of acrylic fibers by pyrolysis–gas chromatography/mass spectrometry*. *Journal of Analytical and Applied Pyrolysis*, 2006. **75**(1): p. 43-48.
169. Chen, C.S., C.W. Brown, and M.J. Bide, *Non–destructive near–infra–red analysis for the identification of dyes on textiles*. *Journal of the Society of Dyers and Colourists*, 1997. **113**(2): p. 51-56.
170. Cleve, E., E. Bach, and E. Schollmeyer, *Using chemometric methods and NIR spectrophotometry in the textile industry*. *Analytica Chimica Acta*, 2000. **420**(2): p. 163-167.
171. Daéid, N.N., W. Meier-Augenstein, and H.F. Kemp, *Investigating the provenance of un-dyed spun cotton fibre using multi-isotope profiles and chemometric analysis*. *Rapid Communications in Mass Spectrometry*, 2011. **25**(13): p. 1812-1816.
172. Fortier, C. and J. Rodgers, *Preliminary examinations for the identification of U.S. domestic and international cotton fibers by near-infrared spectroscopy*. *Fibers*, 2014. **2**(4): p. 264-274.

173. Gilbert, C. and S. Kokot, *Discrimination of cellulosic fabrics by diffuse reflectance infrared Fourier transform spectroscopy and chemometrics*. *Vibrational Spectroscopy*, 1995. **9**(2): p. 161-167.
174. Kokot, S., N. Anh, and T. Rintoul, *Discrimination of reactive dyes on cotton fabric by Raman spectroscopy and chemometrics*. *Applied Spectroscopy*, 1997. **51**(3): p. 387-395.
175. Morgan, S.L., et al. *Pattern recognition methods for the classification of trace evidence textile fibers from UV/visible and fluorescence spectra*. in *2007 Trace Evidence Symposium*. 2007. Clearwater Beach, Florida.
176. Ruckebusch, C., et al., *Quantitative analysis of cotton-polyester textile blends from near-infrared spectra*. *Applied Spectroscopy*, 2006. **60**(5): p. 539-544.
177. Thanasoulas, N.C., et al., *Application of multivariate chemometrics in forensic soil discrimination based on the UV-Vis spectrum of the acid fraction of humus*. *Forensic Science International*, 2002. **130**(2-3): p. 73-82.
178. Dragović, S. and A. Onjia, *Classification of soil samples according to their geographic origin using gamma-ray spectrometry and principal component analysis*. *Journal of Environmental Radioactivity*, 2006. **89**(2): p. 150-158.
179. Baron, M., et al., *Chemometric study on the forensic discrimination of soil types using their infrared spectral characteristics*. *Applied Spectroscopy*, 2011. **65**(10): p. 1151-61.
180. Lee, C.S., et al., *Classification of forensic soil evidences by application of THM-PyGC/MS and multivariate analysis*. *Journal of Analytical and Applied Pyrolysis*, 2012. **96**: p. 33-42.
181. Reidy, L., et al., *Elemental fingerprinting of soils using ICP-MS and multivariate statistics: A study for and by forensic chemistry majors*. *Forensic Science International*, 2013. **233**(1-3): p. 37-44.
182. Bonetti, J. and L. Quarino, *Comparative forensic soil analysis of New Jersey state parks using a combination of simple techniques with multivariate statistics*. *Journal of Forensic Sciences*, 2014. **59**(3): p. 627-636.
183. Jantzi, S.C. and J.R. Almirall, *Elemental analysis of soils using laser ablation inductively coupled plasma mass spectrometry (LA-ICP-MS) and laser-induced breakdown spectroscopy (LIBS) with multivariate discrimination: tape mounting as an alternative to pellets for small forensic transfer specimens*. *Applied Spectroscopy*, 2014. **68**(9): p. 963-974.
184. Petraco, N.D.K., et al., *Statistical discrimination of footwear: A method for the comparison of accidentals on shoe outsoles inspired by facial recognition techniques*. *Journal of Forensic Sciences*, 2010. **55**(1): p. 34-41.
185. Sikirzhytski, V., K. Virkler, and I.K. Lednev, *Discriminant Analysis of Raman Spectra for Body Fluid Identification for Forensic Purposes*. *Sensors*, 2010. **10**(4): p. 2869-2884.

186. Sikirzhyskaya, A., V. Sikirzhyski, and I.K. Lednev, *Raman spectroscopy coupled with advanced chemometrics for forensic analysis of semen and blood mixtures*. Spectroscopy, 2013. **28**(12): p. 25-29.
187. Edelman, G.J., T.G. van Leeuwen, and M.C. Aalders, *Visualization of latent blood stains using visible reflectance hyperspectral imaging and chemometrics*. Journal of Forensic Sciences, 2015. **60**: p. S188-S192.
188. Li, B., et al., *The estimation of the age of a blood stain using reflectance spectroscopy with a microspectrophotometer, spectral pre-processing and linear discriminant analysis*. Forensic Science International, 2011. **212**(1): p. 198-204.
189. Girod, A. and C. Weyermann, *Lipid composition of fingermark residue and donor classification using GC/MS*. Forensic Science International, 2014. **238**: p. 68-82.
190. Frick, A.A., et al., *Investigations into the initial composition of latent fingermark lipids by gas chromatography–mass spectrometry*. Forensic Science International, 2015. **254**: p. 133-147.
191. Zadora, G. and Z. Brozek-Mucha, *The use of chosen methods of statistical and chemometric analysis in forensic examinations of glass*. Z Zagadnien Nauk Sadowych, 1999. **40**: p. 33-71.
192. Zadora, G., *Glass analysis for forensic purposes—a comparison of classification methods*. Journal of Chemometrics, 2007. **21**(5-6): p. 174-186.
193. Kulikov, E., K. Latham, and M.J. Adams, *Classification and discrimination of some cosmetic face powders using XRF spectrometry with chemometric data analysis*. X-Ray Spectrometry, 2012. **41**(6): p. 410-415.
194. Salahioglu, F., M.J. Went, and S.J. Gibson, *Application of Raman spectroscopy for the differentiation of lipstick traces*. Analytical Methods, 2013. **5**(20): p. 5392-5401.
195. Brereton, R.G., *Consequences of sample size, variable selection, and model validation and optimisation, for predicting classification ability from analytical data*. TrAC Trends in Analytical Chemistry, 2006. **25**(11): p. 1103-1111.
196. Badertscher, M. and E. Pretsch, *Bad results from good data*. TrAC Trends in Analytical Chemistry, 2006. **25**(11): p. 1131-1138.
197. Morton, W.E. and J.W.S. Hearle, *An introduction to fibre structure*, in *Physical Properties of Textile Fibres*, W.E. Morton and J.W.S. Hearle, Editors. 2008, Woodhead Publishing: Cambridge, England. p. 1-81.
198. *Identification of Textile Fibers*, ed. M.M. Houck. 2009, Cambridge: Woodhead Publishing.

199. Mather, R.R. and R.H. Wardman, *The scope of textile fibres*, in *Chemistry of Textile Fibres*. 2011, Royal Society of Chemistry: Cambridge.
200. *Historical Perspective of Textiles*, in *Textile Design: Theory and Concepts*, C. Swami, Editor. 2011, New Age International: New Delhi.
201. Roux, C. and J. Robertson, *Fibers: Transfer*, in *Encyclopedia of Forensic Sciences*, J.A. Siegel and P.J. Saukko, Editors. 2013, Academic Press: Waltham. p. 113-116.
202. Robertson, J. and C. Roux, *Fibers: Overview*, in *Encyclopedia of Forensic Sciences*, J.A. Siegel and P.J. Saukko, Editors. 2013, Academic Press: Waltham. p. 109-112.
203. John, M.J. and R.D. Anandjiwala, *Surface Modification and Preparation Techniques for Textile Materials*, in *Surface Modification of Textiles*, Q. Wei, Editor. 2009, Woodhead Publishing: Cambridge. p. 1-25.
204. Jackson, A.R.W. and J.M. Jackson, *Trace and Contact Evidence - Part I: Recoverable Materials*, in *Forensic Science*. 2011, Pearson Education: Harlow, England. p. 61-106.
205. Grieve, M.C., T.W. Biermann, and K. Schaub, *The individuality of fibres used to provide forensic evidence – not all blue polyesters are the same*. *Science & Justice*, 2005. **45**(1): p. 13-28.
206. Blackledge, R.D. and K. Gaenzle, *Characterization of Surface-Modified Fibers in Forensic Analysis on the Cutting Edge*, R.D. Blackledge, Editor. 2007, John Wiley & Sons: New Jersey. p. 221-241.
207. Houck, M., *Textiles*, in *Forensic Chemistry: Fundamentals and Applications*, J.A. Siegel, Editor. 2016, Wiley-Blackwell: Chichester, UK. p. 40-74.
208. David, S.K. and M.T. Pailthorpe, *Classification of Textile Fibres: Production, Structure, and Properties*, in *Forensic Examination of Fibres*, J. Robertson and M. Grieves, Editors. 1999, CRC Press: Boca Raton, Florida. p. 1-33.
209. Houck, M.M. and J.A. Siegel, *Fundamentals of Forensic Science*. 2nd ed. 2010, Burlington, MA: Academic Press.
210. American Society for Testing and Materials, *E228-10: Standard Guide for Microscopical Examination of Fibers*. 2010.
211. Scientific Working Group on Materials Analysis, *Forensic Fiber Examination Guidelines*. 1999.
212. Scientific Working Group on Materials Analysis, *Introduction to Forensic Fiber Examination*. 2011.
213. Bell, S., *Forensic Chemistry*. 2006, Upper Saddle River, NJ: Pearson Education.

214. Hemmings, J.M., *Fiber Microscopy*, in *Encyclopedia of Forensic Sciences*, J.A. Siegel and P.J. Saukko, Editors. 2013, Academic Press: Waltham. p. 143-147.
215. Robertson, J. and C. Roux, *Fibers: Protocols for Examination*, in *Encyclopedia of Forensic Sciences*, J.A. Siegel and P.J. Saukko, Editors. 2013, Academic Press: Waltham. p. 124-128.
216. Nehse, K., *Examination of Fibers and Textiles*, in *Wiley Encyclopedia of Forensic Science*, A. Jamieson and A. Moenssens, Editors. 2009, John Wiley & Sons: New Jersey. p. 985-998.
217. Goodpaster, J.V. and E.A. Liszewski, *Forensic analysis of dyed textile fibers*. *Analytical and Bioanalytical Chemistry*, 2009. **394**(8): p. 2009-2018.
218. Kubic, T., *Forensic analysis of colorless textile fibers by fluorescence microscopy*. *The Microscope Journal*, 1983. **31**(3): p. 213.
219. Robson, D., *Fibre surface imaging*. *Journal of the Forensic Science Society*, 1994. **34**(3): p. 187-191.
220. Palmer, R., *Fibers: Identification and Comparison*, in *Encyclopedia of Forensic Sciences*, J.A. Siegel and P.J. Saukko, Editors. 2013, Academic Press: Waltham. p. 129-137.
221. Siegel, J.A., *Forensic Science: The Basics*. 2007, Boca Raton, Florida: Taylor & Francis.
222. Griffin, R. and J. Speers, *Other Methods of Color Analysis: High Performance Liquid Chromatography*, in *Forensic Examination of Fibres*, J. Robertson and M. Grieves, Editors. 1999, CRC Press: Boca Raton, Florida. p. 311-328.
223. Wiggins, K.G., *Thin Layer Chromatographic Analysis for Fibre Dyes*, in *Forensic Examination of Fibres*, J. Robertson and M. Grieves, Editors. 1999, CRC Press: Boca Raton, Florida. p. 291-391.
224. Grieve, M.C., R.M.E. Griffin, and R. Malone, *Characteristic dye absorption peaks found in the FTIR spectra of coloured acrylic fibres*. *Science & Justice*, 1998. **38**(1): p. 27-37.
225. Lang, P.L., et al., *The identification of fibers by infrared and Raman microspectroscopy*. *Microchemical Journal*, 1986. **34**(3): p. 319-331.
226. Suzuki, E.M., *Forensic Applications of Infrared Spectroscopy*, in *Forensic Science Handbook*, R. Saferstein, Editor. 1993, Prentice Hall: New Jersey. p. 150-152.
227. Houck, M.M., *The Use of Spectroscopy for Textile Fiber Identification*, in *Identification of Textile Fibers*, M.M. Houck, Editor. 2009, Woodhead Publishing: Cambridge. p. 158-164.

228. Abbott, L.C., et al., *Resonance Raman and UV-visible spectroscopy of black dyes on textiles*. Forensic Science International, 2010. **202**(1–3): p. 54-63.
229. Lepot, L., et al., *Application of Raman spectroscopy to forensic fibre cases*. Science & Justice, 2008. **48**(3): p. 109-117.
230. Massonnet, G., *Evaluation of Raman spectroscopy for the analysis of colored fibers: A collaborative study*. Journal of Forensic Sciences, 2005. **50**(5): p. 1028-1038.
231. Massonnet, G., et al., *Raman spectroscopy and microspectrophotometry of reactive dyes on cotton fibres: Analysis and detection limits*. Forensic Science International, 2012. **222**(1–3): p. 200-207.
232. Zięba-Palus, J. and J. Waś-Gubała, *An investigation into the use of micro-Raman spectroscopy for the analysis of car paints and single textile fibres*. Journal of Molecular Structure, 2011. **993**(1–3): p. 127-133.
233. Madariaga, J.M., *Identification of Dyes and Pigments by Vibrational Spectroscopy*, in *Infrared and Raman Spectroscopy in Forensic Science*, J.M. Chalmers, H.G.M. Edwards, and M.D. Hargreaves, Editors. 2012, John Wiley & Sons. p. 383-399.
234. Reffner, J., S. Smith, and F. Adar, *Characterizing colored fibers by FT-IR and Raman spectroscopy*. Spectroscopy, 2010: p. 6-14.
235. Watson, N., *Forensic Sciences: Fibers*, in *Encyclopedia of Analytical Science*, P. Worsfold, A. Townshend, and C. Poole, Editors. 2005, Elsevier: Oxford. p. 406-414.
236. Woods, M. and M.B. Woods, *Ancient Communication Technology: From Hieroglyphics to Scrolls*. 2011, Minneapolis: Twenty-First Century Books.
237. Lindblom, B.S., *Pens and Pencils*, in *Scientific Examination of Questioned Documents*. 2006, CRC Press. p. 147-158.
238. Kunjappu, J., *Ink chemistry - What's in ink? More than you might think*. Chemistry in Britain, 2003.
239. Siegel, J.A., *Ink Analysis*, in *Encyclopedia of Forensic Sciences*, M.M. Houck, J.A. Siegel, and P.J. Saukko, Editors. 2013, Academic Press: Waltham. p. 375-379.
240. LaPorte, G.M., *Chemical Analysis for the Scientific Examination of Questioned Documents*, in *Forensic Chemistry: Fundamentals and Applications*, J.A. Siegel, Editor. 2016, Wiley-Blackwell: Chichester, UK. p. 318-354.
241. Bell, S., *Encyclopedia of Forensic Science*. 2008, New York: Infobase Publishing.

242. Merrill, R.A. and E.G. Bartick, *Analysis of ballpoint pen inks by diffuse reflectance infrared spectrometry*. Journal of Forensic Sciences, 1992. **37**(2): p. 528-541.
243. Ezcurra, M., et al., *Analytical methods for dating modern writing instrument inks on paper*. Forensic Science International, 2010. **197**(1–3): p. 1-20.
244. Brunelle, R.L. and K.R. Crawford, *Advances in the Forensic Analysis and Dating of Writing Ink*. 2003, Springfield, Illinois: Charles C Thomas.
245. Levinson, J., *Writing Inks and Dyes, Pens and Pencils*, in *Questioned Documents: A Lawyer's Handbook*. 2001, Academic Press: London. p. 115-126.
246. Guedes, A. and A.C. Prieto, *Raman Spectroscopy for the Characterisation of Inks on Written Documents*, in *Infrared and Raman Spectroscopy in Forensic Science*, J.M. Chalmers, H.G.M. Edwards, and M.D. Hargreaves, Editors. 2012, John Wiley & Sons, Ltd. p. 137-151.
247. LaPorte, G.M., et al., *An evaluation of matching unknown writing inks with the United States International Ink Library*. Journal of Forensic Sciences, 2006. **51**(3): p. 689-692.
248. Scientific Working Group for Forensic Document Examination, *Standard for Writing Ink Identification*. 2013.
249. Scientific Working Group for Forensic Document Examination, *Standard for Test Methods for Forensic Writing Ink Comparison*. 2013.
250. Causin, V., et al., *The discrimination potential of ultraviolet-visible spectrophotometry, thin layer chromatography, and Fourier Transform infrared spectroscopy for the forensic analysis of black and blue ballpoint inks*. Journal of Forensic Sciences, 2008. **53**(6): p. 1468-1473.
251. Laing, D.K. and M.D.J. Isaacs, *The comparison of nanogram quantities of ink using visible microspectrometry*. Journal of the Forensic Science Society, 1983. **23**(2): p. 147-154.
252. Pfeifferli, P.W., *Application of microspectrophotometry in document examination*. Forensic Science International, 1983. **23**(2–3): p. 129-136.
253. Senior, S., et al., *Characterization and dating of blue ballpoint pen inks using principal component analysis of UV-Vis absorption spectra, IR spectroscopy, and HPTLC*. Journal of Forensic Sciences, 2012. **57**(4): p. 1087-1093.
254. Bell, S.E.J., et al., *Comparison of the discriminating power of Raman and surface-enhanced Raman spectroscopy with established techniques for the examination of liquid and gel inks*. Journal of Raman Spectroscopy, 2013. **44**(4): p. 509-517.

255. Braz, A., M. López-López, and C. García-Ruiz, *Raman spectroscopy for forensic analysis of inks in questioned documents*. Forensic Science International, 2013. **232**(1–3): p. 206-212.
256. Liu, S., et al., *Discrimination of blue ballpoint pen inks in Chinese market with confocal Raman microscope*. Pigment & Resin Technology, 2014. **43**(1): p. 45-51.
257. Vančo, L., et al., *Raman mapping as a tool for discrimination of blue writing inks and their cross lines*. Vibrational Spectroscopy, 2015. **79**: p. 11-15.
258. Nam, Y.S., et al., *Application of micro-attenuated total reflectance Fourier Transform infrared spectroscopy to ink examination in signatures written with ballpoint pen on questioned documents*. Journal of Forensic Sciences, 2014. **59**(3): p. 800-805.
259. Wang, J., et al., *Systematic analysis of bulk blue ballpoint pen ink by FTIR spectrometry*. Journal of Forensic Sciences, 2001. **46**(5): p. 1093-7.
260. Aginsky, V.N., *Forensic examination of "slightly soluble" ink pigments using thin-layer chromatography*. Journal of Forensic Sciences, 1993. **38**(5): p. 1131-1133.
261. Houlgrave, S., G.M. LaPorte, and J.C. Stephens, *The use of filtered light for the evaluation of writing inks analyzed using thin layer chromatography*. Journal of Forensic Sciences, 2011. **56**(3): p. 778-782.
262. Neumann, C., R. Ramotowski, and T. Genessay, *Forensic examination of ink by high-performance thin layer chromatography - The United States Secret Service Digital Ink Library*. Journal of Chromatography A, 2011. **1218**(19): p. 2793-2811.
263. Saini, K., H. Kaur, and M. Gupta, *Analyses of blue gel pen inks using thin-layer chromatography and visible spectrophotometry*. Journal of Forensic Identification, 2014. **64**(1): p. 28-42.
264. Bügler, J.H., H. Buchner, and A. Dallmayer, *Age determination of ballpoint pen ink by thermal desorption and gas chromatography-mass spectrometry**. Journal of Forensic Sciences, 2008. **53**(4): p. 982-988.
265. Li, B., et al., *GC analysis of black gel pen ink stored under different conditions*. Journal of Forensic Sciences, 2014. **59**(2): p. 543-549.
266. Aginsky, V.N. *Current methods for dating ink on documents*. in *60th Annual Conference for the American Society of Questioned Document Examiners*. 2002. San Diego, CA.
267. Gaudreau, M. and L. Brazeau. *Ink dating using a solvent loss ratio method*. in *60th Annual Conference for the American Society of Questioned Document Examiners*. 2002. San Diego, CA.

268. National Fire Protection Association, *Explosions*, in *NFPA 921: Guide for Fire and Explosion Investigation*. 2011, National Fire Protection Association: Quincy, MA. p. 149-165.
269. Todd, C., L. Jones, and M. Marshall, *Explosions*, in *Crime Scene to Court: The Essentials of Forensic Science*, P. White, Editor. 2010, RSC Publishing: Cambridge.
270. Crippin, J.B., *Explosions*, in *Encyclopedia of Forensic Sciences*, J.A. Siegel and P.J. Saukko, Editors. 2013, Academic Press: Waltham, Massachusetts. p. 104-108.
271. *Classification of Explosive Materials*, in *The Chemistry of Explosives*, J. Akhavan, Editor. 2011, Royal Society of Chemistry: Cambridge. p. 27-59.
272. Goodpaster, J., *Explosives*, in *Forensic Chemistry: Fundamentals and Applications*, J.A. Siegel, Editor. 2016, Wiley-Blackwell: Chichester, UK. p. 175-228.
273. *Energetic Materials and Explosive Devices*, in *The Counterterrorism Handbook*, F. Bolz, K.J. Dudonis, and D.P. Schulz, Editors. 2011, CRC Press: Boca Raton, FL. p. 241-260.
274. Hopler, R.B., *The History, Development, and Characteristics of Explosives and Propellants*, in *Forensic Investigation of Explosions*. 2011, CRC Press: Boca Raton, Florida. p. 1-18.
275. Alcohol Tobacco Firearms and Explosives Bureau. *Commerce in Explosives; 2015 Annual List of Explosive Materials*. 2015; Available from: <https://federalregister.gov/a/2015-26994>.
276. Genge, N.E., *The Forensic Casebook: The Science of Crime Scene Investigation*. 2004, London: Ebury Press.
277. Jackson, A.R.W. and J.M. Jackson, *Explosions and Explosives*, in *Forensic Science*. 2011, Pearson Education: Harlow, England. p. 352-368.
278. Saferstein, R., *Forensic Investigation of Explosives*, in *Forensic Science: From the Crime Scene to the Crime Lab*. 2009, Pearson Education: Upper Saddle River, NJ.
279. Australian Federal Police. *ABDC Annual Statistics Reports*. Available from: <http://www.afp.gov.au/en/media-centre/publications/annual-reports/abdc.aspx>.
280. Clyburn, J., *Personal communication*. 2015.
281. Murray, S.G., *Explosives: Mechanism of Explosion*, in *Encyclopedia of Forensic Sciences*, J.A. Siegel, Editor. 2000, Elsevier: Oxford. p. 758-764.

282. *Explosions and Explosives*, in *Forensic Science: An Encyclopedia of History, Methods and Techniques*, W.J. Tilstone, Editor. 2006, ABC-CLIO: Santa Barbara, California.
283. Marshall, M. and J.C. Oxley, *The Threats and the Materials*, in *Aspects of Explosives Detection*, M. Marshall and J.C. Oxley, Editors. 2009, Elsevier: Boston.
284. Murray, S.G., *Explosives: Military*, in *Encyclopedia of Forensic Sciences*, J.A. Siegel and P.J. Saukko, Editors. 2013, Academic Press: Waltham. p. 92-97.
285. Royds, D., S.W. Lewis, and A.M. Taylor, *A case study in forensic chemistry: The Bali bombings*. *Talanta*, 2005. **67**(2): p. 262-268.
286. Technical Working Group for Fire and Explosion, *Recommended Guidelines for Forensic Identification of Intact Explosives*. 2007.
287. Technical Working Group for Fire and Explosion, *Recommended Guidelines for Forensic Identification of Post-Blast Explosive Residues*. 2009.
288. Levine, B. and S.W. Lewis, *Presumptive Chemical Tests*, in *Encyclopedia of Forensic Sciences*, J.A. Siegel and P.J. Saukko, Editors. 2013, Academic Press: Waltham. p. 616-620.
289. Parker, R.G., et al., *Analysis of explosives and explosive residues. Part 1: Chemical tests*. *Journal of Forensic Sciences*, 1975. **20**(1): p. 133-40.
290. Bowerbank, C.R., et al., *Solvating gas chromatography with chemiluminescence detection of nitroglycerine and other explosives*. *Journal of Chromatography A*, 2000. **902**(2): p. 413-419.
291. Burns, D.T. and R.J. Lewis, *Analysis and characterisation of nitroglycerine-based explosives by gas chromatography-mass spectrometry*. *Analytica Chimica Acta*, 1995. **307**(1): p. 89-95.
292. Calderara, S., D. Gardebas, and F. Martinez, *Solid phase micro extraction coupled with on-column GC/ECD for the post-blast analysis of organic explosives*. *Forensic Science International*, 2003. **137**(1): p. 6-12.
293. Yinon, J., R.A. Yost, and S. Bulusu, *Thermal decomposition characterization of explosives by pyrolysis-gas chromatography-mass spectrometry*. *Journal of Chromatography A*, 1994. **688**(1-2): p. 231-242.
294. Perr, J.M., K.G. Furton, and J.R. Almirall, *Gas chromatography positive chemical ionization and tandem mass spectrometry for the analysis of organic high explosives*. *Talanta*, 2005. **67**(2): p. 430-436.
295. Stambouli, A., et al., *Headspace-GC/MS detection of TATP traces in post-explosion debris*. *Forensic Science International*, 2004. **146**: p. S191-S194.

296. Waddell, R., et al., *Determination of nitroaromatic and nitramine explosives from a PTFE wipe using thermal desorption-gas chromatography with electron-capture detection*. Journal of Chromatography A, 2005. **1062**(1): p. 125-131.
297. Furton, K.G., L.M. Wu, and J.R. Almirall, *Optimization of solid-phase microextraction (SPME) for the recovery of explosives from aqueous and post-explosion debris followed by gas and liquid chromatographic analysis*. Journal of Forensic Sciences, 2000. **45**(4): p. 857-864.
298. DeTata, D., P. Collins, and N. Campbell, *The identification of the emulsifier component of emulsion explosives by liquid chromatography-mass spectrometry*. Journal of Forensic Sciences, 2006. **51**(2): p. 303-307.
299. De Tata, D., P. Collins, and N. Campbell, *The identification of the emulsifier component of emulsion explosives by liquid chromatography-mass spectrometry*. Journal of Forensic Sciences, 2006. **51**(2): p. 303-307.
300. Kolla, P., *Gas chromatography, liquid chromatography and ion chromatography adapted to the trace analysis of explosives*. Journal of Chromatography A, 1994. **674**(1-2): p. 309-318.
301. Verweij, A.M.A., et al., *Liquid chromatographic, thermospray/negative ion, tandem mass spectrometric(LC/TSP/MS/MS) analysis of some explosives*. Forensic Science International, 1993. **60**(1-2): p. 7-13.
302. Wood, M., et al., *Recent applications of liquid chromatography-mass spectrometry in forensic science*. Journal of Chromatography A, 2006. **1130**(1): p. 3-15.
303. Dicoski, G.W., R.A. Shellie, and P.R. Haddad, *Forensic identification of inorganic explosives by ion chromatography*. Analytical Letters, 2006. **39**(4): p. 639-657.
304. McCord, B.R., et al., *Forensic analysis of explosives using ion chromatographic methods*. Analytica Chimica Acta, 1994. **288**(1-2): p. 43-56.
305. Tyrrell, É., et al., *Coupled reversed-phase and ion chromatographic system for the simultaneous identification of inorganic and organic explosives*. Journal of Chromatography A, 2011. **1218**(20): p. 3007-3012.
306. Hutchinson, J., et al., *Identification of inorganic improvised explosive devices by analysis of postblast residues using portable capillary electrophoresis instrumentation and indirect photometric detection with a light-emitting diode*. Analytical Chemistry, 2007. **79**(18): p. 7005-7013.
307. Johns, C., et al., *Identification of homemade inorganic explosives by ion chromatographic analysis of post-blast residues*. Journal of Chromatography A, 2008. **1182**(2): p. 205-214.

308. Kolla, P., *Trace analysis of salt based explosives by ion chromatography*. Forensic Science International, 1991. **50**(2): p. 217-226.
309. Cruces-Blanco, C., L. Gámiz-Gracia, and A.M. García-Campaña, *Applications of capillary electrophoresis in forensic analytical chemistry*. Trends in Analytical Chemistry, 2007. **26**(3): p. 215-226.
310. Hopper, K.G., H. LeClair, and B.R. McCord, *A novel method for analysis of explosives residue by simultaneous detection of anions and cations via capillary zone electrophoresis*. Talanta, 2005. **67**(2): p. 304-312.
311. Sarazin, C., et al., *Identification and determination of inorganic anions in real extracts from pre- and post-blast residues by capillary electrophoresis*. Journal of Chromatography A, 2010. **1217**(44): p. 6971-6978.
312. Hargadon, K.A. and B.R. McCord, *Explosive residue analysis by capillary electrophoresis and ion chromatography*. Journal of Chromatography A, 1992. **602**(1-2): p. 241-247.
313. McNesby, K.L. and R.A. Pesce-Rodriguez, *Applications of Vibrational Spectroscopy in the Study of Explosives*, in *Handbook of Vibrational Spectroscopy*. 2006, John Wiley & Sons: New York.
314. Zitrin, S. and T. Tamiri, *Analysis of Explosives by Infrared Spectrometry*, in *Forensic Investigation of Explosions*, A. Beveridge, Editor. 2011, CRC Press: Boca Raton, Florida. p. 671-690.
315. Banas, A. *Synchrotron-based Fourier transform infrared spectroscopy and statistic analysis in detection of post-blast traces of explosive materials*. in *Explosive Materials*. 2011.
316. Banas, A., et al., *Post-blast detection of traces of explosives by means of Fourier transform infrared spectroscopy*. Vibrational Spectroscopy, 2009. **51**(2): p. 168-176.
317. Primera-Pedrozo, O.M., et al., *High explosives mixtures detection using fiber optics coupled: grazing angle probe/Fourier transform reflection absorption infrared spectroscopy*. Sensing and Imaging, 2008. **9**: p. 27-40.
318. Primera-Pedrozo, O.M., et al., *Detection of high explosives using reflection absorption infrared spectroscopy with fiber coupled grazing angle probe/FTIR*. Sensing and Imaging, 2009. **10**: p. 1-13.
319. Ali, E.M.A. and H.G.M. Edwards, *Screening of textiles for contraband drugs using portable Raman spectroscopy and chemometrics*. Journal of Raman Spectroscopy, 2014. **45**(3): p. 253-258.
320. Ali, E.M.A., H.G.M. Edwards, and I.J. Scowen, *Raman spectroscopy and security applications: The detection of explosives and precursors on clothing*. Journal of Raman Spectroscopy, 2009. **40**(12): p. 2009-2014.

321. Moros, J., et al., *Fundamentals of stand-off Raman scattering spectroscopy for explosive fingerprinting*. Journal of Raman Spectroscopy, 2013. **44**(1): p. 121-130.
322. Zachhuber, B., et al., *Stand-off Raman spectroscopy: A powerful technique for qualitative and quantitative analysis of inorganic and organic compounds including explosives*. Analytical and Bioanalytical Chemistry, 2011. **400**(8): p. 2439-2447.
323. Brandl, S.G., *Criminal Investigation*. 2nd ed. 2007, Upper Saddle River, NJ: Prentice Hall.
324. Apsell, P., *What are Dyes? What is Dyeing?*, in *Dyeing Primer*, J.R. Aspland, Editor. 1981, American Association of Textile Chemists and Colorists: Research Triangle Park, NC. p. 4-7.
325. Martin, P., *Fibers: Color Analysis*, in *Encyclopedia of Forensic Sciences*, J.A. Siegel and P.J. Saukko, Editors. 2013, Academic Press: Waltham. p. 148-154.
326. Eng, M., P. Martin, and C. Bhagwandin, *The analysis of metamer blue fibers and their forensic significance*. Journal of Forensic Sciences, 2009. **54**(4): p. 841-845.
327. Eyring, M.B. and B.D. Gaudette, *An Introduction to the Forensic Aspects of Textile Fiber Examination*, in *Forensic Science Handbook*, R. Saferstein, Editor. 2005, Prentice Hall: Englewood Cliffs, NJ. p. 231-296.
328. Grieve, M.C., T. Biermann, and M. Davignon, *The occurrence and individuality of orange and green cotton fibres*. Science & Justice, 2003. **43**(1): p. 5-22.
329. Marcrae, R., R.J. Dudley, and K.W. Smalldon, *The characterization of dyestuffs on wool fibers with special reference to microspectrophotometry*. Journal of Forensic Sciences, 1979. **24**(1): p. 117-129.
330. Suzuki, S., et al., *Microspectrophotometric discrimination of single fibres dyed by indigo and its derivatives using ultraviolet-visible transmittance spectra*. Science & Justice, 2001. **41**(2): p. 107-111.
331. Buzzini, P. and G. Massonnet, *The discrimination of colored acrylic, cotton, and wool textile fibers using micro-Raman spectroscopy. Part 1: In situ detection and characterization of dyes*. Journal of Forensic Sciences, 2013. **58**(6): p. 1593-1600.
332. Jochem, G. and R.J. Lehnert, *On the potential of Raman microscopy for the forensic analysis of coloured textile fibres*. Science & Justice, 2002. **42**(4): p. 215-221.

333. Thomas, J., et al., *Raman spectroscopy and the forensic analysis of black/grey and blue cotton fibres: Part 1. Investigation of the effects of varying laser wavelength*. Forensic Science International, 2005. **152**(2–3): p. 189-197.
334. Houck, M.M., *Ways of Identifying Textile Fibers and Materials*, in *Identification of Textile Fibers*, M.M. Houck, Editor. 2009, Woodhead Publishing: Cambridge. p. 6-26.
335. Scientific Working Group on Materials Analysis, *Ultraviolet-Visible Spectroscopy of Textile Fibers*. 2011.
336. Liu, Y., *Vibrational spectroscopic investigation of Australian cotton cellulose fibres: Part 1 - A Fourier transform Raman study*. Analyst, 1998. **123**(4): p. 633-636.
337. Fisher, R.A., *Statistical Methods for Research Workers*. 13th ed. 1958, Edinburgh: Oliver and Boyd.
338. Fisher, R.A., *On the interpretation of χ^2 from contingency tables, and the calculation of P*. Journal of the Royal Statistical Society, 1922. **85**(1): p. 87-94.
339. Fisher, R.A., *The Design of Experiments*. 8th ed. 1971, New York: Hafner Publishing Company.
340. Mao, J., et al., *Removal of Basic Blue 3 from aqueous solution by Corynebacterium glutamicum biomass: Biosorption and precipitation mechanisms*. Korean Journal of Chemical Engineering, 2008. **25**(5): p. 1060-1064.
341. Sigma Aldrich. *Basic Blue 3*. 2015; Available from: <http://www.sigmaaldrich.com/catalog/product/aldrich/378011?lang=en®ion=AU>.
342. Wawrzekiewicz, M., *Removal of C.I. Basic Blue 3 dye by sorption onto cation exchange resin, functionalized and non-functionalized polymeric sorbents from aqueous solutions and wastewaters*. Chemical Engineering Journal, 2013. **217**: p. 414-425.
343. Speers, S.J., B.H. Little, and M. Roy, *Separation of acid, basic and dispersed dyes by a single-gradient elution reversed-phase high-performance liquid chromatography system*. Journal of Chromatography A, 1994. **674**(1-2): p. 263-70.
344. Iranifam, M., M. Zarei, and A.R. Khataee, *Decolorization of C.I. Basic Yellow 28 solution using supported ZnO nanoparticles coupled with photoelectro-Fenton process*. Journal of Electroanalytical Chemistry, 2011. **659**(1): p. 107-112.

345. Ismail, D., Z. Austad, and W.N.S.M. Desa, *Ultra-violet and visible (UV-Vis) spectroscopy and chemometrics techniques for forensic analysis of ballpoint pen inks: A preliminary study*. Malaysian Journal of Forensic Sciences, 2008. **5**(1): p. 47-52.
346. Andrasko, J., *HPLC analysis of ballpoint pen inks stored at different light conditions*. Journal of Forensic Sciences, 2001. **46**(1): p. 21-30.
347. Locicero, S., et al., *Dynamic of the ageing of ballpoint pen inks: quantification of phenoxyethanol by GC-MS*. Science & Justice, 2004. **44**(3): p. 165-171.
348. Weyermann, C., et al., *Photofading of ballpoint dyes studied on paper by LDI and MALDI MS*. Journal of the American Society for Mass Spectrometry, 2006. **17**(3): p. 297-306.
349. Weyermann, C., et al., *A GC/MS study of the drying of ballpoint pen ink on paper*. Forensic Science International, 2007. **168**(2-3): p. 119-127.
350. Thetford, D., *Triphenylmethane and Related Dyes*, in *Kirk-Othmer Encyclopedia of Chemical Technology*, A. Seidel and M. Bickford, Editors. 2013, John Wiley & Sons: New Jersey.
351. Chen, C.-C., et al., *Photocatalyzed N-de-methylation and degradation of crystal violet in titania dispersions under UV irradiation*. Dyes and Pigments, 2007. **75**(2): p. 434-442.
352. Grim, D.M., J. Siegel, and J. Allison, *Evaluation of desorption/ionization mass spectrometric methods in the forensic applications of the analysis of inks on paper*. Journal of Forensic Sciences, 2001. **46**(6): p. 1411-20.
353. Siegel, J., et al., *The use of laser desorption/ionization mass spectrometry in the analysis of inks in questioned documents*. Talanta, 2005. **67**(2): p. 425-429.
354. Weyermann, C., et al., *Evaluation of the photodegradation of crystal violet upon light exposure by mass spectrometric and spectroscopic methods*. Journal of Forensic Sciences, 2009. **54**(2): p. 339-345.
355. Kuramoto, N. and T. Kitao, *The contribution of singlet oxygen to the photofading of triphenylmethane and related dyes*. Dyes and Pigments, 1982. **3**(1): p. 49-58.
356. Li, X., G. Liu, and J. Zhao, *Two competitive primary processes in the photodegradation of cationic triarylmethane dyes under visible irradiation in TiO₂ dispersions*. New Journal of Chemistry, 1999. **23**(12): p. 1193-1196.
357. Caine, M.A., et al., *The influence of singlet oxygen in the fading of carbonless copy paper primary dyes on clays*. Dyes and Pigments, 2001. **49**(3): p. 135-143.

358. Bajpai, P., *Environmentally Friendly Production of Pulp and Paper*. 2010, New Jersey: John Wiley & Sons.
359. Andrasko, J., *Changes in composition of ballpoint pen inks on aging in darkness*. *Journal of Forensic Sciences*, 2002. **47**(2): p. 324-327.
360. Grim, D.M., J. Siegel, and J. Allison, *Does ink age inside of a pen cartridge?* *Journal of Forensic Sciences*, 2002. **47**(6): p. 1294-1297.
361. Péré, E., et al., *Quantitative assessment of organic compounds adsorbed on silica gel by FTIR and UV-vis spectroscopies: The contribution of diffuse reflectance spectroscopy*. *Vibrational Spectroscopy*, 2001. **25**(2): p. 163-175.
362. Liang, Y.-Z., et al., *Pre-treatment of diffuse reflectance infrared spectra for quantitative analysis of macro porous polymer particles*. *Vibrational Spectroscopy*, 1999. **20**(1): p. 47-57.
363. *How it is Manufactured - Stationery*. 2015; Available from: <http://www.bicworld.com/en/products/how-its-manufactured-stationery/>.
364. Grim, D.M., J. Siegel, and J. Allison, *Evaluation of laser desorption mass spectrometry and UV accelerated aging of dyes on paper as tools for the evaluation of a questioned document*. *Journal of Forensic Sciences*, 2002. **47**(6): p. 1-9.
365. Koenig, A., et al., *Ink dating using thermal desorption and gas chromatography/mass spectrometry: Comparison of results obtained in two laboratories*. *Journal of Forensic Sciences*, 2015. **60**(s1): p. S152-S161.
366. Weyermann, C. and B. Spengler, *The potential of artificial aging for modelling of natural aging processes of ballpoint ink*. *Forensic Science International*, 2008. **180**(1): p. 23-31.
367. Andrasko, J. and M. Kunicki, *Inhomogeneity and aging of ballpoint pen inks inside of pen cartridges*. *Journal of Forensic Sciences*, 2005. **50**(3): p. 1-6.
368. Kalivas, J.H. and P.J. Gemperline, *Calibration*, in *Practical Guide to Chemometrics*. 2006, CRC Press: Boca Raton, Florida. p. 105-166.
369. Esbenson, K.H., et al., *Multivariate Data Analysis – In Practice*. 5th ed. 2002, Oslo, Norway: Camo Process AS.
370. Cantu, A.A., *Comments on the accelerated aging of ink*. *Journal of Forensic Sciences*, 1988. **33**(3): p. 744-750.
371. Habib, M.A., et al., *Photocatalytic decolorization of crystal violet in aqueous nano-ZnO suspension under visible light irradiation*. *Journal Of Nanostructure in Chemistry*, 2013. **3**(70): p. 1-10.
372. Koppenhaver, K.M., *Equipping a Laboratory*, in *Forensic Document Examination: Principles and Practice*. 2007, Humana Press: New Jersey. p. 69-74.

373. Lewis, J.A., *Instrumentation*, in *Forensic Document Examination: Fundamentals and Current Trends*. 2014, Academic Press: Oxford. p. 69-80.
374. Reed, G., et al., *Hyperspectral imaging of gel pen inks: An emerging tool in document analysis*. *Science & Justice*, 2014. **54**(1): p. 71-80.
375. Foster+Freeman. *VSC5000*. [cited 2015 October]; Available from: <http://crimesight.co.za/images/assets/FF%20Brochures/VSC5000.pdf>.
376. Horton, R. and L. Nelson, *An evaluation of the use of laser-induced infrared luminescence to differentiate writing inks*. *Journal of Forensic Sciences*, 1991. **36**(3): p. 838-843.
377. Sun, Q., et al., *How much can a forensic laboratory do to discriminate questioned ink entries?* *Journal of Forensic Sciences*, 2016: p. n/a-n/a.
378. Mokrzycki, G.M., *Advances in document examination: The Video Spectral Comparator 2000*. *Forensic Science Communications*, 1999. **1**(3).
379. Ellen, D., *The Functions of Photography in Document Examination and Other Special Techniques*, in *Scientific Examination of Documents: Methods and Techniques*. 2006, CRC Press: Boca Raton, Florida. p. 199-209.
380. Trubshoe, T., *Personal communication*. 2015.
381. Weyermann, C., et al., *Statistical discrimination of black gel pen inks analysed by laser desorption/ionization mass spectrometry*. *Forensic Science International*, 2012. **217**(1-3): p. 127-133.
382. *Explosives*, in *Criminalistics: Forensic Science, Crime, and Terrorism*, J.E. Girard, Editor. 2011, Jones & Bartlett Learning: Sudbury, MA. p. 415-442.
383. Bender, E.C. and A.D. Beveridge, *Investigation of Pipe Bombs*, in *Forensic Investigation of Explosions*, A. Beveridge, Editor. 2011, CRC Press: Boca Raton, Florida. p. 429-492.
384. Heard, B.J., *Firearms: Propellants - History*, in *Wiley Encyclopedia of Forensic Science*. 2009, John Wiley & Sons: New Jersey.
385. National Research Council - Committee on Smokeless and Black Powder, *Black and Smokeless Powders: Technologies for Finding Bombs and the Bomb Makers*. 1998, Washington, DC: National Academies Press.
386. Heramb, R.M. and B.R. McCord, *The manufacture of smokeless powders and their forensic analysis: A brief review*. *Forensic Science Communications*, 2002. **4**(2).
387. Day, G., *Personal communication*. 2014.
388. Tamiri, T. and S. Zitrin, *Explosives: Analysis*, in *Encyclopedia of Forensic Sciences*, J.A. Siegel, P.J. Saukko, and M.M. Houck, Editors. 2013, Academic Press: Waltham. p. 64-84.

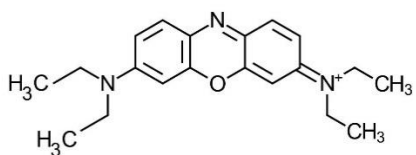
389. DeTata, D.A., P.A. Collins, and A.J. McKinley, *A comparison of common swabbing materials for the recovery of organic and inorganic explosive residues*. *Journal of Forensic Sciences*, 2013. **58**(3): p. 757-763.
390. Perret, D., et al., *LC-MS-MS determination of stabilizers and explosives residues in hand-swabs*. *Chromatographia*, 2008. **68**(7-8): p. 517-524.
391. Song-im, N., *Explosive residue analysis: evaluation and optimisation of sampling, storage and cleanup protocols*. 2011, University of Canberra.
392. Song-im, N., S. Benson, and C. Lennard, *Evaluation of different sampling media for their potential use as a combined swab for the collection of both organic and inorganic explosive residues*. *Forensic Science International*, 2012. **222**(1-3): p. 102-110.
393. Szomborg, K., et al., *Residues from low-order energetic materials: The comparative performance of a range of sampling approaches prior to analysis by ion chromatography*. *Forensic Science International*, 2013. **233**(1-3): p. 55-62.
394. Twibell, J.D., *Assessment of solvents for the recovery of nitroglycerine from hands using cotton swabs*. *Journal of Forensic Sciences*, 1982. **27**(4): p. 792-800.
395. Thompson, R.Q., et al., *Aqueous recovery from cotton swabs of organic explosives residue followed by solid phase extraction*. *Journal of Forensic Sciences*, 1999. **44**(4): p. 795-804.
396. DeTata, D.A., P.A. Collins, and A.J. McKinley, *A comparison of solvent extract cleanup procedures in the analysis of organic explosives*. *Journal of Forensic Sciences*, 2013. **58**(2): p. 500-507.
397. Song-im, N., S. Benson, and C. Lennard, *Stability of explosive residues in methanol/water extracts, on alcohol wipes and on a glass surface*. *Forensic Science International*, 2013. **226**(1-3): p. 244-253.
398. Kolla, P., *Stability of explosives traces on different supports*. *Forensic Science International*, 1993. **60**: p. 127-137.
399. Batlle, R., et al., *Enhanced detection of nitroaromatic explosive vapors combining solid-phase extraction-air sampling, supercritical fluid extraction, and large-volume injection-GC*. *Analytical Chemistry*, 2003. **75**(13): p. 3137-3144.
400. Fryš, O., et al., *Optimization of focused ultrasonic extraction of propellant components determined by gas chromatography/mass spectrometry*. *Talanta*, 2012. **99**: p. 316-322.
401. Vanini, G., et al., *Multivariate optimisation of ICP OES instrumental parameters for Pb/Ba/Sb measurement in gunshot residues*. *Microchemical Journal*, 2015. **120**: p. 58-63.

402. Rainey, C.L., D.E. Bors, and J.V. Goodpaster, *Design and optimization of a total vaporization technique coupled to solid phase microextraction (TV-SPME)*. Analytical Chemistry, 2014. **86**(22): p. 11319-11325.
403. Bors, D. and J. Goodpaster, *Mapping explosive residues on galvanized pipe bomb fragments using total vaporization solid phase microextraction (TV-SPME)*. Analytical Methods, 2015. **7**: p. 9756-9762.
404. Yinon, J. and S. Zitrin, *The Analysis of Explosives*. 1981, Oxford: Pergamon Press.
405. Espinoza, E.O.N. and J.I. Thornton, *Characterization of smokeless gunpowder by means of diphenylamine stabilizer and its nitrated derivatives*. Analytica Chimica Acta, 1994. **288**(1-2): p. 57-69.
406. Joshi, M., K. Rigsby, and J.R. Almirall, *Analysis of the headspace composition of smokeless powders using GC-MS, GC- μ ECD and ion mobility spectrometry*. Forensic Science International, 2011. **208**(1-3): p. 29-36.
407. Marshall, M., *Post-Blast Detection Issues*, in *Aspects of Explosives Detection*, M. Marshall and J.C. Oxley, Editors. 2009, Elsevier: Boston.
408. Strobel, R.A., *Recovery of Material from the Scene of an Explosion*, in *Forensic Investigation of Explosions*, A. Beveridge, Editor. 2011, CRC Press: Boca Raton, Florida. p. 119-158.
409. Peters, F.T., O.H. Drummer, and F. Musshoff, *Validation of new methods*. Forensic Science International, 2007. **165**(2-3): p. 216-24.
410. Borusiewicz, R., G. Zadora, and J. Zieba-Palus, *Chemical analysis of post explosion samples obtained as a result of model field experiments*. Talanta, 2013. **116**: p. 630-636.
411. Kolla, P., *Trace analysis of explosives from complex mixtures with sample pretreatment and selective detection*. Journal of Forensic Sciences, 1991. **36**(5): p. 1342-1359.
412. Voyksner, R., *Trace analysis of explosives by thermospray high-performance liquid chromatography-mass spectrometry*. Journal of Chromatography, 1986. **354**: p. 393-405.
413. Wallace, J.S. and W.J. McKeown, *Sampling procedures for firearms and/or explosives residues*. Journal of the Forensic Science Society, 1993. **33**: p. 107-116.
414. *Material Safety Data Sheet: Alliant Red Dot® Smokeless Powder*. [Online] 2010; Available from: <http://www.alliantpowder.com/downloads/sds/RedDot.pdf>.
415. Mason, R.L., R.F. Gunst, and J.L. Hess, *Statistical Design and Analysis of Experiments*. 2nd ed. 2003, New York: John Wiley & Sons.

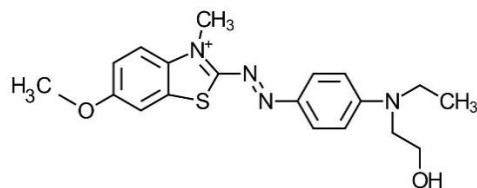
416. Myers, R.H., C.M. Anderson-Cook, and D.C. Montgomery, *Response Surface Methodology: Process and Product Optimization Using Designed Experiments*. 3rd ed. ed. 2014, Somerset, NJ, USA: Wiley.
417. Bors, D., J. Cummins, and J. Goodpaster, *The anatomy of a pipe bomb explosion: The effect of explosive filler, container material and ambient temperature on device fragmentation*. Forensic Science International, 2014. **234**: p. 95-102.
418. Bors, D., J. Cummins, and J. Goodpaster, *The anatomy of a pipe bomb explosion: Measuring the mass and velocity distributions of container fragments*. Journal of Forensic Sciences, 2014. **59**(1): p. 42-51.
419. Causin, V., et al., *A quantitative differentiation method for acrylic fibers by infrared spectroscopy*. Forensic Science International, 2005. **151**(2-3): p. 125-131.
420. European Network for Forensic Science Institutes, *ENFSI Guideline for Evaluative Reporting in Forensic Science*. 2015.
421. Pitts, K., *Personal communication*. 2015.

Every reasonable effort has been made to acknowledge the owners of copyright material. I would be pleased to hear from any copyright owner who has been omitted or incorrectly acknowledged.

Appendices



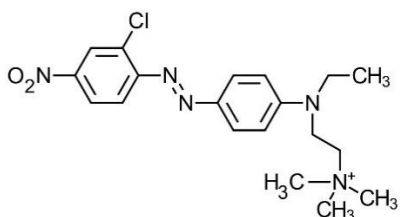
Basic Blue 3
CAS: 55840-82-9



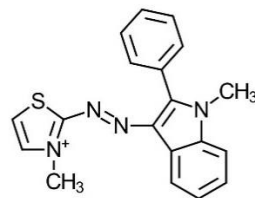
Basic Blue 41
CAS: 12270-13-2

Structure
Unknown

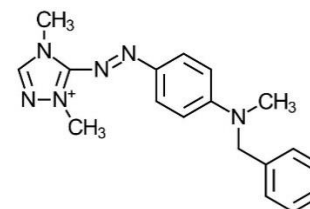
Basic Blue 147
CAS: 99035-77-5



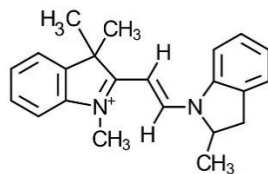
Basic Red 18
CAS: 25198-22-5



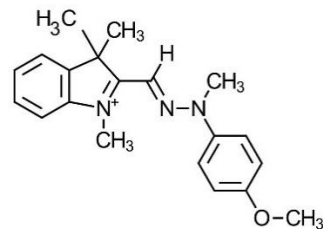
Basic Red 29
CAS: 42373-04-6



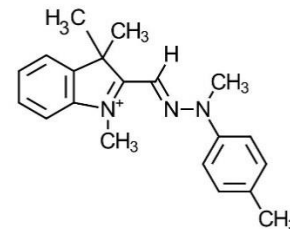
Basic Red 46
CAS: 12221-69-1



Basic Yellow 21
CAS: 6359-50-8

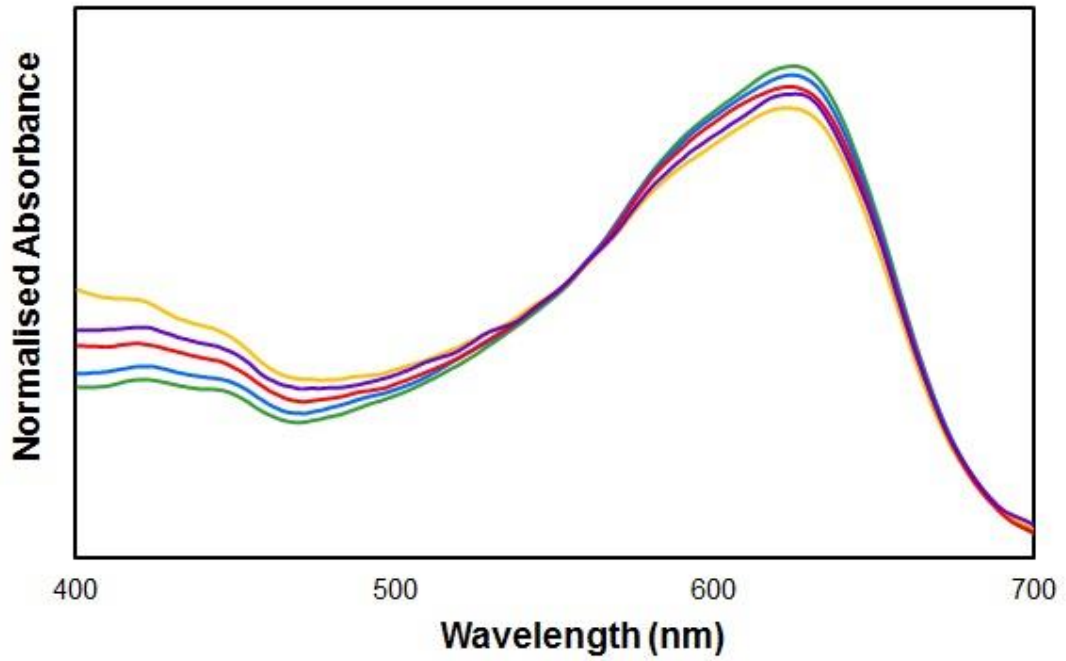


Basic Yellow 28
CAS: 54060-92-3

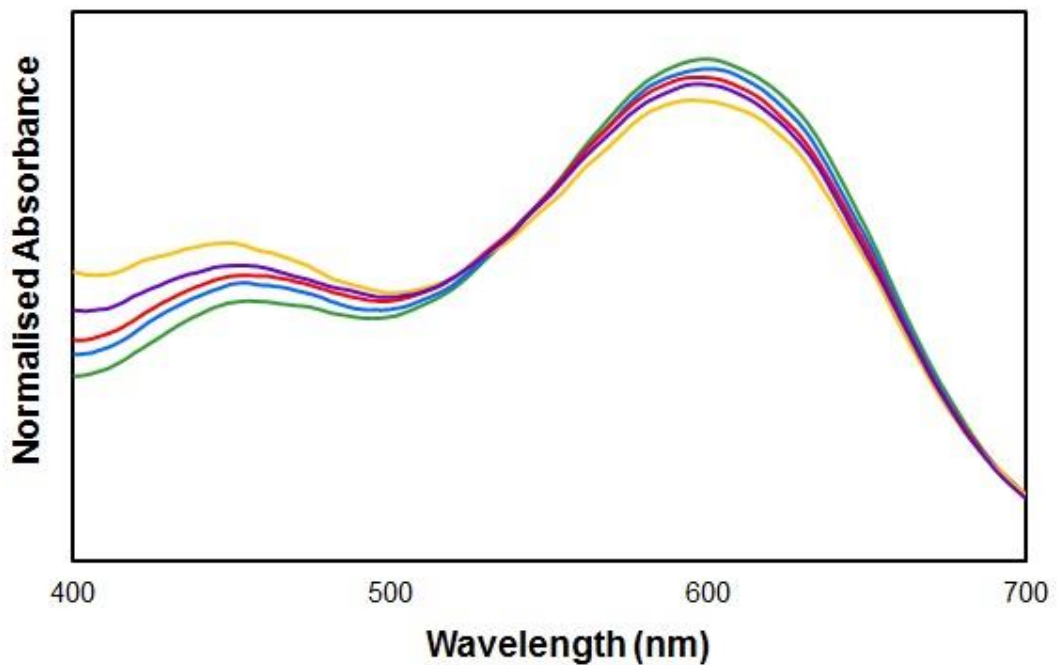


Basic Yellow 29
CAS: 68134-38-3

Appendix 2.1: Chemical structures and CAS registry numbers of cationic dyes present in blue acrylic fibres (structure for Basic Blue 147 dye is unknown).



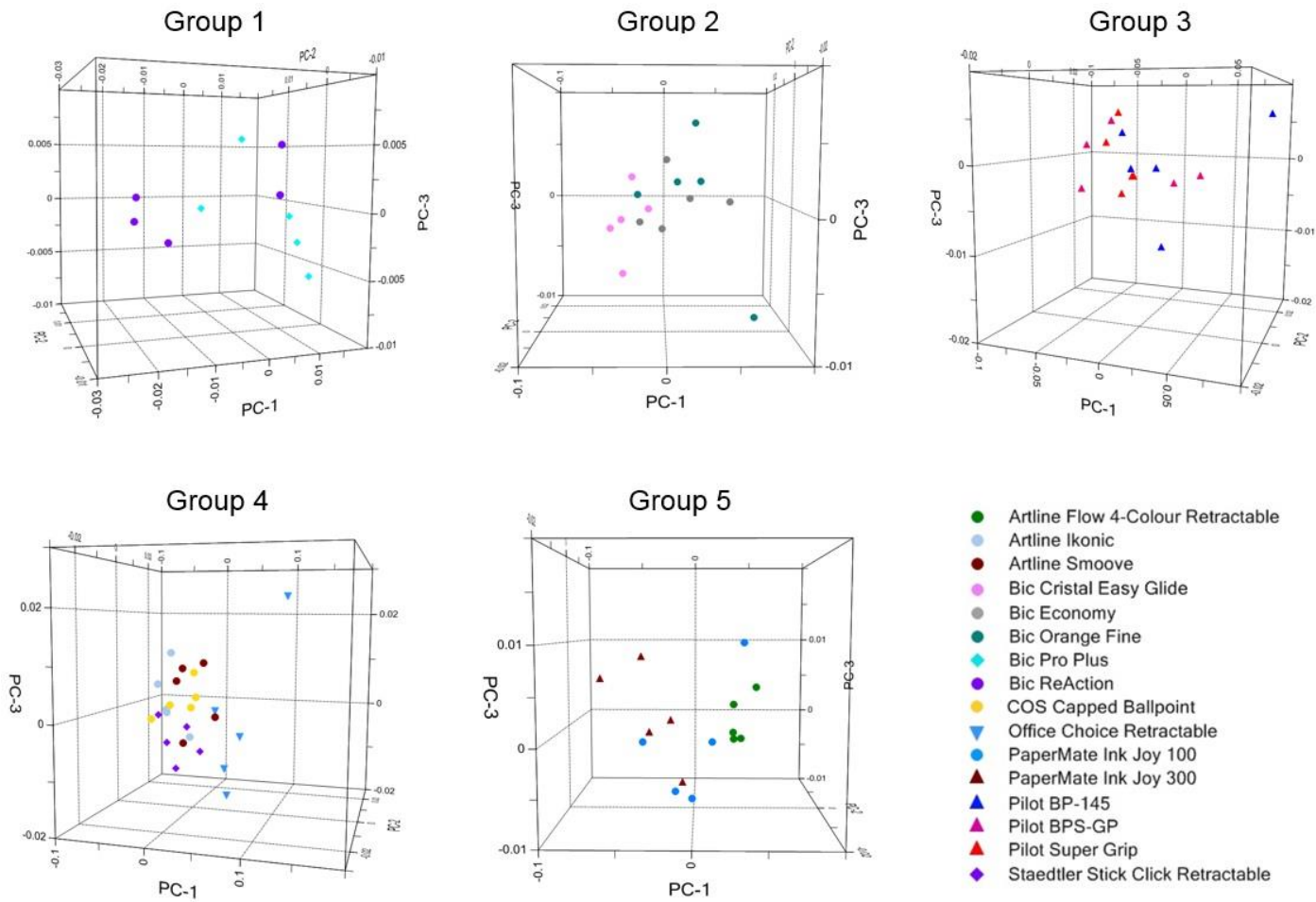
Appendix 2.2: Pre-processed MSP spectra (each averaged across five replicates) obtained from five set D blue acrylic fibres.



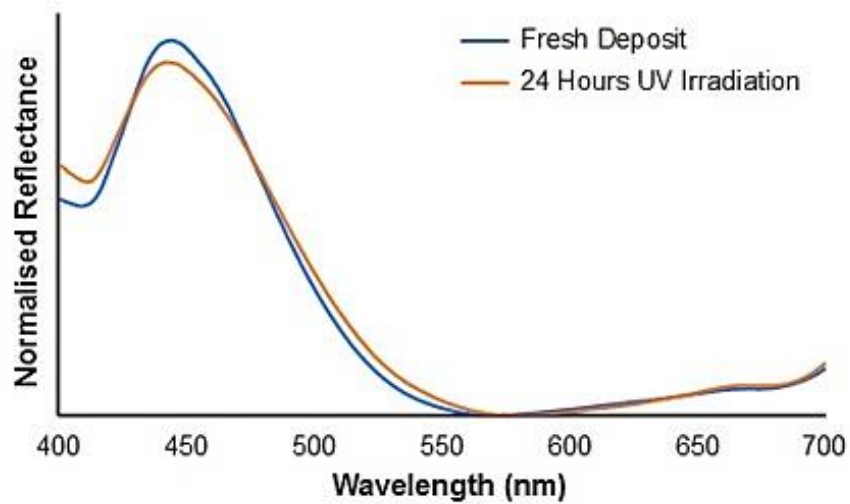
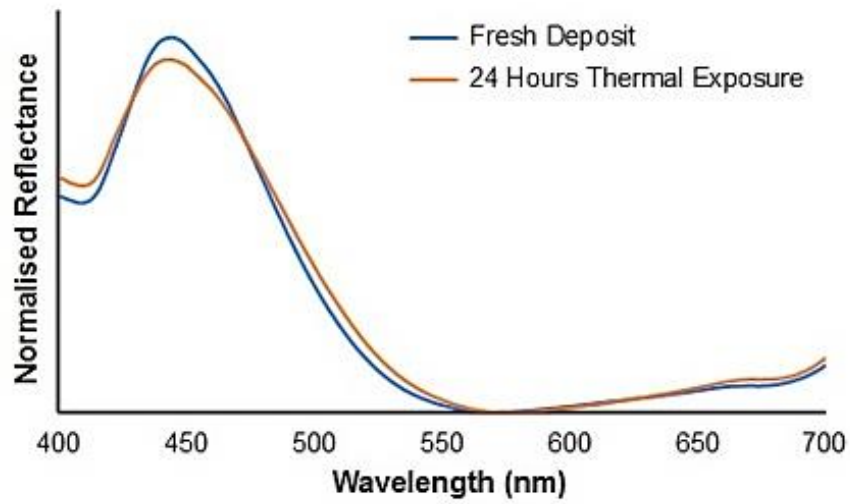
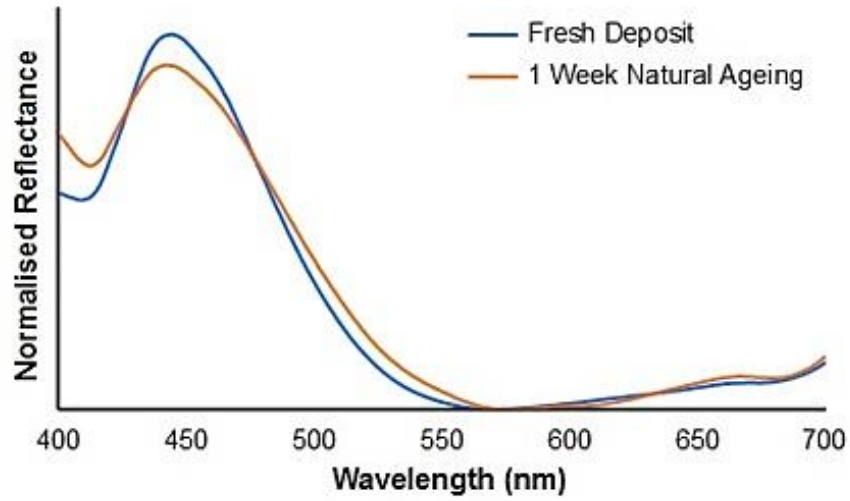
Appendix 2.3: Pre-processed MSP spectra (each averaged across five replicates) obtained from five set E blue acrylic fibres.

Appendix 3.1: A summary of temperature, humidity and dew point data collected using a Digitech QP-6013 data logger on an open office shelf utilised for natural ink ageing studies, acquired between 2-14 months of ageing.

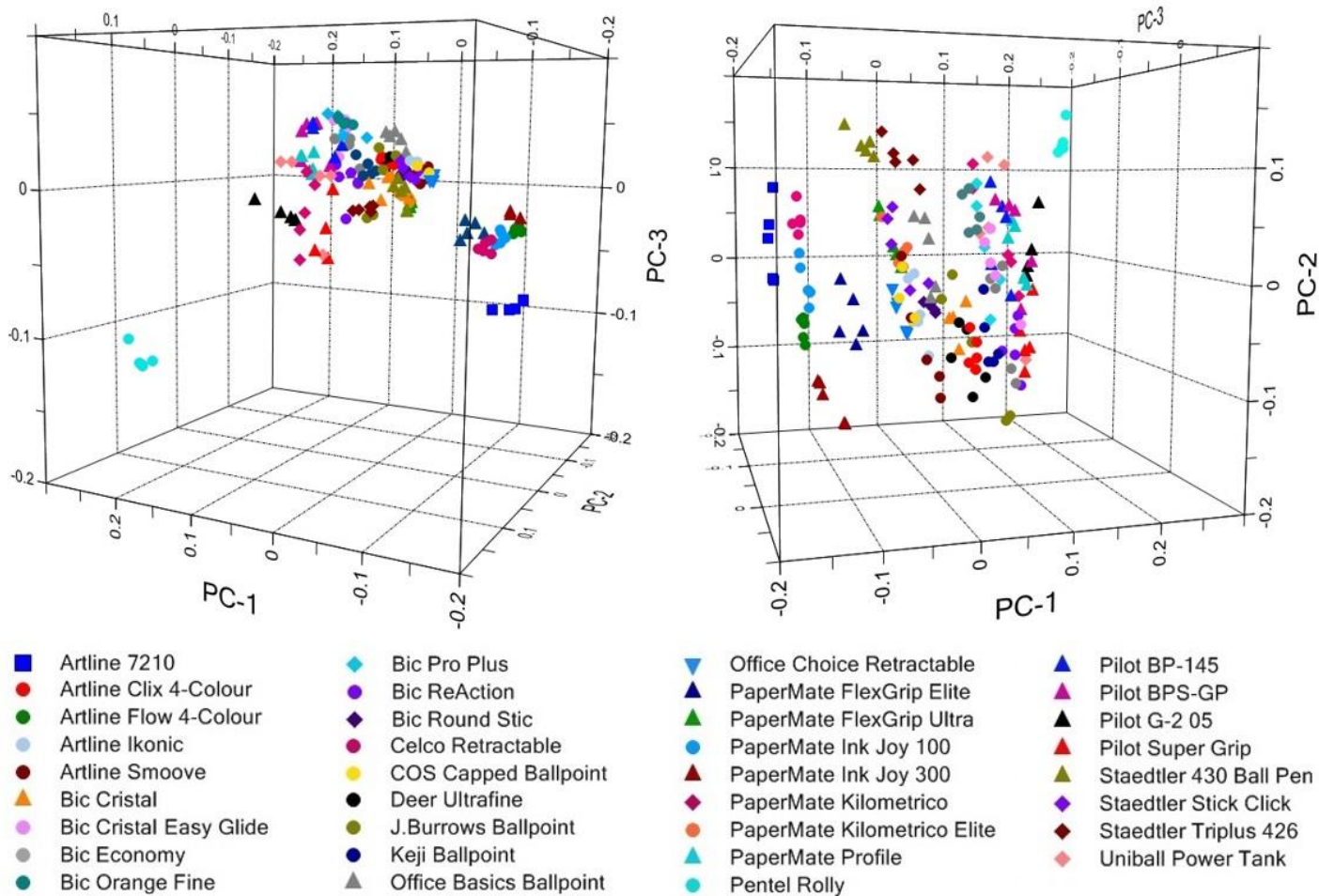
	Temperature (°C)		Relative Humidity (%)		Dew Point (°C)	
	Average	Standard Deviation	Average	Standard Deviation	Average	Standard Deviation
January	24.0	0.3	47.0	4.5	11.9	1.3
February	24.1	0.5	53.1	6.7	13.8	1.8
March	24.0	0.6	50.0	7.1	12.8	2.2
April	24.0	0.7	45.8	8.1	11.4	2.7
May	24.1	0.3	39.6	6.2	9.3	2.5
June	24.0	0.4	42.6	7.0	10.3	2.4
July	23.9	0.3	42.5	8.8	10.1	3.1
August	23.8	0.5	42.3	6.9	10.0	2.4
September	24.0	0.4	39.1	7.6	8.9	2.9
October	24.0	0.2	47.5	7.8	11.9	2.7
November	23.8	0.8	49.8	6.5	12.5	2.4
December	23.8	0.3	50.3	5.9	12.7	2.0



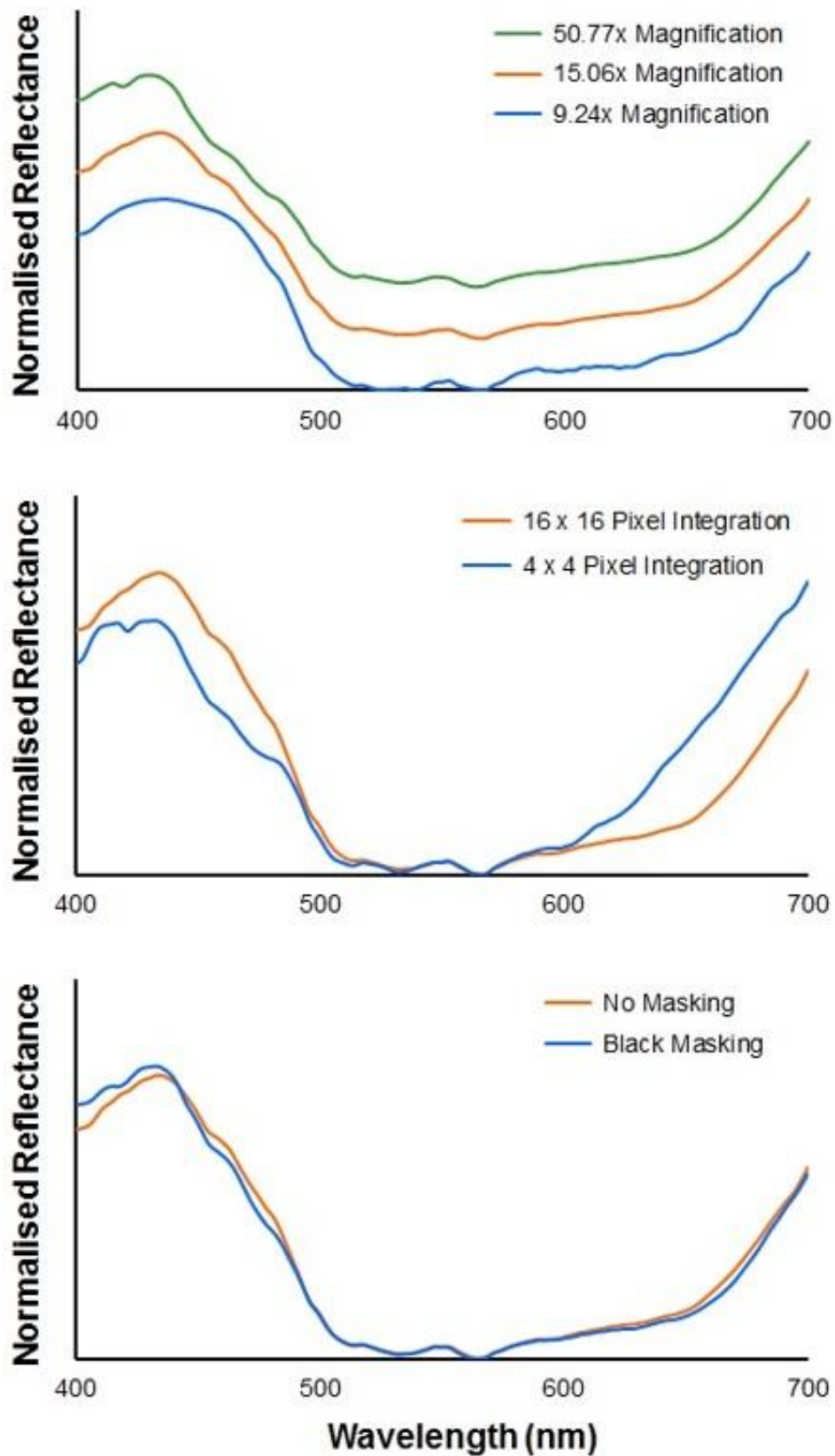
Appendix 3.2: 3-dimensional PCA scores plots generated from individual clusters of inks observed to be visually indistinguishable using PCA of the overall dataset.



Appendix 3.3: Normalised spectra obtained from PaperMate Profile ink, both freshly deposited and following (top) one week of natural ageing under open light; (middle) 24 hours of thermal exposure; and (bottom) 24 hours of UV irradiation.



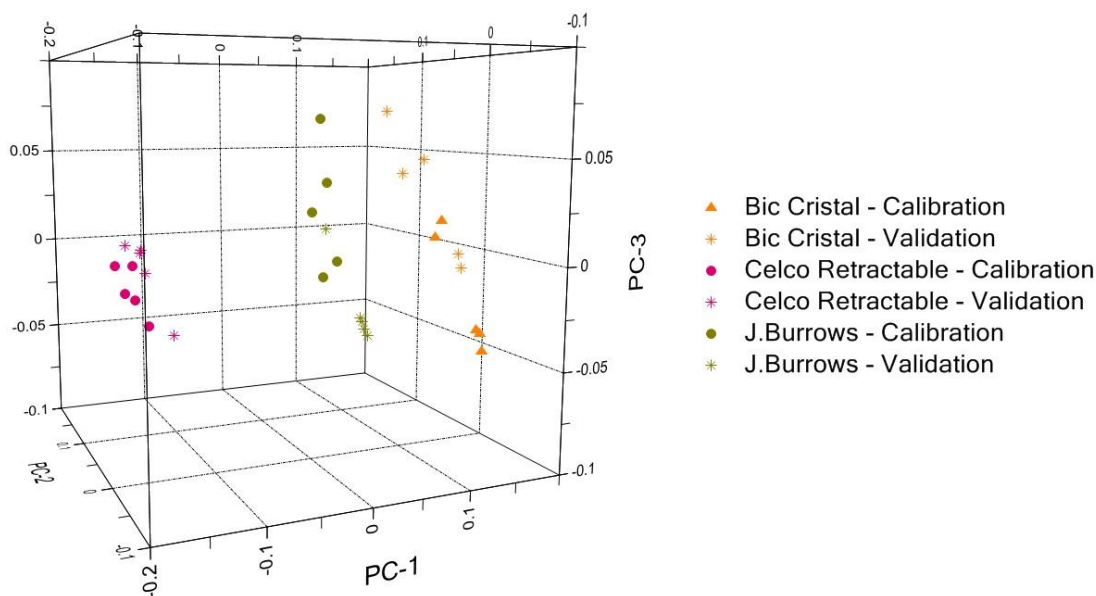
Appendix 4.1: 3-dimensional PCA scores plots generated using the first three PCs, highlighting the distribution of the blue ballpoint ink population based upon their corresponding VSC visible-NIR spectra.



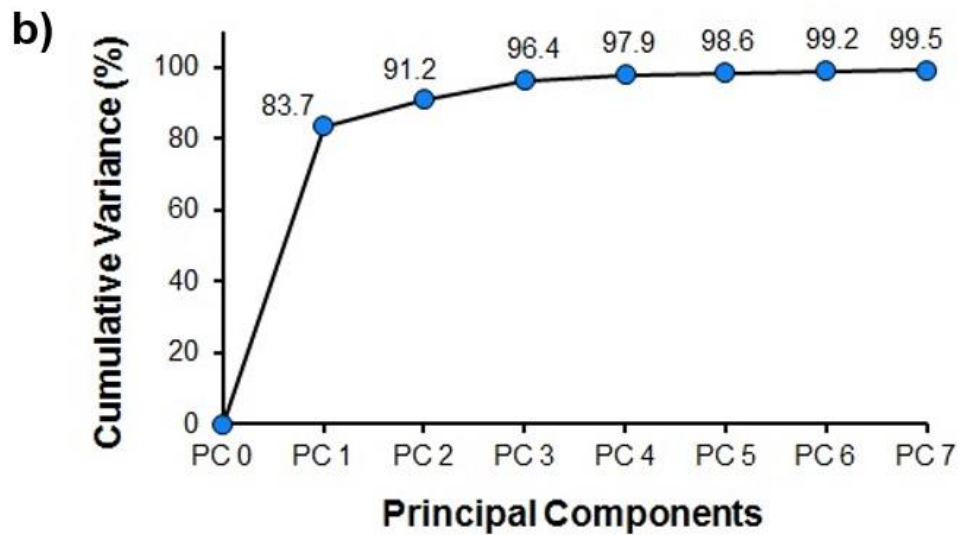
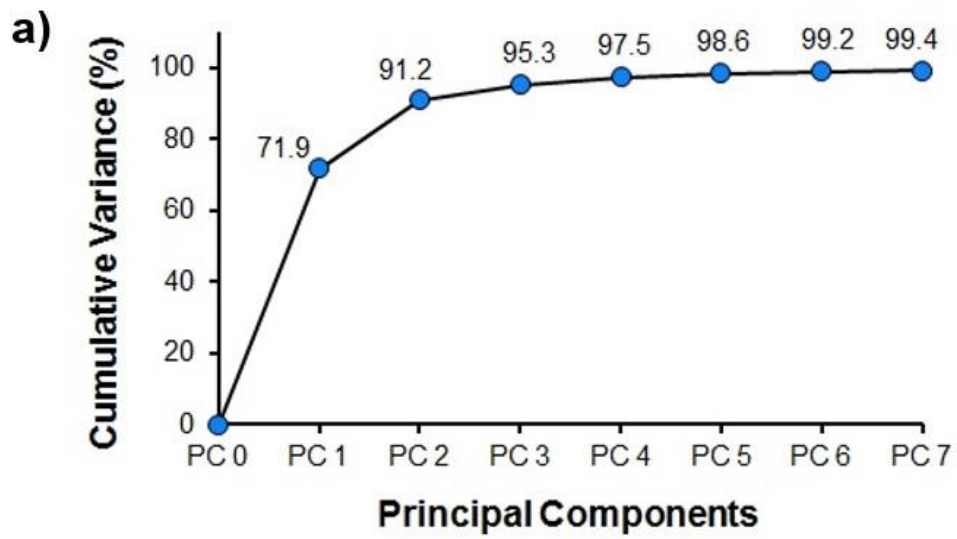
Appendix 4.2: Pre-processed VSC5000 visible spectra showing the effect of (top) varying magnification; (middle) varying integration area; and (bottom) black masking on spectral quality.

Appendix 4.3: Actual and predicted classifications of visible reflectance spectra acquired from 12 inks using the VSC5000, using the statistical model generated using the Cary 4000.

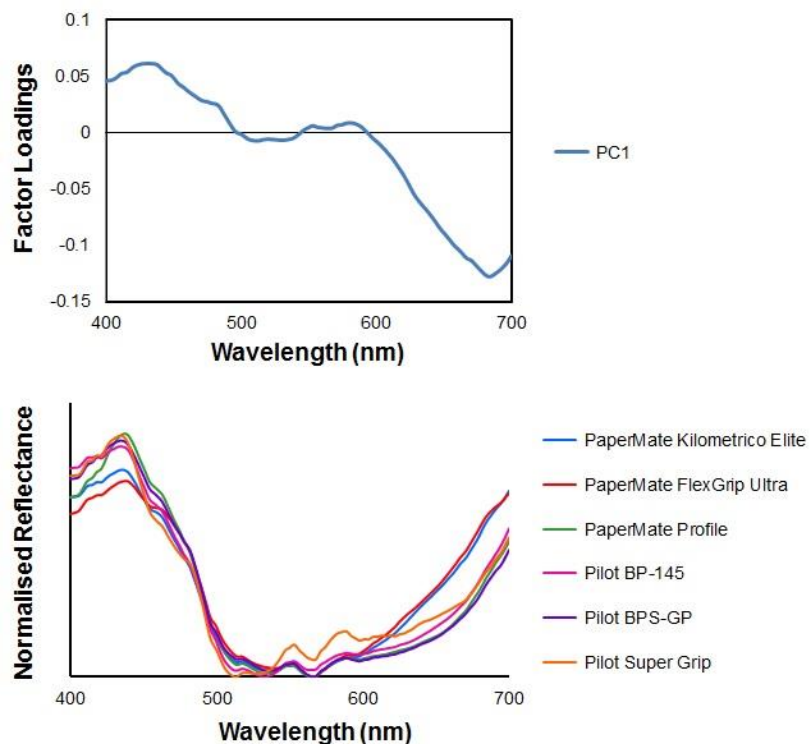
Actual Pen	Predicted Pen(s)
Bic Cristal	Artline Clix 4-Colour / PaperMate Profile
Celco Retractable	Pilot BP-145 / PaperMate Profile
Office Basics Ballpoint	Pilot BP-145 / PaperMate Profile / Artline Clix 4-Colour
J.Burrows Ballpoint	Artline Clix 4-Colour
Bic Economy	Artline Clix 4-Colour
Pilot G-2 05	Artline Clix 4-Colour
Bic Pro Plus	Artline Clix 4-Colour
PaperMate FlexGrip Elite	Artline Clix 4-Colour
Pentel Rolly	Artline Clix 4-Colour
Staedtler Triplus 426	Artline Clix 4-Colour / PaperMate Profile
PaperMate Ink Joy 300	Artline Clix 4-Colour
Office Choice Retractable	Artline Clix 4-Colour / PaperMate Profile



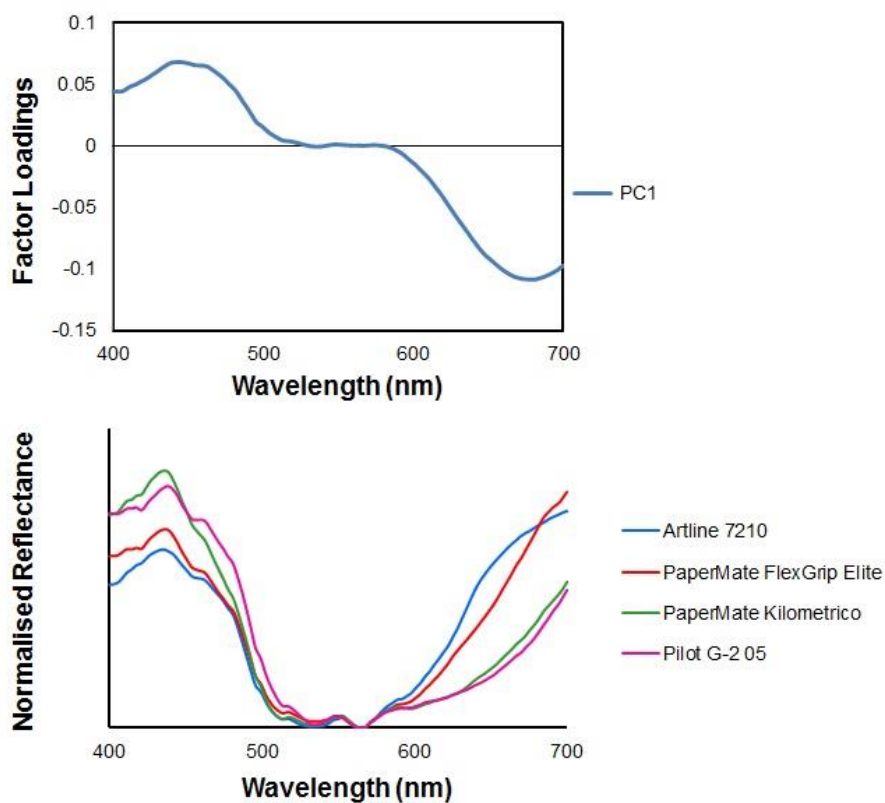
Appendix 4.4: 3-dimensional PCA scores plot showing the relative distribution of calibration and validation spectra acquired from three inks using the VSC5000.



Appendix 4.5: Scree plots depicting the cumulative variance retained by each PC for (a) non-fluorescent; and (b) fluorescent blue ballpoint inks.



Appendix 4.6: PC1 factor loadings and visible reflectance spectra acquired from weakly fluorescent blue ballpoint inks using the VSC5000.



Appendix 4.7: PC1 factor loadings and visible reflectance spectra acquired from moderately fluorescent blue ballpoint inks using the VSC5000.

Appendix 5.1: Distance measurements between fixed steel witness plates and the PVC pipe bomb device containing Alliant Red Dot double-base smokeless powder.

Plate	Distance to Device
North	12.25 inches
East	10.75 inches
South	10.25 inches
West	11.75 inches
Top	8.5 inches
Bottom	12.25 inches